The Role of Pyruvate Kinase Regulation in Tumor Growth and Metabolism

by

William James Israelsen

B.A. Biology; B.A. Economics
Utah State University (2008)

Submitted to the Department of Biology
in Partial Fulfillment of the Requirements for the Degree of

DOCTOR OF PHILOSOPHY

at the

MASSACHUSETTS INSTITUTE OF TECHNOLOGY

September 2014

Signature of Author .....
Department of Biology
July 11, 2014

Certified by .....
Matthew G. Vander Heiden
Associate Professor of Biology
Thesis Supervisor

Accepted by.....
Michael T. Hemann
Professor of Biology
Co-Chair, Graduate Committee

The Role of Pyruvate Kinase Regulation in Tumor Growth and Metabolism

by

William James Israelsen

Submitted to the Department of Biology on July 11, 2014 in Partial Fulfillment of the Requirements for the Degree of Doctor of Philosophy in Biology

ABSTRACT

Cancer is a disease of inappropriate cell proliferation, and central carbon metabolism is highly regulated to support the unique anabolic needs of proliferating cells. Pyruvate kinase, the enzyme catalyzing the final step of glycolysis, is an important point of regulation. Mammals have four pyruvate kinase isoforms, and one in particular, the M2 isoform, is preferentially expressed in proliferative tissues, including cancers. We sought to determine the role and importance of PKM2 in cancer. The activity of pyruvate kinase M2 (PKM2) is down-regulated by pro-proliferative signaling in the cell, and reduced PK activity appears to be important for proliferative metabolism. Because oncogenic signaling reduces PKM2 activity, we hypothesized that artificially high intracellular pyruvate kinase activity would disrupt proliferative metabolism and hinder tumor growth. We found that increased PK activity due to expression of the constitutively-active PKM1 isoform or direct pharmacological activation of PKM2 perturbs metabolism and reduces tumor growth in a lung cancer xenograft model. These results suggested that PKM2 expression is selected for in cancers because PKM2 activity can be down-regulated in a controlled fashion. We next sought to determine if the PKM2 isoform is necessary for tumor proliferation. Deletion of PKM2 in a mouse model of BRCA1-deficient breast cancer demonstrated that PKM2 is not required for tumor formation or growth. PKM2-null tumors exhibited heterogeneous PKM1 expression, and tumor cell proliferation was associated with low PKM1 expression in the absence of PKM2. Analysis of human breast tumors revealed highly variable PKM2 protein expression, and heterozygous PKM2 mutations were found in many cancer types. These mutations cause truncations or amino acid changes in conserved regions of the enzyme. Determination of kinetic parameters of purified wild-type and mutant PKM2 showed that cancer-associated missense mutations reduce affinity of the enzyme for substrate, reduce maximum velocity, or disrupt response of the enzyme to activation by its allosteric activator FBP. These results suggest that cancer cells tolerate or select for reduced pyruvate kinase activity. We conclude that PKM2 is important because its activity is down-regulated to support proliferation, but the PKM2 isoform itself is not required for tumor formation or cancer cell proliferation.

Thesis Supervisor: Matthew G. Vander Heiden
Title: Associate Professor of Biology

BIOGRAPHICAL NOTE

William J. Israelsen

Education:

2009 - 2014: Ph.D. (Biology), Massachusetts Institute of Technology, Cambridge, MA.
2001, 2004 - 2008: B.A. (Biology/Economics) Utah State University, Logan, UT.

Research Experience:

2009 - 2014: Graduate Studies
Laboratory of Dr. Matthew Vander Heiden, MIT.
Investigate the role of pyruvate kinase isoforms in tumor metabolism using a mouse model of breast cancer. Maintain a colony of laboratory mice at MIT.

2008 - 2009: Research Technician
Laboratory of Dr. Paul Cliften, Utah State University
Discovery of novel gene regulatory elements via comparative genomics and yeast genetics and assembly of yeast mitochondrial genomes from sequencing data.

Spring 2008: Undergraduate Research
Laboratory of Dr. Paul Cliften, Utah State University
Discovery of novel gene regulatory elements via comparative genomics and yeast genetics.

2005 - 2007: Undergraduate Research
Laboratory of Dr. Peter Ruben, Utah State University
Investigation of structure/function relationship of voltage-gated sodium channels using site-directed mutagenesis and electrophysiology recording.

Teaching Experience:

Spring 2013: Teaching Assistant, General Biochemistry (7.05), MIT
Fall 2010: Teaching Assistant, Introductory Biology (7.012), MIT
Fall 2004 - Spring 2007: Teaching Assistant, Creative Arts (USU 1330), Utah State University

Awards:

2008: *Summa cum laude* graduate with Honors in Biology, Utah State University
2008: Undergraduate Researcher of the Year, Huntsman School of Business, Utah State U.
2007: Best Paper Award, Business Division, Utah Academy of Sciences, Arts & Letters

Publications:

Israelsen WJ, Dayton TL, Davidson SM, Fiske BP, Hosios AM, Bellinger G, Li J, Yu Y, Sasaki M, Horner JW, Burga LN, Xie J, Jurczak MJ, Depinho RA, Clish CB, Jacks T, Kibbey RG, Wulf GM, Di Vizio D, Mills GB, Cantley LC, Vander Heiden MG. (2013) *PKM2 Isoform-Specific Deletion Reveals a Differential Requirement for Pyruvate Kinase in Tumor Cells.* Cell, 155(2):397-409.

Anastasiou D*, Yu Y*, Israelsen WJ*, Jiang J, Boxer MB, Hong BS, Tempel W, Dimov S, Shen M, Jha A, Yang H, Mattaini KR, Metallo CM, Fiske BP, Courtney KD, Malstrom S, Khan TM, Kung C, Skoumbourdis AP, Veith H, Southall N, Walsh MJ, Brimacombe KR, Leister W, Lunt SY, Johnson ZR, Yen KE, Kunii K, Davidson SM, Christofk HR, Austin CP, Inglese J, Harris MH, Asara JM, Stephanopoulos G, Salituro FG, Jin S, Dang L, Auld DS, Park H, Cantley LC, Thomas CJ, Vander Heiden MG. (2012) *Pyruvate kinase M2 activators promote tetramer formation and suppress tumorigenesis*. Nature Chemical Biology, 8(10):839-47. [*Equal contribution]

Vander Heiden MG, Lunt SY, Dayton TL, Fiske BP, Israelsen WJ, Mattaini K R, Vokes NI, Stephanopoulos G, Cantley LC, Metallo CM, Locasale JW. (2012) *Metabolic Pathway Alterations that Support Cell Proliferation*. Cold Spring Harbor Symposia on Quantitative Biology, 76:325–34.

Walsh MJ, Brimacombe KR, Veith H, Bougie JM, Daniel T, Leister W, Cantley LC, Israelsen WJ, Vander Heiden MG, Shen M, Auld DS, Thomas CJ, Boxer MB. (2011) *2-Oxo-N-aryl-1,2,3,4-tetrahydroquinoline-6-sulfonamides as activators of the tumor cell specific M2 isoform of pyruvate kinase.* Bioorganic & Medicinal Chemistry Letters. 21(21):6322-7.

Israelsen, WJ & Vander Heiden, MG (2010). *ATP consumption promotes cancer metabolism.* Cell, 143(5): 669-71.

Select Presentations:

Talk: "*The Role of Pyruvate Kinase in Tumor Metabolism and Growth*" Seminars in Metabolism, University of Utah School of Medicine, Salt Lake City, UT, Oct. 17, 2013

Talk: "*PKM2 isoform-specific deletion reveals a differential requirement for pyruvate kinase in tumor cells*" Cell Growth Research Symposium of the MIT Physical Sciences-Oncology Center, Cambridge, MA, July 23, 2013

Talk: "*PKM2 isoform-specific deletion reveals a differential requirement for pyruvate kinase in tumor cells*" Broad Institute Cancer Program Meeting, Cambridge, MA, April 26, 2013

Talk: "*Role of PKM2 in Tumor Formation*" Koch Institute Annual Fall Retreat, Hyannis, MA, Oct. 15, 2012

Short Talk: "*Role of PKM2 in Tumor Formation*" Keystone Symposium, Cancer and Metabolism, Banff, AB, Feb. 16, 2012

ACKNOWLEDGEMENTS

I thank my advisor, Matthew Vander Heiden. Matt has been an outstanding mentor and example. Matt has always been willing to drop what he's doing to have a conversation or answer a question. He has been involved in my progression as a scientist and given needed guidance and advice, but he has also been comfortable giving me space and allowing me to manage myself; for this I am grateful. I am also grateful for the effort he has made to ensure that I have had opportunities to learn all aspects of the scientific process, to collaborate with outside labs, to give talks, and to position myself for success in my post-graduation plans. Matt has been exceptionally generous in facilitating my transition to my next position, and I have learned much from his example.

I am grateful to Tyler Jacks and Michael Hemann, who have taken the time to serve as my thesis committee. They have provided sound advice, have written letters for me on short notice, and have helped guide my career aspirations. I thank Mike for taking the time to meet with me outside of committee meetings. Frank Solomon has been a source of advice on everything ranging from which lab to join to postdoctoral plans. I thank him for having served on my committee in the early days and for stepping in at the last minute to attend my defense. I thank Nabeel Bardeesy for serving as the outside member of my thesis defense committee.

I have had the pleasure of meeting and working with many impressive people at MIT. My classmate Talya Dayton has been a great collaborator. I learned many mouse-related techniques from her and am grateful for her work that made our *Cell* paper what it is. I acknowledge the many other outside collaborators who have enriched my graduate school experience and facilitated publications.

I thank my Vander Heiden labmates for enjoyable interactions and the things that I have learned from them. In particular, Katie Mattaini has been a good friend and even better bay-mate since we joined the lab; I have learned from her that incessant mockery is the language of friendship. Brian Fiske is an excellent scientist; I have learned a lot from him technically and I have sought to emulate his "Fiske Rigor." Brian and I have had many great scientific conversations and it was Brian who first got me interested in the metabolism of hibernation. Those early conversations with Brian played a major role in shaping my career trajectory, and I have valued and learned from his attitude toward the scientific process. I have enjoyed working with all other members of the Vander Heiden lab past and present: Amelia Yu, Zach Johnson, Gary Bellinger, Sophia Lunt, Shawn Davidson, Jared Mayers, Aaron Hosios, Dan Gui, Alba Luengo, Caroline Lewis, and Lucas Sullivan.

I have had the good fortune of working with very talented MIT undergraduates. Vivian Liu and Andrea Howell have been committed, fun to work with, and have been hugely helpful in moving my work forward over the past several years. I thank them for their efforts, and I thank also Katie Allsop for the short time she worked with me before defecting to the dismal science of economics.

My parents, Dwight and Jill Israelsen, have always been extremely supportive and have encouraged me to be successful in all my endeavors, graduate school included. I thank them for their support in all aspects of my life. In particular, I am grateful for they way that they valued education, set high expectations by their example and actions, and taught me how to work. I am grateful to them for career and personal advice, the encouragement to take risks and go after big scientific questions, and for their confidence in me.

I acknowledge the examples that were set for me by my grandfathers, who both passed away during my first year of graduate school here at MIT. They were both examples of hard work, sacrifice, and the importance of family.

Finally, I acknowledge the huge role that my wife Lora has played in my success. My time in Cambridge has been a time of change, and all of the changes have been for the better. Lora and I first met when I moved to Cambridge and we were married partway through my PhD. She has improved my life in innumerable ways, but most importantly, she has encouraged me both to work hard and at the same time helped me to see that there is much more to life than working all of the time.

TABLE OF CONTENTS

CHAPTER ONE:
Introduction

INTRODUCTION TO CANCER METABOLISM

The view of cancer as a disease of altered metabolism originated with the work of Otto Warburg in the early 1920s. Warburg's idea that inappropriate tissue proliferation was caused by an imbalance between respiration and glycolysis preceded even the elucidation of the individual glycolytic reactions and the discovery of ATP. Although great progress has been made over the last 90 years in understanding intracellular metabolic networks and the genetic and signaling aspects of cancer biology, the intimate relationship between metabolism and proliferation remains an area of fruitful investigation. Many successful anti-cancer drugs target metabolic processes, and work toward understanding of how proliferating tumor cells adapt metabolism to support uncontrolled growth has been conducted with the hope that additional therapeutic targets will be made manifest. The work reported here is focused on pyruvate kinase, a glycolytic enzyme, and its role in cancer metabolism. The M2 isoform of pyruvate kinase is expressed in the vast majority of cancers and other proliferating cells, and I have investigated the importance of this pyruvate kinase isoform in the regulation of proliferative metabolism.

HISTORICAL PERSPECTIVE

Discovery and Purification of Pyruvate Kinase

Pyruvate kinase catalyzes the conversion ADP and phospho*enol*pyruvate (PEP) to ATP and pyruvate (Figure 1). The enzymatic activity of pyruvate kinase was discovered in the 1930s, as multiple laboratories worked to identify the individual reactions of the glycolytic pathway. Embden and coworkers first observed that 3-phosphoglycerate was converted to pyruvate and inorganic phosphate in muscle tissue (Embden et al, 1933). Lohmann and Meyerhof showed that the conversion of 3-phosphoglycerate to pyruvate and

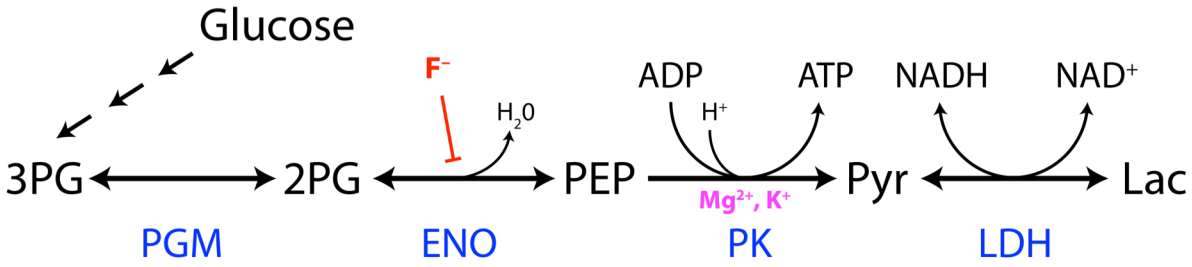

Figure 1. Final Reactions of Lower Glycolysis and Pyruvate Fermentation.
Pyruvate kinase requires mono- and divalent metal cofactors, and enolase can be experimentally inhibited with fluoride. The activity of pyruvate kinase can be measured in an LDH-linked *in vitro* kinetic assay. In the presence of excess NADH and LDH activity, the rate of pyruvate production is equivalent to the rate of pyruvate and NADH consumption, and this rate is observed via change NADH absorbance at 340 nm. Metabolite abbreviations: 3PG, 3-phosphoglycerate; 2PG, 3-phosphoglycerate; PEP, phosphoenolpyruvate; Pyr, pyruvate, Lac, lactate. Enzyme abbreviations: PGM, phosphoglycerate mutase; ENO, enolase; PK, pyruvate kinase; LDH, lactate dehydrogenase.

inorganic phosphate in muscle extract required Mg^{2+} and adenine nucleotide cofactors (Lohmann & Meyerhof, 1934). The absence of these cofactors allowed the accumulation of a new intermediate (PEP) that was identified as “phosphopyruvate." Additionally, the conversion of 3-phosphoglycerate to phosphopyruvate was blocked by fluoride (which was later found to inhibit enolase); this work thus separated the activity of pyruvate kinase from upstream steps and defined ADP and Mg^{2+} as required cofactors. Concurrently, Parnas and coworkers demonstrated that the conversion of 3-phosphoglycerate to lactate maintained ATP levels in muscle lysate and proposed that this process occurred through a direct transfer of phosphate from a phosphorylated intermediate to ADP; Parnas incorrectly identified the phosphocreatine generated in his assay as the likely phosphate donor (Parnas et al, 1934). The ATP-generating results from Parnas’ laboratory were confirmed by workers in London, who correctly suggested a direct reaction between PEP and ADP to produce ATP, and that ATP was the phosphate donor for creatine phosphate

production (Needham & Van Heyningen, 1935). Shortly thereafter, the structures of 2-phosphoglycerate and phospho*enol*pyruvate were determined and the direct transfer of phosphate from PEP to ADP was established (Meyerhof, 1935; Parnas, 1935). Later work showed a requirement for potassium ions at the pyruvate kinase step, which completed the list of necessary cofactors (Boyer et al, 1942).

The pyruvate kinase enzyme was successfully purified from rat muscle and isolated as crystals by 1942 by Negelein in the laboratory of Otto Warburg (Kubowitz & Ott, 1943), but, as was later reported by his contemporaries (Bücher & Pfleiderer, 1955), "[h]is protocols and manuscript related to this work were lost in the confusion at the end of World War II." Negelein also developed the lactate dehydrogenase-linked photometric kinetic assay for pyruvate kinase activity and determined that pyruvate kinase directly bound Mg^{2+} (Kubowitz & Ott, 1943). Negelein's linked assay was later standardized as a method for determining pyruvate kinase activity (Bücher & Pfleiderer, 1955). The first published purification was by Negelein's colleagues Kubowitz and Ott (1943), who purified pyruvate kinase from human muscle tissue. Thus, the identity and structure of the substrates and products of pyruvate kinase, its required metal cofactors, and its purification were all worked out within a decade of its discovery as a step in glycolysis.

Isoforms, Nomenclature, and Cloning

There are four mammalian pyruvate kinase isoforms which have each had multiple designations over time in the English-language literature. The PKM1 isoform, first isolated from muscle by Negelein, was commonly called the M isoform. The PKM2 isoform was referred to as the K isoform because it was commonly purified from the kidney. The main variant isolated from the liver was commonly designated the L isoform, and red blood cells

yielded the R isoform of pyruvate kinase; these designations persist as PKL and PKR, respectively. Many other designations were given to different isoforms by various workers based on alternative conventions such as isoelectric shift, and a more complete table of historical nomenclature is given by Imamura and Tanaka (1982).

Prior to the convergence of biochemical and genetic information on pyruvate kinase isoforms, there was much speculation into the origin and possible biochemical interconversion of different pyruvate kinase isozymes (Ibsen, 1977). Some of this speculation was laid to rest with the determination that PKM1 and PKM2 are translated from different mRNAs (Noguchi & Tanaka, 1982). Around the same time, a spontaneous loss-of-function allele, then termed *PK-3*^{r}, that affected pyruvate kinase activity in the kidney was mapped to mouse chromosome 9 (Johnson et al, 1981). This mutation appeared to be a complete loss-of function because animals heterozygous for the *PK-3*^{r} allele showed a ~50% reduction in pyruvate kinase activity in their kidneys. The *PK-3*^{r} allele was subsequently shown to also affect pyruvate kinase activity levels in the heart (Peters & Andrews, 1984), confirming previous biochemical evidence, such as immunological cross-reactivity, which suggested that the PKM1 and PKM2 isoforms were produced from the same gene. Of note is that *PK-3*^{r} homozygous mice were never obtained from heterozygous crosses (Johnson et al, 1981), and lethality of *PK-3*^{r} homozygous embryos was later shown to occur around the time of implantation (Lewis & Johnson, 1983), suggesting that a product of the *PKM* gene is required during embryonic development.

The rat *PKM* gene was soon cloned and was shown to produce both the PKM1 and PKM2 isoforms by alternative mRNA splicing (Noguchi et al, 1986). This alternative

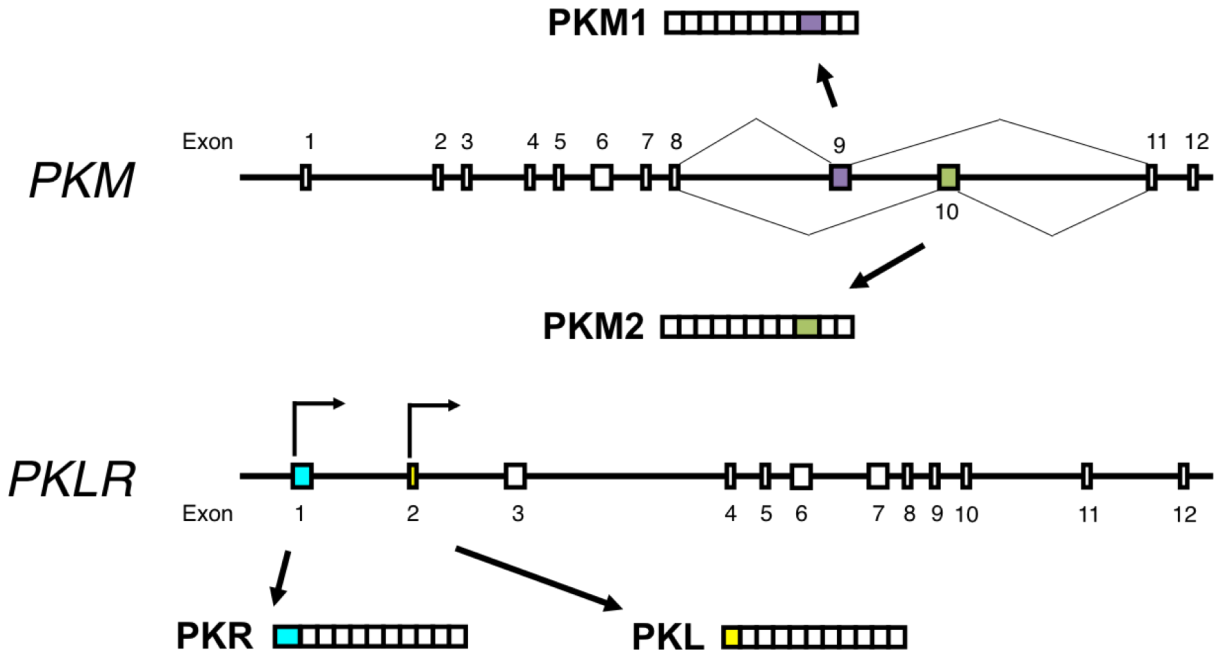

Figure 2. Generation of Pyruvate Kinase Isoforms from the *PKM* and *PKLR* Genes.
PKM1 and PKM2 are produced by alternative splicing from the *PKM* gene. *PKM* exon 9 is included in mature PKM1 mRNA, and exon 10 is included in mature PKM2 mRNA. PKR and PKL are produced from the *PKLR* gene by tissue-specific promoters and share exons 3-12. Primary PKR transcript includes both exons 1 and 2, but exon 2 is removed during splicing.

splicing involves the mutually-exclusive inclusion of one of a pair of adjacent internal exons; inclusion of exon 9 generates PKM1 transcript, and inclusion of exon 10 generates PKM2 transcript (Figure 2). The human *PKM* gene was found to have the same intro-exon structure, with the 9th or 10th exon being included during splicing to produce the PKM1 or PKM2 isoform, respectively (Takenaka et al, 1991). The PKL and PKR isoforms are likewise encoded by a single gene, *PKLR*, but are expressed under the control of separate, tissue-specific promoters (Noguchi et al, 1987). The PKL and PKR mRNAs thus contain unique first exons but are otherwise identical; PKR has a longer first exon and is the larger isoform (Figure 2).

PYRUVATE KINASE GENES, PROTEIN STRUCTURE, AND FUNCTION

Alternative Splicing of the *PKM* Gene

The *PKM* gene is alternatively spliced to allow production of the PKM1 and PKM2 protein isoforms. The human, rat, and mouse genes each have 12 exons (Noguchi et al, 1986; Takenaka et al, 1991). In all mammals, the 9th and 10th exons are isoform-specific: exon 9 is specific to PKM1, exon 10 is specific to PKM2, and only one of the two exons is included in a properly-spliced final transcript. Splicing of the PKM isoforms is tightly controlled by multiple factors, as splicing to produce PKM2 transcript requires both inclusion of exon 10 and repression of exon 9 (Figure 3). Three splicing factors – polypyrimidine tract binding protein (PTB), heterogeneous nuclear ribonucleoprotein A1 (hnRNPA1), and heterogeneous nuclear ribonucleoprotein A1 (hnRNPA2) – act downstream of oncogenic signaling to repress inclusion of exon 9 (Clower et al, 2010; David et al, 2010), while the serine/arginine-rich splicing factor 3 (SRSF3) binds within exon 10 to promote its inclusion in the transcript (Wang et al, 2012a). How the cell

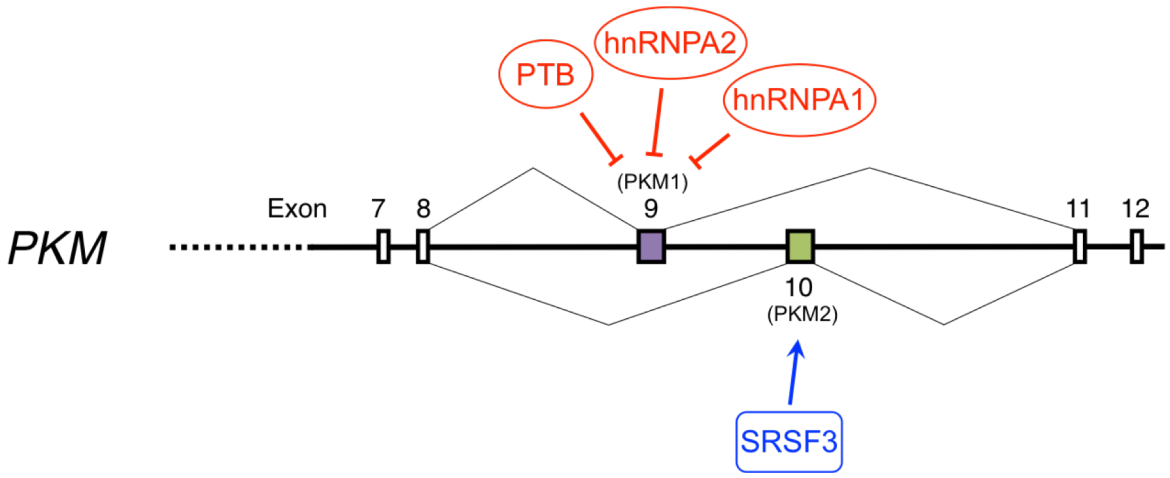

Figure 3. Factors Controlling *PKM* Splicing.
Production of the M2 isoform of pyruvate kinase requires both repression of exon 9 and inclusion of exon 10. PTB, hnRNPA1, and hnRNPA2 repress inclusion of exon 9, while SRSF3 promotes inclusion of exon 10.

controls splicing to generate PKM1 transcript is less well understood. Knockdown of the repressive factors (PTB, hnRNPA1, and hnRNPA2) allows an increase in PKM1 transcript production, but this results in production of less than 50% PKM1 transcript (Clower et al, 2010; David et al, 2010). Similarly, SRSF3 knockdown decreases PKM2 transcript production and increases PKM1 transcript levels, but this effect is also only partial, because a mixture of PKM1 and PKM2 mRNAs is produced in cells lacking SRSF3 (Wang et al, 2012a). The effect of the repressive splicing factor hnRNPA1 on PKM splicing also appears to be concentration dependent. A reduction of the intracellular levels of hnRNPA1 can shift its binding from exon 9 to the PKM2-specific exon 10 and contribute to exon 10 exclusion, thereby promoting PKM1 expression (Chen et al, 2012). In the absence of oncogenic signaling, inclusion of exon 9 and PKM1 expression may thus be the default. Because PKM splicing research has been focused on cancer, it remains to be seen if additional regulatory elements are required to allow exclusive expression of PKM1 in other cell types. If these regulatory elements exist and are required, they are expected to repress inclusion of exon 10 and/or promote inclusion of exon 9. Work toward understanding the splicing factors contributing to PKM1 expression will likely be more difficult than the previous work to understand PKM splicing, as it will require investigation of terminally-differentiated cells or tissues such as myotubes, skeletal muscle, or neurons that normally express only PKM1. Even the A172 glioblastoma cell line, which has been used to study PKM1 expression, produces PKM1 transcript at a rate of only 5-15% (Clower et al, 2010; Wang et al, 2012a; Wang et al, 2012b).

Protein Structure of PKM1 and PKM2

Mammalian pyruvate kinase is a tetrameric protein of identical subunits (Figure 4). Each monomer contains one active site and is composed of three main domains, which are designated A, B, and C (Stammers & Muirhead, 1977), and one small N-terminal domain (Muirhead et al, 1986). The A domain is the largest domain and is a symmetric α_8/β_8 barrel fold called a TIM barrel; the TIM barrel is a common protein fold that was first discovered in another enzyme, triose phosphate isomerase (TIM) (Banner et al, 1975). The A domain hosts the active site, which is found in a cleft "on top" of the barrel and "beneath" the B

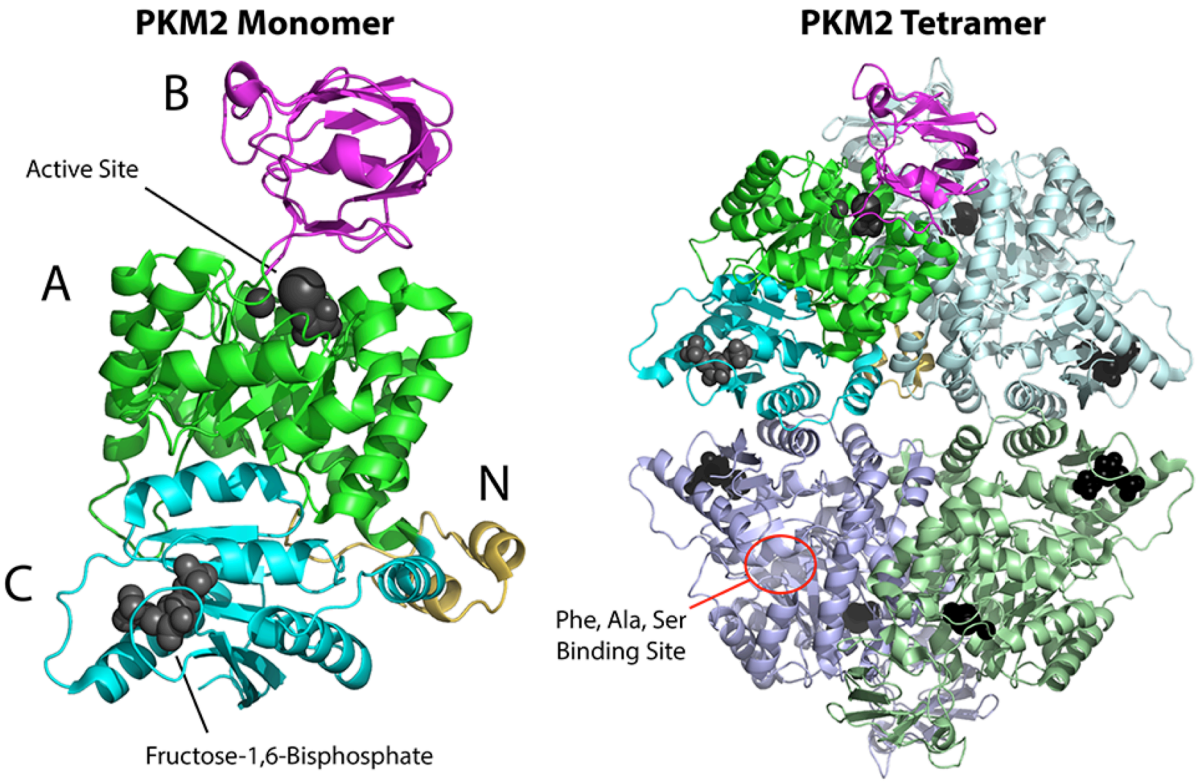

Figure 4. Crystal Structure of Tetrameric PKM2 with Bound Ligands.
The ribbon structure of tetrameric PKM2 (PDB 3BJF) is shown, with a single subunit colored to represent individual domains. The A, B, C, and N-terminal domains are depicted in green, magenta, cyan, and yellow, respectively. Bound ligands are shown as gray spheres. In this structure, the active site is occupied by K^+, Mg^{2+}, and oxalate (a PEP mimetic), and FBP is bound at its binding pocket. The binding site for phenylalanine, alanine, and serine is empty; this site is located in a pocket between the A and C domains.

domain. The B domain is mobile and closes down on the active site upon binding of the Mg^{2+}-ADP substrate complex (Larsen et al, 1998). The C domain is found on the side of the A domain opposite the B domain and contains the fructose-1,6-bisphosphate (FBP) binding pocket which is present in the M2, L, and R isoforms (Jurica et al, 1998; Dombrauckas et al, 2005). FBP is a major allosteric activator of most pyruvate kinase isoforms and its function in regulating PK activity is discussed in a later section. The C domains form the dimer-dimer interface of the fully-associated tetramer. It is the C domain that differs due to alternative splicing of PKM1 and PKM2 (Figure 5); differences in the dimer-dimer interface explain the differences in FBP binding and allosteric regulation between the M1 and M2 isoforms (Jurica et al, 1998).

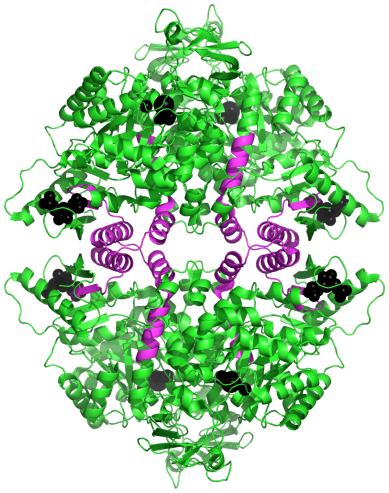

Figure 5. The Isoform-Specific Portion of a PKM2 Tetramer. A ribbon structure of a PKM2 tetramer is shown in green. The part of each subunit that is isoform-specific is highlighted in magenta. The isoform-specific part of the protein forms the bulk of the interface between the dimer of dimers and also forms part of the FBP binding site. Ligands bound to the active sites and FBP binding sites are shown as black spheres.

The pyruvate kinase enzyme normally functions as a tetramer. Solvent denaturation of rabbit PKM1 showed that dimers retain most catalytic activity, but that monomers are inactive (Cottam et al, 1969). However, it is unclear if the monomers remain folded in the 4M urea required to cause full dissociation of the stable PKM1 tetramer. Unlike PKM1, PKM2 is not a constitutive tetramer; the M2 isoform is subject to

reversible dissociation and inactivation when diluted in the absence of FBP (Ashizawa et al, 1991). In these dilute conditions, PKM2 monomers retain catalytic activity but have a very low specific activity: the specific activity of PKM2 in monomer form is only ~4% of that of the FBP-activated tetramer. The reversible association and dissociation of PKM2 tetramers thus provides a method of dynamic regulation of PKM2 enzymatic activity.

Mechanism of Catalysis

Pyruvate kinase catalyzes the direct transfer of phosphate from PEP to ADP to produce ATP and pyruvate. This reaction is energetically favorable due to the extremely high energy of hydrolysis of PEP (Mazurek et al, 2002). During catalysis, the active site is occupied by both substrates (PEP and ADP complexed with Mg^{2+}), one monovalent cation (usually K^{+}) and one additional divalent cation (usually Mg^{2+}) that is bound to the enzyme (Gupta & Oesterling, 1976). These latter two metal ions assist with substrate binding and coordination. Phosphate transfer is assisted by a catalytic lysine, which coordinates the pentacoordinate transition state that exists as the phosphate is transferred directly from PEP to ADP. The conserved catalytic lysine is found at position 270 in mammals, 240 in *S. cerevisiae*, and 221 in *Bacillus*; substitution of the catalytic lysine with methionine in these proteins produces a properly-folded but catalytically-dead version of the enzyme (Bollenbach et al, 1999; Sakai, 2005; Luo et al, 2011).

Transfer of the phosphate from PEP to ADP leaves the energetically less stable enol form of pyruvate bound in the active site (Seeholzer et al, 1991). Tautomerization of enolpyruvate to the more stable keto form releases additional free energy, which contributes to the favorable energetics of the forward reaction. Following phosphate transfer, tautomerization occurs when enolpyruvate accepts a proton from a water

molecule which is held in the proper position by conserved residues (T328 and S326) in active site (Susan-Resiga & Nowak, 2003; Susan-Resiga & Nowak, 2004; Dombrauckas et al, 2005). Following catalysis, the products leave the active site. Substrate binding and release appear to occur in random order (Ainsworth & MacFarlane, 1973).

Pyruvate kinase is not perfectly selective in terms of its nucleotide substrate. In addition to using ADP as a substrate, rabbit PKM1 has been shown to accept other substrates *in vitro*, including GDP, IDP, UDP, dADP, and CDP in order of decreasing affinity at pH 7.5 (Plowman & Krall, 1965). In comparison to ADP binding, the enzyme displays a four-fold increase in K_m for GDP, which was verified by other workers (Hohnadel & Cooper, 1973), and a 15-fold increase in K_m for dADP. Given the low affinity of PKM1 for substrates other than ADP, and the relative abundance of ADP in the cytosol, the *in vivo* activity of PKM1 on substrates other than ADP is likely quite low. The active site of PKM2 shares both primary and tertiary structure with the active site of PKM1 (Morgan et al, 2013), which implies that PKM2 exhibits the same substrate specificity. Careful determination of kinetic parameters of PKM2 with different nucleotide substrates is lacking; however, PKM2 in tumor cell line lysates exhibits activity, in decreasing amounts, when presented with ADP, GDP, and UDP (Mazurek et al, 1998). These results bolster the assumption that PKM1 and PKM2 exhibit the same nucleotide substrate selectivity.

The PKM2 K367M mutant has been reported in the literature as being catalytically dead, and this mutation has been used by various groups in an attempt to separate the catalytic function of the enzyme from putative non-canonical functions of PKM2. (These non-canonical functions are discussed in a following section.) The K367M mutation supposedly abolishes ADP binding (Le Mellay et al, 2002); however, that report does not

include data to support this assertion, and no additional work has been published to show that this mutant is indeed deficient in substrate binding. Crystal structure analysis shows that while K367 is near the nucleotide binding site, it does not interact with the bound nucleotide (Larsen et al, 1998). It is possible that loss of charge at residue 367 does indeed affect the activity of pyruvate kinase, but this published claim awaits experimental verification.

Kinetics and Allosteric Effectors

All mammalian pyruvate kinase isoforms exhibit similar kinetic parameters for their ADP substrate, but they differ in their kinetics and allosteric regulation with respect to PEP (see Appendix B of this thesis). ADP is bound non-cooperatively and with high affinity by all pyruvate kinase isoforms, and this binding is generally insensitive to allosteric effectors. Most regulation of pyruvate kinase activity occurs via changes in PEP binding affinity. In the absence of allosteric activators, the PKM2, PKL, and PKR tetramers have low affinity for PEP and exhibit positive cooperativity of PEP binding. Binding of PEP at the active site of one subunit in the tetramer induces conformational changes in the other subunits, thus increasing their affinity for PEP. The affinity of the enzyme for PEP at low PEP concentrations can be greatly increased by binding of fructose-1,6-bisphosphate (FBP), which is an upstream glycolytic intermediate and the major allosteric activator of pyruvate kinase (Taylor & Bailey, 1967; Koler & Vanbellinghen, 1968). Each PKM2, PKL, and PKR subunit contains one binding site that is specific for FBP and distinct from the active site; FBP binding acts at a distance to increase PEP binding affinity and stabilizes the PKM2, PKL, or PKR tetramer in the active R-state. The fourth isoform, PKM1, does not bind FBP due to structural differences at the FBP binding pocket (Dombrauckas et al, 2005);

however, the PKM1 isoform naturally exists as a stable, active tetramer which is insensitive to most of the allosteric effectors that act on PKM2, PKR, and PKL (Morgan et al, 2013). Constitutively-active PKM1 and FBP-activated PKM2 have almost identical kinetic parameters (Ibsen et al, 1981), and are locked into the same three-dimensional conformation (Morgan et al, 2013), with the only structural differences occurring in areas of the protein that are encoded by isoform-specific exons: the FBP binding site and dimer-dimer interface.

PKM2 activity is affected by a long list of allosteric effectors, which includes amino acids and other small molecules and metabolites (Eigenbrodt et al, 1992; Mazurek, 2011; Morgan et al, 2013). The kinetic effects and physiological relevance of many of these effectors are not well described; however, some of the best-studied allosteric activators and inhibitors are discussed below.

The allosteric inhibitor phenylalanine (Phe) reduces activity of both PKM1 and PKM2 by decreasing affinity of the enzyme for PEP (Vijayvargiya et al, 1969; Weber, 1969; Carminatti et al, 1971). The Phe binding site is distinct from both the active site and the FBP binding site (Williams et al, 2006), and FBP can only partially activate Phe-bound PKM2 (Kung et al, 2012). Crystallographic work shows that Phe binding stabilizes the tetramer in an inactive T-state, where the active site cleft is held in an open conformation(Morgan et al, 2013). Phe binding thus does not oppose the tetramer-forming activity of FBP, but acts to push the tetramer into a less-active state. This tetramer-stabilizing effect of Phe is demonstrated by greater resistance of Phe-bound PKM1 to chaotropic denaturation (Consler & Lee, 1988).

The phenylalanine binding site can also be occupied by alanine (Williams et al, 2006), which, in the case of PKM2 but not PKM1, can also act as an allosteric inhibitor (Morgan et al, 2013). In contrast to inhibition by phenylalanine, alanine inhibition appears to favor dissociation of PKM2 to a dimeric form, and this inhibition can be fully overcome by FBP(Sparmann et al, 1973; Schulz et al, 1975).

Serine binds in the same pocket as alanine and phenylalanine, but serine acts as an allosteric activator of PKM2 (Ibsen & Marles, 1976; Eigenbrodt et al, 1983) with a reported AC_{50} of 1.3 mM (Chaneton et al, 2012). Serine and alanine compete with phenylalanine for binding to PKM1 (Williams et al, 2006), but the effect of combinations of these allosteric effectors on PKM2 has not been explored.

The thyroid hormone triiodo-L-thyronine (T3) is an allosteric inhibitor of PKM2; it binds to the monomeric form of PKM2 and stabilizes the enzyme in its inactive, monomeric state (Ashizawa et al, 1991; Morgan et al, 2013). PKM2 inactivation by T3 is overcome in the presence of FBP, as FBP binding favors tetramerization of the enzyme. The ability of T3 to bind to PKM2 was discovered when a 58 kD thyroid-binding protein was cloned and determined to be PKM2 (Ashizawa et al, 1991). Additional work suggests that T3 has a similar inhibitory effect on PKR (Fanjul & Farias, 1993). The binding location of T3 is unknown and might be revealed by crystallographic studies; however, it is unknown if crystals of monomeric PKM2 can be obtained because high enzyme concentration favors tetramer formation.

More recent reports have shown that PKM2 is activated by succinylaminoimidazolecarboxamide ribose-5' phosphate (SAICAR), which is an intermediate metabolite in the *de novo* purine synthesis pathway (Keller et al, 2012).

Activation of PKM2 by SAICAR was originally reported to occur during glucose starvation. The action of SAICAR is specific to PKM2, as SAICAR does not activate PKM1, PKL or PKR. The reported EC_{50} for SAICAR activation of PKM2 is 300 μM; however, *in vitro* phosphorylation of PKM2 by ERK1/2 significantly increases affinity of PKM2 for SAICAR and lowers the SAICAR EC_{50} to 12 μM (Keller et al, 2014). ERK-dependent phosphorylation is reported to occur on PKM2 S37 (Yang et al, 2012b), but the SAICAR binding site and the conformational effects of phosphorylation on PKM2 S37 are unknown. ERK-dependent SAICAR activation is reported to occur during normal growth conditions, where it is posited to be important for sustained proliferative signaling via a novel protein kinase activity of PKM2 (Keller et al, 2014). This non-canonical activity of PKM2 is discussed in a later section.

Efforts to develop small molecule modulators of PKM2 have resulted in effective allosteric activators of the enzyme (Boxer et al, 2010; Jiang et al, 2010; Walsh et al, 2011; Kung et al, 2012; Parnell et al, 2013). These activators all have EC_{50} values in the low nanomolar range. Structures of PKM2 crystalized with bound activator show that these activators bind at a novel binding site at the subunit interface of the tetramer (Anastasiou et al, 2012; Kung et al, 2012; Parnell et al, 2013); the first of these studies is presented in the next chapter. There are thus two activator binding sites per tetramer, but the endogenous ligand that occupies this site, if any, is unknown. This binding modality differs from that reported for a set of small molecule activators that target yeast pyruvate kinase; the activators of the yeast enzyme are predicted to bind in the FBP binding pocket (Bond et al, 2000). The effect of the PKM2 activators on yeast pyruvate kinase is unknown.

Additional common metabolites have been reported to activate or inactivate PKM2 *in vitro* when present at a concentration of 1 mM (Morgan et al, 2013). These activators include histidine, maleic acid, tartaric acid, and malic acid, and additional inhibitors include tryptophan, oxalic acid, and ribose-5-phosphate. Of these inhibitors, oxalate is well-studied as a PEP mimetic. At high levels, oxalate inhibits both PKM1 and PKM2 by competing with PEP for binding in the active site. At sub-saturating PEP concentrations, oxalate can activate the enzyme by contributing to substrate-binding-induced allosteric activation of the enzyme (Dombrauckas et al, 2005). While many compounds have been shown to have an effect on PKM2 activity, most of them have only modest effects at high concentrations and are not likely to be important for the physiological regulation of PKM2.

Regulation of PKM2 Activity by Intracellular Signaling

In addition to being regulated by allosteric effectors, the activity of mammalian PKM2 is also affected by intracellular signaling (Figure 6). PKM2 activity can be reduced as a consequence of phosphotyrosine growth signaling in the cell (Christofk et al, 2008b;

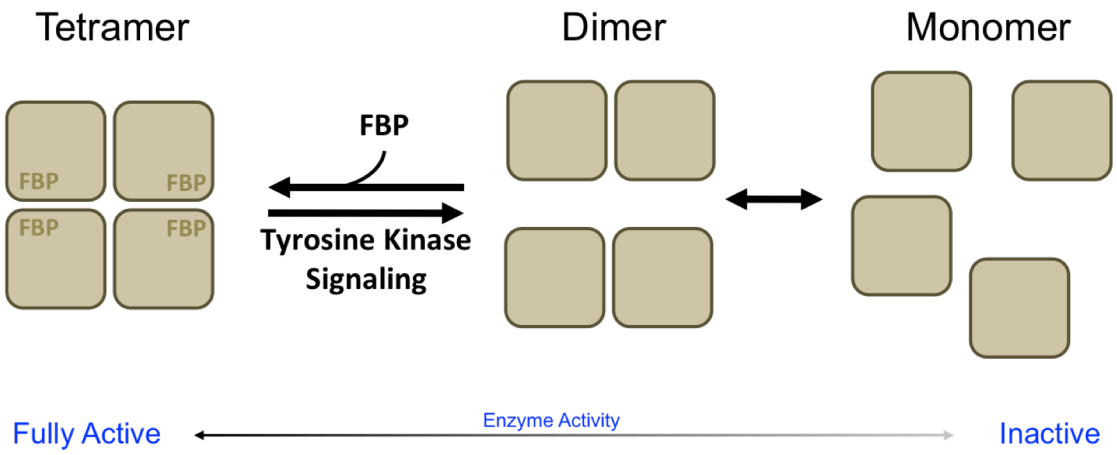

Figure 6. PKM2 Tetramer Stability is Affected by FBP Binding and Intracellular Signaling. PKM2 exists in a tetramer-dimer-monomer equilibrium. FBP binding favors PKM2 tetramer formation and activation. Interaction of PKM2 with tyrosine-phosphorylated proteins induces FBP release and allows dissociation and inactivation of the enzyme.

Varghese et al, 2010). A reduction in PKM2 activity occurs when FBP-bound PKM2 interacts with other proteins that are phosphorylated on tyrosine residues; this interaction causes PKM2 to release bound FBP (Figure 6). The phosphorylated protein inducing FBP release can be PKM2 itself (Hitosugi et al, 2009), or any other protein with a phosphorylated tyrosine in a degenerate context that is a predicted target of many growth factor signaling proteins (Christofk et al, 2008b). The interactions of PKM2 with negatively-charged phosphotyrosine depend on K433, a positively-charged amino acid located at the FBP binding site (Christofk et al, 2008b). Crystal structures of FBP-bound PKM2 show that the side chain of K433 interacts directly with a phosphate group of bound FBP (Dombrauckas et al, 2005). The presence of a protein containing phosphotyrosine, but not unmodified tyrosine, appears to cause FBP release in a phosphate-dependent manner, presumably by interfering with the PKM2-FBP interaction (Christofk et al, 2008b). This interference is reciprocal, as the ability of PKM2 to bind to a phosphotyrosine column was disrupted in a dose-dependent manner when the protein had been incubated with increasing concentrations of FBP. A K433E substitution is reported to disallow phosphotyrosine peptide binding and FBP release but not affect FBP binding (Christofk et al, 2008b). A peptide containing phosphotyrosine was shown to bind to PKM2 by fluorescence polarization; this binding could be outcompeted by high levels of FBP, suggesting that FBP and phosphotyrosine peptides may bind competitively (Allali-Hassani et al, 2009). *In vivo* interactions between PKM2 and other proteins that are phosphorylated on tyrosine residues are likely transient, as a dominant phosphorylated binding partner has not been reported outside of specific situations.

PKM2 is subject to direct phosphorylation on tyrosine residues, including Y105, allowing phosphorylated PKM2 to play a role in inactivating other PKM2 tetramers by stimulating FBP release (Hitosugi et al, 2009). PKM2 is also subject to additional post-translational modifications that directly affect activity of the enzyme. Acetylation of PKM2 K305 occurs under nutrient-replete conditions and reduces pyruvate kinase activity by both lowering affinity for PEP and triggering degradation of the enzyme itself (Lv et al, 2011). PKM2 activity is reduced by oxidation of C358 as a consequence of reactive oxygen species in the cell (Anastasiou et al, 2011), and additional modifications, such as prolyl-hydroxylation, have been reported (Luo et al, 2011).

Tissue Distribution and Function of Pyruvate Kinase Isoforms

Most mammalian tissues express PKM2, with the other three isoforms being found only in specialized tissues (Imamura & Tanaka, 1972; Strandholm et al, 1976; Cardenas & Dyson, 1978). PKM1 is found in muscle, heart, and the brain. PKL is the major isoform in the liver and the minor isoform in the kidney, which also expresses PKM2. PKR is found exclusively in red blood cells. PKM2 is the embryonic isoform, but PKM2 is replaced by the other isoforms in specific tissues during development. This isoform switch can also be observed *in vitro*; C2C12 cells switch isoforms from PKM2 to PKM1 upon differentiation to myotubes (Clower et al, 2010; David et al, 2010).

The constitutively-active PKM1 isoform is found in tissues with high catabolic demand, such as muscle or neurons. Expression of the PKM1 isoform may help support rapid production of ATP via glycolysis in these tissues. The liver isoform is induced by a high-carbohydrate diet, and is responsive to FBP, which allows feed-forward activation of glycolysis in the fed state (Tanaka et al, 1967; Yamada & Noguchi, 1999). The liver isoform

is under tight regulatory control from hormonal signals; it is phosphorylated and inactivated by protein kinase A (PKA) during the glucagon-coordinated switch from glycolysis to gluconeogenesis (Ishibashi & Cottam, 1978; El-Maghrabi et al, 1980). This inactivation is necessary to prevent a futile cycle between pyruvate kinase, phosphoenolcarboxykinase (PEPCK) and pyruvate carboxylase (PC). The red blood cell isoform is likewise activated by FBP and inactivated by phosphorylation. Interestingly, chickens only have one pyruvate kinase gene, which, like mammals, produces PKM1 and PKM2 isoforms. The PKM2 isoform is expressed in chicken liver (Strandholm et al, 1975); however, chicken PKM2 is not phosphorylated by PKA and thus remains active during gluconeogenesis (Ochs & Harris, 1978); chickens appear to compartmentalize liver PEPCK activity in the mitochondria to help avoid futile cycles, but this raises further questions about control of chicken gluconeogenesis that are beyond the scope of this discussion.

In mammals, PKM2 is expressed in obviously proliferating cells, such as cancers, lymphocytes, and the cells of the intestinal epithelium (Imamura & Tanaka, 1972; Netzker et al, 1992), but lack of proliferation does not necessarily mean lack of PKM2 expression. For example, primary mouse embryonic fibroblasts retain PKM2 expression even upon replicative senescence (Sophia Lunt, personal communication), and many differentiated tissues, such as white adipose tissue and the lung, express PKM2 (Imamura & Tanaka, 1972; Eigenbrodt et al, 1983; Clower et al, 2010). The utility of PKM2 expression in cell types such as these is not clear, but PKM2 expression may provide some benefit to anabolic cell types. More study on the importance of PKM2 in the context of normal tissues is warranted.

Heterotetramerization of Pyruvate Kinase Isoforms

In vitro experiments showed that PKM1 and PKL are capable of forming functional heterotetramers (Cardenas & Dyson, 1973), as are PKM1 and PKM2 (Anastasiou et al, 2012). Isolation and kinetic characterization of individual PKL-PKM1 heterotetramer species showed that increasing numbers of PKM1 subunits serve to progressively stabilize the tetramer in an active conformation, as evidenced by a progressive reduction in K_m for PEP and reduction in cooperativity with respect to PEP binding (Cardenas & Dyson, 1973; Hubbard & Cardenas, 1975). The distribution of heterotetramer species obtained from these experiments is consistent with random assortment of individual PKM1 and PKL monomers into all possible heterotetramer species, which indicates a lack of binding preference between the isozymes. The high degree of conservation among vertebrate pyruvate kinase isoforms is further highlighted by the ability of chicken PKM1 to form functional heterotetramers with bovine PKL (Cardenas et al, 1975).

Characterization of the tissue distribution of pyruvate kinase isoforms revealed the presence of pyruvate kinase heterotetramers in specific situations *in vivo*. Co-expression of PKM2 and PKM1 occurs as PKM2 is replaced by PKM1 during development of skeletal muscle and the heart. PKM1-PKM2 heterotetramers are evident during this transition, which can last for several weeks in the rat; heterotetramers of PKL and PKM2 are also observed in rat and bovine fetal liver (Cardenas & Dyson, 1978). PKM1-PKM2 heterotetramers are also observed in the bovine Purkinje fibers, the great vessels, and heart valves (Strandholm et al, 1976). Other adult tissues express more than one pyruvate kinase isoform, but in most cases, heterotetramers are usually not observed, suggesting

that expression of each isoforms is restricted to a particular cell type (Cardenas & Dyson, 1978).

PKM2 AND CANCER METABOLISM

Genesis of the Field

Warburg, who first observed the metabolic alterations in cancer tissue (Warburg et al, 1924), maintained that cancer was rooted in metabolic derangement due to loss of cellular respiratory capacity (Warburg et al, 1924; Warburg, 1956). Interestingly, Crabtree demonstrated a greater range of metabolic phenotypes across a broad array of tumor types, and noted that some tumors have high respiration rates (Crabtree, 1929). These observations laid the foundation for later research on the proliferative metabolism of cancer cells, but a concrete connection between carcinogenic events and altered metabolism was not possible until the discovery of the first oncogenes, protein kinases, and intracellular signaling pathways. Eigenbrodt first speculated that PKM2 was phosphorylated and inactivated by various newly-discovered protein kinases, including the protein kinase encoded by the *src* gene found in Rous sarcoma virus (Eigenbrodt & Glossmann, 1980). Eigenbrodt also suggested that inhibition of the pyruvate kinase step in glycolysis is necessary for channeling of metabolites into the pentose phosphate pathway to support the nucleotide biosynthesis required in a rapidly dividing cell (Eigenbrodt et al, 1992). These two ideas – the connection of PKM2 to both cancer signaling and cancer metabolism – informed the field and set the stage for current work on PKM2 in the context of cancer. PKM2 garnered significant attention due to its ubiquitous expression in all cancer types, and efforts have been made to use PKM2 as a cancer biomarker (Mazurek, 2011). A direct connection between PKM2 and oncogenic signaling was made when PKM2

was shown to interact with peptides and proteins phosphorylated on tyrosine residues; this interaction causes inhibition of the enzyme and was shown to have functional importance in tumor growth (Christofk et al, 2008a; Christofk et al, 2008b). This work provided a foundation for further investigation into the metabolic needs of proliferating cells and how oncogenic signaling modulates cancer metabolism to meet those needs.

Metabolic Needs of Proliferating Cells

Proliferation imposes unique metabolic requirements on a cell that extend well beyond maintenance of homeostasis. The usual housekeeping needs of a cell include maintenance of ion gradients across the cell membrane and basal turnover of damaged proteins or organelles. These housekeeping processes are ATP consuming processes; the muscle cell or neuron is primarily engaged in catabolic metabolism to support the energy-consuming processes of life, which, in the case of the muscle cell, include mechanical work. A proliferating cell must also perform these housekeeping functions, but the proliferating cell has an additional objective: it must accumulate and organize biomass sufficient to produce a daughter cell. This biomass accumulation creates additional metabolic needs and, of necessity, requires a reorganization of intracellular metabolism.

The steps of central carbon metabolism and many metabolic functions of tissues such as muscle, heart, and liver were worked out using tissue lysates or whole tissue preparations; much of this work was done prior to the advent of mammalian tissue culture (Cori, 1974). Tissue culture, particularly the work of Harry Eagle, helped to define the minimum nutritional requirements for *in vitro* growth of cells (Eagle, 1955a; Eagle, 1955b; Eagle, 1955c; Eagle, 1955d; Eagle, 1955e; Eagle, 1956; Eagle et al, 1956), but tissue culture also brought surprises. As was remarked by Cristofalo and Kritchevsky (1966),

> The striking similarity in the metabolism of cultured cells derived from a wide variety of sources remains unexplained. It is conceivable that this similarity reflects an adaptation by populations of cells in culture, irrespective of origin, which best suits them for survival under the artificial conditions of *in vitro* growth.

Culture *in vitro* selects for cells capable of the most rapid proliferation, and in so doing, likely unveils some common characteristics of proliferative metabolism, and to some extent, an adaptation to non-physiological growth conditions. Exceptions can be made for sophisticated growth conditions that allow maintenance of the physiological function of the cells to be studied; however, transition of cells to culture results in changes to their gene expression and behavior. Loss of liver-specific gene expression by primary hepatocytes after only 24 hours in culture provides one such example (Clayton & Darnell, 1983).

Much like Warburg's aerobic glycolysis, cells grown in culture often exhibit high glucose consumption and high lactate production. This behavior, common to most proliferating cells *in vivo* and *in vitro*, has been proposed to be important for supporting biosynthetic metabolism (Vander Heiden et al, 2009). A proliferating cell must provide nucleotide precursors for DNA replication and generation of ribosomal RNA, lipids for new membranes, glucose carbon for protein glycosylation, as well as amino acids and other cellular building blocks (Lunt & Vander Heiden, 2011). Generating and assembling these building blocks requires ATP; but biosynthesis also requires carbon and nitrogen precursors and the reducing equivalents necessary to process them. *De novo* lipid synthesis in particular requires significant expenditure of reducing power in the form of NADPH. Proliferative metabolism thus requires a shift away from the textbook model of

ATP production via glucose-fueled oxidative phosphorylation. Anabolic metabolism stereotypically requires shunting of glucose carbon from glycolysis to biosynthetic pathways, the excretion of most glucose carbons as lactate, and the consumption of glutamine or other nutrients as anaplerotic substrates of the TCA cycle.

Glucose carbon is used in many biosynthetic pathways during proliferation. The pentose phosphate pathway (PPP) produces ribose-5-phosphate and phosphoribosyl pyrophosphate (PRPP), which is used for *de novo* nucleotide biosynthesis. The PPP also generates reducing equivalents in the form of NADPH. Glucose carbon is also shunted from glycolysis to serine and glycine biosynthesis via glyceraldehyde-3-phosphate, and dihydroxyacetone phosphate is used to make glycerol-3-phosphate which can be further processed for use as the three carbon unit of lipid head groups.

The excretion of more than 80% of glucose carbons as lactate appears wasteful, but greatly-increased glucose consumption appears to be important to allow control of flux through branch-points, especially relatively low-flux branches such as the PPP (Newsholme et al, 1985). The conversion of pyruvate to lactate is coupled to the oxidation of NADH to NAD^+, which is required for continued glycolytic flux through the GAPDH step. Inhibition of lactate dehydrogenase, which catalyzes the aforementioned reaction, results in decreased glycolytic rates (Yamagata et al, 1998). This is likely due to the inability of the mitochondria to accept reducing equivalents from the cytosol quickly enough to regenerate the NAD^+ necessary to support rapid glycolysis. The aerobic glycolysis phenotype thus appears to be required to allow the rapid glucose consumption and lactate production that are needed to allow proper control of biosynthetic pathways including the PPP.

PKM2 Facilitates Anabolic Metabolism

Early work showed that various rat tumors express PKM2, including hepatomas (Imamura & Tanaka, 1972; Imamura et al, 1972). Because the liver normally expresses PKL, this work showed that there is a switch of expression from PKL to PKM2 in the hepatomas. Additional work relying on immunostains of tumor tissue found PKM2 expression in a wide variety of cancer types (Reinacher & Eigenbrodt, 1981; Mazurek, 2011). PKM2 appears to be expressed in all proliferating cell types, including the embryo, normal proliferating cells such as the intestinal lining, tumor cells, and cells proliferating in culture (Mazurek, 2011). Various reasons for PKM2 expression in proliferating cells have been proposed, and these reasons can be coarsely divided into two groups. The first is based on the contribution of PKM2 regulation to controlling intracellular metabolism. The second group is contained in a body of more recent literature that ascribes a variety of novel, non-metabolic functions to PKM2. These non-canonical functions of PKM2 will be discussed in a later section.

One of the original ideas put forth to explain the role of PKM2 in proliferative metabolism was based on the idea that PKM2 activity is down-regulated by oncogenic signaling (Eigenbrodt & Glossmann, 1980). The importance of PKM2 to cancer metabolism was attributed to its ability to control the final step of glycolysis. Thus, up-regulation of enzymes committing glucose to glycolysis, along with down-regulation of PKM2 activity, was thought to allow the accumulation of phosphorylated glycolytic intermediates, which were then available to spill into branching biosynthetic pathways (Eigenbrodt et al, 1992). Interestingly, experiments conducted with a large variety of cell types in culture suggest that the ratio of pyruvate kinase activity to phosphofructokinase (PFK) activity is >20 in

neoplastic cells (Board et al, 1990); this finding suggests that the expansion of metabolites may not be due to a bottleneck at the pyruvate kinase step. Modern metabolite measurements have not detected significant changes in the pool sizes of glycolytic intermediates (Anastasiou et al, 2012). It is worth noting that changes in pool sizes do not necessarily correlate with obvious changes in metabolic fluxes, as became evident during the development of the field of Metabolic Control Analysis (Kacser & Burns, 1973; Heinrich & Rapoport, 1974b; Heinrich & Rapoport, 1974a).

The metabolic function of PKM2 has been highlighted by experiments using human lung cancer cell lines (H1299 & A549) that have been engineered to express PKM1 in the place of PKM2. PKM1-expressing cells showed increased oxygen consumption and decreased lactate production, deficiency in growth at 0.5% oxygen, and a reduced capability to form xenograft tumors in immunocompromised mice (Christofk et al, 2008a). These experiments demonstrated global metabolic changes in cellular metabolism. The phosphotyrosine-insensitive K433E mutant was unable to rescue the effects of knockdown of endogenous PKM2 on cell proliferation or synthesis of lipids from glucose (Christofk et al, 2008b), suggesting that the phosphotyrosine-binding activity of the enzyme – and subsequent down-regulation of pyruvate kinase enzymatic activity – is important for proliferative metabolism. Additional experiments have shown that PKM2 is important for regulating the redox status of proliferating cells by favoring oxidative PPP flux (Anastasiou et al, 2011). In this case, down-regulation of PKM2 activity due to oxidation of C358 results in a rewiring of metabolism to deal with oxidative stress. Experiments with small molecule activators of PKM2 showed that artificially increasing intracellular pyruvate kinase activity has an anti-proliferative effect (Anastasiou et al, 2012; Kung et al, 2012; Parnell et al,

2013). The same effect is seen as a consequence of exogenous PKM1 expression (Anastasiou et al, 2012; Israelsen et al, 2013); the effects of PKM1 expression and PKM2 activation appear to be due to disruption of anabolic metabolism.

Non-canonical Pyruvate Kinase Functions

Recent work has reported multiple non-metabolic functions for pyruvate kinase, most of which require translocation of PKM2 into the nucleus, where it is postulated to be involved in control of gene expression or other signaling. These functions are based on interactions between PKM2 and other proteins. Although FBP release is mediated by interaction of the enzyme with other proteins that are phosphorylated by tyrosine (Christofk et al, 2008b), a dominant binding partner has not been determined for this interaction. Given the response of the protein to a range of phosphorylated motifs, there may not be a specific phosphorylated interaction partner responsible for mediating phosphotyrosine-dependent FBP release.

PKM2 appears capable of additional protein-protein interactions. PKM2, but not PKM1, was reported to directly associate with the HIF1α transcription factor (Luo et al, 2011). PKM2 binding transactivates HIF1α, and this activity is regulated by prolyl-hydroxylation of P403 and P408, residues that are encoded by the PKM2-specific exon 10.

PKM2 was reported to act as a protein kinase in signal transduction by phosphorylating and activating the transcription factor STAT3 (Gao et al, 2012). A constitutive-dimer mutant, PKM2 K399E, was shown to have increased protein kinase activity. The reported phosphate donor for this protein kinase activity is PEP; this implies that the PKM2 dimer (or perhaps monomer) is capable of adopting a conformation different from that of the tetramer, where the enzyme is capable of binding both PEP and a

protein substrate. This would likely require significant movement of the B domain to make the bound PEP accessible to a protein substrate, as the active site is buried deep in a cleft between the A and B domains. Other eukaryotic PEP-depended protein kinases have not been reported; however, bacteria use the phosphotransferase system (PTS), to transfer the phosphate from PEP to hexose via a several phosphoprotein intermediates (Kundig et al, 1964; Postma & Lengeler, 1985). This system is used to phosphorylate hexoses and trap them in the cell. The phosphate is transferred from PEP to a histidine residue on Enzyme I of the system; Enzyme I then transfers the phosphate to a histidine on the protein HPr, which then, in turn, transfers the phosphate to an additional enzyme which can then phosphorylate the target sugar. The PTS differs from the proposed PKM2 mechanism in that it involves phosphoenzyme intermediates, while the essentially uncharacterized protein kinase activity of PKM2 is presumed to involve direct transfer of phosphate from PEP to its various protein substrates.

PKM2 was subsequently reported to be translocated to the nucleus in response to EGFR activation. Once in the nucleus, PKM2 binds to and transactivates β-catenin through interactions involving PKM2 K433, which is found at the PKM2 FBP binding site (Yang et al, 2011). This ultimately results in cyclin D1 expression which drives progression through the cell cycle. PKM2 was then shown to bind to and phosphorylate histone H3 as a consequence of EGF signaling; PKM2-dependent histone H3 phosphorylation results in epigenetic changes and is necessary for cyclin D1 and c-Myc expression, which help drive the cell cycle and tumorigenesis in glioblastoma cells (Yang et al, 2012a). Further work by the same group investigated the mechanism of EGF-induced PKM2 nuclear localization (Yang et al, 2012b). Following EGFR activation PKM2 is bound to and phosphorylated on

S37 by ERK. ERK apparently binds to PKM2 via the PKM2 residues I429 and L431, as mutation of these residues to arginine abolishes ERK-dependent phosphorylation of PKM2 on S37. Interestingly, these two resides lie in the hydrophobic interior of the protein. If the reported mechanism is correct, a refolding of PKM2 must occur to allow ERK binding; this rearrangement of secondary/tertiary structure would also reorient the side chain of S37, which is not solvent exposed, to allow access by ERK. Once phosphorylated on S37, PKM2 is then recognized by PIN1, a prolyl isomerase, which causes the cis-trans isomerization of P38 on PKM2. This, in turn, allows recognition of PKM2 by importin α5 and its subsequent nuclear localization.

PKM2 was also further shown to play a role proper mitotic progression and chromosome segregation (Jiang et al, 2014). Here, PKM2 binds to the spindle checkpoint protein Bub3 and phosphorylates it on Y207; this function of PKM2 facilitations proper progression through the cell cycle. Pyruvate kinase dependent Bub3 phosphorylation appears to be a late-evolving mechanism, as this mechanism of cell cycle regulation is not found in *S. cerevisiae*.

The molecular mechanism underlying the protein kinase activity of PKM2 is unknown, as are the factors regulating the choice of substrate (i.e., ADP vs. protein). The metabolite SAICAR, which was shown to activate the pyruvate kinase activity of PKM2, was reported to also activate the protein kinase activity of PKM2 (Keller et al, 2014). Interestingly, SAICAR also activates both activities of the R399E mutant, suggesting that the protein and pyruvate kinase activities are linked, or perhaps somehow both activated by the same mechanisms. Unfortunately, the SAICAR binding site and mode of binding remain unknown. The protein kinase activity of PKM2 is inhibited by ADP, presumably in a

competitive manner (Yang et al, 2012a; Keller et al, 2014), and the conclusion drawn by those workers is that ADP and the target proteins compete for binding at the active site.

The PKM2 active site thus appears to accommodate binding of PEP (the phosphate donor) and multiple phosphate acceptors: the metabolite ADP, and multiple protein substrates with both threonine and tyrosine target residues. Published targets include histone H3 T11 (Yang et al, 2012a), STAT3 Y705 (Gao et al, 2012), BUB3 Y207 (Jiang et al, 2014), and ERK1, with T202 being the likely residue (Keller et al, 2014); additionally, 149 proteins were identified as potential substrates, with 91 of these being protein kinases themselves (Keller et al, 2014). How the enzyme maintains selectivity among nucleotide-diphosphate substrates while accepting a wide variety of protein substrates at the same site is not clear. Pyruvate kinase is highly selective among the nucleotides, with data from PKM1 showing a greater than four-fold selectivity of ADP over GDP, and minimal activity in the presence of other potential substrates (e.g., IDP, UDP, CDP, dADP) (Plowman & Krall, 1965; Hohnadel & Cooper, 1973; Petrescu et al, 1979). The nucleotide-diphosphate selectivity of PKM2 has been less well characterized but appears to be the same as PKM1 (Mazurek et al, 1998).

SUMMARY

Of the four mammalian isoforms, PKM2 is most closely associated with proliferation. PKM2 is expressed in the developing embryo, in proliferative tissues in the adult, and in cancer cells, but a full picture of the benefit provided by PKM2 to the proliferating cell has yet to be painted. PKM2 catalyzes the final step of glycolysis, and its enzymatic activity is regulated by allosteric effectors and intracellular signaling. Novel, non-canonical functions of PKM2 have also been reported over the last few years; nuclear PKM2 is reported to

affect gene expression by engaging in protein-protein interactions, and PKM2 is also reported to act as a dual-specificity protein kinase by transferring phosphate from PEP to threonine or tyrosine residues on target proteins.

The work reported in this thesis seeks to determine how the regulation of pyruvate kinase activity affects proliferative metabolism, whether the PKM2 isoform is required for tumor initiation and growth, and how PKM2 mutations found in human tumors affect enzyme function.

REFERENCES

Ainsworth S, MacFarlane N (1973) A kinetic study of rabbit muscle pyruvate kinase. *Biochem J* 131**:** 223-236

Allali-Hassani A, Wasney GA, Chau I, Hong BS, Senisterra G, Loppnau P, Shi Z, Moult J, Edwards AM, Arrowsmith CH, Park HW, Schapira M, Vedadi M (2009) A survey of proteins encoded by non-synonymous single nucleotide polymorphisms reveals a significant fraction with altered stability and activity. *Biochem J* 424**:** 15-26

Anastasiou D, Poulogiannis G, Asara JM, Boxer MB, Jiang JK, Shen M, Bellinger G, Sasaki AT, Locasale JW, Auld DS, Thomas CJ, Vander Heiden MG, Cantley LC (2011) Inhibition of pyruvate kinase M2 by reactive oxygen species contributes to cellular antioxidant responses. *Science* 334**:** 1278-1283

Anastasiou D, Yu Y, Israelsen WJ, Jiang JK, Boxer MB, Hong BS, Tempel W, Dimov S, Shen M, Jha A, Yang H, Mattaini KR, Metallo CM, Fiske BP, Courtney KD, Malstrom S, Khan TM, Kung C, Skoumbourdis AP, Veith H, Southall N, Walsh MJ, Brimacombe KR, Leister W, Lunt SY, Johnson ZR, Yen KE, Kunii K, Davidson SM, Christofk HR, Austin CP, Inglese J, Harris MH, Asara JM, Stephanopoulos G, Salituro FG, Jin S, Dang L, Auld DS, Park HW, Cantley LC, Thomas CJ, Vander Heiden MG (2012) Pyruvate kinase M2 activators promote tetramer formation and suppress tumorigenesis. *Nat Chem Biol* 8**:** 839-847

Ashizawa K, McPhie P, Lin KH, Cheng SY (1991) An in vitro novel mechanism of regulating the activity of pyruvate kinase M2 by thyroid hormone and fructose 1, 6-bisphosphate. *Biochemistry* 30**:** 7105-7111

Banner DW, Bloomer AC, Petsko GA, Phillips DC, Pogson CI, Wilson IA, Corran PH, Furth AJ, Milman JD, Offord RE, Priddle JD, Waley SG (1975) Structure of chicken muscle triose phosphate isomerase determined crystallographically at 2.5 angstrom resolution using amino acid sequence data. *Nature* 255**:** 609-614

Board M, Humm S, Newsholme EA (1990) Maximum activities of key enzymes of glycolysis, glutaminolysis, pentose phosphate pathway and tricarboxylic acid cycle in normal, neoplastic and suppressed cells. *Biochem J* 265**:** 503-509

Bollenbach TJ, Mesecar AD, Nowak T (1999) Role of lysine 240 in the mechanism of yeast pyruvate kinase catalysis. *Biochemistry* 38**:** 9137-9145

Bond CJ, Jurica MS, Mesecar A, Stoddard BL (2000) Determinants of allosteric activation of yeast pyruvate kinase and identification of novel effectors using computational screening. *Biochemistry* 39**:** 15333-15343

Boxer MB, Jiang JK, Vander Heiden MG, Shen M, Skoumbourdis AP, Southall N, Veith H, Leister W, Austin CP, Park HW, Inglese J, Cantley LC, Auld DS, Thomas CJ (2010) Evaluation of substituted N,N'-diarylsulfonamides as activators of the tumor cell specific M2 isoform of pyruvate kinase. *J Med Chem* 53**:** 1048-1055

Boyer PD, Lardy HA, Phillips PH (1942) The role of potassium in muscle phosphorylations. *J Biol Chem* 146**:** 673–682

Bücher T, Pfleiderer G (1955) Pyruvate kinase from muscle: Pyruvate phosphokinase, pyruvic phosphoferase, phosphopyruvate transphosphorylase, phosphate—transferring enzyme II, etc. Phosphoenolpyruvate+ ADP⇌ Pyruvate+ ATP. *Methods Enzymol* 1**:** 435–440

Cardenas JM, Dyson RD (1973) Bovine pyruvate kinases. II. Purification of the liver isozyme and its hybridization with skeletal muscle pyruvate kinase. *J Biol Chem* 248**:** 6938-6944

Cardenas JM, Blachly EG, Ceccotti PL, Dyson RD (1975) Properties of chicken skeletal muscle pyruvate kinase and a proposal for its evolutionary relationship to the other avian and mammalian isozymes. *Biochemistry* 14**:** 2247-2252

Cardenas JM, Dyson RD (1978) Mammalian pyruvate kinase hybrid isozymes: tissue distribution and physiological significance. *J Exp Zool* 204**:** 361-367

Carminatti H, Jimenez de Asua L, Leiderman B, Rozengurt E (1971) Allosteric properties of skeletal muscle pyruvate kinase. *J Biol Chem* 246**:** 7284-7288

Chaneton B, Hillmann P, Zheng L, Martin AC, Maddocks OD, Chokkathukalam A, Coyle JE, Jankevics A, Holding FP, Vousden KH, Frezza C, O'Reilly M, Gottlieb E (2012) Serine is a natural ligand and allosteric activator of pyruvate kinase M2. *Nature* 491**:** 458-462

Chen M, David CJ, Manley JL (2012) Concentration-dependent control of pyruvate kinase M mutually exclusive splicing by hnRNP proteins. *Nat Struct Mol Biol* 19**:** 346-354

Christofk HR, Vander Heiden MG, Harris MH, Ramanathan A, Gerszten RE, Wei R, Fleming MD, Schreiber SL, Cantley LC (2008a) The M2 splice isoform of pyruvate kinase is important for cancer metabolism and tumour growth. *Nature* 452**:** 230-233

Christofk HR, Vander Heiden MG, Wu N, Asara JM, Cantley LC (2008b) Pyruvate kinase M2 is a phosphotyrosine-binding protein. *Nature* 452**:** 181-186

Clayton DF, Darnell JE, Jr. (1983) Changes in liver-specific compared to common gene transcription during primary culture of mouse hepatocytes. *Mol Cell Biol* 3**:** 1552-1561

Clower CV, Chatterjee D, Wang Z, Cantley LC, Vander Heiden MG, Krainer AR (2010) The alternative splicing repressors hnRNP A1/A2 and PTB influence pyruvate kinase isoform expression and cell metabolism. *Proc Natl Acad Sci U S A* 107**:** 1894-1899

Consler TG, Lee JC (1988) Domain interaction in rabbit muscle pyruvate kinase. I. Effects of ligands on protein denaturation induced by guanidine hydrochloride. *J Biol Chem* 263**:** 2787-2793

Cori CF (1974) Some highlights of the early period of bioenergetics. *Mol Cell Biochem* 5**:** 47-53

Cottam GL, Hollenberg PF, Coon MJ (1969) Subunit structure of rabbit muscle pyruvate kinase. *J Biol Chem* 244**:** 1481-1486

Crabtree HG (1929) Observations on the carbohydrate metabolism of tumours. *Biochem J* 23**:** 536-545

Cristofalo VJ, Kritchevsky D (1966) Respiration and glycolysis in the human diploid cell strain WI-38. *J Cell Physiol* 67**:** 125-132

David CJ, Chen M, Assanah M, Canoll P, Manley JL (2010) HnRNP proteins controlled by c-Myc deregulate pyruvate kinase mRNA splicing in cancer. *Nature* 463**:** 364-368

Dombrauckas JD, Santarsiero BD, Mesecar AD (2005) Structural basis for tumor pyruvate kinase M2 allosteric regulation and catalysis. *Biochemistry* 44**:** 9417-9429

Eagle H (1955a) The specific amino acid requirements of a mammalian cell (strain L) in tissue culture. *J Biol Chem* 214**:** 839-852

Eagle H (1955b) The specific amino acid requirements of a human carcinoma cell (strain HeLa) in tissue culture. *J Exp Med* 102**:** 37-48

Eagle H (1955c) The growth requirements of two mammalian cell lines in tissue culture. *Trans Assoc Am Physicians* 68**:** 78-81

Eagle H (1955d) Nutrition needs of mammalian cells in tissue culture. *Science* 122**:** 501-514

Eagle H (1955e) The minimum vitamin requirements of the L and HeLa cells in tissue culture, the production of specific vitamin deficiencies, and their cure. *J Exp Med* 102**:** 595-600

Eagle H (1956) The salt requirements of mammalian cells in tissue culture. *Arch Biochem Biophys* 61**:** 356-366

Eagle H, Oyama VI, Levy M, Horton CL, Fleischman R (1956) The growth response of mammalian cells in tissue culture to L-glutamine and L-glutamic acid. *J Biol Chem* 218**:** 607-616

Eigenbrodt E, Glossmann H (1980) Glycolysis - one of the keys to cancer? *Trends Pharmacol Sci* 1**:** 240-245

Eigenbrodt E, Leib S, Kramer W, Friis RR, Schoner W (1983) Structural and kinetic differences between the M2 type pyruvate kinases from lung and various tumors. *Biomed Biochim Acta* 42**:** S278-282

Eigenbrodt E, Reinacher M, Scheefers-Borchel U, Scheefers H, Friis R (1992) Double role for pyruvate kinase type M2 in the expansion of phosphometabolite pools found in tumor cells. *Crit Rev Oncog* 3**:** 91-115

El-Maghrabi MR, Haston WS, Flockhart DA, Claus TH, Pilkis SJ (1980) Studies on the phosphorylation and dephosphorylation of L-type pyruvate kinase by the catalytic subunit of cyclic AMP-dependent protein kinase. *J Biol Chem* 255**:** 668-675

Embden G, Deuticke HJ, Kraft G (1933) Über die Intermediären Vorgänge bei der Glykolyse in der Muskulatur. *Klin Wochenschr* 12**:** 213-215

Fanjul AN, Farias RN (1993) Cold-sensitive cytosolic 3,5,3'-triiodo-L-thyronine-binding protein and pyruvate kinase from human erythrocytes share similar regulatory properties of hormone binding by glycolytic intermediates. *J Biol Chem* 268**:** 175-179

Gao X, Wang H, Yang JJ, Liu X, Liu ZR (2012) Pyruvate kinase M2 regulates gene transcription by acting as a protein kinase. *Mol Cell* 45**:** 598-609

Gupta RK, Oesterling RM (1976) Dual divalent cation requirement for activation of pyruvate kinase; essential roles of both enzyme- and nucleotide-bound metal ions. *Biochemistry* 15**:** 2881-2887

Heinrich R, Rapoport TA (1974a) A linear steady-state treatment of enzymatic chains. Critique of the crossover theorem and a general procedure to identify interaction sites with an effector. *Eur J Biochem* 42**:** 97-105

Heinrich R, Rapoport TA (1974b) A linear steady-state treatment of enzymatic chains. General properties, control and effector strength. *Eur J Biochem* 42**:** 89-95

Hitosugi T, Kang S, Vander Heiden MG, Chung TW, Elf S, Lythgoe K, Dong S, Lonial S, Wang X, Chen GZ, Xie J, Gu TL, Polakiewicz RD, Roesel JL, Boggon TJ, Khuri FR, Gilliland DG, Cantley LC, Kaufman J, Chen J (2009) Tyrosine phosphorylation inhibits PKM2 to promote the Warburg effect and tumor growth. *Sci Signal* 2**:** ra73

Hohnadel DC, Cooper C (1973) The effect of structural alterations on the reactivity of the nucleotide substrate of rabbit muscle pyruvate kinase. *FEBS Lett* 30**:** 18-20

Hubbard DR, Cardenas JM (1975) Kinetic properties of pyruvate kinase hybrids formed with native type L and inactivated type M subunits. *J Biol Chem* 250**:** 4931-4936

Ibsen KH, Marles SW (1976) Inhibition of chicken pyruvate kinases by amino acids. *Biochemistry* 15**:** 1073-1079

Ibsen KH (1977) Interrelationships and functions of the pyruvate kinase isozymes and their variant forms: a review. *Cancer Res* 37**:** 341-353

Ibsen KH, Chiu RH, Park HR, Sanders DA, Roy S, Garratt KN, Mueller MK (1981) Purification and properties of mouse pyruvate kinases K and M and of a modified K subunit. *Biochemistry* 20**:** 1497-1506

Imamura K, Tanaka T (1972) Multimolecular forms of pyruvate kinase from rat and other mammalian tissues. I. Electrophoretic studies. *J Biochem* 71**:** 1043-1051

Imamura K, Taniuchi K, Tanaka T (1972) Multimolecular forms of pyruvate kinase. II. Purification of M2-type pyruvate kinase from Yoshida ascites hepatoma 130 cells and comparative studies on the enzymological and immunological properties of the three types of pyruvate kinases, L, M1, and M2. *J Biochem* 72**:** 1001-1015

Imamura K, Tanaka T (1982) Pyruvate kinase isozymes from rat. *Methods Enzymol* 90 Pt E**:** 150-165

Ishibashi H, Cottam GL (1978) Glucagon-stimulated phosphorylation of pyruvate kinase in hepatocytes. *J Biol Chem* 253**:** 8767-8771

Israelsen WJ, Dayton TL, Davidson SM, Fiske BP, Hosios AM, Bellinger G, Li J, Yu Y, Sasaki M, Horner JW, Burga LN, Xie J, Jurczak MJ, DePinho RA, Clish CB, Jacks T, Kibbey RG, Wulf GM, Di Vizio D, Mills GB, Cantley LC, Vander Heiden MG (2013) PKM2 isoform-specific deletion reveals a differential requirement for pyruvate kinase in tumor cells. *Cell* 155**:** 397-409

Jiang JK, Boxer MB, Vander Heiden MG, Shen M, Skoumbourdis AP, Southall N, Veith H, Leister W, Austin CP, Park HW, Inglese J, Cantley LC, Auld DS, Thomas CJ (2010) Evaluation of thieno[3,2-b]pyrrole[3,2-d]pyridazinones as activators of the tumor cell specific M2 isoform of pyruvate kinase. *Bioorg Med Chem Lett* 20**:** 3387-3393

Jiang Y, Li X, Yang W, Hawke DH, Zheng Y, Xia Y, Aldape K, Wei C, Guo F, Chen Y, Lu Z (2014) PKM2 regulates chromosome segregation and mitosis progression of tumor cells. *Mol Cell* 53**:** 75-87

Johnson FM, Chasalow F, Anderson G, Macdougal P, Hendren RW, Lewis SE (1981) A variation in mouse kidney pyruvate kinase activity determined by a mutant gene on chromosome 9. *Genet Res* 37**:** 123-131

Jurica MS, Mesecar A, Heath PJ, Shi W, Nowak T, Stoddard BL (1998) The allosteric regulation of pyruvate kinase by fructose-1,6-bisphosphate. *Structure* 6**:** 195-210

Kacser H, Burns JA (1973) The control of flux. *Symp Soc Exp Biol* 27**:** 65-104

Keller KE, Tan IS, Lee YS (2012) SAICAR stimulates pyruvate kinase isoform M2 and promotes cancer cell survival in glucose-limited conditions. *Science* 338**:** 1069-1072

Keller KE, Doctor ZM, Dwyer ZW, Lee YS (2014) SAICAR induces protein kinase activity of PKM2 that is necessary for sustained proliferative signaling of cancer cells. *Mol Cell* 53**:** 700-709

Koler RD, Vanbellinghen P (1968) The mechanism of precursor modulation of human pyruvate kinase I by fructose diphosphate. *Adv Enzyme Regul* 6**:** 127-142

Kubowitz F, Ott P (1943) Isolierung von Gärungsfermenten aus menschlieben Muskeln. *Biochem Z* 317**:** 193-203

Kundig W, Ghosh S, Roseman S (1964) Phosphate bound to histidine in a protein as an intermediate in a novel phospho-transferase system. *Proc Natl Acad Sci U S A* 52**:** 1067-1074

Kung C, Hixon J, Choe S, Marks K, Gross S, Murphy E, DeLaBarre B, Cianchetta G, Sethumadhavan S, Wang X, Yan S, Gao Y, Fang C, Wei W, Jiang F, Wang S, Qian K, Saunders J, Driggers E, Woo HK, Kunii K, Murray S, Yang H, Yen K, Liu W, Cantley LC, Vander Heiden MG, Su SM, Jin S, Salituro FG, Dang L (2012) Small molecule activation of PKM2 in cancer cells induces serine auxotrophy. *Chem Biol* 19**:** 1187-1198

Larsen TM, Benning MM, Rayment I, Reed GH (1998) Structure of the bis(Mg2+)-ATP-oxalate complex of the rabbit muscle pyruvate kinase at 2.1 A resolution: ATP binding over a barrel. *Biochemistry* 37**:** 6247-6255

Le Mellay V, Houben R, Troppmair J, Hagemann C, Mazurek S, Frey U, Beigel J, Weber C, Benz R, Eigenbrodt E, Rapp UR (2002) Regulation of glycolysis by Raf protein serine/threonine kinases. *Adv Enzyme Regul* 42**:** 317-332

Lewis SE, Johnson FM (1983) Dominant and recessive effects of electrophoretically detected specific locus mutations. In *Utilization of Mammalian Specific Locus Studies in Hazard Evaluation and Estimation of Genetic Risk*, de Serres FJ, Sheridan W (eds), pp 267-278. New York: Plenum Press

Lohmann K, Meyerhof O (1934) Über die enzymatische Umwandlung von Phosphoglycerinsäure in Brenztraubensäure und Phosphorsäure. *Biochem Z* 273**:** 60-72

Lunt SY, Vander Heiden MG (2011) Aerobic glycolysis: meeting the metabolic requirements of cell proliferation. *Annu Rev Cell Dev Biol* 27**:** 441-464

Luo W, Hu H, Chang R, Zhong J, Knabel M, O'Meally R, Cole RN, Pandey A, Semenza GL (2011) Pyruvate kinase M2 is a PHD3-stimulated coactivator for hypoxia-inducible factor 1. *Cell* 145**:** 732-744

Lv L, Li D, Zhao D, Lin R, Chu Y, Zhang H, Zha Z, Liu Y, Li Z, Xu Y, Wang G, Huang Y, Xiong Y, Guan KL, Lei QY (2011) Acetylation targets the M2 isoform of pyruvate kinase for degradation through chaperone-mediated autophagy and promotes tumor growth. *Mol Cell* 42**:** 719-730

Mazurek S, Grimm H, Wilker S, Leib S, Eigenbrodt E (1998) Metabolic characteristics of different malignant cancer cell lines. *Anticancer Res* 18**:** 3275-3282

Mazurek S, Grimm H, Boschek CB, Vaupel P, Eigenbrodt E (2002) Pyruvate kinase type M2: a crossroad in the tumor metabolome. *Br J Nutr* 87 Suppl 1**:** S23-29

Mazurek S (2011) Pyruvate kinase type M2: a key regulator of the metabolic budget system in tumor cells. *Int J Biochem Cell Biol* 43**:** 969-980

Meyerhof O (1935) Über umkehrbare Reaktionen im Verlauf der biologischen Zuckersplatung. *Naturwissenschaften* 23**:** 490-493

Morgan HP, O'Reilly FJ, Wear MA, O'Neill JR, Fothergill-Gilmore LA, Hupp T, Walkinshaw MD (2013) M2 pyruvate kinase provides a mechanism for nutrient sensing and regulation of cell proliferation. *Proc Natl Acad Sci U S A* 110**:** 5881-5886

Muirhead H, Clayden DA, Barford D, Lorimer CG, Fothergill-Gilmore LA, Schiltz E, Schmitt W (1986) The structure of cat muscle pyruvate kinase. *EMBO J* 5**:** 475-481

Needham DM, Van Heyningen WE (1935) Linkage of chemical changes in muscle. *Nature* 135**:** 585-586

Netzker R, Greiner E, Eigenbrodt E, Noguchi T, Tanaka T, Brand K (1992) Cell cycle-associated expression of M2-type isozyme of pyruvate kinase in proliferating rat thymocytes. *J Biol Chem* 267**:** 6421-6424

Newsholme EA, Crabtree B, Ardawi MS (1985) The role of high rates of glycolysis and glutamine utilization in rapidly dividing cells. *Biosci Rep* 5**:** 393-400

Noguchi T, Tanaka T (1982) The M1 and M2 subunits of rat pyruvate kinase are encoded by different messenger RNAs. *J Biol Chem* 257**:** 1110-1113

Noguchi T, Inoue H, Tanaka T (1986) The M1- and M2-type isozymes of rat pyruvate kinase are produced from the same gene by alternative RNA splicing. *J Biol Chem* 261**:** 13807-13812

Noguchi T, Yamada K, Inoue H, Matsuda T, Tanaka T (1987) The L- and R-type isozymes of rat pyruvate kinase are produced from a single gene by use of different promoters. *J Biol Chem* 262**:** 14366-14371

Ochs RS, Harris RA (1978) Studies on the relationship between glycolysis, lipogenesis, gluconeogenesis, and pyruvate kinase activity of rat and chicken hepatocytes. *Arch Biochem Biophys* 190**:** 193-201

Parnas JK, Ostern P, Mann T (1934) Über die Verkettung der chemischen Vorgänge im Muskel. *Biochem Z* 272**:** 64-70

Parnas JK (1935) Über die Verkettung der chemischen Vorgänge im Muskel. *Klin Wochenschr* 14**:** 1017–1023

Parnell KM, Foulks JM, Nix RN, Clifford A, Bullough J, Luo B, Senina A, Vollmer D, Liu J, McCarthy V, Xu Y, Saunders M, Liu XH, Pearce S, Wright K, O'Reilly M, McCullar MV, Ho KK, Kanner SB (2013) Pharmacologic activation of PKM2 slows lung tumor xenograft growth. *Mol Cancer Ther* 12**:** 1453-1460

Peters J, Andrews SJ (1984) The Pk-3 gene determines both the heart, M1, and the kidney, M2, pyruvate kinase isozymes in the mouse; and a simple electrophoretic method for separating phosphoglucomutase-3. *Biochem Genet* 22**:** 1047-1063

Petrescu I, Bojan O, Saied M, Barzu O, Schmidt F, Kuhnle HF (1979) Determination of phosphoenolpyruvate carboxykinase activity with deoxyguanosine 5'-diphosphate as nucleotide substrate. *Anal Biochem* 96**:** 279-281

Plowman KM, Krall AR (1965) A kinetic study of nucleotide interactions with pyruvate kinase. *Biochemistry* 4**:** 2809-2814

Postma PW, Lengeler JW (1985) Phosphoenolpyruvate:carbohydrate phosphotransferase system of bacteria. *Microbiol Rev* 49**:** 232-269

Reinacher M, Eigenbrodt E (1981) Immunohistological demonstration of the same type of pyruvate kinase isoenzyme (M2-Pk) in tumors of chicken and rat. *Virchows Arch B Cell Pathol Incl Mol Pathol* 37**:** 79-88

Sakai H (2005) Mutagenesis of the active site lysine 221 of the pyruvate kinase from Bacillus stearothermophilus. *J Biochem* 137**:** 141-145

Schulz J, Sparmann G, Hofmann E (1975) Alanine-mediated reversible inactivation of tumour pyruvate kinase caused by a tetramer-dimer transition. *FEBS Lett* 50**:** 346-350

Seeholzer SH, Jaworowski A, Rose IA (1991) Enolpyruvate: chemical determination as a pyruvate kinase intermediate. *Biochemistry* 30**:** 727-732

Sparmann G, Schulz J, Hofmann E (1973) Effects of L-alanine and fructose (1,6-diphosphate) on pyruvate kinase from ehrlich ascites tumour cells. *FEBS Lett* 36**:** 305-308

Stammers DK, Muirhead H (1977) Three-dimensional structure of cat muscle pyruvate kinase at 3-1 A resolution. *J Mol Biol* 112**:** 309-316

Strandholm JJ, Cardenas JM, Dyson RD (1975) Pyruvate kinase isozymes in adult and fetal tissues of chicken. *Biochemistry* 14**:** 2242-2246

Strandholm JJ, Dyson RD, Cardenas JM (1976) Bovine pyruvate kinase isozymes and hybrid isozymes. Electrophoretic studies and tissue distribution. *Arch Biochem Biophys* 173**:** 125-131

Susan-Resiga D, Nowak T (2003) The proton transfer step catalyzed by yeast pyruvate kinase. *J Biol Chem* 278**:** 12660-12671

Susan-Resiga D, Nowak T (2004) Proton donor in yeast pyruvate kinase: chemical and kinetic properties of the active site Thr 298 to Cys mutant. *Biochemistry* 43**:** 15230-15245

Takenaka M, Noguchi T, Sadahiro S, Hirai H, Yamada K, Matsuda T, Imai E, Tanaka T (1991) Isolation and characterization of the human pyruvate kinase M gene. *Eur J Biochem* 198**:** 101-106

Tanaka T, Harano Y, Sue F, Morimura H (1967) Crystallization, characterization and metabolic regulation of two types of pyruvate kinase isolated from rat tissues. *J Biochem* 62**:** 71-91

Taylor CB, Bailey E (1967) Activation of liver pyruvate kinase by fructose 1,6-diphosphate. *Biochem J* 102**:** 32C-33C

Vander Heiden MG, Cantley LC, Thompson CB (2009) Understanding the Warburg effect: the metabolic requirements of cell proliferation. *Science* 324**:** 1029-1033

Varghese B, Swaminathan G, Plotnikov A, Tzimas C, Yang N, Rui H, Fuchs SY (2010) Prolactin inhibits activity of pyruvate kinase M2 to stimulate cell proliferation. *Mol Endocrinol* 24**:** 2356-2365

Vijayvargiya R, Schwark WS, Singhal RL (1969) Pyruvate kinase: modulation by L-phenylalanine and L-alanine. *Can J Biochem* 47**:** 895-898

Walsh MJ, Brimacombe KR, Veith H, Bougie JM, Daniel T, Leister W, Cantley LC, Israelsen WJ, Vander Heiden MG, Shen M, Auld DS, Thomas CJ, Boxer MB (2011) 2-Oxo-N-aryl-1,2,3,4-tetrahydroquinoline-6-sulfonamides as activators of the tumor cell specific M2 isoform of pyruvate kinase. *Bioorg Med Chem Lett* 21**:** 6322-6327

Wang Z, Chatterjee D, Jeon HY, Akerman M, Vander Heiden MG, Cantley LC, Krainer AR (2012a) Exon-centric regulation of pyruvate kinase M alternative splicing via mutually exclusive exons. *J Mol Cell Biol* 4**:** 79-87

Wang Z, Jeon HY, Rigo F, Bennett CF, Krainer AR (2012b) Manipulation of PK-M mutually exclusive alternative splicing by antisense oligonucleotides. *Open Biol* 2**:** 120133

Warburg O (1956) On the origin of cancer cells. *Science* 123**:** 309-314

Warburg OH, Posener K, Negelein E (1924) Über den Stoffwechsel der Carcinomzelle. *Biochem Z* 152**:** 309-344

Weber G (1969) Inhibition of human brain pyruvate kinase and hexokinase by phenylalanine and phenylpyruvate: possible relevance to phenylketonuric brain damage. *Proc Natl Acad Sci U S A* 63**:** 1365-1369

Williams R, Holyoak T, McDonald G, Gui C, Fenton AW (2006) Differentiating a ligand's chemical requirements for allosteric interactions from those for protein binding. Phenylalanine inhibition of pyruvate kinase. *Biochemistry* 45**:** 5421-5429

Yamada K, Noguchi T (1999) Nutrient and hormonal regulation of pyruvate kinase gene expression. *Biochem J* 337 (Pt 1)**:** 1-11

Yamagata M, Hasuda K, Stamato T, Tannock IF (1998) The contribution of lactic acid to acidification of tumours: studies of variant cells lacking lactate dehydrogenase. *Br J Cancer* 77**:** 1726-1731

Yang W, Xia Y, Ji H, Zheng Y, Liang J, Huang W, Gao X, Aldape K, Lu Z (2011) Nuclear PKM2 regulates beta-catenin transactivation upon EGFR activation. *Nature* 480**:** 118-122

Yang W, Xia Y, Hawke D, Li X, Liang J, Xing D, Aldape K, Hunter T, Alfred Yung WK, Lu Z (2012a) PKM2 phosphorylates histone H3 and promotes gene transcription and tumorigenesis. *Cell* 150**:** 685-696

Yang W, Zheng Y, Xia Y, Ji H, Chen X, Guo F, Lyssiotis CA, Aldape K, Cantley LC, Lu Z (2012b) ERK1/2-dependent phosphorylation and nuclear translocation of PKM2 promotes the Warburg effect. *Nat Cell Biol* 14**:** 1295-1304

CHAPTER TWO:
Pyruvate Kinase M2 Activators Promote Tetramer Formation and Suppress Tumorigenesis

Dimitrios Anastasiou[1,2*], Yimin Yu[3*], William J. Israelsen[3*], Jian-kang Jiang[4], Matthew B. Boxer[4], Bum Soo Hong[5], Wolfram Tempel[5], Svetoslav Dimov[5], Min Shen[4], Abhishek Jha[6], Hua Yang[7], Katherine R. Mattaini[3], Christian M. Metallo[8], Brian P. Fiske[3], Kevin D. Courtney[1,2,9], Scott Malstrom[3], Tahsin M. Khan[3], Charles Kung[7], Amanda P. Skoumbourdis[4], Henrike Veith[4], Noel Southall[4], Martin J. Walsh[4], Kyle R. Brimacombe[4], William Leister[4], Sophia Y. Lunt[3], Zachary R. Johnson[3], Katharine E. Yen[7], Kaiko Kunii[7], Shawn M. Davidson[3], Heather R. Christofk[1], Christopher P. Austin[4], James Inglese[4], Marian H. Harris[10], John M. Asara[1,11], Gregory Stephanopoulos[6], Francesco G. Salituro[7], Shengfang Jin[7], Lenny Dang[7], Douglas S. Auld[4], Hee-Won Park[5,12], Lewis C. Cantley[1,2], Craig J. Thomas[4], Matthew G. Vander Heiden[3,9]

1. Department of Medicine-Division of Signal Transduction, Beth Israel Deaconess Medical Center, Boston, MA 02115, USA.
2. Department of Systems Biology, Harvard Medical School, Boston, MA 02115, USA.
3. Koch Institute for Integrative Cancer Research, Massachusetts Institute of Technology Cambridge, MA 02139, USA.
4. NIH Chemical Genomics Center, National Human Genome Research Institute, National Institutes of Health, 9800 Medical Center Drive, Rockville, Maryland 20850, USA.
5. Structural Genomics Consortium, University of Toronto, Toronto, ON, M5G 1L7, Canada.
6. Department of Chemical Engineering, Massachusetts Institute of Technology, Cambridge, MA 02139, USA.
7. Agios Pharmaceuticals, Cambridge, MA 02139, USA.
8. Department of Bioengineering, University of California, San Diego, CA 92093, USA.
9. Dana-Farber Cancer Institute, Harvard Medical School, Boston, MA 02115, USA.
10. Department of Pathology, Children's Hospital, Boston, MA 02115, USA.
11. Department of Medicine, Harvard Medical School, Boston, MA 02115, USA.
12. Department of Pharmacology, University of Toronto, Toronto, ON M5G 1L7, Canada.
*These authors contributed equally to this work.

A version of chapter has been published: Pyruvate kinase M2 activators promote tetramer formation and suppress tumorigenesis. *Nat Chem Biol* (2012) 8: 839-847.

WJI assisted in planning and coordinating the study, performed or assisted with experiments presented in Figures 2, 3, 11, 15, and Table S3, and contributed to writing the manuscript. Contributions by all 43 authors are listed in a section near the end of this chapter.

ABSTRACT

Cancer cells engage in a metabolic program to enhance biosynthesis and support cell proliferation. The regulatory properties of pyruvate kinase M2 (PKM2) influence altered glucose metabolism in cancer. PKM2 interaction with phosphotyrosine-containing proteins inhibits enzyme activity and increases availability of glycolytic metabolites to support cell proliferation. This suggests that high pyruvate kinase activity may suppress tumor growth. We show that expression of PKM1, the pyruvate kinase isoform with high constitutive activity, or exposure to published small molecule PKM2 activators inhibit growth of xenograft tumors. Structural studies reveal that small molecule activators bind PKM2 at the subunit interaction interface, a site distinct from that of the endogenous activator fructose-1,6-bisphosphate (FBP). However, unlike FBP, binding of activators to PKM2 promotes a constitutively active enzyme state that is resistant to inhibition by tyrosine-phosphorylated proteins. These data support the notion that small molecule activation of PKM2 can interfere with anabolic metabolism.

INTRODUCTION

Cancer cells differ from many normal cells in the way they utilize extracellular nutrients, providing a strategy to interfere with tumor growth (Tennant et al, 2010; Vander Heiden, 2011). The increased cell proliferation that characterizes tumor growth imposes an enhanced need for biological building blocks to support production of new cells (Vander Heiden et al, 2009). To provide for this increased biosynthetic demand, cancer cells exhibit higher uptake of nutrients such as glucose. In addition, the metabolic pathways of cancer cells are altered to allow production of macromolecules and withstand oxidative stress

associated with tumorigenesis (Trachootham et al, 2009; Vander Heiden et al, 2009; Levine & Puzio-Kuter, 2010; Tennant et al, 2010; Cairns et al, 2011).

Enhanced glucose uptake is a hallmark of several cancers and is exploited in the clinic as a diagnostic tool through PET imaging of the glucose analogue ^{18}F-deoxyglucose (^{18}FDG-PET) (Weissleder, 2006). Moreover, in contrast to most normal tissues where much of the glucose is oxidized through the TCA cycle in mitochondria, cancer cells preferentially convert glucose to lactate (Vander Heiden et al, 2009). The fate of glucose inside cells is influenced by the enzymatic properties of the specific glycolytic gene products expressed. Expression of the M2 isoform of pyruvate kinase (PKM2) can contribute to the characteristic glucose metabolism of tumors and replacement of PKM2 with its splice variant PKM1 cannot efficiently support biosynthesis and tumor growth (Christofk et al, 2008a). Thus, pyruvate kinase regulates a step in glucose metabolism that can be critical for controlling cell proliferation.

Pyruvate kinase catalyzes the last step of glycolysis, transferring the phosphate from phosphoenolpyruvate (PEP) to adenosine diphosphate (ADP) to yield adenosine triphosphate (ATP) and pyruvate. In mammals, two genes encode a total of four pyruvate kinase isoforms. The *Pkrl* gene encodes the PKL and PKR isoforms, which are expressed in the liver and red blood cells respectively. Most tissues express either the PKM1 or PKM2 isoform encoded by the *Pkm* gene. PKM1 is found in many normal differentiated tissues whereas PKM2 is expressed in most proliferating cells including all cancer cell lines and tumors tested (Mazurek, 2011). PKM1 and PKM2 are derived from alternative splicing of a *Pkm* gene transcript by mutual exclusion of a single conserved exon encoding 56 amino acids (Noguchi et al, 1986; Yamada & Noguchi, 1999; Clower et al, 2010). Despite very

similar primary sequences, PKM1 and PKM2 have different catalytic and regulatory properties. PKM1 exhibits high constitutive enzymatic activity (Ikeda et al, 1997). In contrast, PKM2 is less active, but can be allosterically activated by the upstream glycolytic metabolite fructose-1,6-bisphosphate (FBP) (Ikeda & Noguchi, 1998). It has been hypothesized that FBP binding induces conformational changes that promote the association of the protein into homotetramers that comprise the most active form of the enzyme (Ashizawa et al, 1991a; Ashizawa et al, 1991b).

Unlike other pyruvate kinase isoforms, PKM2 can interact with proteins harboring phosphorylated tyrosine residues leading to release of FBP, which, in turn, reduces the activity of the enzyme (Christofk et al, 2008b). Low PKM2 activity, in conjunction with increased glucose uptake, facilitates the flux of glucose carbons into anabolic pathways derived from glycolysis (Eigenbrodt et al, 1992; Christofk et al, 2008b; Vander Heiden et al, 2009; Mazurek, 2011). Also, PKM2, but not PKM1, can be inhibited by direct oxidation of cysteine 358 as an adaptive response to increased intracellular reactive oxygen species (ROS) (Anastasiou et al, 2011). Additionally, PKM2 expression in cancer cells is associated with enhanced phosphorylation of H11 on phosphoglycerate mutase 1 (PGAM1) by PEP (Vander Heiden et al, 2010b). This pathway provides an alternative route for pyruvate production while bypassing the generation of ATP via the pyruvate kinase step and thereby allows glycolysis to proceed at high rates (Locasale et al, 2010). Replacement of PKM2 with the constitutively active isoform PKM1 results in reduced lactate production, enhanced oxygen consumption, and a decrease in PGAM1 phosphorylation (Christofk et al, 2008a; Vander Heiden et al, 2010b). Furthermore, there appears to be selection for PKM2 expression for growth *in vivo*. However, it is also possible that PKM2 expression reflects

selection against high pyruvate kinase activity and therefore against expression of PKM1, raising the possibility that activation of PKM2 may impede cancer cell proliferation by interfering with regulatory mechanisms critical for proliferative metabolism.

Recently, we identified small molecules that selectively activate PKM2 over other pyruvate kinase isoforms *in vitro* (Boxer et al, 2010; Jiang et al, 2010). Here we show that synthetic PKM2 activators can increase PKM2 activity in cells to levels that are comparable to PKM1 expression. PKM2 activators bind to a pocket at the PKM2 subunit interface and thereby enhance association of PKM2 subunits into stable tetramers. Importantly, this mechanism of tetramer stabilization is refractory to inhibition by tyrosine-phosphorylated proteins and influences cell metabolism. Among the two classes of PKM2 activators described here, a member of the thieno[3,2-b]pyrrole[3,2-d]pyridazinones class, TEPP-46, has pharmacokinetic properties amenable to experiments in mice. Expression of PKM1 or continuous dosing of mice with TEPP-46, decreases development of human cancer cell xenografts, suggesting that increased pyruvate kinase activity can impair tumorigenesis.

RESULTS

Increased Pyruvate Kinase Activity Impairs Tumor Growth

We have previously demonstrated that replacement of PKM2 with PKM1 impairs the ability of H1299 human non-small cell lung cancer cells to form xenograft tumors in mice (Christofk et al, 2008a). This observation may reflect selection for PKM2 expression in tumors. However, because the ability to decrease PKM2 activity correlates with increased cell proliferation (Christofk et al, 2008b), it is also possible that high pyruvate kinase activity associated with the expression of the constitutively active PKM1 isoform can

suppress tumor growth. To address whether PKM1 expression alone affects tumor formation *in vivo*, we engineered H1299 cells to stably express Flag-tagged PKM1 in the presence of endogenous PKM2 (henceforth referred to as H1299-PKM1 cells). Expression of Flag-PKM1 did not affect endogenous PKM2 levels (Figure 1a), but resulted in a 35±17% increase in total cellular pyruvate kinase activity (Figure 2a). Both PKM1 and PKM2 can associate into tetramers (Kato et al, 1989; Ikeda et al, 2000). To determine if PKM1 can associate with endogenous PKM2 we used an anti-Flag antibody to immunoprecipitate Flag-PKM1. SDS-PAGE of the immunoprecipitated protein followed by silver staining revealed the presence of stoichiometric amounts of Flag-PKM1 and endogenous co-precipitating PKM2 (Figure 1b). The identity of PKM2 was confirmed by mass spectrometry (Figure 1c). These data show that PKM1 can form heterocomplexes with endogenous PKM2, and that immunoprecipitation of exogenously expressed Flag-tagged

Figure 1. Expression and Interaction of PKM1 and PKM2.
(a) Expression of Flag-PKM1 or Flag-PKM2 in H1299 human lung cancer cells does not alter endogenous PKM2 levels. H1299 cells were infected with retroviruses to express Flag-tagged mouse PKM1 (mM1) or mouse PKM2 (mM2). 2007 and 2008 denote two independent derivatizations of Flag-PKM1- or Flag-PKM2-expressing cells. "Rescue knockdown cells" denotes cells as above that were further infected with a lentivirus encoding an shRNA that targets endogenous human PKM2 but does not affect exogenous pyruvate kinase expression levels. Lysates of mouse muscle or liver tissue (which express exclusively PKM1 and PKL, respectively) and 293T cells (which express exclusively PKM2) were utilized as controls for isoform-specificity of the antibodies. Lysates were analyzed by SDS-PAGE and Western blot with antibodies specific to the indicated isoforms or an antibody (PKM) that recognizes both PKM1 and PKM2. **(b)** Lysates of H1299 cells expressing Flag-PKM1 or Flag-PKM2 generated as in (a) were subjected to immunoprecipitation with Flag-antibodies to immunoprecipitate Flag-PKM1 or Flag-PKM2. Immunoprecipitated proteins were visualized by silver staining. **(c)** Peptide maps derived from mass spectrometry analysis of the corresponding bands in (b). Yellow highlights indicate protein sequence coverage; green lines indicate detected peptides; red lines indicate the protein sequence encoded by the PKM1-specific or PKM2-specific exons. This spans a region of 55 amino acids (residues 381-435) of which 21 are distinct between the two isoforms allowing unequivocal identification. It remains unclear if the increased pyruvate kinase activity in cells following PKM1 expression results from PKM1 alone or the ability of PKM1 to increase the activity of PKM1/PKM2 heterocomplexes. However, the latter possibility seems likely as Flag-PKM1 co-precipitates equivalent amounts of endogenous PKM2 (Figure 5e).

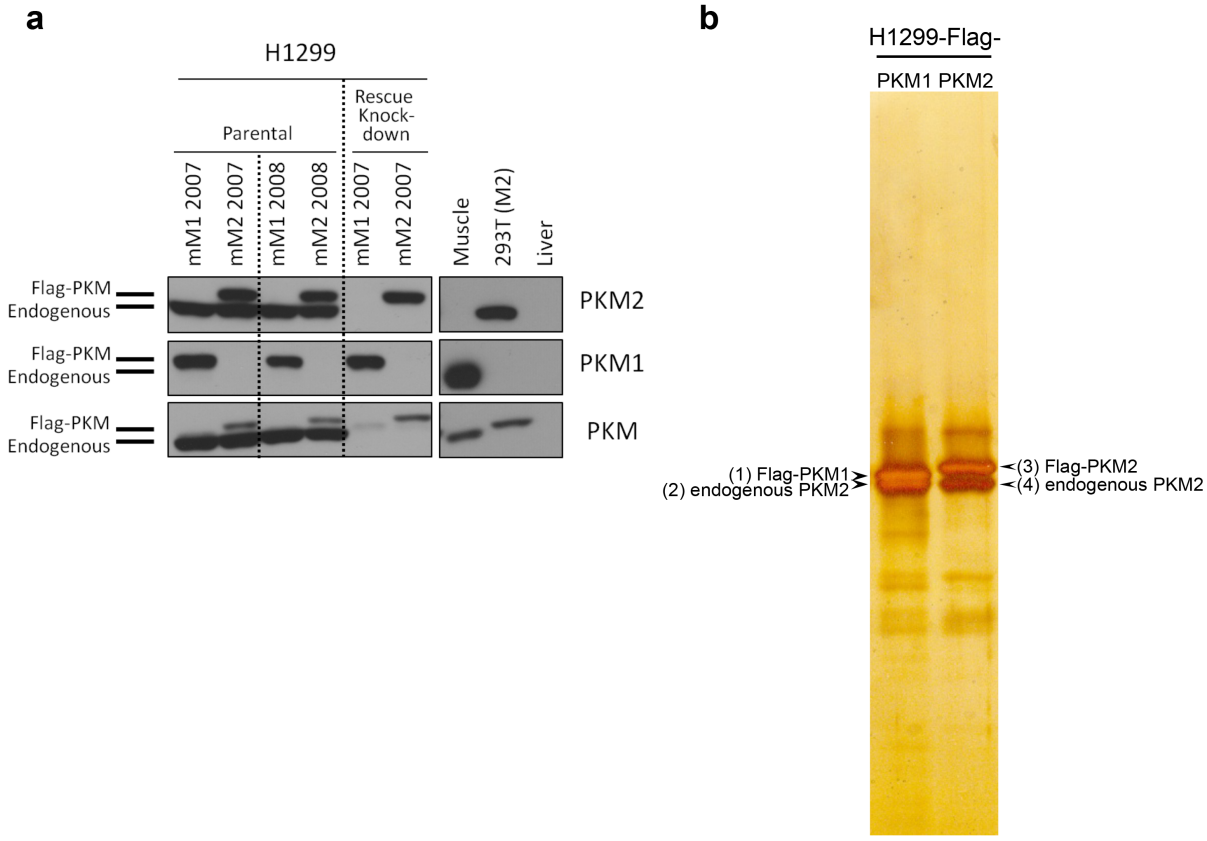

c

Band 1-PKM1

Band 3-PKM2

Band 2-PKM2

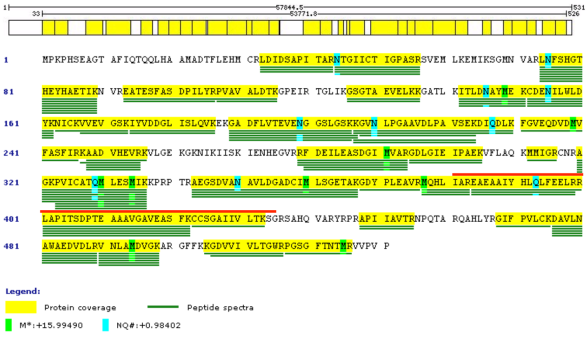

Band 4-PKM2

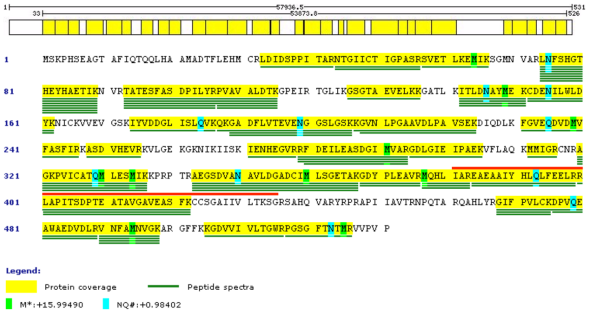

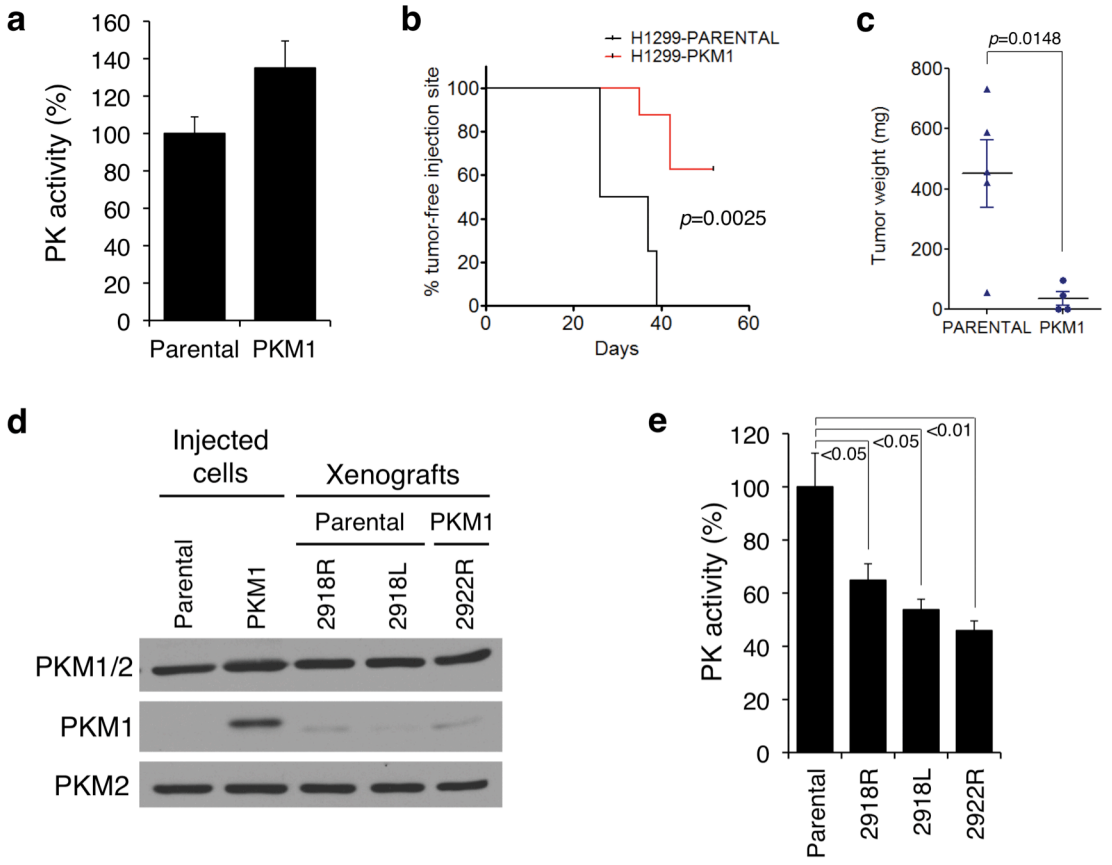

Figure 2. PKM1 Expression in Cancer Cells Impairs Xenograft Tumor Growth.
(a) H1299 human lung cancer cells were infected with a retrovirus to stably express Flag-PKM1 (referred to as H1299-PKM1 cells in the text) or empty vector (Parental) and after selection, cells were lysed and pyruvate kinase activity in the lysates was assayed. **(b)** Tumor formation over time of parental or H1299-PKM1 cells generated as in (a) and injected subcutaneously at equal numbers in *nu/nu* mice [*p* value calculated by logrank (Mantel-Cox) test]. **(c)** Final tumor weights from the experiment in (b). Mean tumor weights ± s.e.m. are shown and *p* value was calculated by unpaired Student's t-test. **(d)** Expression of Flag-PKM1 and endogenous PKM2 in the cells used in (b) and (c) was determined by western blot with isoform-specific antibodies. **(e)** Pyruvate kinase activity assays in lysates of the tumors shown in (d) (*N*=3, 1-way ANOVA and Tukey's post-test).

pyruvate kinase can be used to assess formation of multimeric pyruvate kinase complexes in cells. Furthermore, these data suggest that expression of PKM1 in PKM2-expressing cells suffices to increase total pyruvate kinase activity.

To determine whether PKM1 expression with enhanced pyruvate kinase activity interferes with tumor growth, we compared the ability of H1299-PKM1 versus parental

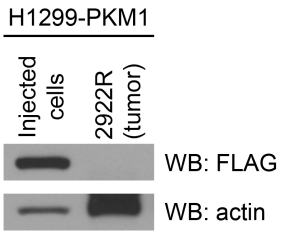

Figure 3. Xenograft Tumors Derived From PKM1-Expressing Cells Have Reduced PKM1 Expression.
To confirm loss of PKM1 expression in xenograft tumors derived from H1299- PKM1 cells, lysates of H1299-PKM1 cells and of tumor 2922R (shown in Figure 2d) were analyzed by Western blot with Flag antibodies.

H1299 cells to form tumors in immunocompromised (*nu/nu*) mice. Tumors emerged in all sites where parental cells were injected after a median of 31.5 days (Figure 2b). However, only 4 out of 10 sites injected with H1299-PKM1 cells gave rise to tumors. Notably, tumors derived from H1299-PKM1 cells were significantly smaller (Figure 2c), occurred later and had reduced expression of Flag-PKM1 relative to the injected H1299-PKM1 cells (Figure 2d and Figure 3). Furthermore, pyruvate kinase activity in tumor lysates was consistently lower than that seen in parental H1299 cells (Figure 2e). As the same numbers of parental or PKM1-expressing cells were injected to initiate tumors, the low pyruvate kinase activity in all tumors suggests that the small tumors derived from H1299-PKM1 cells arose from a subset of cells that lost PKM1 expression. These data support the notion that decreased pyruvate kinase activity is associated with tumor growth, and suggest that high pyruvate kinase activity can suppress formation of cancer cell xenograft tumors in mice.

Small Molecules Can Specifically Activate PKM2 in Cells

A recent screen identified two structurally distinct classes of small-molecule PKM2 activators (Boxer et al, 2010; Jiang et al, 2010). A representative compound from each class was selected for further studies; the **t**hi**e**no[3,2-*b*]**p**yrrole[3,2-*d*]**p**yridazinone NCGC00186528 (TEPP-46; ML265, PubChem CID: 44246499) and the substituted *N*,*N*'-**di**aryl**s**ulfon**a**mide NCGC00185916 (DASA-58; ML203, PubChem CID: 44543605) are both potent activators of recombinant PKM2 (TEPP-46: AC_{90}=470 nM, AC_{50}=92 nM; DASA-58:

AC_{90}=680 nM, AC_{50}=38 nM; Figure 4a) and are soluble in aqueous solution (Boxer et al, 2010; Jiang et al, 2010). Furthermore, TEPP-46 and DASA-58 are selective for PKM2 as they do not activate recombinant PKM1 *in vitro* (Figure 4b). To investigate whether these compounds are able to activate PKM2 selectively in cells, we engineered A549 cells to express Flag-PKM1 or Flag-PKM2 with concomitant knockdown of endogenous PKM2 (referred to as A549-PKM1/kd and A549-PKM2/kd, respectively) (Figure 4c). We treated these cells with 40 μM DASA-58 and assayed pyruvate kinase activity in the corresponding cell lysates. Consistent with our results in H1299 cells, lysates from DMSO-treated A549-PKM1/kd cells had 233±27% more pyruvate kinase activity than A549-PKM2/kd cells. We observed no increase in pyruvate kinase activity following treatment of A549-PKM1/kd cells with DASA-58; however DASA-58 treatment resulted in a 248 ±21% increase of pyruvate kinase activity in A549-PKM2/kd cell lysates. These data suggest that DASA-58 can selectively activate PKM2 in cells.

In a manner analogous to FBP, both TEPP-46 and DASA-58 decrease the K_m of PKM2 for PEP with no effect on the K_m for ADP (Boxer et al, 2010; Jiang et al, 2010), suggesting that TEPP-46 and DASA-58 activate PKM2 by a mechanism similar to that of the endogenous activator FBP. To determine whether FBP could further activate PKM2 in activator-treated cells, we incubated A549 cells with increasing concentrations (0-100 μM) of DASA-58 and assayed PKM2 activity in the corresponding lysates in the presence or absence of FBP. In the absence of FBP, DASA-58 activated PKM2 in a dose-dependent manner with an effective cellular half-activation concentration (EC_{50}) of 19.6 μM (Figure 4d). However, in the presence of high physiological levels of FBP (200 μM), we observed no significant additional increase in activity as a result of activator treatment. These data

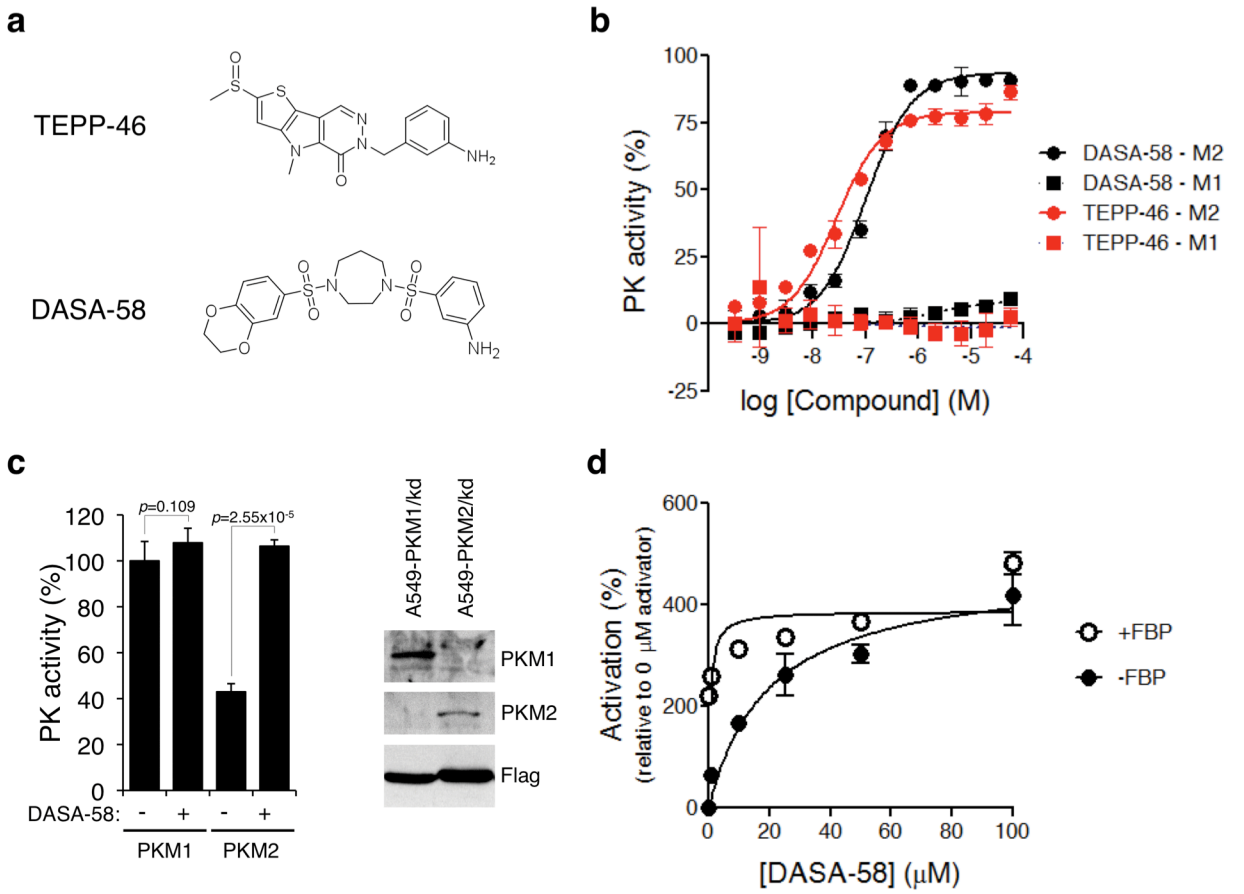

Figure 4. TEPP-46 and DASA-58 Isoform Specificity *In Vitro* and in Cells.
(a) Structures of the PKM2 activators TEPP-46 and DASA-58 used in this study. **(b)** Purified recombinant human PKM1 or PKM2 expressed in bacteria were subjected to pyruvate kinase activity assays in the presence of increasing concentrations of TEPP-46 or DASA-58. **(c)** A549 cells were engineered to stably express Flag-PKM1 or Flag-PKM2 in the absence of endogenous PKM2 which was knocked down by shRNA. As the PKM1 and PKM2 cDNAs correspond to the mouse orthologs, their expression was resistant to knockdown (Christofk et al, 2008a). Expression of Flag-PKM1 and Flag-PKM2 was confirmed by western blot with isoform-specific antibodies (right panel). These cell lines were then treated with 40 μM DASA-58 for 3 hours and the respective lysates were assayed for pyruvate kinase activity (*N*=3, Student's t-test). Similar results were observed in H1299 cells (not shown). **(d)** A549 cells were treated with the indicated doses of DASA-58 for 3 hours, lysed and assayed for pyruvate kinase activity in the presence or absence of 200 μM FBP.

are consistent with the *in vitro* kinetic analysis suggesting that DASA-58 enhances PKM2 activity by a mechanism similar to FBP.

PKM2 Activators Stabilize Subunit Interactions

The most active form of PKM2 is as a tetramer, and subunit association is thought to be promoted by FBP. To test this hypothesis, we separated bacterially expressed recombinant PKM2 into monomers and tetramers by size exclusion chromatography (Figure 5a) and assayed the ability of FBP to increase PKM2 activity. PKM2 tetramers showed greater than 50-fold higher activity compared to PKM2 monomers (Figure 5b). Addition of FBP had minimal effects on PKM2 tetramer activity (consistent with bacterial FBP being trapped on the stable tetramers (Christofk et al, 2008b)), but FBP increased the

Figure 5. Effects of Activators on PKM2 Tetramerization and Response to pTyr Signaling.
(a) Size-exclusion chromatography of purified recombinant PKM2 expressed in bacteria. **(b)** Fractions from (a) corresponding to monomeric or tetrameric PKM2 were assayed for pyruvate kinase activity. **(c)** FBP activates PKM2 monomers but not tetramers. Fractions as in (b) were assayed in the presence or absence of 100 μM FBP. Percent activity changes with FBP relative to without FBP are shown. **(d)** Sucrose gradient ultracentrifugation profiles of purified recombinant PKM1 or PKM2 and effects of FBP, TEPP-46 and DASA-58 on PKM2 subunit stoichiometry. After centrifugation, fractions were collected, analyzed by SDS-PAGE and stained with Coomassie Blue. Relative protein amounts were calculated by band densitometry on a LiCOR Odyssey infrared imaging system. **(e)** A549-PKM1 and A549-PKM2 cells were treated for 3 hours with 20 μM of DASA-58, an inactive analogue (NCGC00181801-01) or a DASA-58 analogue of the same family with intermediate activity (DASA-56, NCGC00185921-01) (Boxer et al., 2010). Following immunoprecipitation with Flag antibodies, association of endogenous PKM2 with Flag-PKM1 or Flag-PKM2 was determined by Western blotting with the indicated antibodies. The association of PKM1 with PKM2 suggests that PKM1 expression may increase activity of PKM1/PKM2 heterocomplexes by stabilizing the active tetramer conformation of the enzyme. **(f)** A549 cells expressing Flag-PKM2 as in (e), were treated for 3 hours with DMSO, 20 μM of DASA-58 or 20 μM of TEPP-46, lysed and subjected to immunoprecipitation with Flag antibodies. Immunoprecipitates were analyzed by SDS-PAGE and the amount of endogenous PKM2 co-precipitating with Flag-PKM2 was assessed by Western blot with a PKM2 antibody. **(g)** H1299 cells were treated with 100 μM pervanadate for 10 minutes in the presence or absence of TEPP-46, lysed hypotonically, and were analyzed by size exclusion chromatography. Chromatographic fractions were then subjected to Western blotting with a pyruvate kinase antibody to assess the stoichiometry of PKM2 subunit association under these conditions. **(h)** Purified recombinant PKM2 expressed in bacteria was treated with a phosphotyrosine-containing peptide with amino acid sequence corresponding to the optimal PKM2 binding sequence (pM2tide) or a peptide with the same sequence but lacking the phosphate on the tyrosine (M2tide). Following incubation with the peptides, PKM2 subunit composition in each sample was analyzed by size-exclusion chromatography. **(i)** Purified recombinant PKM2 was treated with M2tide or pM2tide as in (h) in the presence of increasing concentrations of TEPP-46 and assayed for pyruvate kinase activity.

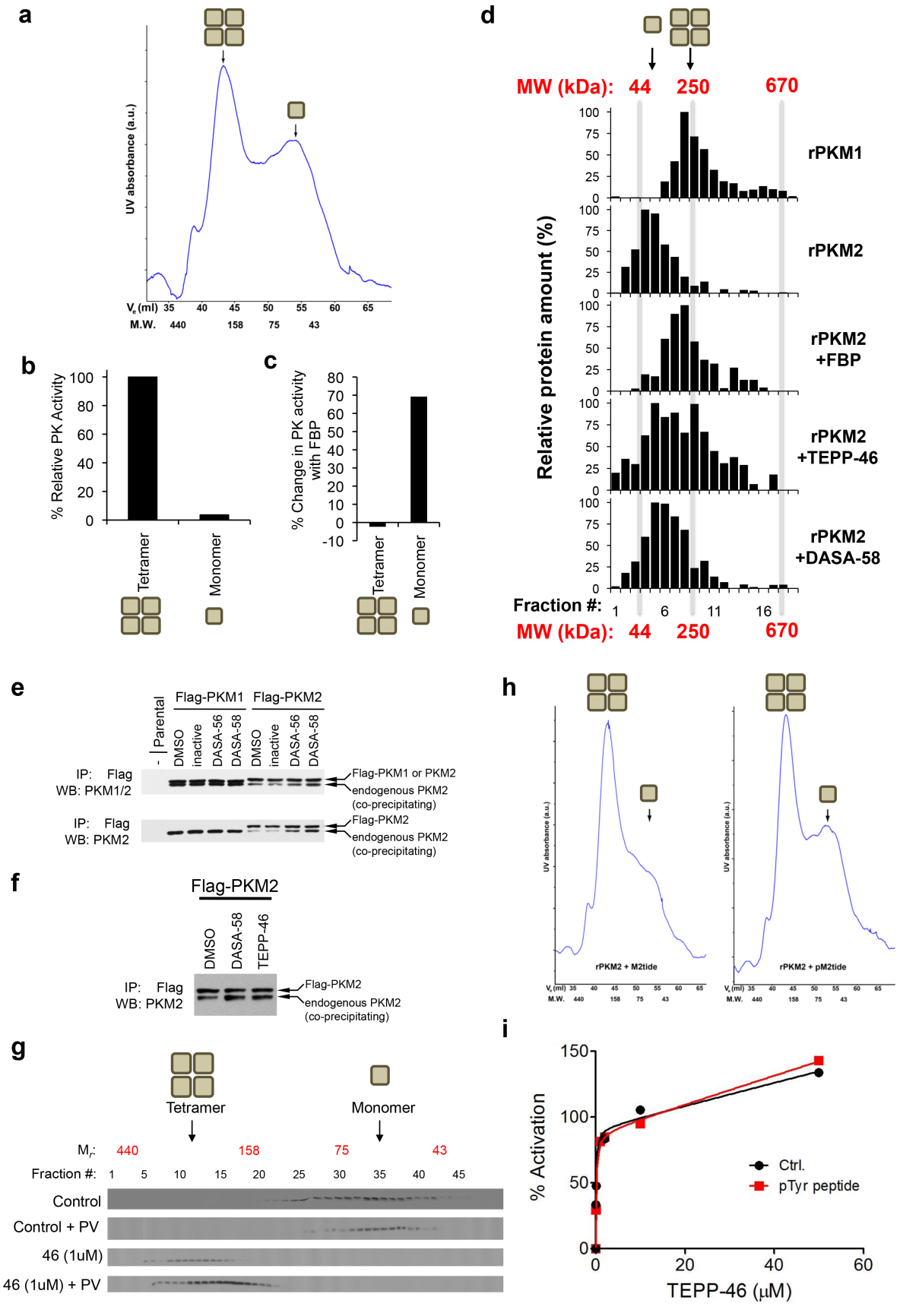
a
UV absorbance (a.u.)
Ve (ml) 35 40 45 50 55 60 65
M.W. 440 158 75 43
b
% Relative PK Activity
Tetramer
Monomer
c
% Change in PK activity with FBP
Tetramer
Monomer
d
MW (kDa): 44 250 670
Relative protein amount (%)
rPKM1
rPKM2
rPKM2 +FBP
rPKM2 +TEPP-46
rPKM2 +DASA-58
Fraction #: 1 6 11 16
MW (kDa): 44 250 670
e
Parental
Flag-PKM1
Flag-PKM2
DMSO
inactive
DASA-56
DASA-58
IP: Flag
WB: PKM1/2
Flag-PKM1 or PKM2
endogenous PKM2 (co-precipitating)
IP: Flag
WB: PKM2
Flag-PKM2
endogenous PKM2 (co-precipitating)
f
Flag-PKM2
DMSO
DASA-58
TEPP-46
IP: Flag
WB: PKM2
Flag-PKM2
endogenous PKM2 (co-precipitating)
g
Tetramer
Monomer
Mr: 440 158 75 43
Fraction #: 1 5 10 15 20 25 30 35 40 45
Control
Control + PV
46 (1uM)
46 (1uM) + PV
h
rPKM2 + M2tide
rPKM2 + pM2tide
i
% Activation
Ctrl.
pTyr peptide
TEPP-46 (μM)

activity of PKM2 monomers by approximately 70% (Figure 5c). The relatively modest activation of the monomers likely reflects the slow kinetics of assembling tetramers from monomers under dilute conditions. To determine if FBP activation of monomers is accompanied by changes in PKM2 subunit composition, we performed sucrose gradient ultracentrifugation on purified recombinant PKM2. Under these conditions, the majority of PKM2 is found to dissociate into monomers (Figure 6a). Exposure of PKM2 to FBP throughout the experiment results in a shift of the protein into a tetrameric configuration that is comparable to that seen with the constitutively active PKM1 isoform (Figure 5d). To investigate if small-molecule activators also promote pyruvate kinase subunit association into tetramers, we incubated purified PKM2 with TEPP-46 or DASA-58. We observed only a partial shift of PKM2 into tetramers with both activators alone (Figure 5d). As only a fraction of bacterially expressed PKM2 is bound to FBP (Figure 5a-c) we reasoned that the activators may only stabilize FBP-bound PKM2. Consistent with this hypothesis, transient incubation of PKM2 with FBP prior to addition of TEPP-46 resulted in the activator fully stabilizing the PKM2 tetramer. Overall, these data suggest that unlike PKM2, PKM1 is a stable tetrameric enzyme, and both FBP and small-molecule activators increase PKM2 activity by promoting the tetrameric state.

To investigate whether PKM2 activators promote pyruvate kinase subunit association in cells, we generated A549 cells stably expressing Flag-PKM1 or Flag-PKM2 and treated them with DMSO or DASA-58. Following lysis and immunoprecipitation with Flag antibodies, we determined the relative amount of endogenous PKM2 that co-precipitated under the various conditions by western blot using an antibody that recognizes an epitope common to both pyruvate kinase isoforms. Flag-PKM1

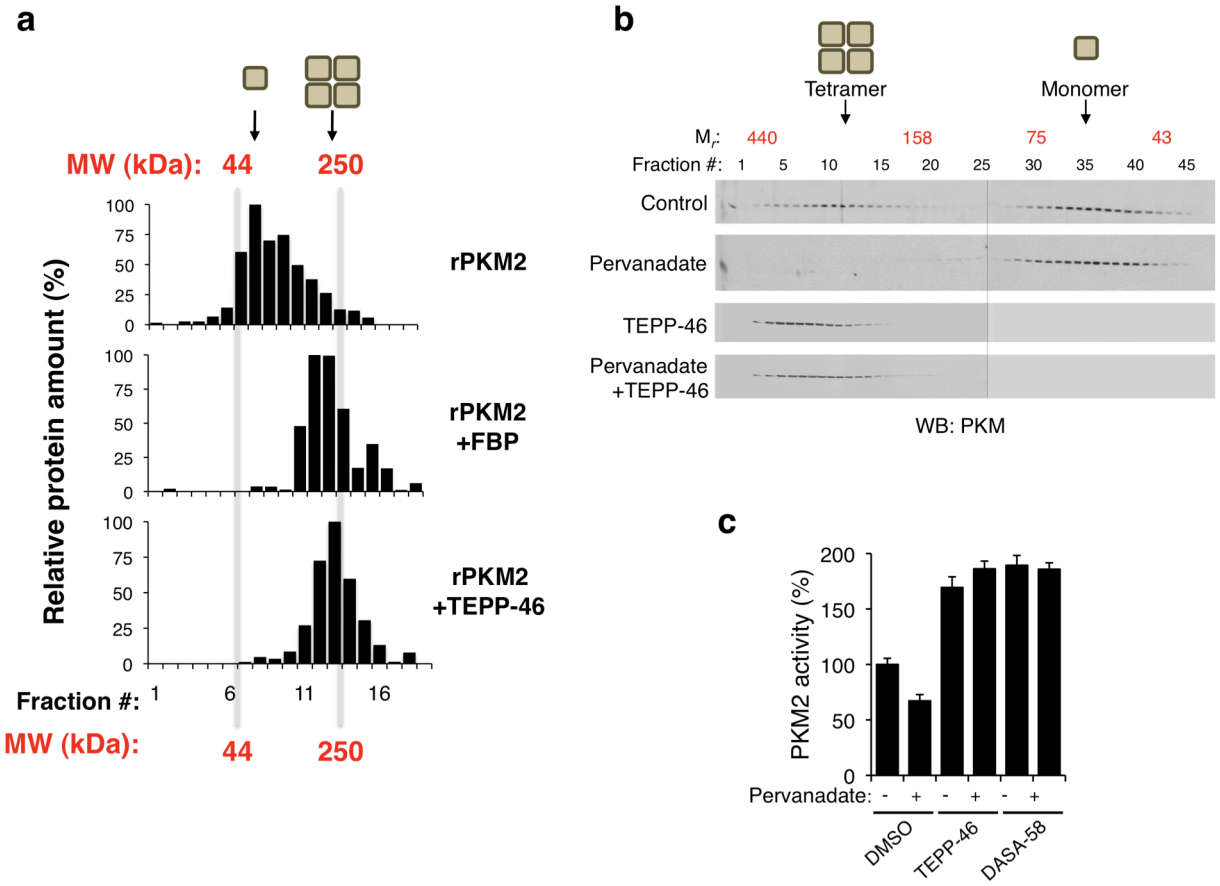

Figure 6. Activators Promote PKM2 Tetramer Formation and Prevent Inhibition by pTyr Signaling.
(a) Sucrose gradient ultracentrifugation profiles of purified recombinant PKM2 and effects of FBP and TEPP-46 on PKM2 subunit stoichiometry. Recombinant PKM2 was transiently exposed to FBP prior to addition of TEPP-46. After centrifugation, fractions were collected, analyzed by SDS-PAGE and stained with Coomassie Blue. Relative protein amounts were calculated by band densitometry on a LiCOR Odyssey infrared imaging system. **(b)** A549 cells were treated with 100 μM pervanadate for 10 min. in the presence or absence of TEPP-46, lysed hypotonically, and were analyzed by size exclusion chromatography. Chromatographic fractions were then subjected to western blotting with a pyruvate kinase antibody to assess the stoichiometry of PKM2 subunit association under these conditions. **(c)** Pyruvate kinase activity assays in A549 cells treated with pervanadate as in (b) in the presence of DMSO, 1 μM TEPP-46 or 1 μM DASA-58 (N=3, p=0.0044 by 2-way ANOVA).

immunoprecipitated equivalent amounts of endogenous PKM2 irrespective of activator treatment (Figure 5e). In contrast, DASA-58 treatment resulted in increased levels of endogenous PKM2 immunoprecipitating with Flag-PKM2 when compared with DMSO-treated cells or cells treated with an inactive analog of DASA-58 (Boxer et al, 2010). Similar

results were obtained with TEPP-46 (Figure 5f). These data indicate that PKM2 activators can promote stable association of PKM2 subunits in cells.

Phosphotyrosine interaction with PKM2 downstream of growth factor signaling is critical for both cell proliferation and metabolic changes that promote anabolism (Christofk et al, 2008b). Binding to phosphotyrosine decreases PKM2 activity by catalyzing release of FBP from the enzyme (Christofk et al, 2008b; Hitosugi et al, 2009). Pervanadate inhibits tyrosine phosphatases to acutely increase levels of tyrosine-phosphorylated proteins, and pervanadate treatment of cells results in inhibition of PKM2 but not inhibition of PKM1 activity (Christofk et al, 2008b; Vander Heiden et al, 2010b). To determine whether PKM2 activity inhibition caused by increased tyrosine phosphorylated proteins results in destabilization of PKM2 tetramers in cells, we treated cells with pervanadate and determined the stoichiometry of PKM2 subunit composition by size exclusion chromatography. In logarithmically growing A549 cells, approximately half of the PKM2 elutes as a tetramer while the other half dissociates to monomers during size exclusion chromatography (Figure 6b). Under these conditions we do not detect a significant population of dimeric PKM2. Pervanadate treatment caused disappearance of PKM2 tetramers and the entire PKM2 population was detected as monomers in this assay. We then tested whether PKM2 activators influence regulation of PKM2 tetramerization by tyrosine phosphorylated proteins. In logarithmically growing cells treated with TEPP-46 all PKM2 was found as a tetramer (Figure 6b). Moreover, PKM2 tetramers were preserved even after treatment of cells with pervanadate (Figure 6b). Similar results were obtained with H1299 cells (Figure 5g).

To test whether PKM2 activators also affect PKM2 activity when levels of tyrosine-phosphorylated proteins are increased, we assayed PKM2 activity in lysates of cells treated with DMSO, TEPP-46 or DASA-58 followed by pervanadate treatment. Pre-treatment of cells with TEPP-46 or DASA-58 prevented pervanadate-induced inhibition of PKM2 activity (Figure 6c). It is plausible that activator binding renders PKM2 resistant to an inhibitory modification induced by pervanadate treatment. However, a phosphotyrosine-containing peptide corresponding to the optimal PKM2 interaction motif (Christofk et al, 2008b) can promote dissociation of PKM2 tetramers (Figure 5h), but does not inhibit the ability of TEPP-46 to activate recombinant PKM2 (Figure 5i). These results indicate that activators render PKM2 tetramers resistant to dissociation induced by phosphotyrosine signaling.

Overall, these data argue that PKM2 activators enhance PKM2 activity by promoting the stable (active) tetrameric form of PKM2. However, similar to PKM1 but unlike the endogenous activator FBP, small-molecule PKM2 activators promote the active form of the enzyme even in the presence of increased phosphotyrosine levels that would otherwise lower PKM2 activity.

Structural Analysis of PKM2 Activator Mode of Binding

Based on these biochemical studies, it is possible that these agents activate PKM2 by binding at the same site as FBP but fail to be released following interaction with phosphotyrosine. Alternatively, PKM2 activators may stabilize the tetramer in another way. To explore these possibilities, purified recombinant PKM2 was crystallized in the presence of TEPP-46 or DASA-58. Our refined model shows that one tetrameric PKM2 contains two activators and four FBP molecules (Figure 7a, Supplementary Table 1, and Figure 8a). The four FBP molecules co-purified from the *E. coli* cells where PKM2 was

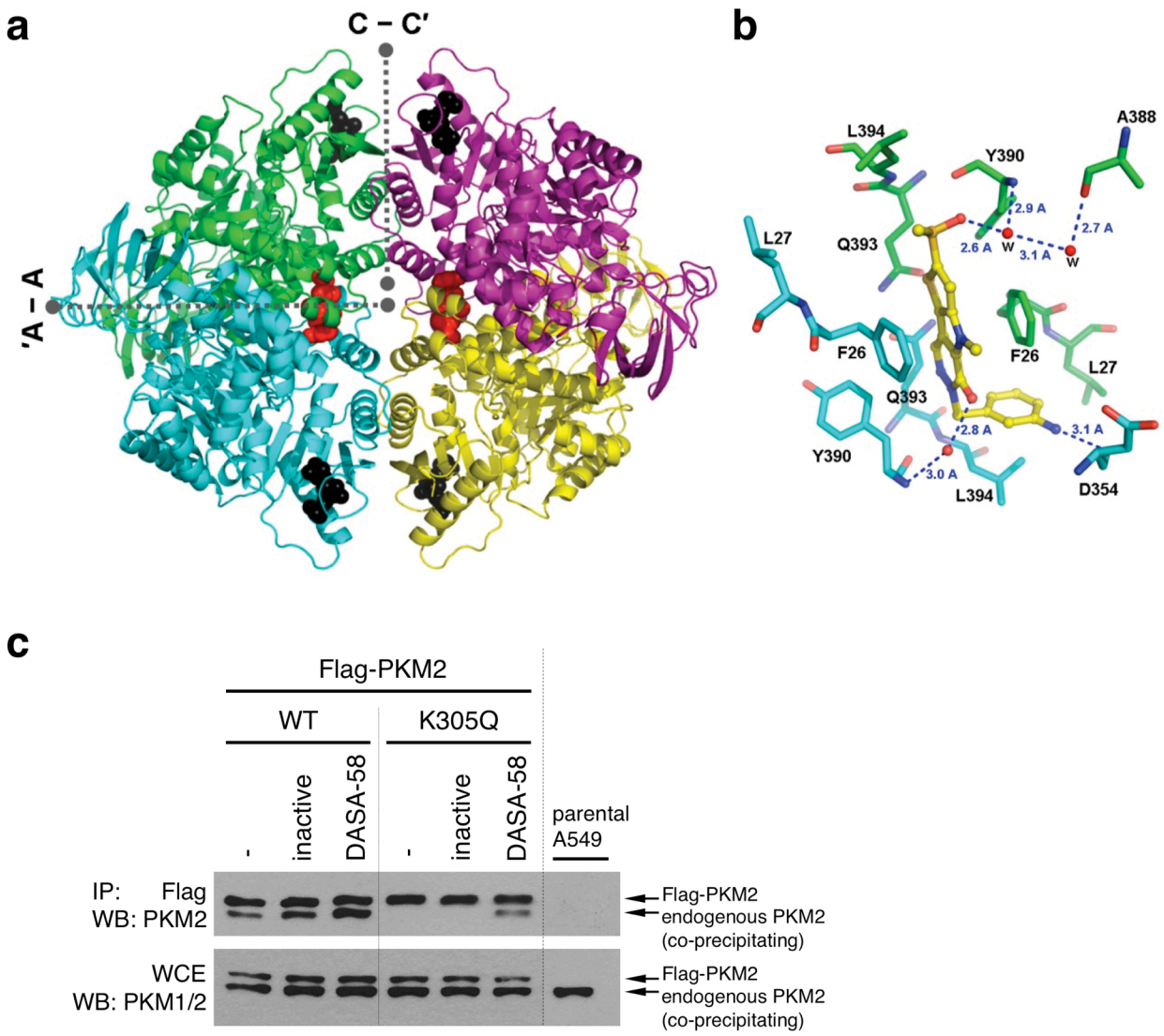

Figure 7. Structural Analysis of PKM2 Activator Mode of Action.
(a) Interaction between tetrameric PKM2 and TEPP-46. The four PKM2 monomers are represented in cartoon mode with different colors, respectively. The bound FBP and the activator molecules are colored black and red, respectively, and shown as space-filling models. The interfaces between two monomers are indicated by dotted lines. **(b)** Interaction between TEPP-46 and surrounding residues. The bound activator is colored yellow and represented by ball and stick model. The residues involved in the interaction from two monomers are labeled and colored green and cyan, respectively. Hydrogen bonds are indicated by blue dotted lines with distance (Å). **(c)** DASA-58 stabilizes the interaction of Flag-PKM2(K305Q) with endogenous PKM2. Flag-PKM2(K305Q) stably expressed in A549 cells was immunoprecipitated from corresponding lysates and the levels of co-precipitating endogenous PKM2 were assessed by western blotting with a PKM2 antibody.

produced and they were found to occupy all four of the FBP binding pockets of the PKM2 tetramer. In comparison, one activator was found in the interface (named A-A′) between the A domains of each dimer, approximately 35Å away from the FBP binding pocket (Figure 7a and Figure 8a). The bound activator was completely buried within the A-A′ interface. The activator binding pocket was lined with equivalent sets of residues provided by each of the PKM2 molecules forming the A-A′ interface, where the activator was accommodated through polar and van der Waals interactions with pocket-lining residues (Figure 7b and Figure 8b). Particularly in the case of TEPP-46, crystallographic evidence suggests that the binding orientation of the activator alternates based on a pseudo-twofold axis that is co-linear with both the nitrogen-methyl carbon bond of the N-methyl pyrrole moiety of TEPP-46 and the pseudo-twofold axis of the A-A' interface. The extra space in the pocket was filled with solvent molecules or ions, which also mediate hydrogen bonds between the activator and the pocket-lining residues (Figure 7b). These data show that TEPP-46 and DASA-58 bind PKM2 through a binding pocket distinct from that of FBP and that they stabilize a tetrameric conformational state.

FBP is thought to contribute to tetramer formation by stabilizing the C-C' interface. Given the distinct location of the activator binding pocket, we investigated whether activator binding results in stabilization of subunit interaction along the A-A' interface. A recent study showed that acetylation of K305 results in decreased PKM2 subunit association as another way to inactivate the enzyme (Lv et al, 2011). The ε-amino group of K305 interacts *via* a salt bridge with E384 in the neighboring subunit along the A-A' interface (Figure 8c). Acetylation may interfere with this interaction resulting in destabilization of the PKM2 tetramer. We mutated K305 to Q to mimic acetylation. Flag-

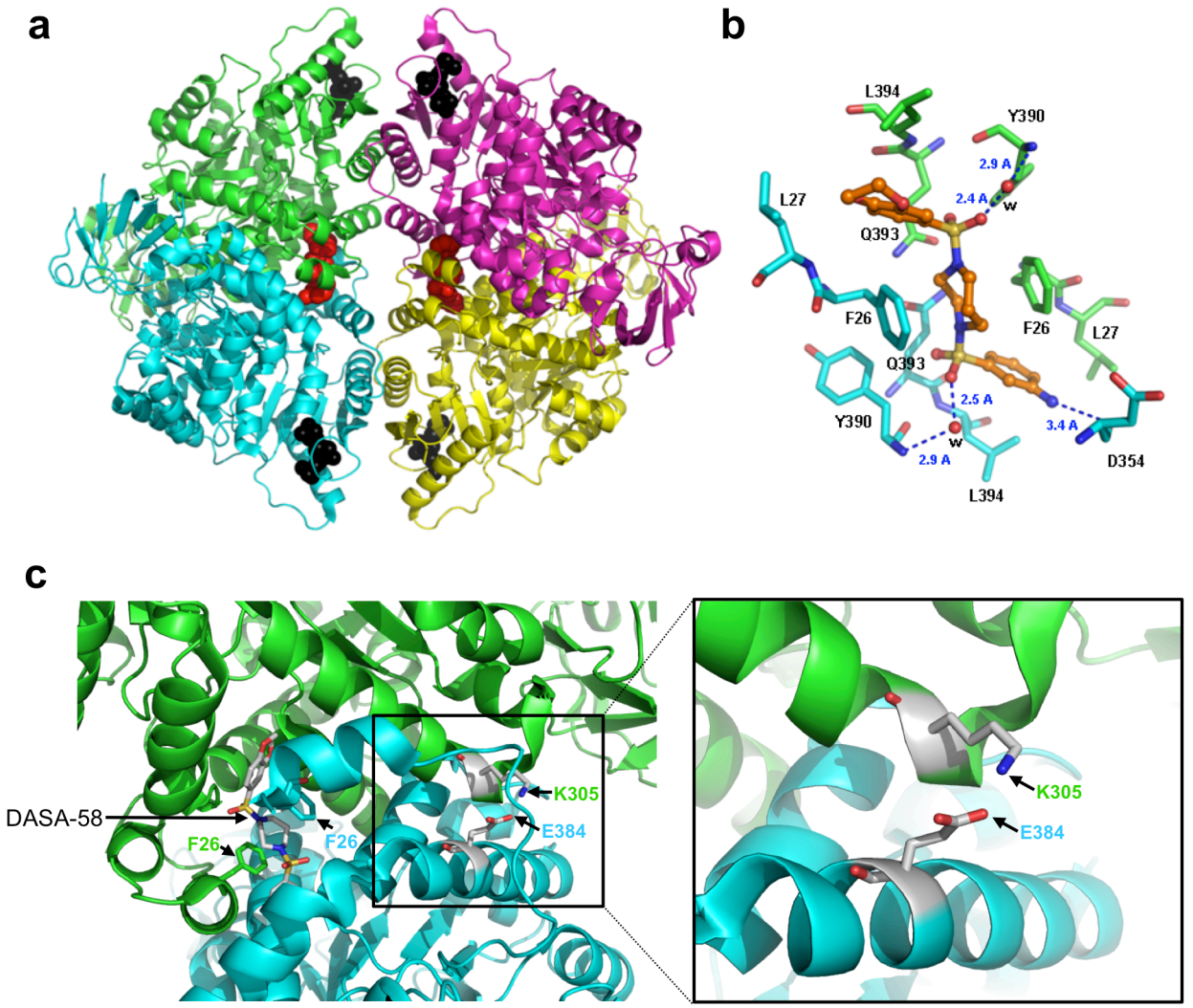

Figure 8. Structural Basis of DASA-58 Binding and PKM2 Subunit Interactions.
(a) Interaction between tetrameric PKM2 and DASA-58. The four PKM2 monomers are represented in cartoon mode with different colors, respectively. The bound FBP and the activator molecules are colored black and red, respectively, with space-filling models. **(b)** Interaction between DASA-58 and surrounding residues. The bound activator is colored orange and represented by ball and stick model. The residues involved in the interaction from two monomers are labeled and colored green and cyan, respectively. The hydrogen bonds are indicated by blue dotted lines with distance (Å). **(c)** Close up of the activator binding site and neighboring 'A-A interface showing the interaction between K305 and E384. Green and cyan indicate the two neighboring PKM2 subunits.

PKM2(K305Q) failed to co-precipitate endogenous PKM2 (Figure 7c). Given that the activator binds between two PKM2 subunits at the A-A' interface where K305 and E384 reside, we asked if PKM2 activator can rescue the interaction between Flag-PKM2(K305Q)

and endogenous PKM2. Indeed, treatment of cells with DASA-58 restored the ability of Flag-PKM2(K305Q) to co-precipitate endogenous PKM2 (Figure 7c). These data further support a model where PKM2 activators function by binding at the A-A' interface and stabilize the PKM2 tetramer, and suggest that the activators could circumvent *in vivo* mechanisms for inhibition of PKM2 activity.

PKM2 Activators Alter Metabolism in Cultured Cells

Overall, our results suggest that PKM2 activators will mimic the regulatory properties of constitutively active PKM1, thereby promoting high PKM2 activity regardless of the known mechanisms cells use to decrease pyruvate kinase activity. Therefore, we next examined the effects of activator treatment on cellular proliferation. Similar to results observed when PKM2 is replaced with PKM1 (Christofk et al, 2008a), under standard tissue culture conditions PKM2 activators had no significant effects on cell proliferation when tested across several lines (Figure 9a and Figure 10). In contrast, when we assayed proliferation under hypoxic conditions (1% O_2), PKM2 activator treatment resulted in a decreased rate of cell proliferation compared to DMSO-treated cells (Figure 9a). Similarly, expression of PKM1 in the presence of endogenous PKM2 had no effect on cell proliferation in standard tissue culture conditions, but inhibited cell proliferation under hypoxia to a similar degree as treatment with activators. These observations are consistent with previous data showing that replacement of PKM2 with PKM1 also impairs cell proliferation under low oxygen (Christofk et al, 2008a).

To test our hypothesis that PKM2 activators mimic a metabolic state found in PKM1-expressing cells, we interrogated the effects of activator treatment on cell metabolism. Replacement of PKM2 with PKM1 in cultured cells results in reduced lactate production

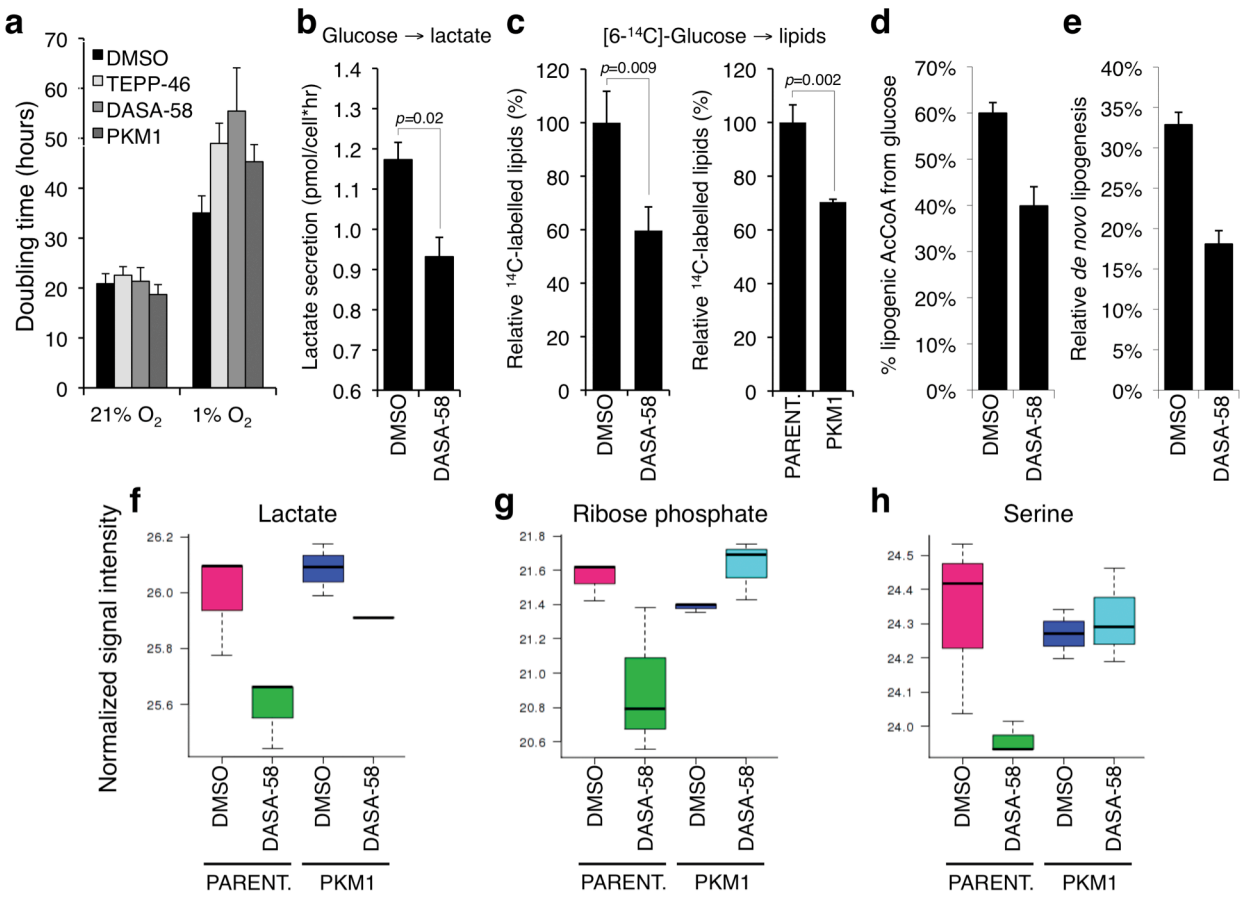

Figure 9. Metabolic Effects of Cell Treatment with PKM2 Activators.
(a) Effects of TEPP-46, DASA-58 (both used at 30 μM), or PKM1 expression on the doubling time of H1299 cells under normoxia (21% O_2) or hypoxia (1% O_2). **(b)** Effects of DASA-58 on lactate production from glucose. Logarithmically growing H1299 cells were washed with Krebs buffer and incubated in Krebs buffer containing glucose in the presence of 50 μM DASA-58 (*N*=3, Student's t-test). Produced lactate in the incubation medium was assayed after 20 min. as described in Methods. **(c)** Logarithmically growing H1299 cells (left), or parental H1299 and H1299-PKM1 cells (right) were incubated for 2 hours with 4 μCi/ml [6-^{14}C]-glucose in the presence of DMSO or 30 μM DASA-58, cellular lipids were extracted and lipid-incorporated ^{14}C was quantified by scintillation counting. **(d)** Contribution of [U-$^{13}C_6$]glucose to the lipogenic AcCoA pool, and fractional new synthesis of palmitate **(e)** were determined by isotopomer spectral analysis in A549 cells treated with DMSO or 100 mM DASA-58. Error bars indicate 95% confidence intervals. **(f-h)** Intracellular concentrations of lactate, ribose phosphate and serine in parental H1299 or H1299-PKM1 cells treated with DMSO or 25 mM of TEPP-46 for 36 hours were determined by targeted LC-MS/MS.

and enhanced oxygen consumption (Christofk et al, 2008a). Acute treatment of H1299 cells with DASA-58 also resulted in decreased lactate production (Figure 9b). Unlike cells where PKM2 is replaced with PKM1, expression of PKM1 in the presence of endogenous

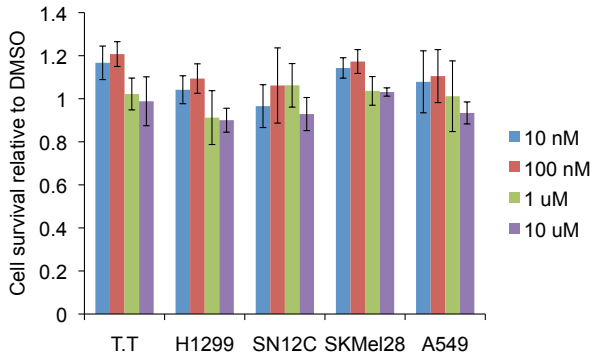

Figure 10. Effects of DASA-58 Treatment on Survival of Various Cancer Cell Lines. T.T: human medullary thyroid carcinoma, H1299: human non-small cell lung carcinoma, SN12C: human renal cell carcinoma, SKMel28: human melanoma, A549: human non-small cell lung carcinoma. Cells were treated with the indicated doses of DASA-58 for 72 hours at which point viability was assayed using an MTS assay.

PKM2 or activator treatment had no significant effect on oxygen consumption (Figure 11a). Furthermore, DASA-58 treatment did not affect glucose or glutamine consumption (Figure 11b-c), indicating that changes in uptake of major nutrients are unlikely to underlie the observed metabolic phenotypes. Inhibition of PKM2 activity mediated by phosphotyrosine signaling results in more efficient incorporation of glucose carbons into lipids (Christofk et al, 2008b). To determine if PKM2 activator treatment inhibits glucose carbon incorporation into lipids, cells were incubated with [6-^{14}C]-glucose in the presence of DMSO or DASA-58, cellular lipids were extracted, and ^{14}C-labelled lipids were quantified by scintillation counting. DASA-58 treatment resulted in a significant decrease in glucose-derived carbon incorporation into lipids (Figure 9c). Similarly, we observed a decrease in glucose carbon incorporation into lipids in H1299-PKM1 cells (Figure 9c). We also used gas chromatography-mass spectrometry (GC-MS) to analyze metabolite extracts of cells incubated with ^{13}C-labeled glucose. DASA-58 treatment resulted in diminished incorporation of glucose carbons into acetyl-CoA used for *de novo* palmitate synthesis (Figure 9d and Figure 11d) and a decrease in overall *de novo* lipogenesis (Figure 9e). TEPP-46 also induced a decrease in the intracellular levels of acetyl-coA, lactate, ribose phosphate and serine (Figure 9f-h and Figure 11e). Ribose phosphate is a key intermediate

for the biosynthesis of nucleotides via the pentose phosphate pathway, and serine, in addition to being incorporated directly into proteins can serve as a precursor for lipid head groups and glycine as well as provide carbon to the folate pool. Notably, these changes, along with overall changes in other intracellular metabolite concentrations (Figure 11f), were evident only in parental cells and not PKM1-expressing cells, indicating that the effects of the activator on cellular metabolism are specific to PKM2. No significant differences in the concentrations of lactate, ribose phosphate or serine were observed between PKM1-expressing and parental cells, most likely reflecting that, unlike transient activation of PKM2 by small molecules, selection for PKM1 expression in cells may lead to adaptive changes in metabolite levels to compensate for the effects of chronic pyruvate kinase activity elevation. Regardless, these data indicate that small-molecule activation of PKM2 can alter glucose metabolism and can decrease the intracellular concentrations of intermediates required for biosynthesis.

Low PKM2 activity is also associated with increased phosphorylation of PGAM1 on the catalytic histidine residue (His11) (Vander Heiden et al, 2010b). To determine if activator treatment decreases PGAM1 phosphorylation, we treated cells with DMSO or DASA-58, and analyzed the corresponding lysates by 2-D SDS-PAGE/isoelectric focusing to

Figure 11. Effects of DASA-58 Treatment on Cell Metabolism.
Oxygen consumption **(a)**, glucose uptake **(b)** and glutamine consumption **(c)** in parental H1299 or H1299-PKM1 cells treated with DASA-58 as in Figure 9f-h. **(d)** Mass isotopomer distribution (MIDs) of palmitate labeling in A549 cells grown for 3 days with [U-$^{13}C_6$]glucose in the presence of DMSO or 100 μM DASA-58. MIDs were corrected for natural isotope abundance using in-house algorithms adapted from Fernandez et al (1996) and were used to determine glucose carbon enrichment in lipogenic AcCoA and fractional new palmitate synthesis as described in the Methods. Error bars indicate s.e.m. (*N*=3). **(e)** Intracellular acetyl-coA concentration in H1299 cells treated as in Figure 9f-h determined by LC-MS/MS via selected reaction monitoring (SRM). **(f)** Heatmap of metabolite concentrations in parental H1299 or H1299-PKM1 cells treated with DMSO (Vehicle) or DASA-58 as in Figure 9f-h.

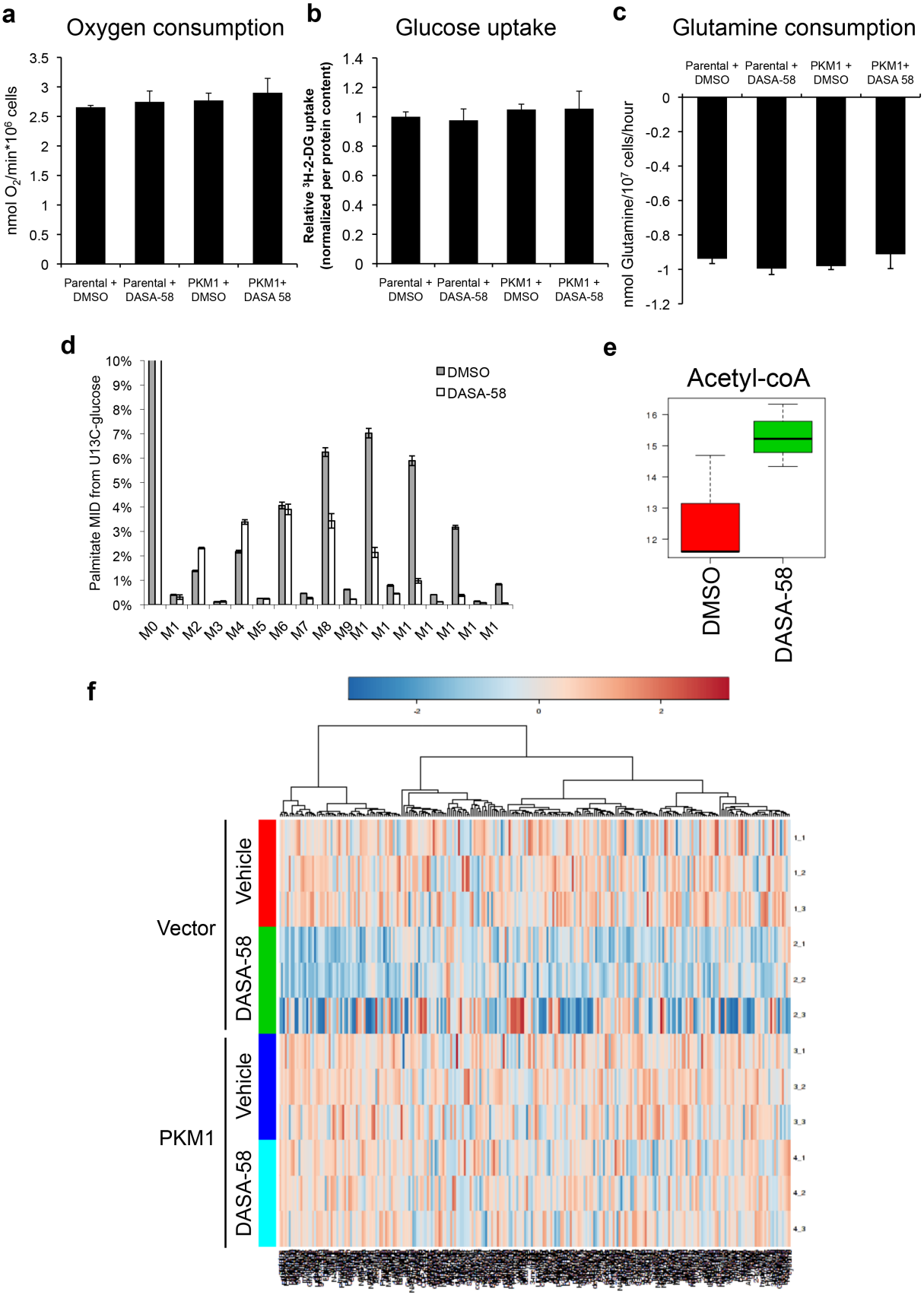
a
Oxygen consumption
nmol O2/min*10^6 cells
3.5
3
2.5
2
1.5
1
0.5
0
Parental + DMSO
Parental + DASA-58
PKM1 + DMSO
PKM1+ DASA 58
b
Glucose uptake
Relative 3H-2-DG uptake (normalized per protein content)
1.4
1.2
1
0.8
0.6
0.4
0.2
0
Parental + DMSO
Parental + DASA-58
PKM1 + DMSO
PKM1 + DASA-58
c
Glutamine consumption
Parental + DMSO
Parental + DASA-58
PKM1 + DMSO
PKM1+ DASA 58
nmol Glutamine/10^7 cells/hour
0
-0.2
-0.4
-0.6
-0.8
-1
-1.2
d
Palmitate MID from U13C-glucose
10%
9%
8%
7%
6%
5%
4%
3%
2%
1%
0%
DMSO
DASA-58
M0
M1
M2
M3
M4
M5
M6
M7
M8
M9
e
Acetyl-coA
16
15
14
13
12
DMSO
DASA-58
f
Vector
PKM1
Vehicle
DASA-58
Vehicle
DASA-58

resolve PGAM1 species in cells (Vander Heiden et al, 2010b). Similar to PKM1-expressing cells (Vander Heiden et al, 2010b), we observed a decrease in PGAM1 phosphorylation as a result of activator treatment (Figure 12). Together, these data suggest that PKM2 activators induce a metabolic state in cells comparable to, but distinct from, that seen with PKM1 expression.

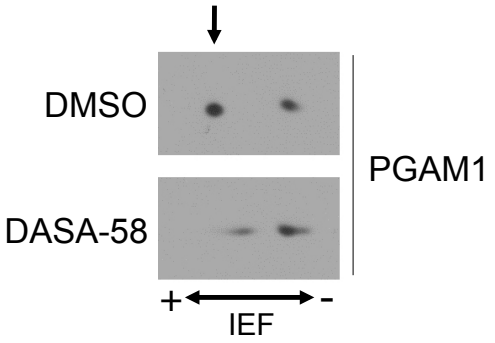

Figure 12. Effect of DASA-58 Treatment on PGAM1 Phosphorylation.
H1299 cells were treated with 50 μM DASA-58 for 1 hour, lysed and analyzed by 2-D electrophoresis followed by Western blot with a PGAM1 antibody. Phosphorylated PGAM1 is indicated with an arrow.

PKM2 activator inhibits xenograft tumor growth

PKM1 expression impairs the ability of cancer cells to grow *in vivo* as xenografts. To determine whether PKM2 activators also impede xenograft tumor growth, we determined which compound was suitable for experiments in mice. Based on *in vitro* absorption, distribution, metabolism and excretion (ADME) profiling studies, we predicted that TEPP-46 would have superior *in vivo* drug exposure compared to other analogs. To determine appropriate repeated drug doses for the mouse experiments, we performed single-dose pharmacokinetic and acute pharmacodynamic (PK-PD) studies with TEPP-46. Figure 13 shows mouse plasma drug concentration over time after a single intravenous, intraperitoneal or oral dose. TEPP-46 exhibits good oral bioavailability with relatively low clearance, long half-life, and good volume of distribution - parameters that predict for drug

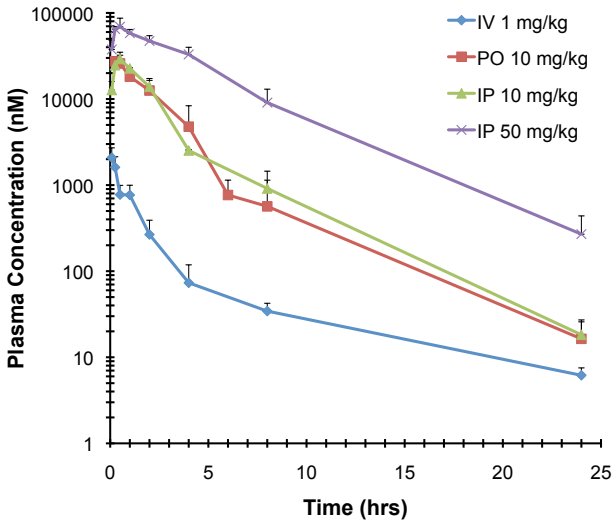

Figure 13. Comparison of TEPP-46 Dosing Methods in Mice.
Plasma drug concentration-time profile of TEPP-46 in BALB/c mice following intravenous (IV, 1 mg/kg), intraperitoneal (IP, 10 and 50 mg/kg), and oral administration (PO, 10 mg/kg). Error bars indicate SD with *N*=3 per time point.

exposure in tumor tissues (Supplementary Table 2). Acute oral-dose of TEPP-46 at 150 mg/kg readily achieved maximal PKM2 activation measured in A549 xenograft tumors (Figure 14a). To ensure that drug treatment could be carried out safely for a multi-day dosing regimen, we also performed a 5-day repeat-dose tolerability study in mice and showed that 50 mg/kg twice daily was well-tolerated with no sign of weight loss (Figure 14b).

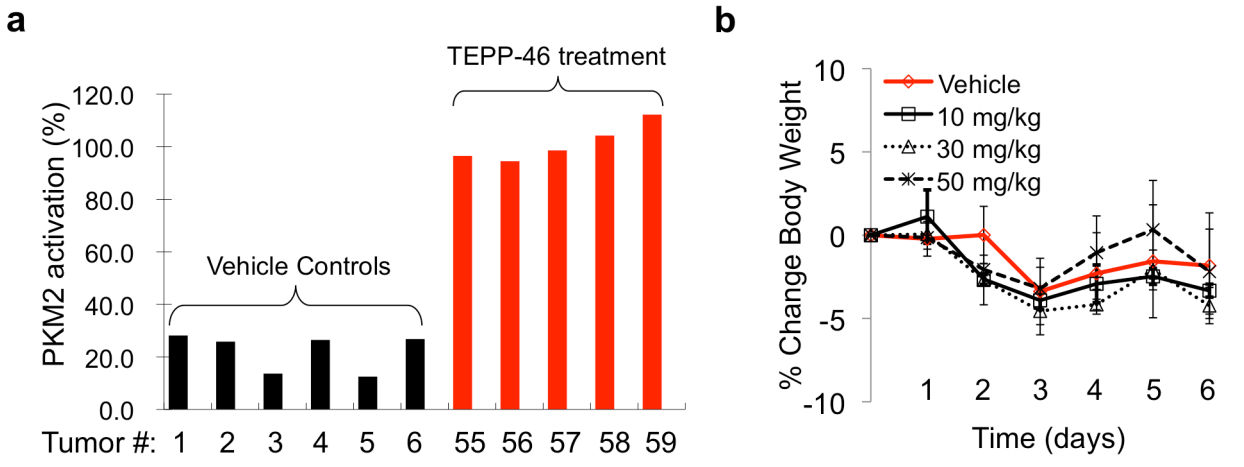

Figure 14. Pharmacodynamic Study of TEPP-46 in a Mouse A549 Xenograft Model.
(a) Pyruvate kinase activity in tumor lysates following two consecutive days of BID (twice daily) dosing of TEPP-46. **(b)** Monitoring of changes in the body weight of mice treated orally bi-daily with the indicated doses of TEPP-46.

Because 50 mg/kg twice daily oral dosing of TEPP-46 was well tolerated and led to reasonable plasma levels in mice, we tested whether this dose of TEPP-46 could promote PKM2 tetramerization in xenograft tumors. We treated mice bearing H1299 xenograft tumors with vehicle or TEPP-46 and analyzed tumor lysates by size exclusion chromatography. In xenografts from vehicle-treated mice, very little PKM2 was found as tetramers (Figure 15a). In contrast, tumors exposed to TEPP-46 harbored exclusively tetrameric PKM2. Metabolomic analysis revealed that, similar to the effects observed in cultured cells following treatment with TEPP-46, tumors derived from mice treated with TEPP-46 had lower concentrations of lactate, ribose phosphate and serine (Figure 15b). We then tested whether these changes in PKM2 activity and tumor metabolism impact the ability of H1299 cells to form xenografts. H1299 cells were injected into immunocompromised (*nu/nu*) mice and the animals were randomly divided into two cohorts, one treated with vehicle and the other treated with 50 mg/kg of TEPP-46, dosed twice daily for the duration of the experiment. No apparent toxicity was observed in any mice, despite over 7 weeks of continuous drug exposure based on blood counts and serum chemistries (Supplementary Table 3) as well as histological examination of blood, bone marrow, liver, kidney, heart and the gastrointestinal tract. Tumors in activator-treated mice emerged with a delayed latency compared to tumors in vehicle-treated mice (Figure 15c). In addition, the tumors from activator-treated mice were smaller than those arising in vehicle-treated animals (Figure 15d). TEPP-46 was detectable in tumors from activator-treated mice suggesting that cells in the tumor were exposed to the drug.

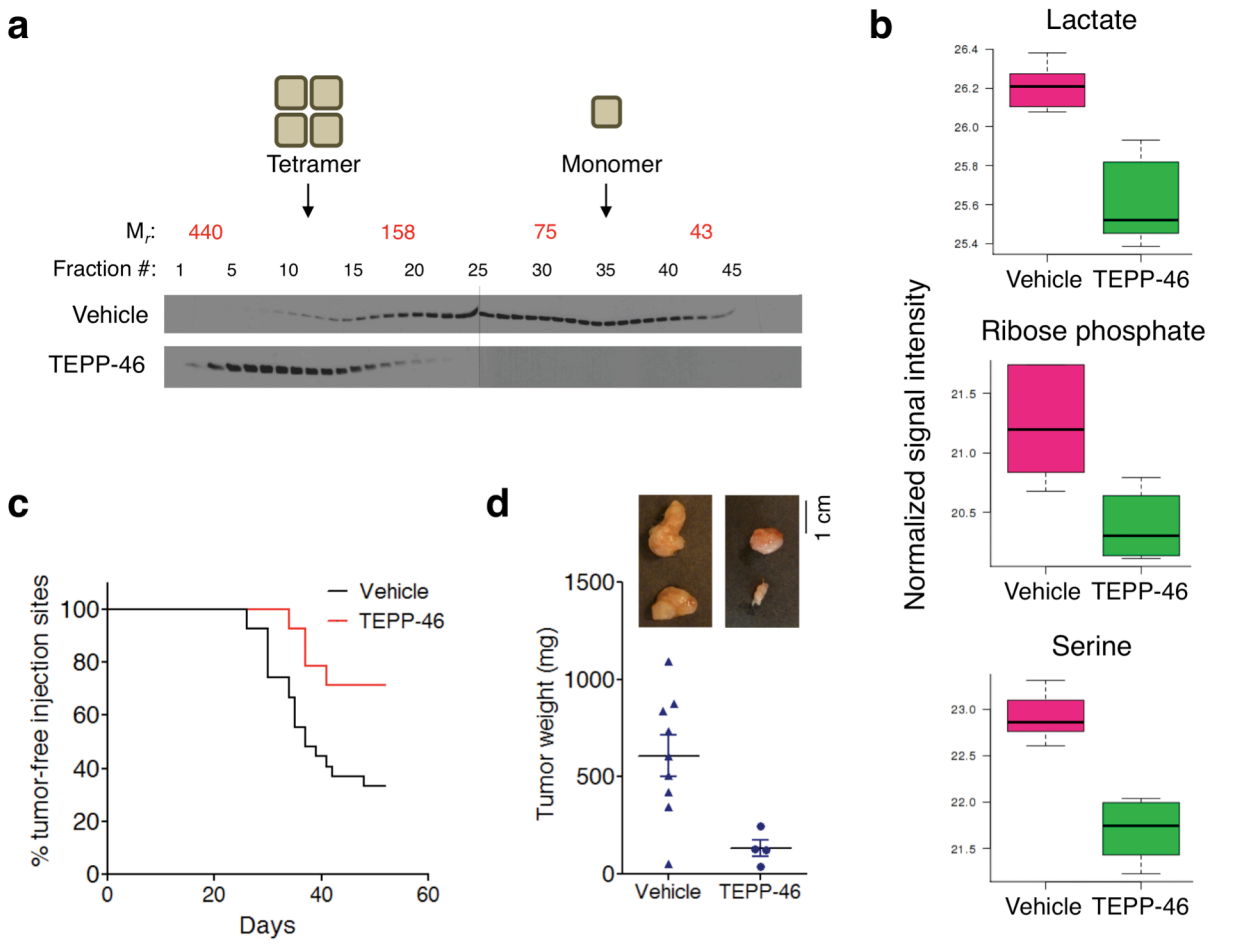

Figure 15. PKM2 Activators Impair Xenograft Growth.
(a) Mice bearing H1299 xenograft tumors received bolus doses of TEPP-46 at 50 mg/kg 16 hours and 4 hours before sacrifice. Tumors were dissected and PKM2 complex stoichiometry in tumor lysates was determined by size exclusion chromatography. **(b)** Concentrations of lactate, ribose phosphate and serine in H1299 xenograft tumors from mice treated with vehicle or TEPP-46 as in (a). **(c)** H1299 cells were injected subcutaneously into *nu/nu* mice which were subsequently randomly divided into two cohorts, one given vehicle and the other TEPP-46 at 50 mg/kg twice-daily throughout the duration of the experiment. Injection sites were monitored for tumor emergence [*p* value calculated by logrank (Mantel-Cox) test]. After 52 days, the tumors were dissected and final tumor weights were measured **(d)**. Mean tumor weights ± s.e.m. are shown and *p* value was calculated by unpaired Student's t-test.

These data demonstrate that cancer cells in xenograft tumors are exposed to TEPP-46 after several weeks of oral dosing, and that this can mimic PKM1 expression to impair growth of H1299 cells as xenograft tumors.

DISCUSSION

Cancer cells harbor genetic changes that allow them to increase nutrient uptake and alter metabolism to support anabolic processes, and interfering with this metabolic program is a strategy for cancer therapy (Tennant et al, 2010; Vander Heiden, 2011). Altered glucose metabolism in cancer cells is mediated in part by expression of PKM2, which has unique regulatory properties. Unlike its splice variant PKM1, which is found in many normal tissues, PKM2 is allosterically activated by FBP and can interact with tyrosine-phosphorylated proteins to release FBP and decrease enzyme activity. Thus, growth factor signaling promotes decreased PKM2 activity and availability of glycolytic metabolites for anabolic pathways that branch from glycolysis. This suggests that activation of PKM2 might oppose the effects of growth signaling and interfere with anabolic glucose metabolism.

Consistent with this hypothesis, our data show that high pyruvate kinase activity caused by PKM1 expression or small-molecule PKM2 activation impedes the ability of cancer cells to form tumors in mice. PKM1 can associate with endogenous PKM2 and form heterocomplexes that are likely insensitive to FBP regulation and thus exhibit higher activity. Recent publications have described non-enzymatic functions for PKM2 (Hoshino et al, 2007; Steták et al, 2007; Luo et al, 2011). While these non-classical PKM2 activities may also play a role in tumor formation, our data suggest that the ability to decrease enzyme activity is also an important property of the enzyme that may drive PKM2 selection in tumors. Furthermore, these experiments provide evidence that elevated pyruvate kinase activity can be incompatible with efficient tumor growth.

Small-molecule PKM2 activators can mimic the enzymatic properties of PKM1 in PKM2-expressing cells and alter cell metabolism. Our studies focused on DASA-58 and TEPP-46, which are representative of two classes of PKM2-activating compounds (Boxer et al, 2010; Jiang et al, 2010). These small molecules induce changes in the kinetic properties of PKM2 that are identical to those induced by the endogenous PKM2 activator FBP, suggesting that PKM2 could adopt a PKM1-like state in cells when FBP is high and/or in the absence of phosphotyrosine signaling. Surprisingly, structural analyses of the activators bound to PKM2 tetramers revealed a binding pocket at the interface of subunit interaction that is distinct from the site of FBP binding. Furthermore, unlike FBP, which stabilizes the C-C' interface of the active tetramer, the small-molecule activators stabilize the A-A' interface. Interestingly, FBP was also observed in the crystals containing small-molecule activators, and activators stabilize PKM2 tetramers more effectively in the presence of FBP. This raises the possibility that FBP binding is still required for small-molecule activation and that stabilization of the A-A' interface inhibits FBP release. Nevertheless, these compounds enhance PKM2 enzymatic activity in a manner that renders PKM2 resistant to inhibition by phosphotyrosine binding, and interaction with phosphotyrosine is the only mechanism described to release FBP from PKM2. No natural ligands have been identified that bind PKM2 in the same site as the PKM2 activators, but given that multiple activator classes bind in the same pocket, it is possible that this represents a previously unknown site of pyruvate kinase regulation.

Our findings are consistent with PKM2 existing in a monomer-tetramer equilibrium that can be altered by the presence of FBP, TEPP-46 or DASA-58. Although this study agrees with previous reports demonstrating that the fully associated tetrameric form of

PKM2 is the active form of the enzyme, dimeric PKM2 was not a predominant form of the enzyme observed in our assays. Previous studies have described PKM2 dimers following isoelectric focusing chromatography (Mazurek, 2011). It is possible that the methods we used to assess PKM2 multimeric state favor complete tetramer dissociation to monomers. We suspect that much of the PKM2 *in vivo* exists in an equilibrium between loosely associated tetramers with low activity and tightly associated tetramers exhibiting high activity, and that this equilibrium is influenced by FBP levels and phosphotyrosine signaling or post-translational modifications that destabilize the loosely-associated (low activity) tetramer (Christofk et al, 2008b; Hitosugi et al, 2009; Anastasiou et al, 2011; Lv et al, 2011).

PKM2 activators may impair tumor cell proliferation by interfering with anabolic metabolism. Activator treatment *in vitro* and *in vivo* results in decreased pools of ribose-phosphate and serine, which are key precursors for nucleotide, lipid and amino acid metabolism. However, no change in metabolite pools were seen when pyruvate kinase activity was elevated by chronic PKM1 expression *in vitro,* suggesting that the metabolic states elicited by these two treatments may not be equivalent. It is possible that this response to PKM1 expression may reflect adaptive events that can more effectively compensate for increased pyruvate kinase activity *in vitro*. PKM2 activator treatment also reduced incorporation of glucose carbons into lactate and lipids, thus interfering with the increased lactate production used by many tumors to establish a redox balance compatible with high glycolytic rates (Vander Heiden et al, 2009). Lipids are essential components of new cells and reduced lipid production has been shown to inhibit proliferation (Hatzivassiliou et al, 2005). Interestingly, the effects of PKM2 activation on proliferation in

cell culture are only evident under hypoxic conditions, suggesting that glucose-dependent anabolic pathways may only be important for proliferation under some conditions. Oxidation-induced inhibition of PKM2 under hypoxia may support NADPH production via the oxidative branch of the pentose phosphate pathway to sustain antioxidant responses (Anastasiou et al, 2011). While the source of NADPH for biosynthetic processes, including lipid synthesis, remains a subject of active investigation, the ability of PKM2 to control cellular redox state may partly underlie the selective effects of PKM2 activation on proliferation under hypoxia.

While our data indicate that small-molecule activation of PKM2 can impede the proliferation of cancer cells in xenograft models, it remains to be determined whether such compounds will be similarly effective in autochthonous mouse tumor models or be efficacious as a cancer therapy in humans. PKM2 activators can also sensitize cells to oxidative stress-induced death raising the possibility that such compounds could enhance tumor killing in combination with drugs that increase cellular ROS (Trachootham et al, 2009; Anastasiou et al, 2011). Regardless, this study further supports the notion that pyruvate kinase acts as an important regulatory node in glycolysis to control glucose fate in cells and argues that high pyruvate kinase activity is not conducive to the anabolic metabolism necessary for tumor growth.

SUPPLEMENTARY TABLES

Supplementary Table 1 – Data collection and refinement statistics (molecular replacement)

	DASA-58	TEPP-46
Data collection		
Space group	$P2_1$	$P2_1$
Cell dimensions		
a, *b*, *c* (Å)	80.88, 152.56, 93.04	80.76, 151.16, 93.21
α, β, γ (°)	90.00, 103.17, 90.00	90.00, 102.94, 90.00
Resolution (Å)	40.00-1.95 (1.98-1.95) *	50.00-2.10 (2.14-2.10)
R_{sym} or R_{merge}	0.080 (0.857)	0.086 (0.533)
$I / \sigma I$[a]	19.4 (1.4)	19.9 (2.1)
Completeness (%)	99.8 (97.4)	98.4 (91.8)
Redundancy	3.6 (3.0)	3.5 (2.8)
Refinement		
Resolution (Å)	26.71-1.95	44.45-2.10
No. reflections used/free	156884 / 1914	123466 / 1524
R_{work} / R_{free}	0.219 / 0.262	0.190 / 0.231
No. atoms (excl. unknown atoms)[b]	16003	15875
Protein	15167	15326
Ligands (FBP and activator)	140	180
Water	676	369
B-factors (Å^2)	29.6[b], 23.4[c]	35.4[b], 28.3[d]
Protein	29.6	35.6
Ligands (FBP and activator)	27.9	26.2
Water	29.2	31.7
R.m.s. deviations		
Bond lengths (Å)	0.014	0.014
Bond angles (°)	1.4	1.4

[a] ratio of average I and average error columns in SCALEPACK statistics table
[b] from program MOLEMAN (G.J Kleywegt, Uppsala University, Sweden), excl. unknown atoms
[c] Mean for all atoms reported by REFMAC
[d] Mean for atoms excl. unknown reported by REFMAC
*Highest-resolution shell is shown in parentheses.

Supplementary Table 2 – Pharmacokinetic parameters of TEPP-46 in male Balb/c mice following intravenous (IV), intraperitoneal (IP) or oral (PO) administration

Group	Dose (mg/kg)	T_{max} (hr)	C_{max} (ng/mL)	C0 (ng/mL)	AUC_{last} (hr*ng/mL)	AUC_{INF} (hr*ng/mL)	$T_{1/2}$ (hr)	CL (mL/min/kg)	Vss (L/kg)	%F
IV	1	-	-	877	958	976	5.80	17.1	3.14	-
PO	10	0.25	10179	-	24328	24350	-	-	-	> 100
IP	10	0.50	10854	-	26966	26994	-	-	-	> 100
IP	50	0.50	25751	-	130627	131034	-	-	-	> 100

IV: 40% *w/v* beta hydroxy cyclodextrin in water
IP: 40% *w/v* beta hydroxy cyclodextrin in water
PO: 0.5% *w/v* carboxy methyl cellulose (400 -1000 cps) with 0.1 % v/v Tween 80

Supplementary Table 3 – Blood counts and serum chemistries of mice treated with TEPP-46 *via* various administration routes

Mouse #	Treatment	Sex	WBC * ($\times 10^3$)	Differential	HEMATOCRIT (% PCV §)	PLATELETS ($\times 10^3$)	ALKALINE PHOSPHATASE (IU/L)	SGPT (ALT) (IU/L)	SGOT (AST) (IU/L)	CPK (IU/L)	ALBUMIN (mg/dL)	TOTAL PROTEIN (mg/dL)	TOTAL BILIRUBIN (mg/dL)	DIRECT BILIRUBIN (mg/dL)	BUN (mg/dL)	CREATININE (mg/dL)	CHOLESTEROL (mg/dL)	GLUCOSE (mg/dL)	CALCIUM (mg/dL)	PHOSPHORUS (mg/dL)	BICARBONATE (mEq/L)
1	Vehicle PO BID x 52 days	F	5.4	n	41	854	75	38	109	280	3.3	5.8	< 0.3	< 0.3	27	< 0.3	116	367	12.1	13.3	9
2	50 mg/kg x 1 dose	F	5.4	n	43	1264	93	36	56	178	< 3	6.8	< 0.3	< 0.3	30	< 0.3	85	218	10.1	12.5	10
3	50 mg/kg x 1 dose	F	17	n	45	960	106	48	87	283	< 3	5	< 0.3	< 0.3	28	< 0.3	90	258	10.2	17.7	8
4	50 mg/kg PO BID x 52 days	F	1.6	n	40	378	84	26	61	102	< 3	5.3	< 0.3	< 0.3	23	< 0.3	90	274	11.3	17.8	9
5	50 mg/kg PO BID x 52 days	F	2.7	n	42	536	84	26	61	102	3	5.2	< 0.3	< 0.3	20	< 0.3	90	274	11.3	11.8	9

* WBC: White Blood Cells

§ PCV: Packed Cell Volume

METHODS

All mouse studies were performed in accordance with institutional guidelines and approved by the MIT Committee on Animal Care.

Cell Lines and Cell Culture

293T (human embryonic kidney) and A549 (human non-small cell lung carcinoma) cells were obtained from ATCC and cultured in DMEM (Mediatech) supplemented with 10% fetal calf serum (FCS), 2 mM glutamine, 100 U/ml penicillin and 100 μg/ml streptomycin. H1299 (human non-small cell lung carcinoma), T.T (human medullary thyroid carcinoma), SN12C (human renal cell carcinoma), and SKMel28 (human melanoma) were obtained from ATCC and cultured in RPMI (Mediatech) supplemented as above. All cells were cultured in a humidified incubator at 37°C and 5% CO_2 unless otherwise stated. Glucose concentration in the media was 25 mM (4.5 g/l) unless otherwise stated. Hypoxia treatments were performed using an InVivo2 400 humidified workstation (Ruskinn, Pencoed, UK). For all hypoxia treatments (and corresponding normoxic control cultures), the media were supplemented with 20 mM HEPES buffer. Cells expressing specific Flag-tagged isoforms of mouse pyruvate kinase M, or mutants thereof, in the absence of endogenous PKM2 were derived as described (Christofk et al, 2008a).

Western Blot

Cells or tissues were lysed in RIPA buffer with 2mM DTT and protease inhibitors and clarified by centrifugation at 21,000 *g*. The protein content of supernatants was quantified by Bradford assay, and analyzed by SDS-PAGE followed by Western blot using standard protocols and the following primary antibodies: anti-pyruvate kinase (Abcam, ab6191), anti-PKM1 (Sigma, SAB4200094), anti-PKM2 (Cell Signaling, 4053), anti-Flag (Sigma,

F3165), and anti-actin (Abcam, ab1801). Iso-electric focusing/SDS-PAGE two-dimensional Western blot analysis was performed as described previously (Vander Heiden et al, 2010b) after incubation of cells with DMSO or drug as indicated for one hour.

Immunoprecipitation

Cells attached to culture dishes were quickly washed once with a large volume (20-30 ml) of ice-cold PBS, snap-frozen in a liquid nitrogen bath and stored at -80°C until further processing. Cells were lysed in 700 µl PK lysis buffer (50 mM Tris-HCl pH 7.5, 1 mM EDTA, 150 mM NaCl, 1% Igepal-630) supplemented freshly prior to use with protease inhibitors [10 µg/ml phenymethylsulfonyl fluoride, 4 µg/ml aprotinin, 4 µg/ml leupeptin, and 4 µg/ml pepstatin (pH 7.4)] and 1 mM dithiothreitol (DTT). Lysates were centrifuged (20,000 *g*, 10', at 4°C), supernatants were transferred to fresh eppendorf tubes containing 20 µl of 50% Flag-agarose (Sigma-A2220) bead slurry in PK lysis buffer and incubated rotating at 4°C for 1 hr. Under these conditions, lysates were immunodepleted of detectable Flag-tagged proteins. Immunoprecipitates were washed 4 times with PK lysis buffer (1ml=100 bead-volumes per wash) then eluted from beads with 3xFlag peptide (150 µg/ml final concentration, Sigma, F4799, dissolved in 50 mM Tris-HCl pH 7.4, 150 mM NaCl) for 30' rotating at 4°C. Following a brief centrifugation of the beads, eluates were transferred to fresh eppendorf tubes, supplemented with SDS-PAGE loading buffer and analyzed by SDS-PAGE.

Xenograft Experiments

H1299 parental and H1299 cells with constitutive expression of a mouse PKM1 cDNA (H1299-PKM1 cells) were propagated in RPMI supplemented with 10% fetal bovine serum, penicillin/streptomycin, 2 mM glutamine, and hygromycin for transgene selection. Cells

were harvested, resuspended in sterile PBS, and $5x10^6$ cells were injected subcutaneously into *nu/nu* mice. Tumor growth was monitored by caliper measurement, the mice were sacrificed and tumors harvested after the time indicated. Tumors were weighed, divided and either flash-frozen in liquid nitrogen or fixed in formalin for later analysis.

PKM2 Activity Assay

Pyruvate kinase activity was measured by monitoring pyruvate-dependent conversion of NADH to NAD^+ by lactate dehydrogenase (LDH) as described previously (Vander Heiden et al, 2010a). Briefly, for cell line experiments, the medium was replaced with fresh medium 1 hour prior to the start of treatment with DMSO or activator. Also, where indicated, 100 μM pervanadate was added 10 minutes prior to cell lysis. Cells were lysed on ice with NP-40 buffer containing 2mM DTT and protease inhibitors and clarified by centrifugation at 21,000 *g*. 5 μl of the supernatant was used to assess pyruvate kinase activity (Vander Heiden et al, 2010a). Pyruvate kinase activity was subsequently normalized for total protein content. For the experiment in Figure 5h, the amino acid sequences of the peptides were: GGAVDDDYAQFANGG (M2tide) and GGAVDDDpYAQFANGG (P-M2tide) (Christofk et al, 2008b).

Sucrose-Gradient Ultracentrifugation

Approximately 2.3 ml of a 10-40% sucrose gradient was layered in ultracentrifuge tubes and left to equilibrate overnight. Recombinant PKM2 (purified as described below) was incubated with 500 nM TEPP-46, 1 μM DASA-58, or 100 μM FBP for 30 minutes on ice before layering on top of the gradient. For assessing the ability of FBP to stabilize PKM2 tetramers, 100 μM FBP was included in the sucrose gradient. Where indicated, recombinant PKM2 was transiently exposed to 100 μM FBP prior to addition of TEPP-46,

but FBP was not present in the sucrose gradient. The gradients were then spun at 55,000 rpm for 10 hours using a Beckman TLS-55 rotor and fractions collected. The resulting fractions were analyzed by SDS-PAGE and Coomassie blue staining. Intensity of staining was quantified using IR fluorescence on a LiCOR Odyssey instrument.

Size Exclusion Chromatography

Recombinant protein or ~2 mg of cellular protein from hypotonically lysed cells was separated on a HiPrep 16/60 Sephacryl S-200 HR column (GE) in 50 mM sodium phosphate, 150 mM sodium chloride, pH 7.2. Fractions were analyzed by UV absorbance or SDS-PAGE and Western blot as indicated. For the experiment in Figure 5d the peptides used are the same as described under "PKM2 activity assay."

Cloning, Expression, and Purification of Full Length PKM2 for Crystallization

The cDNA sequence of full-length human PKM2 was amplified by PCR and cloned into the expression plasmid pET28a-LIC, and the construct was verified by DNA sequencing. The resultant plasmid was transformed into *Escherichia coli* strain BL21(DE3) and the cells were grown in Terrific Broth at 37°C with 50 μg/ml kanamycin. When the OD_{600} reached 1.0, the cells were induced by the addition of 0.5 mM isopropyl β-D-thiogalactoside (IPTG) for overnight at 18°C and the recombinant PKM2 was expressed as a His-tagged fusion protein containing 19 N-terminal amino acid residues (MGSSHHHHHHSSGLVPRGS). Cells were harvested by centrifugation, frozen in liquid nitrogen, and stored at -80°C. The thawed cell pellet was resuspended in binding buffer (10 mM HEPES, pH 7.5; 300 mM KCl; 5 mM imidazole, 5 mM $MgCl_2$; 5% glycerol; 2.5 mM TCEP) supplemented with protease inhibitor cocktail (Sigma) and 0.5% CHAPS, and then lysed by sonication. The lysate was clarified by centrifugation, and the supernatant was loaded onto DE52 column (Whatman)

pre-equilibrated with binding buffer. The collected flow-through was loaded again onto Ni-NTA gravity flow column (Qiagen) equilibrated with binding buffer, and the bound His-tagged PKM2 protein was then eluted with elution buffer (10 mM HEPES, pH 7.5; 300 mM KCl; 5 mM imidazole; 5 mM $MgCl_2$; 5% glycerol; 2.5 mM TCEP). The fractions eluted from Ni-NTA column were pooled, concentrated, and loaded onto a HiLoad 26/60 Superdex 200 column (Amersham Biosciences) pre-equilibrated with 10 mM HEPES, pH 7.5; 100 mM KCl; 5 mM MgCl2; 5% glycerol; 2.5 mM TCEP. The fractions containing PKM2 protein were collected, concentrated to 20 mg/mL using Amicon Ultra-15 centrifugal filter device (Millipore), and stored at -80°C until use. The final protein purity was confirmed by SDS-PAGE.

Protein Crystallization, Data Collection and Structure Determination

For co-crystallization, the purified PKM2 was incubated overnight at room temperature in the presence of 5 mM activators (TEPP-46 or DASA-58) and then crystallization trays were set up using the sitting-drop vapor diffusion method with droplets of protein solution (0.5 µl) and reservoir solution (0.5 µl). The best diffracting crystals were obtained within 2 days from a reservoir solution containing 25% P3350, 0.2 M NH_4OAc and 0.1 M Bis-Tris pH 6.5. Crystals were cryo-protected with 50% Paratone-N, 50% mineral oil for freezing them directly in liquid nitrogen for x-ray data collection. Data collection was carried out at the Advanced Photon Source beamline 23ID-B. For each complex crystal, 360 0.5° oscillation images were collected in a continuous sweep. Data were reduced with HKL-2000 (Otwinowski & Minor, 1997) (DASA-58) or HKL-3000 (Minor et al, 2006) (TEPP-46). Crystals belonged to space group P21. Structures were solved by direct replacement with the isomorphous Protein Data Bank (PDB) (Berman et al, 2000) entry 3GQY. Activator

geometry restraints were obtained at the PRODRG36 server. Iterations of model rebuilding, refinement and geometry validation were performed with COOT (Emsley et al, 2010), REFMAC (Murshudov et al, 1997) and MOLPROBITY (Davis et al, 2004), respectively. The refined models were deposited (Yang et al, 2004) in the PDB. Data collection and refinement statistics are provided in Supplementary Table 1.

Expression and Purification of Recombinant PKM2 for Other Studies

Recombinant His-tagged PKM2 was prepared for ultracentrifugation essentially as above, except that transformed *E. coli* BL21(DE3) cells were grown in LB broth containing 2mM $MgCl_2$ at 37°C with 50 µg/ml kanamycin until OD_{600} reached 0.7. The culture was transferred to room temperature, induced with 0.5 mM IPTG for 6 hours and harvested as described. The cell pellet was resuspended in binding buffer (50 mM Tris, pH 8.5; 10 mM $MgCl_2$; 300 mM NaCl; 10% glycerol; 5mM imidazole), and sonicated. The lysate was clarified by centrifugation, supplemented with 0.1% (v/v) 2-mercaptoethanol, and bound to pre-equilibrated Ni-NTA agarose beads (Qiagen) by gentle shaking on ice for 3 hours. The beads were batch-washed four times in wash buffer (50 mM Tris, pH 8.5; 10 mM $MgCl_2$; 300 mM NaCl; 10% glycerol; 30mM imidazole), then packed into a gravity flow column. Bound protein was eluted in elution buffer (50 mM Tris, pH 8.5; 10 mM $MgCl_2$; 250 mM NaCl; 10% glycerol; 250mM imidazole) and fractions were collected and analyzed by Bradford assay or SDS-PAGE with Coomassie blue staining prior to pooling. Pooled fractions were dialyzed overnight in dialysis buffer (50 mM Tris, pH 7.5; 10 mM $MgCl_2$; 25 mM NaCl; 20% glycerol; 0.15% 2-mercaptoethanol), then for an additional 8 hours in fresh dialysis buffer.

Cell Doubling Time

20,000 cells were seeded in 12-well plates at day -1 in media containing 5.6 mM D-glucose and incubated at the indicated O_2 concentrations. In all cases media contained 10% dialyzed FCS and 20 mM HEPES pH 8.0. At day 0 the media were replaced with fresh media that had been equilibrated since the time of cell seeding at 37°C under the corresponding oxygen concentrations. At days 0, 2, 4 and 6 cells were fixed with 10% formalin and at the end of the experiment stained with 0.1% w/v crystal violet in 20% methanol, shaking for 15' at room temperature, and washed with water twice for 10' each; the plates were then dried on air. Cell-bound crystal violet was solubilized in 1 ml 10% v/v acetic acid and, because the amount of dye bound to cells is proportional to the number of cells, accumulation of cell mass was assessed by measurement of crystal violet absorbance at 595 nm in a spectrophotometer. Doubling times were calculated using exponential regression (http://www.doubling-time.com/compute.php).

Protein Identification by LC-MS/MS

For all mass spectrometry (MS) experiments, pyruvate kinase immunoprecipitates were separated using SDS-PAGE, the gel was stained with Coomassie blue, destained and the pyruvate kinase band was excised. Samples were washed with 50% acetonitrile, subjected to reduction with 10mM dithiothreitol (DTT) for 30 minutes, alkylation with 55mM iodoacetamide with 45 minutes, and in-gel digestion with TPCK modified trypsin (Promega) or chymotrypsin (Princeton Scientific) overnight at pH 8.3, followed by reversed-phase microcapillary/tandem mass spectrometry (LC/MS/MS). LC/MS/MS was performed using an EASY-nLC splitless nanoflow HPLC (Thermo Fisher Scientific) with a self-packed 75 μm i.d. x 15 cm C18 Picofrit column (New Objective) coupled to a LTQ-

Orbitrap XL mass spectrometer (Thermo Scientific) in data-dependent positive ion mode at 300 nL/min with one full MS-FT scan followed by six MS/MS-IT scans via collision induced dissociation (CID). MS/MS spectra were searched against the concatenated target and decoy (reversed) Swiss-Prot protein database using Sequest (Proteomics Browser Software (PBS), Thermo Fisher Scientific) with differential modifications for Met oxidation (+15.99), deamidation of Asn and Gln (+0.984) and fixed Cys alkylation (+57.02). Peptide sequences were identified if they initially passed the following Sequest scoring thresholds against the target database: 1+ ions, Xcorr ≥ 2.0 Sf ≥ 0.4, P ≥ 5; 2+ ions, Xcorr ≥ 2.0, Sf ≥ 0.4, P ≥ 5; 3+ ions, Xcorr ≥ 2.60, Sf ≥ 0.4, P ≥ 5 against the target protein database. Passing MS/MS spectra were manually inspected to be sure that all b- and y- fragment ions aligned with the assigned sequence. False discovery rates (FDR) of peptide hits were estimated below 1.5% based on reversed database hits.

Metabolism Measurements

For measurement of glucose-dependent lipid synthesis (Hatzivassiliou et al, 2005), 10^5 cells per well were seeded in 12-well plates at t=-24 hours. At t=-1 hour the medium was changed to fresh growth medium containing activator as indicated in the legend of Figure 9c. At t=0 the medium was replaced with fresh growth medium containing 4 µCi/ml [6-^{14}C]glucose (final concentration=72 µM) and activator as indicated. Cells were then incubated for 2 hours at 37°C and 5% CO_2. The labeling medium was then removed, cells were washed once with PBS at room temperature and lipids were extracted twice with 500 µl hexane:isopropanol (3:2 v/v), extracts were pooled and dried under nitrogen. Dried lipids were resuspended in 100 µl chloroform and radioactivity was measured in a scintillation counter. Lactate levels were measured using YSI 7100 Select Biochemistry

Analyzer (YSI Incorporated). Oxygen consumption rates were measured using a polarographic oxygen electrode (Schumacker et al, 1993).

MTS Cell Viability Assay

2,000 cells were seeded in 96-well plates 24 h prior to treatment start. CellTiter96® AQ_{ueous} (Promega-G5421) was used according to the manufacturer's protocol to assess cell viability following oxidant and PKM2 activator combination treatments. MTS: (3-(4,5-dimethylthiazol-2-yl)-5- (3-carboxymethoxyphenyl)-2-(4-sulfophenyl)-2H-tetrazolium).

GC/MS and Analysis of Lipid Synthesis

For determination of [U-$^{13}C_6$]glucose enrichment in lipogenic AcCoA, A549 cells were cultured for 3 days in the presence of tracer and either DMSO or 100 μM DASA-58. For extraction, cells were rinsed with 1 ml ice cold PBS and quenched with 0.4 ml ice-cold methanol. An equal volume of water was added, and cells were collected in tubes by scraping with a pipette. One volume of ice-cold chloroform was added to each tube, and the extracts were vortexed for 15 minutes. Samples were centrifuged at 14,000 *g* for 5 minutes at room temperature, and the non-polar fraction was collected in a fresh tube and evaporated under airflow. Fatty acid methyl esters were generated from lipid biomass by dissolving dried chloroform fractions in 50 μl of Methyl-8 reagent (Pierce) and incubating at 60°C for 1 hour. GC/MS analysis was performed using an Agilent 6890 GC equipped with a 30m DB-35MS capillary column connected to an Agilent 5975B MS operating under electron impact (EI) ionization at 70 eV. One μl of sample was injected in splitless mode at 270°C, using helium as the carrier gas at a flow rate of 1 ml min^{-1}. The GC oven temperature was held at 100°C for 5 minutes after injection, increased to 200°C at 15° min^{-1}, then to 250°C at 5° min^{-1}, and finally to 300°C at 15° min^{-1}. The MS source and

quadrupole were held at 230°C and 150°C, respectively, and the detector was run in scanning mode, recording ion abundance in the range of 100 – 350 m/z. Mass isotopomer distributions (MIDs) were determined by integrating palmitate ion fragments in the *m/z* range of 270 to 286. Computational estimation of AcCoA enrichment and fractional new palmitate synthesis was accomplished as previously described (Kharroubi et al, 1992; Grassian et al, 2011). Associated 95% confidence intervals were calculated by performing parameter continuation as described (Antoniewicz et al, 2006; Young et al, 2008).

Metabolite Analysis by Targeted Liquid-Chromatography Tandem Mass Spectrometry (LC-MS/MS)

For tissue culture experiments, 48 hours prior to each experiment, $2.5x10^5$ cells were seeded in 6 cm dishes in media without sodium pyruvate, containing 10% dialyzed FCS, 2 mM glutamine, 100 U/ml penicillin and 100 µg/ml streptomycin. Media were changed at t=-24 h and t=- 2 h. At t=0h cells were harvested at the indicated time points as follows: media were aspirated and metabolites were extracted with 1.5 ml of 4:1 v/v MeOH/H_2O equilibrated at -80°C. The extract and cells were scraped and collected into 15 ml conical tubes and centrifuged for 5 minutes at 690 *g* and solvent in the resulting supernatant was evaporated using a speed-vac. For xenograft experiments, mice bearing H1299 xenograft tumors were treated orally with TEPP-46 at 50mg/kg 16 and 4 hours before tumor harvest. Metabolites from snap-frozen xenograft tumor tissue were extracted with 4:1 v/v MeOH/H2O equilibrated at -80°C, and supernatants were dried under nitrogen gas. Samples were re-suspended in 20µL HPLC-grade water for mass spectrometry. 8 µL were injected and analyzed using a 5500 QTRAP triple quadrupole mass spectrometer (AB/SCIEX) coupled to a Prominence UFLC system (Shimadzu) via selected reaction

monitoring (SRM) of 253 in total endogenous water-soluble metabolites (Yuan et al, 2012). Some metabolites were targeted in both positive and negative ion mode for a total of 287 SRM transitions. ESI voltage was +4900V in positive ion mode and –4500V in negative ion mode via positive/negative polarity switching. The dwell time was 3 ms per SRM transition and the total cycle time was 1.57 seconds. Approximately 10-14 data points were acquired per detected metabolite. Samples were delivered to the MS via normal phase chromatography using a 4.6 mm i.d. x 10 cm Amide XBridge HILIC column (Waters) at 350 µL/minutes. Gradients were run starting from 85% buffer B (HPLC grade acetonitrile) to 42% B from 0-5 minutes; 42% B to 0% B from 5-16 minutes; 0% B was held from 16-24 minutes; 0% B to 85% B from 24-25 minutes; 85% B was held for 7 minutes to re-equilibrate the column. MS data were acquired during the first 15 minutes of the LC gradient. Buffer A was comprised of 20 mM ammonium hydroxide/20 mM ammonium acetate (pH=9.0) in 95:5 water:acetonitrile. Peak areas from the total ion current (TIC) for each metabolite SRM transition were integrated using MultiQuant v2.0 software (AB/SCIEX). Integrated TIC areas corresponding to metabolite concentrations were imported into Metaboanalyst (Xia et al, 2012) software, subjected to quantile normalization and statistical significance of changes in metabolite concentrations between different genotypes and treatments were determined by ANOVA.

ADME and PK/PD Methods

Pharmacokinetic studies were performed in male BALB/c mice fasted from 2 hr pre-dose to 2 hr post-dose. TEPP-46 was formulated as 40% beta-hydroxy cyclodextrin in water (for IV, IP) or 0.5% carboxy methyl cellulose (400-1000 cps) with 0.1 % v/v Tween 80 (for PO). For intravenous administration, the solution of TEPP-46 was administered as bolus

injection at 1 mg/kg dose via tail vein with 5 mL/kg volume at a slow and steady rate. For intraperitoneal route, TEPP-46 was administered at 10 mg/kg and 50 mg/kg doses through the peritoneum cavity with a dosing volume of 10 mL/kg. For oral dosing, the test compound was administered as uniform suspension at 10 mg/kg dose via stomach intubation using a 16-gauge oral feeding needle with a dosing volume of 10 mL/kg. Blood samples (0.06 mL) were collected from retro-orbital sinus of a set of three mice each at t=0, 0.08 (IV and IP), 0.25, 0.5, 1, 2, 4, 6 (only for PO), 8 and 24 hr in pre-labeled microtubes containing EDTA as anticoagulant. The plasma samples were stored at -70°C until bioanalysis by LC-MS/MS with lowest level of quantitation (LLOQ) = 0.636 ng/mL. Pharmacokinetics parameters (Cmax, Tmax, T1/2, AUC) were calculated using non-compartmental model with WinNonlin Ver 5.2 as statistics software (Pharsight Corporation, California, USA).

ACKNOWLEDGEMENTS

The Structural Genomics Consortium is a registered charity (Number 1097737) and receives funds from the Canadian Institutes for Health Research, the Canadian Foundation for Innovation, Genome Canada through the Ontario Genomics Institute, GlaxoSmithKline, Karolinska Institutet, the Knutand Alice Wallenberg Foundation, the Ontario Innovation Trust, the Ontario Ministry for Research and Innovation, Merck and Co., Inc., the Novartis Research Foundation, the Swedish Agency for Innovation Systems, the Swedish Foundation for Strategic Research, and the Wellcome Trust. Crystallography results shown in this report are derived from work performed at Argonne National Laboratory, Structural Biology Center at the Advanced Photon Source. Argonne is operated by UChicago Argonne, LLC, for the U.S. Department of Energy, Office of Biological and Environmental Research

under contract DE-AC02-06CH11357. The authors thank Paul Chang for experimental advice related to sucrose gradient ultracentrifugation and SAI Advantium Pharma Ltd. for help with pharmacokinetics studies. We also thank Mitali Kini for experimental help; and acknowledge Min Yuan and Susanne Breitkopf for help with mass spectrometry experiments. This work was supported by the Molecular Libraries Initiative of the National Institutes of Health Roadmap for Medical Research and the Intramural Research Program of the National Human Genome Research Institute, National Institutes of Health and by R03MH085679. This work was also funded by R01 GM56203 (L.C.C.). J.M.A. acknowledges funding from NIH 5P01CA120964 and NIH DF/HCC Cancer Center Support Grant 5P30CA006516. M.V.H. acknowledges additional funding support from the Smith Family Foundation, the Burroughs Wellcome Fund, the Damon Runyon Cancer Research Foundation, the Stern family, and the National Cancer Institute.

AUTHOR CONTRIBUTIONS

D.A., Y.Y. W.J.I. and M.V.H. designed and coordinated the study. M.B.B., C.J.T. L.C.C. H.-W.P. and L.D. advised on various aspects of the study. J.-K. J., M.B.B., M.S.; A.P.S., H.V., N.S., M.J.W., K.R.B., W.L., C.P.A., J.I., D.S.A., and C.J.T. designed and provided compounds. B.S.H., W.T., S.D. and H.-W.P. performed all structural studies; A.J. did additional structural analysis. H.Y., C.K., K.E.Y., K.K., F.G.S., S.J. and L.D. performed *in vivo* pharmacology and ADME studies. C.M.M., J.M.A, and G.S. did mass spectrometry. M.H.H. reviewed pathology. D.A., Y.Y., W.J.I., K.R.M., B.P.F., K.D.C., S.M., T.M.K., C.K., S.Y.L., Z.R.J., S.M.D., H.R.C, and M.V.H. all performed experiments. D.A. and M.V.H. wrote the paper with significant input from Y.Y. and W.J.I.

REFERENCES

Anastasiou D, Poulogiannis G, Asara JM, Boxer MB, Jiang JK, Shen M, Bellinger G, Sasaki AT, Locasale JW, Auld DS, Thomas CJ, Vander Heiden MG, Cantley LC (2011) Inhibition of pyruvate kinase M2 by reactive oxygen species contributes to cellular antioxidant responses. *Science* 334**:** 1278-1283

Antoniewicz MR, Kelleher JK, Stephanopoulos G (2006) Determination of confidence intervals of metabolic fluxes estimated from stable isotope measurements. *Metab Eng* 8**:** 324-337

Ashizawa K, McPhie P, Lin KH, Cheng SY (1991a) An in vitro novel mechanism of regulating the activity of pyruvate kinase M2 by thyroid hormone and fructose 1, 6-bisphosphate. *Biochemistry* 30**:** 7105-7111

Ashizawa K, Willingham MC, Liang CM, Cheng SY (1991b) In vivo regulation of monomer-tetramer conversion of pyruvate kinase subtype M2 by glucose is mediated via fructose 1,6-bisphosphate. *J Biol Chem* 266**:** 16842-16846

Berman HM, Westbrook J, Feng Z, Gilliland G, Bhat TN, Weissig H, Shindyalov IN, Bourne PE (2000) The Protein Data Bank. *Nucleic Acids Res* 28**:** 235-242

Boxer MB, Jiang JK, Vander Heiden MG, Shen M, Skoumbourdis AP, Southall N, Veith H, Leister W, Austin CP, Park HW, Inglese J, Cantley LC, Auld DS, Thomas CJ (2010) Evaluation of substituted N,N'-diarylsulfonamides as activators of the tumor cell specific M2 isoform of pyruvate kinase. *J Med Chem* 53**:** 1048-1055

Cairns RA, Harris IS, Mak TW (2011) Regulation of cancer cell metabolism. *Nat Rev Cancer* 11**:** 85-95

Christofk HR, Vander Heiden MG, Harris MH, Ramanathan A, Gerszten RE, Wei R, Fleming MD, Schreiber SL, Cantley LC (2008a) The M2 splice isoform of pyruvate kinase is important for cancer metabolism and tumour growth. *Nature* 452**:** 230-233

Christofk HR, Vander Heiden MG, Wu N, Asara JM, Cantley LC (2008b) Pyruvate kinase M2 is a phosphotyrosine-binding protein. *Nature* 452**:** 181-186

Clower CV, Chatterjee D, Wang Z, Cantley LC, Vander Heiden MG, Krainer AR (2010) The alternative splicing repressors hnRNP A1/A2 and PTB influence pyruvate kinase isoform expression and cell metabolism. *Proc Natl Acad Sci U S A* 107**:** 1894-1899

Davis IW, Murray LW, Richardson JS, Richardson DC (2004) MOLPROBITY: structure validation and all-atom contact analysis for nucleic acids and their complexes. *Nucleic Acids Res* 32**:** W615-619

Eigenbrodt E, Reinacher M, Scheefers-Borchel U, Scheefers H, Friis R (1992) Double role for pyruvate kinase type M2 in the expansion of phosphometabolite pools found in tumor cells. *Crit Rev Oncog* 3**:** 91-115

Emsley P, Lohkamp B, Scott WG, Cowtan K (2010) Features and development of Coot. *Acta Crystallogr D Biol Crystallogr* 66**:** 486-501

Grassian AR, Metallo CM, Coloff JL, Stephanopoulos G, Brugge JS (2011) Erk regulation of pyruvate dehydrogenase flux through PDK4 modulates cell proliferation. *Genes Dev* 25**:** 1716-1733

Hatzivassiliou G, Zhao F, Bauer DE, Andreadis C, Shaw AN, Dhanak D, Hingorani SR, Tuveson DA, Thompson CB (2005) ATP citrate lyase inhibition can suppress tumor cell growth. *Cancer Cell* 8**:** 311-321

Hitosugi T, Kang S, Vander Heiden MG, Chung TW, Elf S, Lythgoe K, Dong S, Lonial S, Wang X, Chen GZ, Xie J, Gu TL, Polakiewicz RD, Roesel JL, Boggon TJ, Khuri FR, Gilliland DG, Cantley LC, Kaufman J, Chen J (2009) Tyrosine phosphorylation inhibits PKM2 to promote the Warburg effect and tumor growth. *Sci Signal* 2**:** ra73

Hoshino A, Hirst JA, Fujii H (2007) Regulation of cell proliferation by interleukin-3-induced nuclear translocation of pyruvate kinase. *J Biol Chem* 282**:** 17706-17711

Ikeda Y, Tanaka T, Noguchi T (1997) Conversion of Non-allosteric Pyruvate Kinase Isozyme into an Allosteric Enzyme by a Single Amino Acid Substitution. *J Biol Chem* 272**:** 20495-20501

Ikeda Y, Noguchi T (1998) Allosteric regulation of pyruvate kinase M2 isozyme involves a cysteine residue in the intersubunit contact. *J Biol Chem* 273**:** 12227-12233

Ikeda Y, Taniguchi N, Noguchi T (2000) Dominant negative role of the glutamic acid residue conserved in the pyruvate kinase M(1) isozyme in the heterotropic allosteric effect involving fructose-1,6-bisphosphate. *J Biol Chem* 275**:** 9150-9156

Jiang JK, Boxer MB, Vander Heiden MG, Shen M, Skoumbourdis AP, Southall N, Veith H, Leister W, Austin CP, Park HW, Inglese J, Cantley LC, Auld DS, Thomas CJ (2010) Evaluation of thieno[3,2-b]pyrrole[3,2-d]pyridazinones as activators of the tumor cell specific M2 isoform of pyruvate kinase. *Bioorg Med Chem Lett* 20**:** 3387-3393

Kato H, Fukuda T, Parkison C, McPhie P, Cheng SY (1989) Cytosolic thyroid hormone-binding protein is a monomer of pyruvate kinase. *Proc Natl Acad Sci U S A* 86**:** 7861-7865

Kharroubi AT, Masterson TM, Aldaghlas TA, Kennedy KA, Kelleher JK (1992) Isotopomer spectral analysis of triglyceride fatty acid synthesis in 3T3-L1 cells. *Am J Physiol* 263**:** E667-675

Levine AJ, Puzio-Kuter AM (2010) The control of the metabolic switch in cancers by oncogenes and tumor suppressor genes. *Science* 330**:** 1340-1344

Locasale JW, Vander Heiden MG, Cantley LC (2010) Rewiring of glycolysis in cancer cell metabolism. *Cell Cycle* 9**:** 4253

Luo W, Hu H, Chang R, Zhong J, Knabel M, O'Meally R, Cole RN, Pandey A, Semenza GL (2011) Pyruvate kinase M2 is a PHD3-stimulated coactivator for hypoxia-inducible factor 1. *Cell* 145**:** 732-744

Lv L, Li D, Zhao D, Lin R, Chu Y, Zhang H, Zha Z, Liu Y, Li Z, Xu Y, Wang G, Huang Y, Xiong Y, Guan KL, Lei QY (2011) Acetylation targets the M2 isoform of pyruvate kinase for degradation through chaperone-mediated autophagy and promotes tumor growth. *Mol Cell* 42**:** 719-730

Mazurek S (2011) Pyruvate kinase type M2: a key regulator of the metabolic budget system in tumor cells. *Int J Biochem Cell Biol* 43**:** 969-980

Minor W, Cymborowski M, Otwinowski Z, Chruszcz M (2006) HKL-3000: the integration of data reduction and structure solution--from diffraction images to an initial model in minutes. *Acta Crystallogr D Biol Crystallogr* 62**:** 859-866

Murshudov GN, Vagin AA, Dodson EJ (1997) Refinement of macromolecular structures by the maximum-likelihood method. *Acta Crystallogr D Biol Crystallogr* 53**:** 240-255

Noguchi T, Inoue H, Tanaka T (1986) The M1- and M2-type isozymes of rat pyruvate kinase are produced from the same gene by alternative RNA splicing. *J Biol Chem* 261**:** 13807-13812

Otwinowski Z, Minor W (1997) Processing of X-ray diffraction data collected in oscillation mode. *Macromolecular Crystallography, Pt A* 276**:** 307-326

Schumacker PT, Chandel N, Agusti AG (1993) Oxygen conformance of cellular respiration in hepatocytes. *Am J Physiol* 265**:** L395-402

Steták A, Veress R, Ovádi J, Csermely P, Kéri G, Ullrich A (2007) Nuclear translocation of the tumor marker pyruvate kinase M2 induces programmed cell death. *Cancer Res* 67**:** 1602-1608

Tennant DA, Duran RV, Gottlieb E (2010) Targeting metabolic transformation for cancer therapy. *Nat Rev Cancer* 10**:** 267-277

Trachootham D, Alexandre J, Huang P (2009) Targeting cancer cells by ROS-mediated mechanisms: a radical therapeutic approach? *Nat Rev Drug Discov* 8**:** 579-591

Vander Heiden MG, Cantley LC, Thompson CB (2009) Understanding the Warburg effect: the metabolic requirements of cell proliferation. *Science* 324**:** 1029-1033

Vander Heiden MG, Christofk HR, Schuman E, Subtelny AO, Sharfi H, Harlow EE, Xian J, Cantley LC (2010a) Identification of small molecule inhibitors of pyruvate kinase M2. *Biochem Pharmacol* 79**:** 1118-1124

Vander Heiden MG, Locasale JW, Swanson KD, Sharfi H, Heffron GJ, Amador-Noguez D, Christofk HR, Wagner G, Rabinowitz JD, Asara JM, Cantley LC (2010b) Evidence for an alternative glycolytic pathway in rapidly proliferating cells. *Science* 329**:** 1492-1499

Vander Heiden MG (2011) Targeting cancer metabolism: a therapeutic window opens. *Nat Rev Drug Discov* 10**:** 671-684

Weissleder R (2006) Molecular imaging in cancer. *Science* 312**:** 1168-1171

Xia J, Mandal R, Sinelnikov IV, Broadhurst D, Wishart DS (2012) MetaboAnalyst 2.0--a comprehensive server for metabolomic data analysis. *Nucleic Acids Res* 40**:** W127-133

Yamada K, Noguchi T (1999) Regulation of pyruvate kinase M gene expression. *Biochem Biophys Res Commun* 256**:** 257-262

Yang H, Guranovic V, Dutta S, Feng Z, Berman HM, Westbrook JD (2004) Automated and accurate deposition of structures solved by X-ray diffraction to the Protein Data Bank. *Acta Crystallogr D Biol Crystallogr* 60**:** 1833-1839

Young JD, Walther JL, Antoniewicz MR, Yoo H, Stephanopoulos G (2008) An elementary metabolite unit (EMU) based method of isotopically nonstationary flux analysis. *Biotechnol Bioeng* 99**:** 686-699

Yuan M, Breitkopf SB, Yang X, Asara JM (2012) A positive/negative ion-switching, targeted mass spectrometry-based metabolomics platform for bodily fluids, cells, and fresh and fixed tissue. *Nat Protoc* 7**:** 872-881

CHAPTER THREE:
PKM2 Isoform-Specific Deletion Reveals a Differential Requirement for Pyruvate Kinase in Tumor Cells

William J. Israelsen[1], Talya L. Dayton[1], Shawn M. Davidson[1], Brian P. Fiske[1], Aaron M. Hosios[1], Gary Bellinger[1], Jie Li[2], Yimin Yu[1], Mika Sasaki[3], James W. Horner[4,5], Laura N. Burga[3], Jianxin Xie[6], Michael J. Jurczak[7], Ronald A DePinho[4,8], Clary B. Clish[9], Tyler Jacks[1], Richard G. Kibbey[7,10], Gerburg M. Wulf[3], Dolores Di Vizio[11], Gordon B. Mills[2], Lewis C. Cantley[3,12], Matthew G. Vander Heiden[1,4]

[1] Koch Institute for Integrative Cancer Research at Massachusetts Institute of Technology, Cambridge, MA 02139, USA.
[2] Department of Systems Biology, University of Texas M. D. Anderson Cancer Center, Houston, TX 77030, USA.
[3] Beth Israel Deaconess Medical Center, Department of Medicine-Division of Signal Transduction, Boston, MA 02115, USA.
[4] Department of Medical Oncology, Dana-Farber Cancer Institute, Boston, MA 02115, USA
[5] Institute for Applied Cancer Science and the Department of Genomic Medicine, University of Texas M. D. Anderson Cancer Center, Houston, TX 77030, USA. (Current address)
[6] Cell Signaling Technology, Inc., Danvers, MA 01923, USA.
[7] Department of Internal Medicine, Yale University School of Medicine, New Haven, CT 06510, USA.
[8] Department of Cancer Biology, University of Texas M. D. Anderson Cancer Center, Houston, TX 77030, USA. (Current address)
[9] Metabolite Profiling Platform, Broad Institute, Cambridge, MA 02142, USA.
[10] Department of Cellular & Molecular Physiology, Yale University School of Medicine, New Haven, CT 06510, USA.
[11] Division of Cancer Biology and Therapeutics, Cedars-Sinai Medical Center, Los Angeles, CA; the Urological Diseases Research Center, Boston Children's Hospital; and Department of Surgery, Harvard Medical School, Boston, MA 02115, USA.
[12] Department of Systems Biology, Harvard Medical School, Boston, MA 02115, USA.

A version of this chapter has been published previously: PKM2 isoform-specific deletion reveals a differential requirement for pyruvate kinase in tumor cells. *Cell* (2013) 155**:** 397-409.

WJI performed experiments presented in Figures 1-12, with exceptions as follows: TLD generated some tumor cell lines and contributed Figures 3C-E and 12A-D. DDV scored pathology to assist with Figure 12A-D. SMD, MJJ, and RGK contributed Figures 10D and 11E-G. BPF contributed Figure 6G. AMH contributed Figure 6H. JL and GBM provided TCGA data. JWH generated the $PKM2^{flox}$ mouse using ES cells generated by MGVH, who contributed Figure 2A.

ABSTRACT

The pyruvate kinase M2 isoform (PKM2) is expressed in cancer and plays a role in regulating anabolic metabolism. To determine whether PKM2 is required for tumor formation or growth, we generated mice with a conditional allele that abolishes PKM2 protein production without disrupting PKM1 expression. PKM2 deletion accelerated mammary tumor formation in a *Brca1*-loss driven model of breast cancer. PKM2-null tumors displayed heterogeneous PKM1 expression, with PKM1 found in non-proliferating tumor cells and no detectable pyruvate kinase expression in proliferating cells. This suggests PKM2 is not necessary for tumor cell proliferation and implies that the inactive state of PKM2 is associated with the proliferating cell population within tumors, while non-proliferating tumor cells require active pyruvate kinase. Consistent with these findings, variable PKM2 expression and heterozygous PKM2 mutations are found in human tumors. These data suggest regulation of PKM2 activity supports the different metabolic requirements of proliferating and non-proliferating tumor cells.

INTRODUCTION

Alterations in cell metabolism are a characteristic of many cancers (Cairns et al, 2011), and the metabolic program of rapidly proliferating cancer cells supports the biomass production needed to produce daughter cells (Vander Heiden et al, 2009). The M2 isoform of pyruvate kinase (PKM2) is preferentially expressed in cancer, where complex regulation of its activity is important for control of cell metabolism (Mazurek, 2011; Chaneton & Gottlieb, 2012). While most studies addressing the role of PKM2 in cancer metabolism have relied on analysis of cultured cells, cell culture does not recapitulate the metabolic tumor microenvironment (Vaupel et al, 1989) or the tumor cell heterogeneity

that exists *in vivo* (Salk et al, 2010). Knockdown of PKM2 in xenograft tumors has yielded contradictory results regarding the requirement for PKM2 in tumor growth (Goldberg & Sharp, 2012; Cortes-Cros et al, 2013), further highlighting the need to investigate the role of PKM2 in the context of spontaneous tumors arising *in situ*.

Pyruvate kinase catalyzes the final step in glycolysis by transferring the phosphate from phosphoenolpyruvate (PEP) to ADP, thereby generating pyruvate and ATP. In mammals, pyruvate kinase is encoded by two genes that can each produce two isoforms. Tissue-specific promoters drive expression of the PKL or PKR isoforms from the *PKLR* gene. PKR expression is exclusive to red blood cells, while PKL is expressed primarily in the liver, with low expression in the kidney (Imamura & Tanaka, 1972; Mazurek, 2011). All other tissues studied express a product of the *PKM* gene, which generates either the PKM1 or PKM2 isoforms by including one of two mutually-exclusive exons during mRNA splicing (Noguchi et al, 1986). The regulation of PKM splicing is dependent on multiple splicing factors that bind within the PKM1 and PKM2 exons to promote or suppress their inclusion in the mature transcript (Clower et al, 2010; David et al, 2010; Wang et al, 2012). PKM1 expression is found predominantly in differentiated adult tissues with high ATP requirements, such as the heart, brain, and muscle. PKM2 is expressed during development and in many adult tissues including the spleen, lung, and all cancers and cancer cell lines studied to date (Imamura & Tanaka, 1972; Clower et al, 2010; Mazurek, 2011).

PKM1 and PKM2 differ by 22 amino acids and have distinct regulatory properties (Mazurek, 2011). While PKM1 forms a stable, constitutively active tetramer, PKM2 activity is controlled by numerous allosteric effectors and post-translational modifications that

affect its tetramer stability. Binding of fructose-1,6-bisphosphate (FBP), an upstream intermediate in glycolysis, causes PKM2 to adopt a stable, active conformation similar to that of PKM1 (Christofk et al, 2008b; Anastasiou et al, 2012). PKM2 activation by FBP can be overridden by interaction of PKM2 with tyrosine-phosphorylated proteins produced in response to growth factor signaling (Christofk et al, 2008b; Varghese et al, 2010). PKM2 activity is reduced by other post-translational modifications (Anastasiou et al, 2011; Lv et al, 2011), and metabolites other than FBP can promote PKM2 activation (Chaneton et al, 2012; Keller et al, 2012). These events illustrate the complex regulation of PKM2 activity, and although PKM2 can exist in active or inactive states as a glycolytic enzyme, the physiological significance of these states in cells or tumors is not well understood.

It is reported that PKM2 is upregulated in cancer cells and that PKM2 is the isoform expressed in all tumors. This suggests that PKM2 expression provides a selective advantage over other pyruvate kinase isoforms. Selection for PKM2 over PKM1 during xenograft tumor growth has been observed (Christofk et al, 2008a), and down-regulation of PKM2 enzymatic activity by phosphotyrosine growth signaling (Christofk et al, 2008a) (Hitosugi et al, 2009; Varghese et al, 2010), cellular redox state (Anastasiou et al, 2011) and lysine acetylation (Lv et al, 2011) has been associated with tumor growth and anabolic metabolism. Conversely, high pyruvate kinase activity due to exogenous PKM1 expression or pharmacological activation of PKM2 can impair tumor growth and decrease levels of metabolites critical for biosynthesis *in vivo* (Anastasiou et al, 2012). Taken together, these studies support a model where the ability of PKM2 to be inactivated is important for cancer cell proliferation. However, this model creates a quandary: if low pyruvate kinase activity is favored by proliferating cancer cells, why is there selection for PKM2 expression in

cancer and not inactivation of pyruvate kinase by gene mutation, deletion, or epigenetic silencing?

One possibility is that the enzymatically inactive, non-tetramer form of pyruvate kinase has an important function in cancer outside of glycolysis. Multiple non-metabolic functions unique to PKM2 have been proposed to play a vital role in cancer cell proliferation and tumor growth (Luo et al, 2011; Yang et al, 2011; Gao et al, 2012; Yang et al, 2012a; Yang et al, 2012b). In all cases, these non-metabolic functions are found only with PKM2, and not with PKM1, suggesting that one or all may be driving PKM2 selection in cancer. However, it remains unknown which, if any, are the critical functions promoting PKM2 expression in tumors.

Another possibility is that PKM2 is selected because it can exist in states of low or high enzymatic activity to allow for metabolic adaptation to different physiological situations. While reduced PKM2 activity is associated with cell proliferation, it is possible that enzyme reactivation is important for non-proliferating cancer cells that constitute a sizable fraction of tumor cells *in vivo*. If this hypothesis is correct, there must be a subpopulation of tumor cells where high pyruvate kinase activity is required. Studies of PKM2 in cancer to date have relied on exogenous protein overexpression or RNA interference of PKM2 expression in cell culture or xenograft tumor models (Christofk et al, 2008a; Anastasiou et al, 2011; Luo et al, 2011; Yang et al, 2011; Goldberg & Sharp, 2012; Yang et al, 2012a; Yang et al, 2012b; Cortes-Cros et al, 2013). Although these methods modulate PKM2 expression, they impair the endogenous, cell-autonomous regulation of pyruvate kinase.

In this study we report a conditional allele (*Pkm2*^{fl}) that allows Cre recombinase-mediated deletion of the PKM2 isoform-specific exon. Excision of *Pkm* exon 10 selectively abrogates PKM2 protein production while still allowing PKM1 splicing and protein expression. Loss of PKM2 in a mouse model of breast cancer accelerates tumor formation. Mammary tumors from *Pkm2*$^{fl/fl}$ mice show efficient deletion, suggesting that PKM2 is not absolutely required for cell proliferation or tumor growth. Only a subset of cells in *Pkm2*$^{\Delta/\Delta}$ tumors show compensatory PKM1 expression, and high PKM1 expression is anti-correlated with cell proliferation, supporting a model where PKM2 expression in tumors facilitates low pyruvate kinase activity needed for proliferation. Nonsense and missense mutations in *PKM2* occur in human tumors. These mutations include recurrent heterozygous stop mutations in *PKM* exon 10, consistent with the idea that tumors tolerate or favor low pyruvate kinase activity, lending further support to a model where regulation of PKM2 glycolytic activity is driving selection for this enzyme isoform in tumors.

RESULTS

Generation and Characterization of a Conditional PKM2 Allele

Pre-mRNA transcribed from the *Pkm* gene is spliced to produce PKM1 or PKM2 mRNA by inclusion of exon 9 or exon 10, respectively (Figure 1A). To study the role of PKM2 in tumors *in vivo*, we generated a mouse model that allows conditional deletion of the PKM2-specific exon 10. LoxP sites flanking exon 10 were introduced into the *Pkm* locus of mouse embryonic stem (ES) cells using homologous recombination (Figures 1A, 2A). These ES cells were used to generate chimeric mice, and mice generated from germline transmission of the targeted allele were crossed with mice expressing FLP recombinase to delete the neomycin resistance gene (*Neo*^{r}). Breeding of these mice resulted in

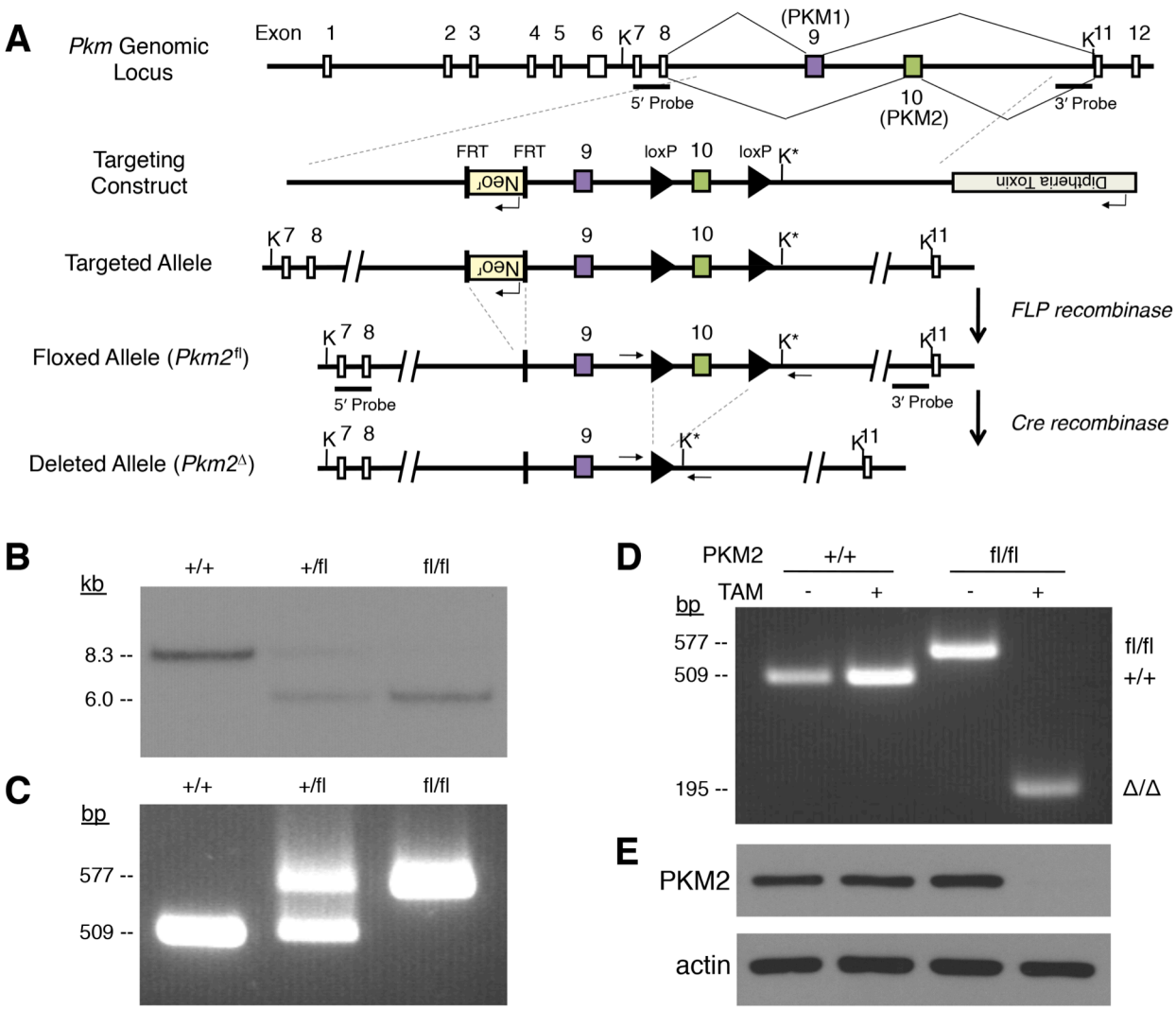

Figure 1. **Generation and Validation of PKM2 Conditional Mice.**
(A) The mouse *Pkm* locus, targeting construct, and the resulting targeted, floxed and deleted alleles. The KpnI sites used for Southern blot analysis are marked with "K", and the new KpnI site introduced by the targeting vector is marked with "K*". The locations of the 5' and 3' Probes used for Southern blot analysis are also shown. **(B)** Southern blot analysis of KpnI-digested genomic DNA using a 5' Probe. Digestion of the wild-type *Pkm* allele yields an ~8.3 kb fragment and the floxed allele yields a ~6.0 kb fragment. **(C)** PCR genotyping of genomic DNA from $Pkm2^{+/+}$, $Pkm2^{+/fl}$, and $Pkm2^{fl/fl}$ mice. Genotyping primers anneal outside of the loxP sites as indicated by arrows in panel (A), and produce amplicons of 509 bp from the $Pkm2^{+}$ allele and 577 bp from the $Pkm2^{fl}$ allele. **(D)** PCR genotyping of $Pkm2^{+/+}$ *Cre-ER* and $Pkm2^{fl/fl}$ *Cre-ER* MEFs that were treated with 4-hydroxytamoxifen (TAM) or mock treated. PCR genotyping of the $Pkm2^{\Delta}$ allele produces a 195 bp amplicon. **(E)** Western blot analysis of PKM2 protein from MEFs as specified in (D).

transmission of the PKM2 conditional allele ($Pkm2^{fl}$) in Mendelian ratios. $Pkm2^{fl/+}$ and $Pkm2^{fl/fl}$ progeny were healthy and had no overt phenotype. The presence of the $Pkm2^{fl}$ allele in adult mice was demonstrated by Southern blot (Figures 1B, 2B, 2C). To facilitate

husbandry and analysis we developed a PCR-based strategy for determination of *Pkm2* genotypes (Figure 1C). We next sought to verify that the *Pkm2*^{fl} allele allows disruption of PKM2 expression via Cre-mediated excision of *Pkm* exon 10. Mice with *Pkm2*^{fl} and inducible Cre recombinase (*Cre-ER*) alleles were crossed to produce mouse embryonic fibroblasts (MEFs) for analysis. Treatment of these MEFs with 4-hydroxytamoxifen resulted in excision of *Pkm* exon 10 in *Pkm2*$^{fl/fl}$ cells (Figure 1D), and western blot analysis showed loss of PKM2 protein in the *Pkm2*$^{\Delta/\Delta}$ MEFs (Figure 1E). These data confirm that the *Pkm2*^{fl} allele allows exon 10 deletion and disruption of PKM2 protein production.

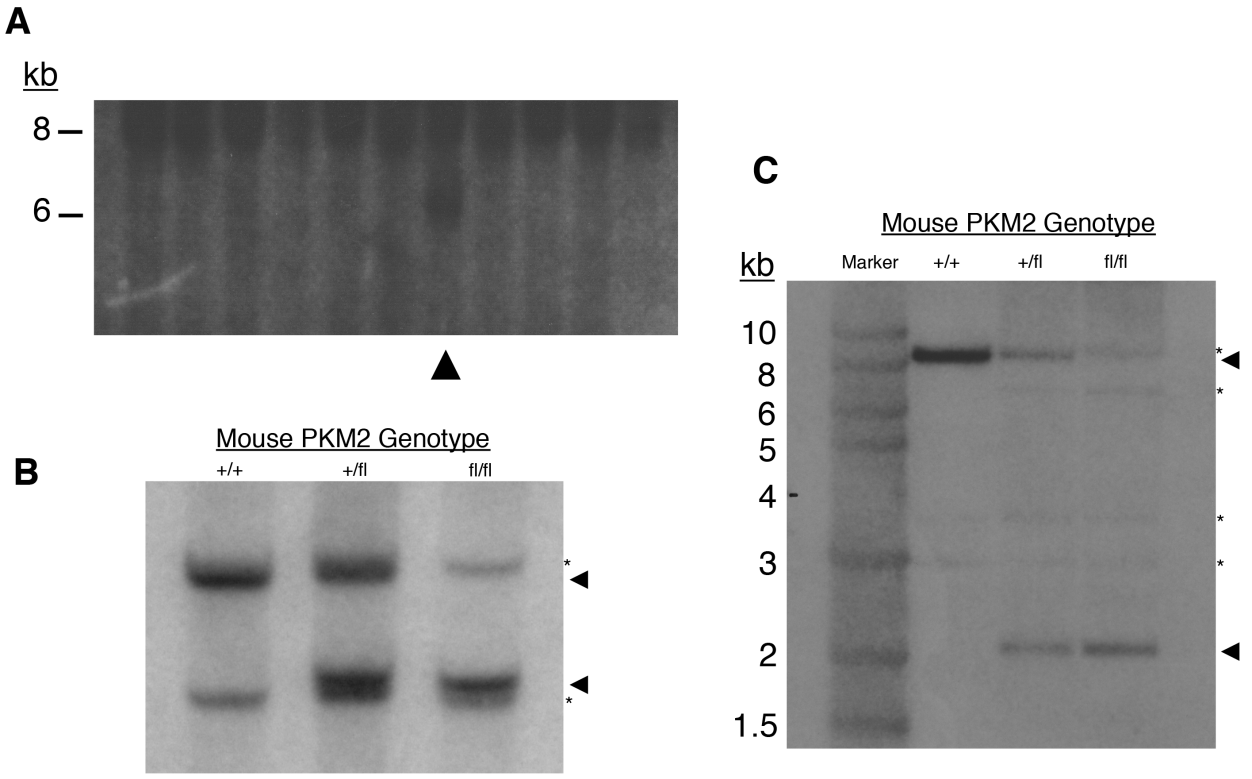

Figure 2. Characterization of the *Pkm2* flox Allele.
(A) Southern blot screening of embryonic stem cell clones for homologous recombination of the targeting construct using a 5' probe. Insertion of a novel KpnI site creates a new band at ~6.0 kb. A clone with successful integration is marked with an arrowhead. **(B)** Southern blot analysis of mouse genomic DNA using a probe on the 5' side of the inserted KpnI site; this probe is the same as was used in (A). Specific bands at 8.3 kb (*Pkm2*$^{+}$) and 6.0 kb (*Pkm2*^{fl} allele) are marked with arrowheads; nonspecific bands are marked with an asterisk (*). **(C)** Southern blot analysis of mouse genomic DNA using a probe on the 3' side of the inserted KpnI site. Specific bands at 8.3 kb (*Pkm2*$^{+}$ allele) and 2.3 kb (*Pkm2*^{fl} allele) are marked with arrowheads; nonspecific bands are marked with an asterisk (*).

PKM2 Loss Accelerates Tumor Formation and Promotes Liver Metastasis in a Mouse Model of Breast Cancer

To investigate the role of PKM2 in tumor formation, *Pkm2* conditional mice were crossed to an established model of breast cancer (Xu et al, 1999). In this model, loss of the *Brca1* tumor suppressor in *Brca1*$^{fl/fl}$ *MMTV-Cre Trp53*$^{+/-}$ mice results in mammary tumors by approximately one year of age. The *Pkm2*^{fl} allele should also undergo recombination in the Cre-expressing epithelial cells that give rise to tumors in this model. Because PKM2 has been implicated as playing an important role in cancer, we expected *Pkm2* deletion to result in fewer tumors or delayed tumor onset. Surprisingly, *Pkm2*$^{fl/fl}$ mice showed accelerated tumor-associated mortality when compared to their *Pkm2*$^{+/+}$ counterparts (Figure 3A).

We characterized tumors from *Pkm2*$^{+/+}$ and *Pkm2*$^{fl/fl}$ mice to investigate potential factors accounting for accelerated mortality in *Pkm2*$^{fl/fl}$ mice. One possibility is that PKM2 loss changes the balance of proliferation and apoptosis. Staining of tumor sections for the proliferative marker Ki-67 and for the apoptosis marker cleaved caspase-3 did not reveal overt differences between the genotypes (Figure 4A). However, macroscopic metastases were observed in livers from 3 of 5 *Pkm2*$^{fl/fl}$ mice compared to 0 of 7 *Pkm2*$^{+/+}$ mice evaluated for possible metastases (Figure 4B). To our knowledge, metastasis to the liver has not been reported in this mouse model of breast cancer.

To confirm that PKM2 is deleted in tumors from *Pkm2*$^{fl/fl}$ mice, we examined the efficiency of Cre-mediated exon 10 deletion by PCR. Qualitative deletion of *Pkm* exon 10 was observed in all tumors derived from *Pkm2*$^{fl/fl}$ mice (Figure 3B), and quantitative PCR (qPCR) analysis of tumor transcripts showed very low levels of PKM2 mRNA compared to

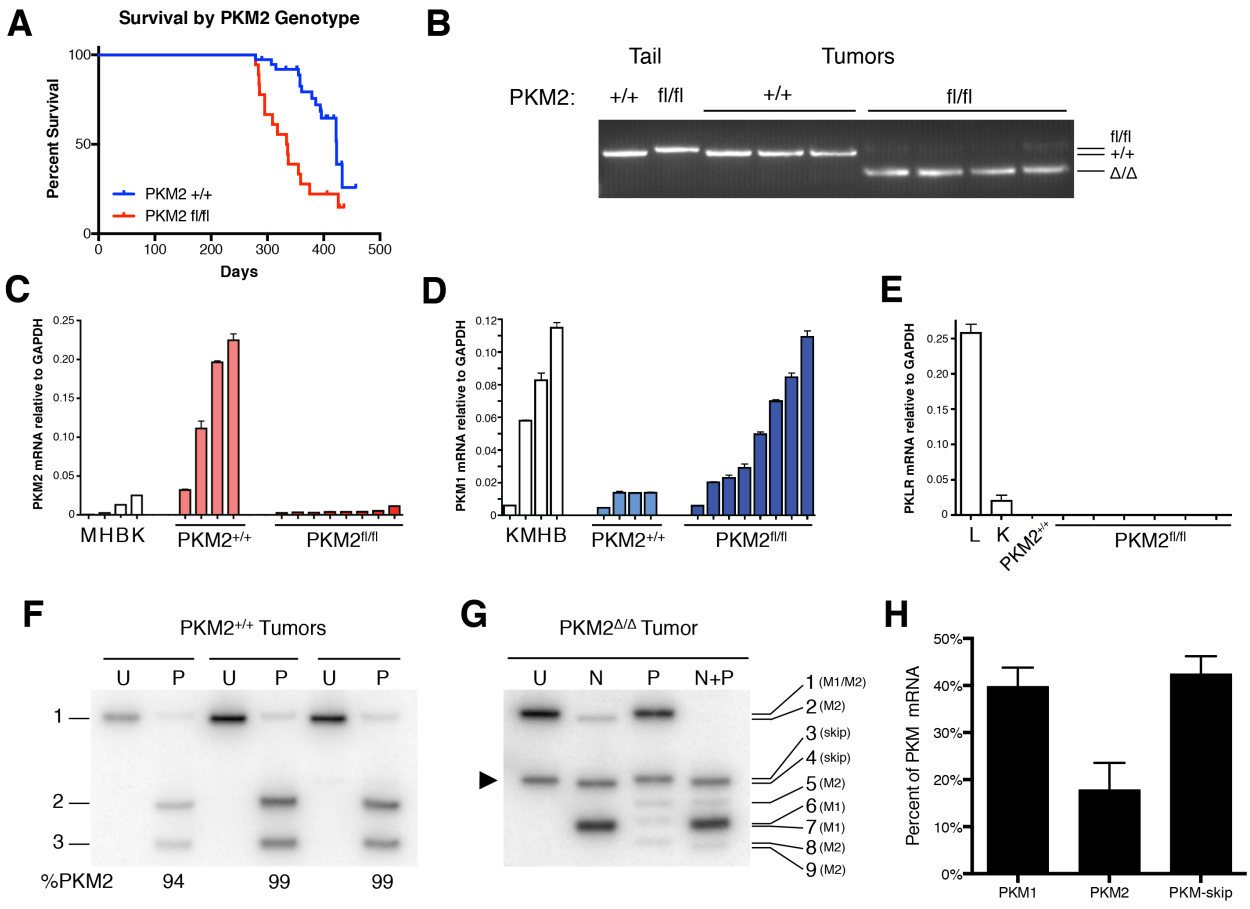

Figure 3. *Pkm* Exon 10 Deletion in Mammary Tumors Results in Accelerated Mortality and Variable Production of PKM1 mRNA.

(A) Kaplan-Meier survival curve comparing *Pkm2*$^{+/+}$ and *Pkm2*$^{fl/fl}$ mice with *Brca1*$^{fl/fl}$ *MMTV-Cre* Tr*p53*$^{+/-}$ alleles. **(B)** PCR genotyping of the *Pkm2* allele in *Pkm2*$^{+/+}$ and *Pkm2*$^{\Delta/\Delta}$ mammary tumors. Analysis of tail DNA from *Pkm2*$^{+/+}$ and *Pkm2*$^{fl/fl}$ mice is shown as a control. **(C)** PKM2 mRNA levels in *Pkm2*$^{+/+}$ and *Pkm2*$^{\Delta/\Delta}$ tumors by quantitative RT-PCR, with normal mouse tissue controls: M, muscle; H, heart; B, brain; K, kidney. **(D)** PKM1 mRNA levels in *Pkm2*$^{+/+}$ and *Pkm2*$^{\Delta/\Delta}$ tumors by quantitative RT-PCR, with normal mouse tissue controls: K, kidney; M, muscle; H, heart; B, brain **(E)** PKLR mRNA levels in *Pkm2*$^{+/+}$ and *Pkm2*$^{\Delta/\Delta}$ tumors by quantitative RT-PCR, with normal mouse tissue controls: L, liver; K, kidney. **(F)** Autoradiograph of Uncut [U] and PstI [P] digested *Pkm* cDNA amplicons. Uncut PKM1 and PKM2 amplicons are of identical length (band 1). PstI digests only the PKM2 amplicon to produce bands 2 and 3. Results from three representative *Pkm2*$^{+/+}$ tumors are shown with quantification. See Figures 4C and E for a schematic of how each band is generated. **(G)** Autoradiograph of Uncut [U] and digested PKM cDNA amplicons from a representative *Pkm2*$^{\Delta/\Delta}$ tumor. Uncut PKM1 and PKM2 amplicons are of identical length (band 1), and the amplicon corresponding to the PKM-skip mis-spliced product is marked with an arrowhead (band 3). NcoI [N] digests the PKM1 amplicon and PstI [P] digests the PKM2 amplicon. Figures 4C,D,F show how each band is generated. **(H)** Quantification of PKM splicing in *Pkm2*$^{\Delta/\Delta}$ tumors, as determined from autoradiographs as in (G). Data are displayed as means ± s.e.m, n=4.

wild-type tumors (Figure 3C). Because *Pkm2*$^{\Delta/\Delta}$ tumor cells can potentially generate PKM1 protein by inclusion of exon 9 during mRNA splicing, we quantified PKM1 mRNA levels by qPCR. Some *Pkm2*$^{\Delta/\Delta}$ tumors had low PKM1 expression at levels similar to *Pkm2*$^{+/+}$ tumors, while others had PKM1 mRNA levels approaching those found in the brain, a tissue that normally expresses PKM1 (Figure 3D). To determine whether *Pkm2*$^{\Delta/\Delta}$ tumors had compensatory expression of the other two pyruvate kinase isoforms, PKL or PKR, we examined tumor PKLR mRNA levels by qPCR. We did not observe any mRNA expression from the *Pklr* gene in tumors of any genotype, suggesting that protein derived from the *Pkm* gene was the only pyruvate kinase present (Figure 3E).

PKM2 Deletion Results in Production of Either PKM1 or a Mis-spliced mRNA

We further characterized PKM mRNA splicing in tumors from *Pkm2*$^{+/+}$ and *Pkm2*$^{fl/fl}$ mice. Exons 9 and 10 are of identical length but contain unique restriction enzyme sites that allow for relative quantification of PKM1 and PKM2 transcript levels (Clower et al, 2010; David et al, 2010). The alternatively spliced region between PKM exons 8 and 11 was amplified from *Pkm2*$^{+/+}$ and *Pkm2*$^{\Delta/\Delta}$ tumor cDNA and digested for analysis (Figures 4C, 4E). Consistent with the qPCR results, PKM2 was the dominant transcript found in *Pkm2*$^{+/+}$ tumors (Figure 3F). *Pkm2*$^{\Delta/\Delta}$ tumors displayed an overall decrease in PKM2 mRNA, with PKM1 message comprising a larger fraction of the total *Pkm*-derived mRNAs (Figure 3G); however, this analysis also revealed an additional PKM splice variant not found in wild type tumors (compare leftmost lanes of Figures 2F and 2G). This mRNA species accounted for approximately 40% of the PKM transcript in *Pkm2*$^{\Delta/\Delta}$ tumors (Figure 3H), was identified by sequencing to result from the splicing of exon 8 to exon 11 (Figures 4D, 4F, 4G), and is hereafter referred to as PKM-skip.

Splicing of PKM pre-mRNA to produce PKM2 transcript involves repression of exon 9 inclusion and activation of exon 10 inclusion by the binding of specific splicing factors to sequences within the alternatively spliced exons (Clower et al, 2010; David et al, 2010; Wang et al, 2012). Thus, the absence of exon 10 together with repression of exon 9 likely explains the presence of the PKM-skip mRNA species in *Pkm2*$^{\Delta/\Delta}$ tumors (Chen et al, 2012). Splicing of PKM exon 8 to 11 causes a frameshift at the exon 8-11 junction which results in 38 missense codons and a premature stop codon more than 500 base pairs upstream of the exon 11-12 junction (Figure 4G). Aberrant splicing of PKM transcript to create a premature stop codon upstream of the exon 11-12 junction leads to message degradation by nonsense-mediated decay (Chen et al, 2012).

Figure 4. Analysis of Tumor Histology and PKM Splicing Following Exon 10 Excision.
(A) Staining of *Pkm2*$^{+/+}$ and *Pkm2*$^{\Delta/\Delta}$ tumors for Ki-67 and cleaved caspase 3 (CC3). Scale bars represent 200 μm. **(B)** Histology showing livers from a *Pkm2*$^{+/+}$ *Brca1*$^{fl/fl}$ *MMTV-Cre Trp53*$^{+/-}$ mouse with a breast tumor (left panels), and a *Pkm2*$^{fl/fl}$ *Brca1*$^{fl/fl}$ *MMTV-Cre Trp53*$^{+/-}$ mouse with a breast tumor (right panels). Metastases are marked with arrowheads. Scale bars represent 500 μm and 20 μm in the low and high magnification images, respectively. **(C)** Diagram showing normal alternative PKM splicing (top) and possible resulting amplicons used in RT-PCR analysis (bottom). Inclusion of exon 9 with NcoI sites yields the PKM1 transcript and inclusion of exon 10 with a PstI site yields the PKM2 transcript. RT-PCR amplification of spliced PKM transcripts using PCR primers in exons 8 and 11 (depicted as small arrows, top) produces amplicons of identical length that can be distinguished by different restriction sites (PstI & NcoI). **(D)** Diagram showing PKM splicing following exon 10 deletion (top) and resulting amplicons (bottom). Inclusion of exon 9 creates PKM1 transcript, while exclusion of exon 9 in the absence of exon 10 results in PKM-skip transcript. RT-PCR amplification of these spliced transcripts using primers annealing to exons 8 and 11 (depicted as small arrows, top) results in the amplicons depicted (bottom). These amplicons lack any PstI sites, and the location of NcoI restriction sites is shown. **(E)** The amplicons and digestion fragments as numbered in Figure 3F. The PstI restriction site is marked with a "P". **(F)** The amplicons and digestion fragments as numbered in Figure 3G. The NcoI and PstI restriction sites are marked with "N" and "P", respectively. **(G)** Alignment of partial PKM2 and PKM-skip cDNA sequences in the region including parts of exons 8 to 11 (top). A diagram of the PKM-skip message showing the frameshift at the exon 8-11 junction, the location of the stop codon, and the distance to the following exon-exon junction is also shown.

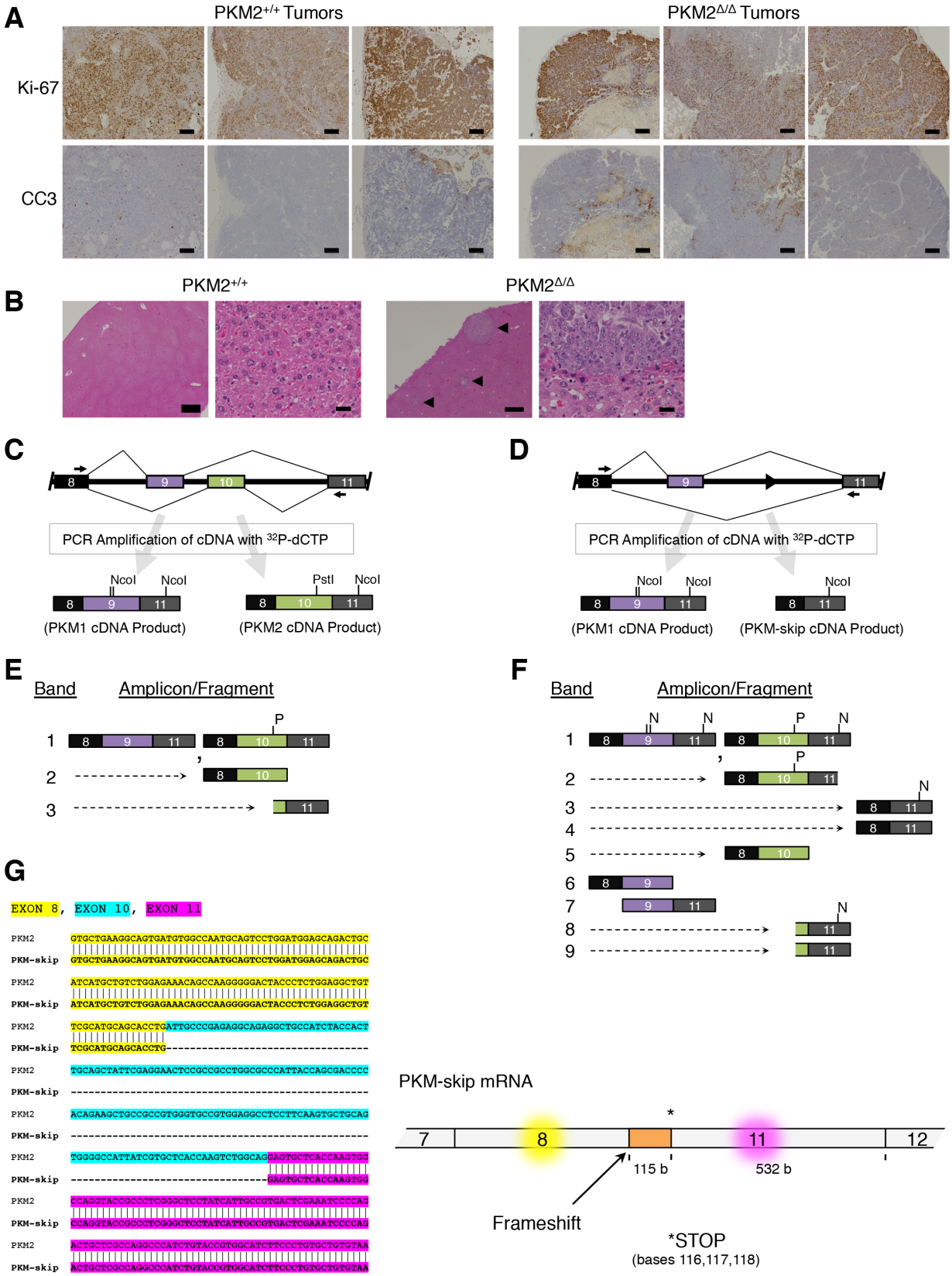
A
PKM2+/+ Tumors
PKM2Δ/Δ Tumors
Ki-67
CC3
B
PKM2+/+
PKM2Δ/Δ
C
PCR Amplification of cDNA with 32P-dCTP
NcoI
NcoI
PstI
NcoI
(PKM1 cDNA Product)
(PKM2 cDNA Product)
D
PCR Amplification of cDNA with 32P-dCTP
NcoI
NcoI
NcoI
(PKM1 cDNA Product)
(PKM-skip cDNA Product)
E
Band
Amplicon/Fragment
F
Band
Amplicon/Fragment
G
EXON 8, EXON 10, EXON 11
PKM2 GTGCTGAAGGCAGTGATGTGGCCAATGCAGTCCTGGATGGAGCAGACTGC
PKM-skip GTGCTGAAGGCAGTGATGTGGCCAATGCAGTCCTGGATGGAGCAGACTGC
PKM2 ATCATGCTGTCTGGAGAAACAGCCAAGGGGGACTACCCTCTGGAGGCTGT
PKM-skip ATCATGCTGTCTGGAGAAACAGCCAAGGGGGACTACCCTCTGGAGGCTGT
PKM2 TCGCATGCAGCACCTGATTGCCCGAGAGGCAGAGGCTGCCATCTACCACT
PKM-skip TCGCATGCAGCACCTG----------
PKM2 TGCAGCTATTCGAGGAACTCCGCCGCCTGGCGCCCATTACCAGCGACCCC
PKM-skip ----------
PKM2 ACAGAAGCTGCCGCCGTGGGTGCCGTGGAGGCCTCCTTCAAGTGCTGCAG
PKM-skip ----------
PKM2 TGGGGCCATTATCGTGCTCACCAAGTCTGGCAGGAGTGCTCACCAAGTGG
PKM-skip ----------GAGTGCTCACCAAGTGG
PKM2 CCAGGTACCGCCCTCGGGCTCCTATCATTGCCGTGACTCGAAATCCCCAG
PKM-skip CCAGGTACCGCCCTCGGGCTCCTATCATTGCCGTGACTCGAAATCCCCAG
PKM2 ACTGCTCGCCAGGCCCATCTGTACCGTGGCATCTTCCCTGTGCTGTGTAA
PKM-skip ACTGCTCGCCAGGCCCATCTGTACCGTGGCATCTTCCCTGTGCTGTGTAA
PKM-skip mRNA
7
8
11
12
115 b
532 b
Frameshift
*STOP
(bases 116,117,118)

PKM2 Deletion results in Variable PKM1 Protein Levels but No PKM-skip Protein

Because deletion of *Pkm* exon 10 does not always lead to exon 9 inclusion and production of PKM1 mRNA, and because PKM1 mRNA levels varied widely across tumors, we determined the effects of *Pkm2* deletion on pyruvate kinase protein levels in *Pkm2*$^{\Delta/\Delta}$ tumors. Western blotting of tumor lysates confirmed the loss of PKM2 protein in *Pkm2*$^{\Delta/\Delta}$ tumors (Figure 5A). Variable amounts of PKM1 protein were observed in *Pkm2*$^{\Delta/\Delta}$ tumor lysates, and overall expression of pyruvate kinase was decreased in *Pkm2*$^{\Delta/\Delta}$ tumors relative to *Pkm2*$^{+/+}$ tumors, such that even tumors with the highest PKM1 expression had lower levels than PKM1-expressing skeletal muscle.

We next determined whether the PKM-skip mRNA generates a protein product in *Pkm2*$^{\Delta/\Delta}$ tumors. Wild type PKM1 and PKM2 are both 531 residues long with subunit masses of approximately 58 kD, while the predicted PKM-skip protein is 418 residues long with a predicted mass of 45 kD (Figure 6A). To verify that we could detect PKM-skip protein via western blot, PKM-skip cDNA was expressed in *E. coli* with an N-terminal 6x-His tag and purified using affinity chromatography. The same approach is used to produce PKM2 protein that is active both as a glycolytic enzyme (Dombrauckas et al, 2005; Anastasiou et al, 2012) and as a putative protein kinase (Gao et al, 2012; Yang et al, 2012a). Some PKM-skip product was recovered from the soluble fraction after bacterial

Figure 5. *Pkm* Exon 10 Deletion in Mammary Tumors Leads to Variable Expression of PKM1. **(A)** PKM2, PKM1, and total PKM protein levels in *Pkm2*$^{+/+}$ and *Pkm2*$^{\Delta/\Delta}$ tumors. Muscle and 293T cell lysates serve as PKM1 and PKM2 protein controls, respectively, with GAPDH as loading control. **(B)** PKM protein in *Pkm2*$^{+/+}$ and *Pkm2*$^{\Delta/\Delta}$ tumors visualized using a monoclonal anti-PKM antibody with an epitope common to PKM1 and PKM2. Muscle and 293T cell lysates serve as PKM1 and PKM2 protein controls, respectively. The size of full-length PKM-skip is marked with an arrowhead and PKM-skip degradation products are marked with asterisks. This blot was intentionally over-exposed. **(C)** Histology and staining of one *Pkm2*$^{+/+}$ tumor and three *Pkm2*$^{\Delta/\Delta}$ tumors for PKM2 or PKM1. Scale bars represent 200 μm. **(D)** High power micrographs of the same tumors as in (C). Scale bars represent 20 μm.

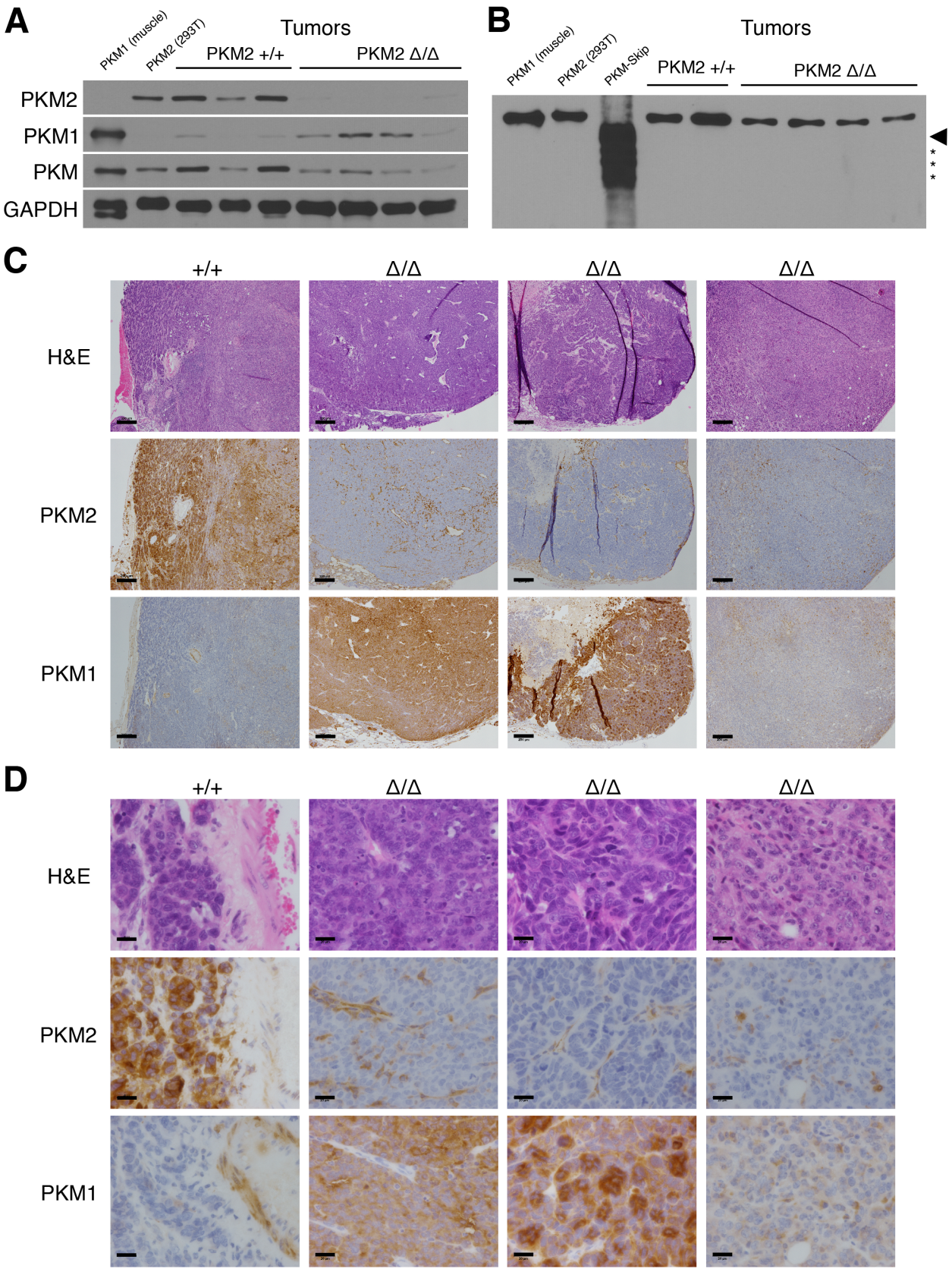
A
PKM1 (muscle)
PKM2 (293T)
Tumors
PKM2 +/+
PKM2 Δ/Δ
PKM2
PKM1
PKM
GAPDH
B
PKM1 (muscle)
PKM2 (293T)
PKM-Skip
Tumors
PKM2 +/+
PKM2 Δ/Δ
C
+/+
Δ/Δ
Δ/Δ
Δ/Δ
H&E
PKM2
PKM1
D
+/+
Δ/Δ
Δ/Δ
Δ/Δ
H&E
PKM2
PKM1

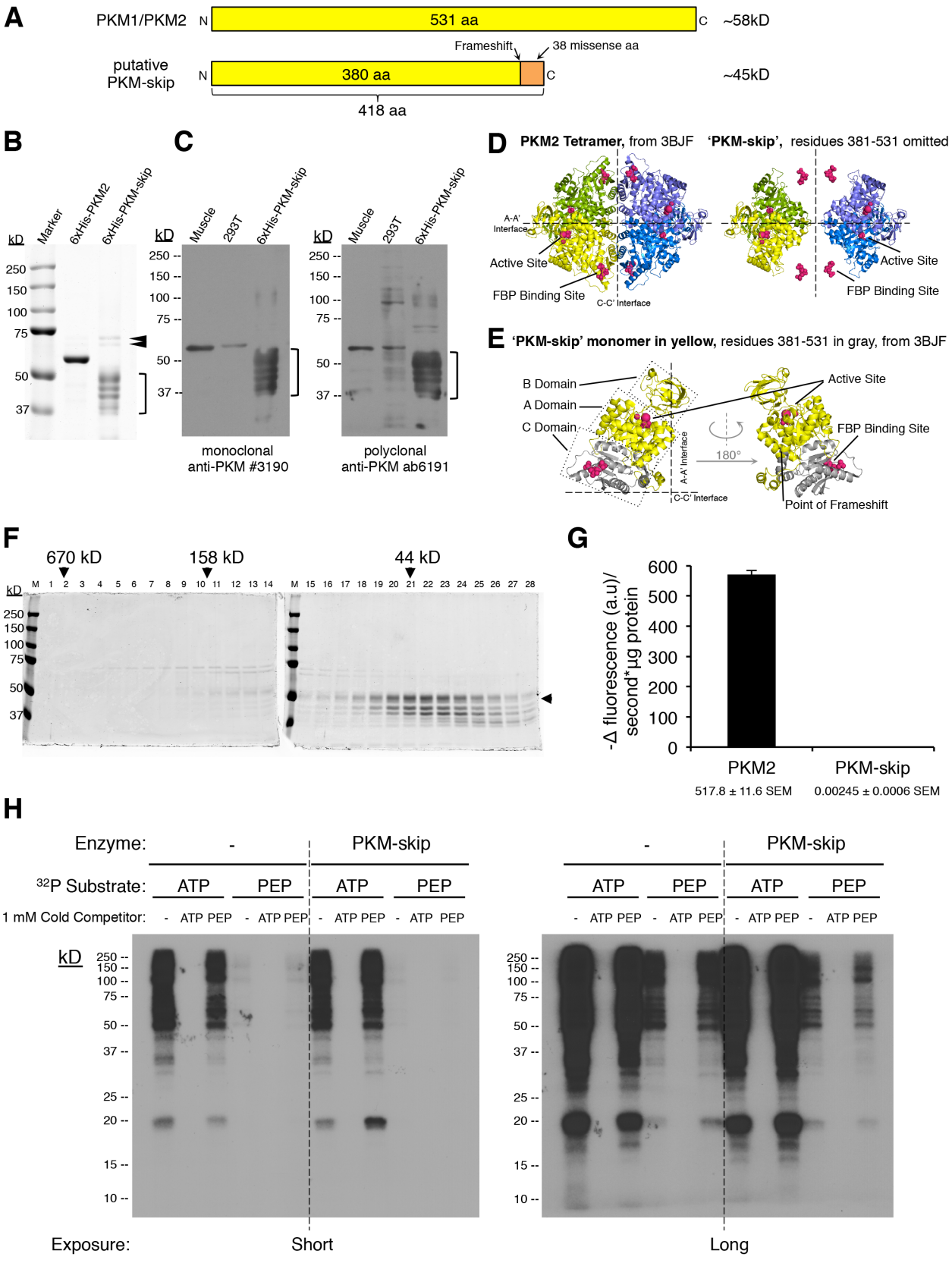
A
PKM1/PKM2
N
531 aa
C
~58kD
Frameshift
38 missense aa
putative
PKM-skip
380 aa
~45kD
418 aa
B
kD
Marker
6xHis-PKM2
6xHis-PKM-skip
250
150
100
75
50
37
C
Muscle
293T
6xHis-PKM-skip
monoclonal
anti-PKM #3190
polyclonal
anti-PKM ab6191
D
PKM2 Tetramer, from 3BJF
'PKM-skip', residues 381-531 omitted
A-A' Interface
Active Site
FBP Binding Site
C-C' Interface
E
'PKM-skip' monomer in yellow, residues 381-531 in gray, from 3BJF
B Domain
A Domain
C Domain
180°
Point of Frameshift
F
670 kD
158 kD
44 kD
G
-Δ fluorescence (a.u)/ second*µg protein
600
500
400
300
200
100
0
PKM2
PKM-skip
517.8 ± 11.6 SEM
0.00245 ± 0.0006 SEM
H
Enzyme:
PKM-skip
32P Substrate:
ATP
PEP
1 mM Cold Competitor:
Exposure:
Short
Long

lysis; however, the expected protein was accompanied by a series of smaller products consistent with partial degradation of an unstable protein in *E. coli* (Figure 6B). Both the full length and smaller polypeptides were recognized by two different anti-PKM antibodies during western blot analysis (Figure 6C). We next performed western blot analysis of tumor lysates using recombinant PKM-skip protein as a control; however, we failed to detect a band smaller than the full-length protein in any tumors (Figure 5B). These data show that PKM-skip protein is not present in appreciable quantities in *Pkm2*$^{\Delta/\Delta}$ tumors.

Figure 6. Analysis of *Pkm2*$^{\Delta/\Delta}$ Mouse Mammary Tumors.
(A) Schematic showing relative lengths and molecular masses of PKM1 and PKM2 protein (top), as well as the putative PKM-skip protein (bottom). **(B)** Recombinant 6x-His-PKM2 and 6x-His-PKM-skip protein preparations were separated via SDS-PAGE and stained with Coomassie blue. 6x-His-PKM-skip protein and degradation fragments are indicated with a bracket; arrowheads indicate unrelated contaminating bacterial proteins. **(C)** Western blots showing that two separate anti-PKM antibodies recognize recombinant PKM-skip protein. The location of 6x-His-PKM-skip protein and degradation fragments is indicated with a bracket. The monoclonal antibody recognizes a defined epitope around G200. **(D)** Ribbon structure of a PKM2 tetramer (left) from the PDB (3BJF) (Christofk et al, 2008b), and the same structure shown when residues missing in the putative PKM-skip protein are omitted (right). The PKM-skip truncation eliminates the endogenous PKM dimer-dimer interface and the binding site of the allosteric activator fructose-1,6-bisphosphate (FBP). Ligands found at the active site and FBP binding site are shown in magenta. **(E)** The ribbon structure of one subunit of a PKM2 tetramer is shown in gray, with residues retained in the putative PKM-skip protein highlighted in yellow. The A, B, and C domains are boxed with a dashed line. Ligands found at the active site and FBP binding site are shown in magenta. **(F)** A 6xHis-PKM-skip protein preparation was subjected to size exclusion chromatography, and collected fractions were analyzed by SDS-PAGE and Coomassie blue staining. The full-length 6xHis-PKM-skip protein is marked by an arrowhead on the right side of the panel; arrowheads at the top of the panel indicate fractions corresponding to the eluent volume of the indicated molecular weight standards. Marker lanes are indicated with an "M". **(G)** Pyruvate kinase activity of recombinant 6xHis-PKM2 and 6xHis-PKM-skip, as determined using an LDH coupled assay. Values are reported as means ± s.e.m., n=3. **(H)** The protein kinase activity of PKM-skip protein with nuclear lysate as a substrate was investigated using the conditions indicated. Reacted lysate was analyzed by SDS-PAGE and autoradiography. Two autoradiographs of the same experiment are shown to allow visualization of proteins phosphorylated in the presence of radioactive ATP and PEP. Similar labeling patterns are observed with each substrate, and the labeling is the same with and without PKM-skip protein. In addition, cold ATP effectively competes for all phosphorylation events observed, while cold PEP is unable to compete for any of these events. This suggests transfer of phosphate from radioactive PEP to ATP is responsible for any phosphorylation events observed.

Because small amounts of catalytic activity are potentially meaningful, we considered that levels of putative PKM-skip below our detection limit might retain some PKM2 activity. By comparison with published PKM2 protein structures (Dombrauckas et al, 2005; Christofk et al, 2008b), PKM-skip protein is predicted to lack the FBP binding site and the dimer-dimer interface found in the native PKM2 tetramer (Figure 6D). However, with a few amino acid changes the predicted PKM-skip monomer retains the primary structure necessary to produce the domains hosting the active site (Figure 6E). We thus evaluated whether recombinant PKM-skip retained catalytic activity and whether this protein could form dimers or tetramers. Using size exclusion chromatography, we found that recombinant PKM-skip eluted at volumes consistent with it being a population of 45 kD or smaller monomers (Figure 6F). PKM-skip protein was >230,000-fold less active per microgram than recombinant PKM2 for glycolytic pyruvate kinase activity (Figure 6G) and had no detectable protein kinase activity (Figure 6H), suggesting that PKM-skip protein would not have meaningful catalytic activity even if it were present in *Pkm2*$^{\Delta/\Delta}$ tumors. Taken together, these data suggest that PKM-skip protein is not a confounding factor in the analysis of *Pkm2*$^{\Delta/\Delta}$ tumors, and that *Pkm* exon 10 deletion effectively precludes PKM2 protein production while still allowing cells to express PKM1.

Expression of PKM1 in PKM2 Knockout Tumors is Spatially Heterogeneous

To understand which cells in *Pkm2*$^{\Delta/\Delta}$ tumors express PKM1, we performed immunohistochemistry (IHC) on fixed tumor sections. Consistent with previous reports (Christofk et al, 2008a; Mazurek, 2011), most cells in *Pkm2*$^{+/+}$ tumors stained for PKM2, but not for PKM1 (Figures 5C, 5D). *Pkm2*$^{\Delta/\Delta}$ tumors showed PKM2 staining only in adipose or other stromal tissue associated with the tumor, with no PKM2 staining in tumor cells.

PKM1 staining was variable and was not observed in every tumor cell in *Pkm2*$^{\Delta/\Delta}$ tumors (Figures 5C, 5D). Taken together, these data suggest that PKM2 is not required by all tumor cells and that there is a differential requirement for pyruvate kinase among different tumor cell populations.

Generation of Tumor Cell Lines Selects for PKM2 Expression

To further characterize *Pkm2*$^{\Delta/\Delta}$ tumor cells, we derived cell lines from mammary tumors arising in *Pkm2*$^{+/+}$ and *Pkm2*$^{fl/fl}$ *Brca*$^{fl/fl}$ *MMTV-Cre Trp53*$^{+/-}$ mice. Generation of cell

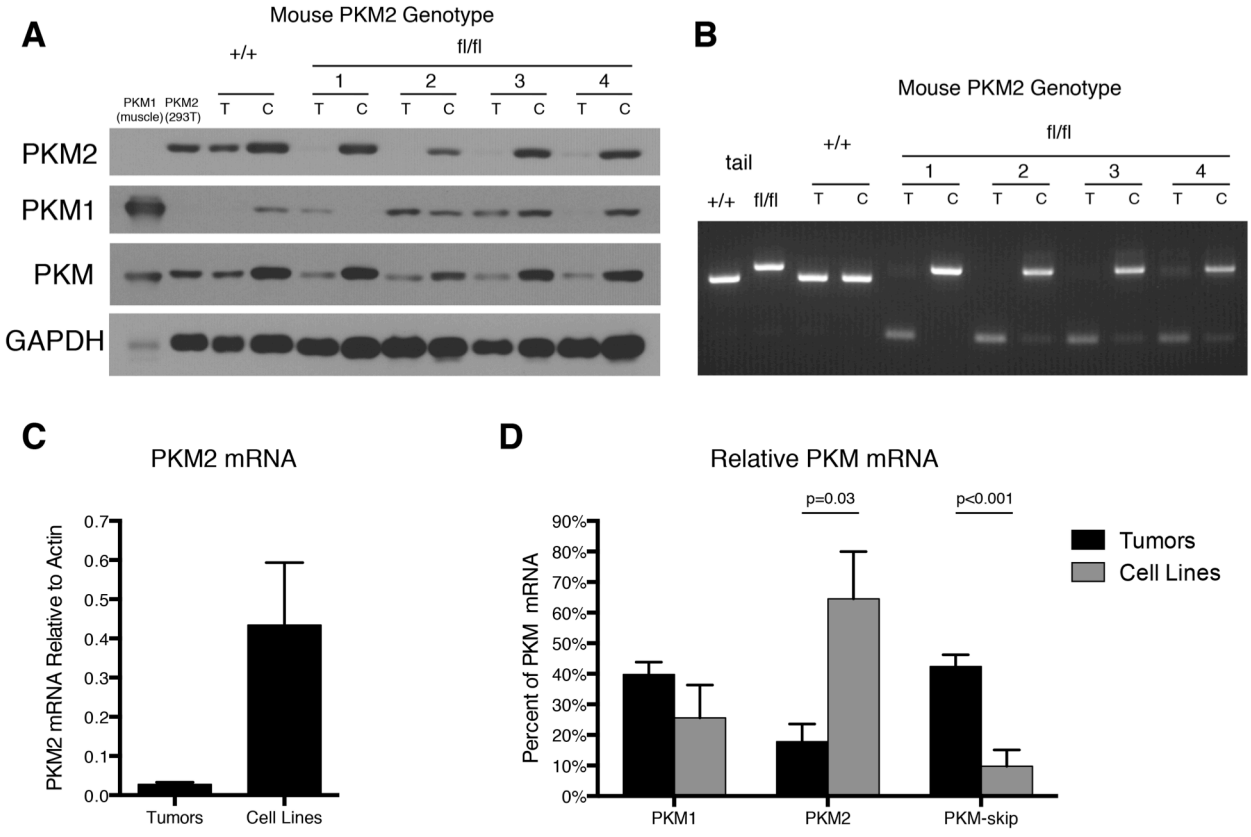

Figure 7. Cell Lines Derived from *Pkm2*$^{\Delta/\Delta}$ Mammary Tumors Retain Expression of PKM2. **(A)** PKM2, PKM1, and total PKM protein levels in tumors [T] from *Pkm2*$^{+/+}$ and *Pkm2*$^{fl/fl}$ mice and their derivative cell lines [C]. Muscle and 293T cell lysates serve as PKM1 and PKM2 protein controls, respectively, with GAPDH as loading control. **(B)** PCR genotyping of tumors [T] from *Pkm2*$^{+/+}$ and *Pkm2*$^{fl/fl}$ mice and their derivative cell lines [C]. Analysis of tail DNA from *Pkm2*$^{+/+}$ and *Pkm2*$^{fl/fl}$ mice is shown as control. **(C)** PKM2 mRNA levels in *Pkm2*$^{\Delta/\Delta}$ tumors and derivative cell lines by quantitative RT-PCR. Data are shown as means ± s.e.m, n=4 tumors, n=3 cell lines. **(D)** Quantification of PKM splicing in *Pkm2*$^{\Delta/\Delta}$ tumor-derived cell lines and parent tumors determined as shown in Figure 5G. Data are displayed as means ± s.e.m, n=4 tumors, n=4 cell lines. P-values were obtained by Student's t-test.

lines from *Pkm2*$^{\Delta/\Delta}$ tumors took several weeks, and in all cases the cell lines showed high levels of PKM2 protein expression despite the deletion of PKM2 observed in the parental tumors (Figure 7A). PCR genotyping of the cell lines showed retention of at least one *Pkm2*^{fl} allele in all cases (Figure 7B), suggesting that the transition to tissue culture selected for rare tumor cells that had not undergone recombination at both *Pkm* loci. In sharp contrast to the tumors from which they were derived, the tumor cell lines showed increased PKM2 mRNA levels (Figures 7C, 7D) and a reduction in PKM-skip transcript (Figure 7D).

Introduction of inducible Cre-recombinase (*Cre-ER*^{T2}) into two tumor cell lines allowed for deletion of the remaining *Pkm2*^{fl} allele *in vitro* (Figure 8A), and we found that

Figure 8. Effects of PKM2 Deletion on Cells.
(A) Genotyping PCR of two *Pkm2*$^{fl/\Delta}$ *Cre-ER*^{T2} tumor cell lines showing *PKM2* exon 10 excision following two treatments with 1 μm 4-hydroxytamoxifen (4-OHT). **(B)** The oxygen consumption rate of tumor cells with or without PKM2 expression was measured using a Clark electrode. An inhibitor of fatty acid β-oxidation, *R*-etomoxir, was applied at 50 μM where indicated. Values are reported as means ± s.e.m., n=4. **(C)** Effect of PKM2 deletion in Tumor Cell Line 1 on response to hypoxia. Data are reported as HRE-luciferase induction normalized to control Renilla luciferase expression. **(D)** Effect of PKM2 deletion in Tumor Cell Line 2 on response to hypoxia. Data are reported as HRE-luciferase induction normalized to control Renilla luciferase expression. **(E)** Effect of PKM2 deletion in Cell Lines 1 and 2 on Glut1 induction in response to hypoxia. Glut1 transcript levels were determined relative to β-actin by qPCR. **(F)** Effect of PKM2 deletion in Cell Lines 1 and 2 on PDK1 induction in response to hypoxia. PDK1 transcript levels were determined relative to β-actin by qPCR. **(G)** Effect of PKM2 deletion in Cell Lines 1 and 2 on LDHA induction in response to hypoxia. LDHA transcript levels were determined relative to β-actin by qPCR. **(H)** Effect of PKM2 deletion on β-catenin nuclear function in Cell Line 1. Cells were treated with 10 mM LiCl to stabilize β-catenin, or with 10 mM NaCl as control. The TOPFLASH or β-catenin-insensitive FOPFLASH luciferase reporters were co-transfected with a control Renilla luciferase construct. Reporter luciferase induction was determined relative to Renilla luciferase control, and data are presented as fold induction due to lithium treatment. **(I)** Effect of PKM2 deletion on β-catenin nuclear function in Cell Line 2. Cells were treated with 10 mM LiCl to stabilize β-catenin, or with 10 mM NaCl as control. The TOPFLASH luciferase reporter was co-transfected with a control Renilla luciferase construct. Reporter luciferase induction was determined relative to Renilla luciferase control, and data are presented as fold induction due to lithium treatment. **(J)** Effect of PKM2 deletion on induction of Axin2, a β-catenin target gene, in response to 10 mM LiCl treatment, using Cell Line 2. 10 mM NaCl was used as control. Axin2 transcript levels were determined via qPCR and are reported relative to β-actin. **(C-J)** All values are reported as means ± s.e.m., n=3.

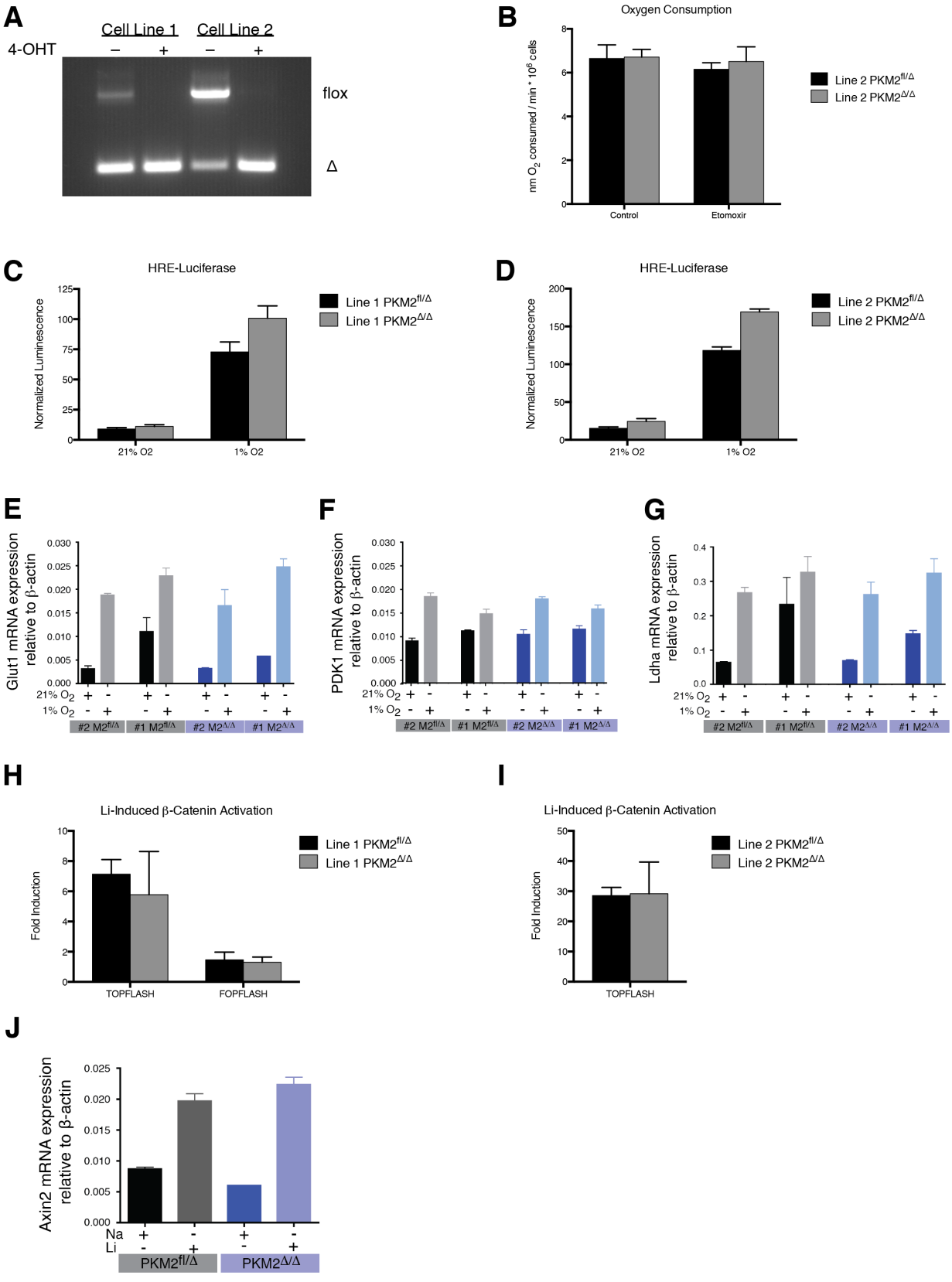
A
Cell Line 1
Cell Line 2
4-OHT
– + – +
flox
Δ
B
Oxygen Consumption
nm O2 consumed / min * 10^6 cells
Control
Etomoxir
Line 2 PKM2fl/Δ
Line 2 PKM2Δ/Δ
C
HRE-Luciferase
Normalized Luminescence
21% O2
1% O2
Line 1 PKM2fl/Δ
Line 1 PKM2Δ/Δ
D
HRE-Luciferase
Normalized Luminescence
21% O2
1% O2
Line 2 PKM2fl/Δ
Line 2 PKM2Δ/Δ
E
Glut1 mRNA expression relative to β-actin
21% O2
1% O2
#2 M2fl/Δ
#1 M2fl/Δ
#2 M2Δ/Δ
#1 M2Δ/Δ
F
PDK1 mRNA expression relative to β-actin
21% O2
1% O2
#2 M2fl/Δ
#1 M2fl/Δ
#2 M2Δ/Δ
#1 M2Δ/Δ
G
Ldha mRNA expression relative to β-actin
21% O2
1% O2
#2 M2fl/Δ
#1 M2fl/Δ
#2 M2Δ/Δ
#1 M2Δ/Δ
H
Li-Induced β-Catenin Activation
Fold Induction
TOPFLASH
FOPFLASH
Line 1 PKM2fl/Δ
Line 1 PKM2Δ/Δ
I
Li-Induced β-Catenin Activation
Fold Induction
TOPFLASH
Line 2 PKM2fl/Δ
Line 2 PKM2Δ/Δ
J
Axin2 mRNA expression relative to β-actin
Na
Li
PKM2fl/Δ
PKM2Δ/Δ

PKM2 loss did not affect the rate of oxygen consumption in these cells or cause dependence on β-oxidation (Figure 8B). We also investigated whether non-glycolytic functions of PKM2 were active in these cells. PKM2 was not required for hypoxia- or β-catenin-induced gene expression (Figures 8C–8J), suggesting that maintenance of those functions was not the basis for the outgrowth of rare PKM2-expressing cells during cell line establishment. Thus, despite selection for PKM2 during cell line generation, a functional PKM2 allele was not required for *in vitro* proliferation.

Selection Against PKM1 Expression, but Not for PKM2 Expression, in Allograft Tumors

Given that tissue culture conditions appear to select for PKM2-expressing cells, we focused on *in vivo* analysis of *Pkm2*$^{\Delta/\Delta}$ tumor-derived cell lines to examine the consequences of constitutive PKM1 or PKM2 expression on tumor growth in the absence of endogenous PKM2. A representative cell line was stably infected with *Cre-ER*^{T2} and either no cDNA (empty vector control), FLAG-PKM1, or FLAG-PKM2. The presence of a FLAG-epitope tag does not impair the ability of exogenously expressed PKM2 to rescue any known function of the protein (Christofk et al, 2008a; Christofk et al, 2008b; Yang et al, 2011). The cells were treated to delete the remaining *Pkm2*^{fl} allele and injected subcutaneously into nude mice. While the control cells and the cells expressing FLAG-PKM2 were competent to form tumors, the cells expressing FLAG-PKM1 were not (Figure 9A). IHC using an anti-FLAG antibody showed that the FLAG-PKM1 expressing cells were

Figure 9. Allograft Tumor Growth Does Not Select for PKM2 Expression.
(A) Growth curves of tumors formed by *Pkm2*$^{\Delta/\Delta}$ cells expressing empty vector, FLAG-PKM1, or FLAG-PKM2 following injection into nude mice. **(B)** Representative anti-FLAG and H&E staining of tumor sections from the allograft experiment shown in (A). Scale bars represent 200 μm and 20 μm at low and high magnification, respectively. **(C)** Anti-PKM2 and H&E staining of a representative *Pkm2*$^{\Delta/\Delta}$ *empty vector* tumor and three *Pkm2*$^{\Delta/\Delta}$ *FLAG-PKM2* tumors. The top right *Pkm2*$^{\Delta/\Delta}$ *FLAG-PKM2* tumor is the same *Pkm2*$^{\Delta/\Delta}$ *FLAG-PKM2* tumor shown in (B). Scale bars represent 200 μm and 20 μm at low and high magnification, respectively.

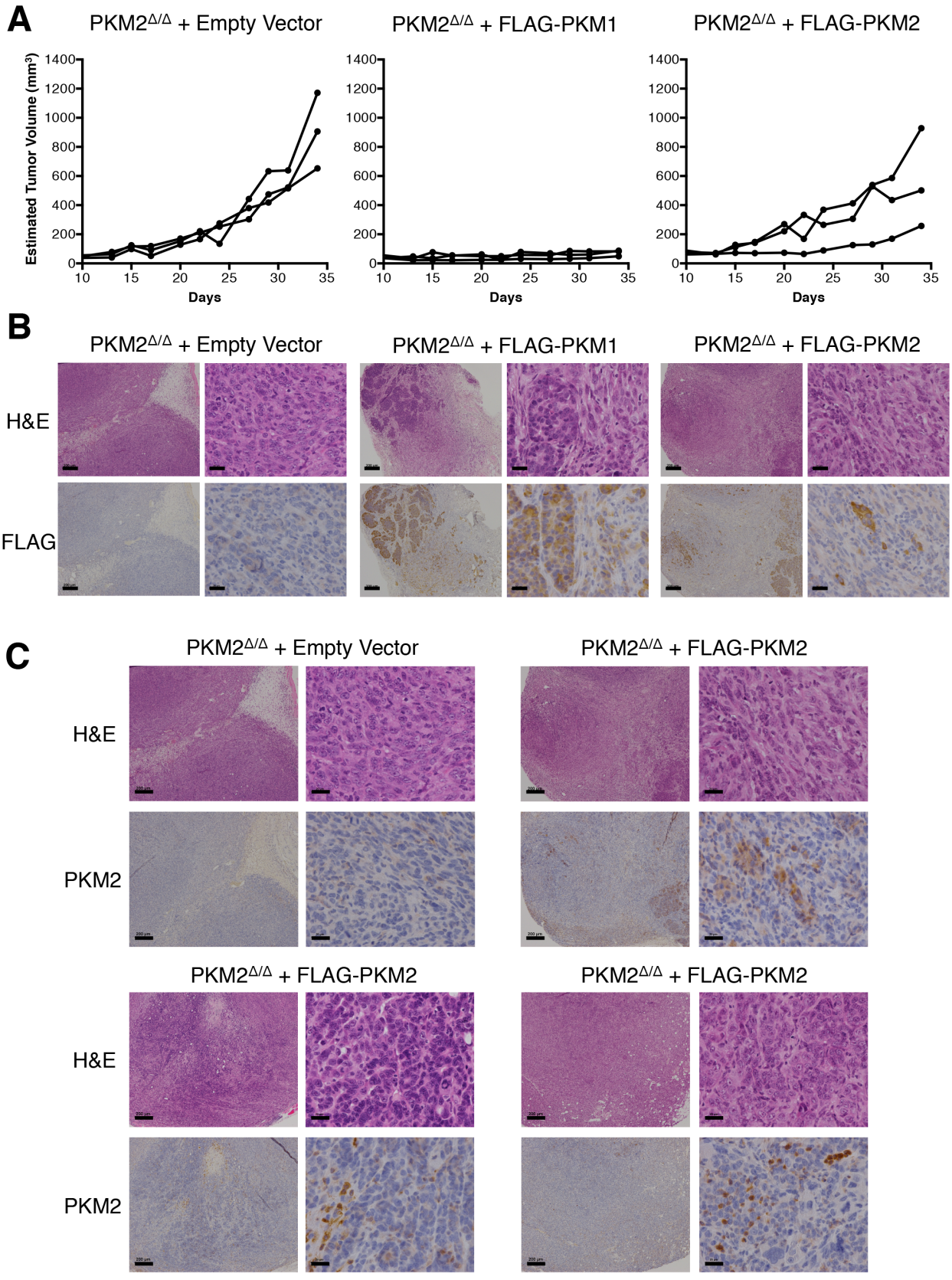
A
PKM2Δ/Δ + Empty Vector
PKM2Δ/Δ + FLAG-PKM1
PKM2Δ/Δ + FLAG-PKM2
Estimated Tumor Volume (mm³)
Days
B
H&E
FLAG
C
PKM2
H&E

detectable upon injection site biopsy 34 days later (Figure 9B). This suggests that constitutive PKM1 expression did not result in decreased viability, but instead promoted a state not conducive to proliferation. Interestingly, tumors derived from FLAG-PKM2-expressing cells showed heterogeneous FLAG staining with only a minority of cells staining positive (Figure 9B), and most cancer cells in these tumors did not stain for PKM2 (Figure 9C). These data suggest that there was no selective pressure to retain FLAG-PKM2 expression despite deletion of the endogenous gene, and confirm that constitutive, exogenous PKM1 expression suppresses proliferation.

PKM1 Expression is Found Only in Non-Proliferating Tumor Cells

PKM1 staining of *Pkm2*$^{\Delta/\Delta}$ allograft tumors showed that PKM1 is endogenously expressed in only a subpopulation of the tumor cells (Figure 10A). Because PKM1 expression suppresses tumor growth and decreased PKM2 activity is associated with pro-proliferative signaling events and anabolic metabolism (Christofk et al, 2008a; Varghese et al, 2010; Anastasiou et al, 2012), we reasoned that proliferating tumor cells might be included in the subset of cells that do not express PKM1. Sections of *Pkm2*$^{\Delta/\Delta}$ allograft tumors were dual stained for PKM1 and the proliferative marker PCNA. Areas of high PKM1 staining had few proliferating cells, while areas of little to no PKM1 staining had many proliferating cells (Figures 10A, 11A). Quantification of this phenotype revealed that 26% of cells counted stained positive for PCNA, and of the 614 PCNA-positive cells counted, the majority (419) had low or no PKM1 staining.

To confirm that PKM1 expression is also associated with the non-proliferating tumor cells in endogenous tumors, we dual stained tumors from *Pkm2*$^{fl/fl}$ *Brca*$^{fl/fl}$ *MMTV-Cre* *Trp53*$^{+/-}$ mice for PKM1 and PCNA. We again saw a correlation between low PKM1

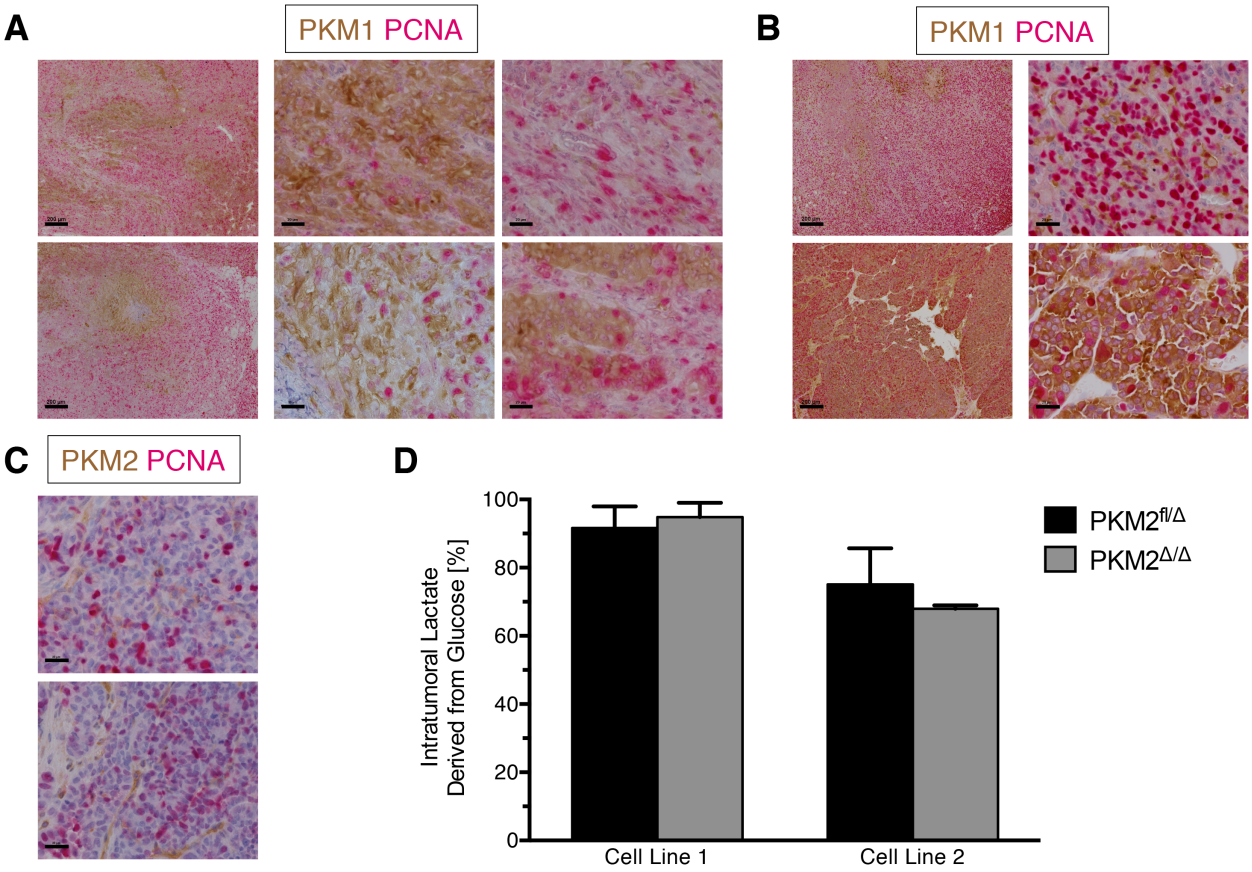

Figure 10. Tumor Cells Proliferate in the Absence of PKM2, but Not in the Presence of PKM1. **(A)** *Pkm2*$^{\Delta/\Delta}$ allograft tumors dual-stained for PKM1 (brown) and PCNA (red). Scale bars represent 200 μm and 20 μm at low and high magnification, respectively. **(B)** *Pkm2*$^{\Delta/\Delta}$ tumors from *Brca1*$^{fl/fl}$ *MMTV-Cre Trp53*$^{+/-}$ mice dual-stained for PKM1 (brown) and PCNA (red). Scale bars represent 200 μm and 20 μm at low and high magnification, respectively. **(C)** *Pkm2*$^{\Delta/\Delta}$ tumors from *Brca1*$^{fl/fl}$ *MMTV-Cre Trp53*$^{+/-}$ mice dual-stained for PKM2 (brown) and PCNA (red). Scale bars represent 20 μm. **(D)** The percent lactate derived from glucose in *Pkm2*$^{fl/\Delta}$ and *Pkm2*$^{\Delta/\Delta}$ allograft tumors was determined from ^{13}C-lactate labeling in tumors normalized to ^{13}C-glucose serum enrichment levels. Results from two independent tumor cell line allografts are displayed as means ± s.e.m (n=8 for Line 1 tumors of both genotypes; n=4 for Line 2 *Pkm2*$^{fl/\Delta}$ tumors and n = 5 for Line 2 *Pkm2*$^{\Delta/\Delta}$ tumors).

expression and staining with PCNA (Figures 10B, 11B). In these tumors, PCNA positive cells made up 21% of the cells counted, and 85% of PCNA positive cells had low to no PKM1 expression. Dual PKM2, PCNA staining of tumors from *Pkm2*$^{fl/fl}$ *Brca*$^{fl/fl}$ *MMTV-Cre Trp53*$^{+/-}$ mice confirmed that cells stained positive for PCNA despite a lack of PKM2 expression (Figure 10C), supporting the notion that *Pkm2*$^{\Delta/\Delta}$ tumor cells are capable of proliferation.

Variable PKM1 Expression Allows Normal Glucose Metabolism in PKM2-null Tumors

Our observation of low PKM1 expression in *Pkm2*$^{\Delta/\Delta}$ tumor cells raises the possibility that glycolysis is disrupted in *Pkm2*$^{\Delta/\Delta}$ tumors. We therefore sought to determine if PKM2 loss resulted in gross metabolic perturbations that would be detectable as changes in glycogen or lipid storage. Spontaneous *Pkm2*$^{+/+}$ and *Pkm2*$^{\Delta/\Delta}$ tumors exhibited similar periodic acid-Schiff staining with and without diastase pretreatment, consistent with tumors of both genotypes having similar glycogen content (Figure 11C). Oil red O staining of neutral lipid stores was also comparable between *Pkm2*$^{+/+}$ and *Pkm2*$^{\Delta/\Delta}$ tumors, with most tumors showing very little lipid accumulation in areas devoid of fat cells (Figure 11D).

Lactate production has been associated with PKM2 expression (Christofk et al, 2008a). To investigate the effect of PKM2 deletion on tumor glucose metabolism, we determined whether *Pkm2*$^{\Delta/\Delta}$ tumors were impaired in glucose to lactate conversion.

Figure 11. Proliferative and Metabolic Phenotypes of Wild-Type and PKM2-deficient Tumors. **(A)** Additional PKM1/PCNA dual-staining of allograft tumors. Quantification of the PCNA+ and PCNA-, as well as PKM1 high and low expressing cells is shown below. Four fields were scored for each of 3 tumors. Scale bars represent 20 μm. **(B)** Additional images showing PKM1/PCNA dual staining of autochthonous tumors. Quantification of the PCNA+ and PCNA-, as well as PKM1 high and low expressing cells is shown below. Four fields were scored for each of 4 tumors. Scale bars represent 20 μm. **(C)** PAS staining for glycogen content without and with diastase treatment of *Pkm2*$^{+/+}$ and *Pkm2*$^{\Delta/\Delta}$ tumors. Scale bars represent 500 μm. **(D)** Oil Red O staining for neutral lipid stores in *Pkm2*$^{+/+}$ and *Pkm2*$^{\Delta/\Delta}$. Scale bars represent 100 μm and 20 μm in the low and high magnification images, respectively. **(E)** Percent enrichment of fully-labeled ^{13}C-glucose in the serum of mice at the time of tumor harvest. Cohorts of mice harboring allograft tumors derived from Tumor Cell Lines 1 and 2 were infused to different glucose serum enrichments. Percentages are calculated as (M+6 Glucose)/(Total Glucose)*100 and reported as means ± s.e.m.; n=8 mice for each genotype of Line 1; n=6 for Line 2 *Pkm2*$^{fl/\Delta}$ mice and n=4 for Line 2 *Pkm2*$^{\Delta/\Delta}$ mice. All calculations have been corrected for natural ^{13}C-isotope abundance. **(F)** Absolute lactate concentrations were determined in Cell Line 2 allograft tumors via mass spectrometry. Values are reported as means ± s.e.m.; n=5 *Pkm2*$^{fl/\Delta}$ tumors and n=3 *Pkm2*$^{\Delta/\Delta}$ tumors. **(G)** Relative abundance of fully-labeled ^{13}C-lactate in serum and tumors formed from cell lines that were or were not deleted for PKM2 as shown from mice that were infused with fully-labeled ^{13}C-glucose. Relative enrichment percent is calculated as (M+3 Lactate)/(Total Lactate)*100 and reported as means ± s.e.m.; n=8. All calculations have been corrected for natural ^{13}C-isotope abundance.

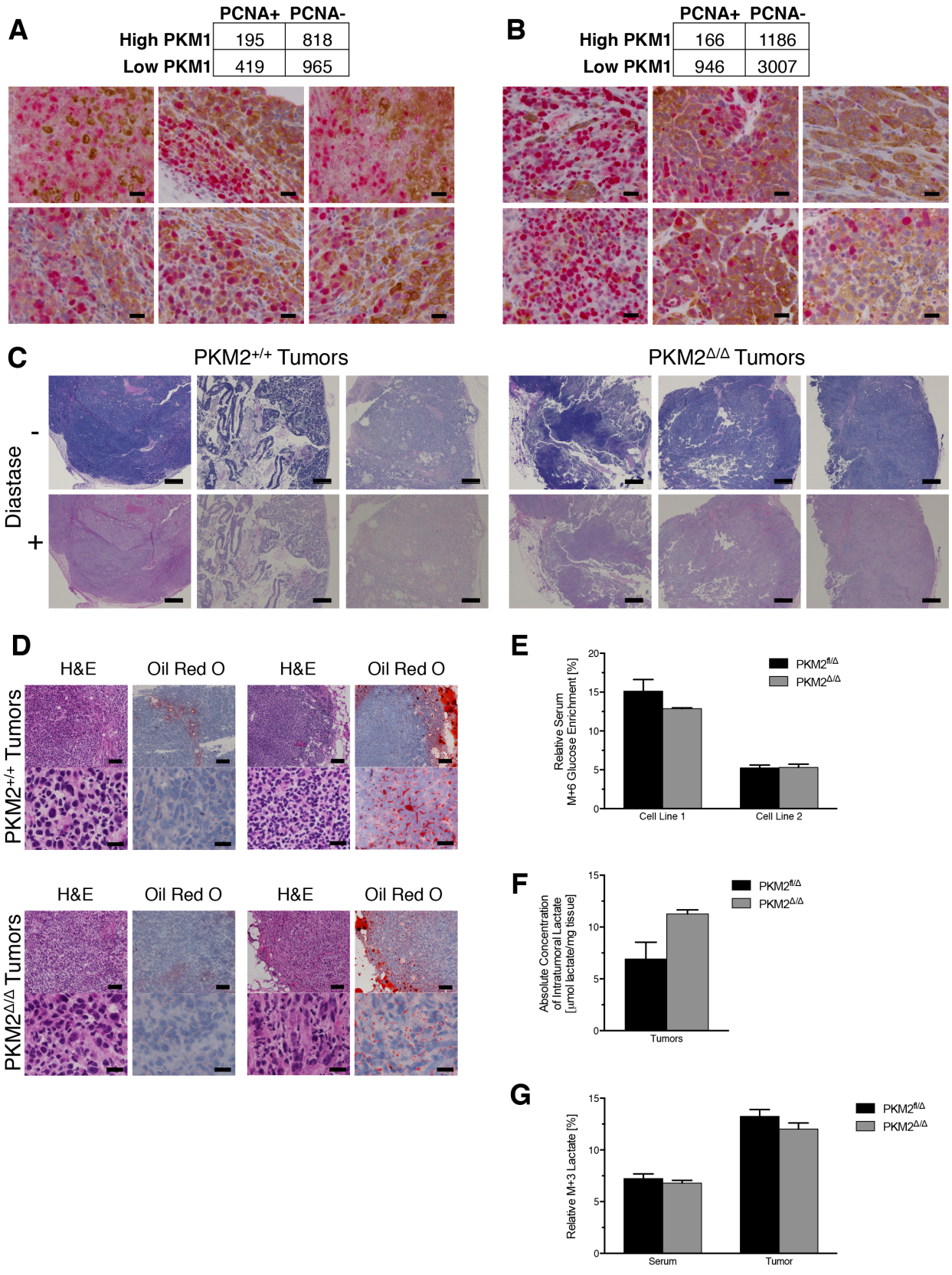
A
PCNA+ PCNA-
High PKM1 195 818
Low PKM1 419 965
B
PCNA+ PCNA-
High PKM1 166 1186
Low PKM1 946 3007
C
PKM2+/+ Tumors
PKM2Δ/Δ Tumors
Diastase
-
+
D
H&E
Oil Red O
H&E
Oil Red O
PKM2+/+ Tumors
PKM2Δ/Δ Tumors
E
Relative Serum M+6 Glucose Enrichment [%]
PKM2fl/Δ
PKM2Δ/Δ
Cell Line 1
Cell Line 2
F
Absolute Concentration of Intratumoral Lactate [μmol lactate/mg tissue]
Tumors
G
Relative M+3 Lactate [%]
Serum
Tumor

Conscious mice harboring *Pkm2*$^{fl/\Delta}$ or *Pkm2*$^{\Delta/\Delta}$ allograft tumors were intravenously infused with fully-labeled ^{13}C-glucose to achieve stable steady-state enrichment of labeled glucose in the serum (Ayala et al, 2010; Figure 11E). Levels of labeled lactate derived from glucose, as well as the absolute concentration of lactate, were similar in both PKM2-expressing and PKM2-null tumors (Figures 10D, 11F). The relative abundance of fully-labeled lactate in tumors was greater than that found in serum regardless of *Pkm2* genotype, providing additional support that the tumors produce similar amounts of lactate from glucose (Figure 11G). These data are consistent with heterogeneous PKM1 expression allowing populations of *Pkm2*$^{\Delta/\Delta}$ tumor cells to recapitulate the metabolism found in PKM2-expressing tumors.

Human Cancers Have PKM2 Mutations and Variable PKM2 Expression

Given the dispensability of PKM2 for tumor growth, and the variability in pyruvate kinase expression observed in our mouse model, we sought to determine whether variable PKM2 expression might be found in primary human tumors. We performed PKM2 and PKM1 IHC on two sets of breast tumor tissue arrays containing a total of 317 cores (Figure 12A, 12B). PKM2 staining intensity scores revealed that, while 71% of the scored tumors show expression of PKM2, the majority of these had weak PKM2 staining (score 1). Moreover, a sizable fraction of the tumors were completely negative for PKM2 staining (score 0), suggesting that PKM2 expression is not consistently upregulated in human tumors (Figure 12C). An absolute requirement for high or low PKM2 expression was not found in any breast cancer subtype, although the more aggressive HER2 positive and triple negative breast tumor subtypes contained the highest percentage of PKM2 negative (score 0) tumors (Figure 12D). We found a statistically significant difference in the distribution of

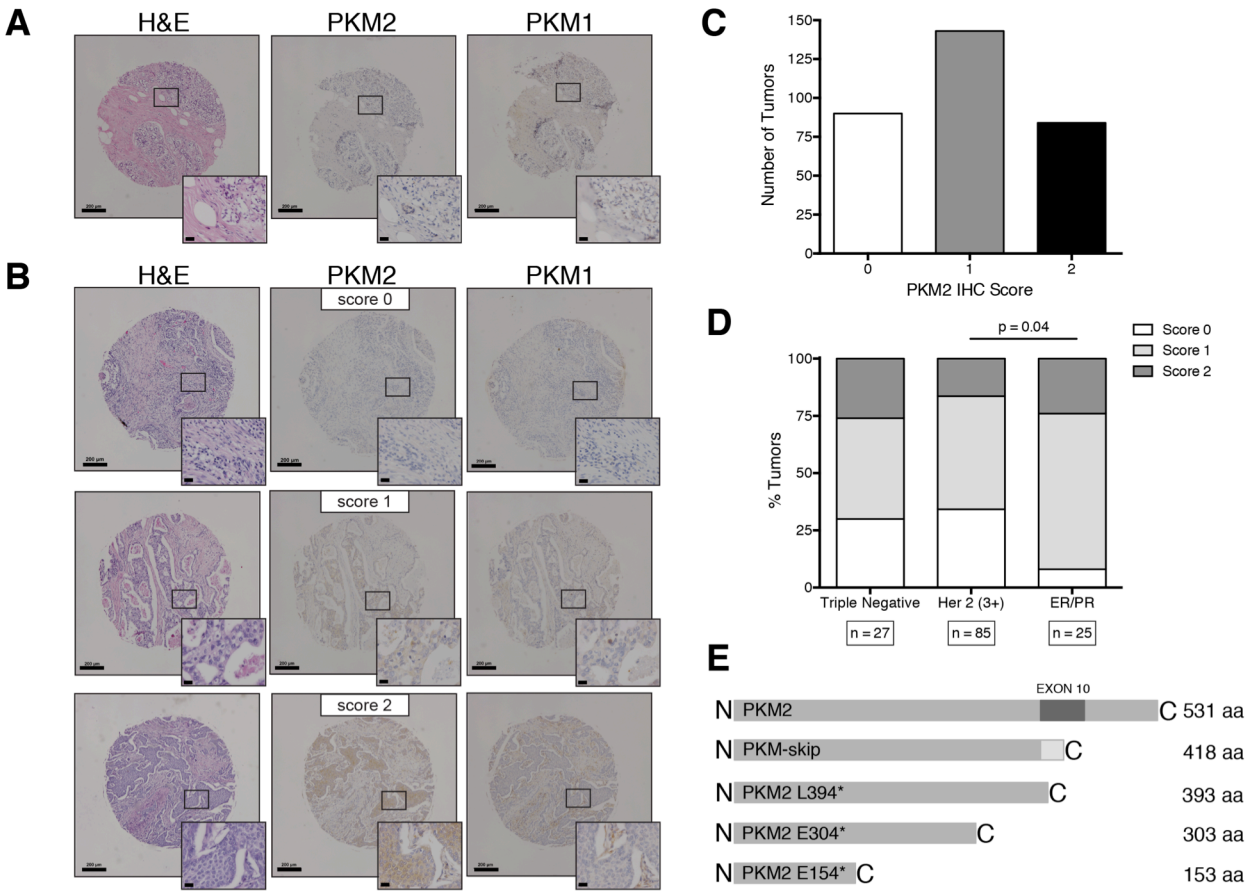

Figure 12. Human Breast Tumors Show Variable Expression of PKM2.
(A) Representative TMA cores containing normal human breast stained with H&E, and for PKM2 and PKM1. Insets show higher magnification. Scale bars represent 200 μm and 20 μm at low and high magnification, respectively. **(B)** Representative TMA cores containing human breast tumor samples stained with H&E, and for PKM2 and PKM1. An example of each PKM2 IHC intensity score is shown (0=negative; 1=weak; 2=strong). Insets show higher magnification. Scale bars represent 200 μm and 20 μm at low and high magnification, respectively. **(C)** Distribution of PKM2 IHC intensity scores of 317 tumors from two different TMAs containing breast tumor samples. **(D)** Quantification of PKM2 expression in human breast tumors relative to breast tumor subtype (triple negative, *HER2* amplified, or ER/PR positive). The distribution of PKM2 scores is significantly different between *HER2* amplified samples and ER/PR positive samples by Chi-square test (P=0.038). **(E)** Schematic showing truncations of PKM2 caused by mutations found in human cancers.

PKM2 IHC scores between *HER2* amplified tumors and tumors that were ER/PR positive (P=0.038, Chi-square test).

Because we observed acceleration of tumor-related mortality in our mice due to PKM2 loss, we wondered whether genetic loss or inactivation of PKM2 might also occur in

some human cancers. Sequencing of human endometrial tumor samples revealed the presence of a recurrent heterozygous nonsense mutation (L394*) within exon 10 of *PKM2* (Figure 12E). If translated, this message would result in a non-functional protein product similar to PKM-skip, arguing that this is a loss-of-function mutation.

Analysis of large-scale efforts to sequence human tumor tissue via The Cancer Genome Atlas (TCGA) revealed additional PKM2 mutations in 7 cancer types (Table S1). These mutations include two additional nonsense mutations (E154* and E304*) that can only generate truncated proteins smaller than PKM-skip (Figure 12E), and one frameshift mutation at V375 that results in a premature stop codon. These mutations all occur upstream of the *PKM* isoform-specific exons (Figure 12E, Table S1) and are expected to result in nonsense-mediated decay of the transcripts (Maquat, 2004) and render any protein product non-functional. The remaining mutations are missense mutations that are predicted to lower enzyme activity. These data are consistent with selection for loss of PKM2 activity under some situations in human cancer.

DISCUSSION

Breast tumors in *Brca*$^{fl/fl}$ *MMTV-Cre Trp53*$^{+/-}$ mice progressed faster despite *Pkm2* deletion, and proliferation within *Pkm2*$^{\Delta/\Delta}$ tumors was associated with low PKM1 expression. These results are in alignment with the known regulation of PKM2 activity in tumor cells, whereby PKM2 can exist in an active state like that of PKM1, or in an inactive state that is promoted by signaling events that drive cell proliferation (Christofk et al, 2008b; Lv et al, 2011; Mazurek, 2011). Following *Pkm* exon 10 deletion, the tumor cells can create analogous states of high and low pyruvate kinase activity by titrating expression of the constitutively active PKM1 isoform. Thus, the low pyruvate kinase activity state

normally induced by growth signaling can still be maintained after PKM2 deletion by repression of exon 9 during splicing to preclude PKM1 expression.

Regulation of PKM2 activity may act as an adaptive response to different cellular metabolic needs, suggesting that increased pyruvate kinase activity is important during different phases of tumor formation and progression. Tumor initiation, either at a primary or metastatic site, involves the ability to grow in a new, inappropriate tissue context. An inadequate blood supply or lack of exogenous growth and survival signals are both possible sources of nutrient stress that might limit the proliferation and survival of individual cancer cells (Vaupel et al, 1989; Vander Heiden et al, 2001). Survival during these periods of stress requires a metabolic program geared away from anabolic metabolism and toward efficient ATP production, which may explain why non-proliferating tumor cells need high pyruvate kinase activity. The ability to activate PKM2 when proliferation is not favored likely drives retention of PKM2 expression in cancer and may explain why loss of function mutations observed in human cancers are heterozygous. In this case, a reduction of pyruvate kinase activity in the cell due to mutation is beneficial for proliferative metabolism, but retention of one functional *PKM* allele provides metabolic flexibility to survive periods of stress experienced by cancer cells *in vivo*.

The *PKM* missense mutations found in multiple human cancer types are noteworthy because PKM2 activity is sensitive to amino acid substitution. A functional characterization of 17 mutations in PKM2 caused by rare SNPs in the human population showed that missense mutations, even in solvent exposed residues, resulted in reduced enzyme activity and stability, and in some cases altered the allosteric regulation of PKM2 (Allali-Hassani et al, 2009). Furthermore, our evaluation of a large panel of breast tumors demonstrated that

PKM2 protein levels are low in many of these cancers. Because PKM2 mutations have not been found at high frequencies, the observed lower expression in some tumors may be due to decreased transcription or translation, or be the result of epigenetic silencing.

Apart from its role as a glycolytic enzyme, multiple non-metabolic functions that are specific to PKM2 have been implicated in cancer, suggesting that these non-canonical activities may drive selection for PKM2 expression in tumor cells. The fact that cells are able to form spontaneous tumors and proliferate after PKM2 deletion implies that non-metabolic functions of the PKM2 isoform are not absolutely necessary for proliferation or tumor progression. While recent reports have suggested that PKM2-dependent phosphorylation of histone H3 is required for cyclin D1 expression and progression through the cell cycle (Yang et al, 2012a), our results indicate that this mechanism is not absolutely required for cell cycle control and is dispensable for cell proliferation in at least some tumors. Other non-metabolic functions of PKM2 that promote gene expression through interactions with HIF1 (Luo et al, 2011), β-catenin (Yang et al, 2011), or by phosphorylation of the stat3 transcription factor (Gao et al, 2012), may occur in and be advantageous for populations of tumor cells, but are not required for growth of all tumors.

The ability of tumor cells to proliferate without PKM2 raises the question of whether cells with PKM2 loss and no apparent PKM1 expression require any pyruvate kinase. It is possible that very low levels of PKM1 expression provide sufficient pyruvate kinase activity to maintain glycolytic flux, which accounts for the continued conversion of glucose to lactate in *Pkm2*$^{\Delta/\Delta}$ tumors. If so, then pyruvate kinase in cancer cells must be in excess of what is needed to allow sufficient PEP to pyruvate conversion, and pyruvate kinase activity would thus never be rate limiting at normal expression levels. However,

this possibility is not consistent with the observation that both PKM1 expression and pyruvate kinase activators can suppress tumor growth by increasing pyruvate kinase activity (Anastasiou et al, 2012). If the level of pyruvate kinase activity is rate limiting in proliferating cells, then the observed loss of PKM2 without compensatory expression of other isoforms suggests that a pyruvate kinase independent mechanism for conversion of PEP to pyruvate might exist to allow glycolytic flux to continue in the absence of pyruvate kinase. The presence of such an activity has been suggested, and may allow cells to decouple glycolytic ATP generation from incorporation of glucose into central metabolic pathways (Vander Heiden et al, 2010).

The ability of *Pkm2*$^{\Delta/\Delta}$ tumors to convert glucose to lactate despite negligible pyruvate kinase expression in many cells has another possible explanation. It may be that tumor lactate production is restricted to non-proliferating cells with high pyruvate kinase activity, while cells with low pyruvate kinase activity consume another substrate. A similar metabolic symbiosis has been suggested to support cells in hypoxic regions of tumors (Sonveaux et al, 2008).

A differential requirement for pyruvate kinase activity among tumor cell populations complicates the development of strategies to target PKM2 for cancer therapy. While PKM2 knockdown inhibits growth *in vitro*, the same does not hold true *in vivo*, as inducible knockdown of PKM2 has no effect on established xenograft tumors (Cortes-Cros et al, 2013). That finding, together with our observation of accelerated tumor mortality after PKM2 deletion, suggests that pharmacological inhibition or therapeutic knockdown of PKM2 may not be effective standalone cancer therapies. Increasing pyruvate kinase activity in the cell with small molecule activators can inhibit tumor growth (Anastasiou et

al, 2012; Parnell et al, 2013); however, our finding that PKM1-expressing cancer cells persist in a non-proliferative state *in vivo* raises the possibility that increased pyruvate kinase activity favors survival of cancer cells under some conditions. Additionally, pharmacological activation of PKM2 activity may have no effect on the non-proliferating tumor cell population and be at best a cytostatic therapy. Finally, as at least some tumors can tolerate loss of PKM2, the deletion, mutation, or epigenetic silencing of PKM2 may provide a mechanism for resistance to PKM2 activators in a therapeutic setting. Activation or inhibition of pyruvate kinase as an adjuvant therapy may still be effective in situations where targeting PKM2 opposes the biological regulation of PKM2 activity. For example, effective PKM2 inhibition might disrupt the metabolism of the non-proliferating tumor fraction and cause cell death or sensitize the cells to cytotoxic therapy. The findings of this study highlight the importance of understanding the context-dependent metabolic needs of cancer cells to effectively target metabolism for therapeutic benefit.

Table S1. PKM2 Mutations in Human Cancers, Related to Figure 7

PKM2 mutations from 8 different human cancer types. Mutations are reported by amino acid alteration and mutation type: Nonsense, Missense, or frameshift due to deletion (FS Deletion). The center reporting the mutation, number of mutations found, and the number of cases for each cancer type sequenced are also reported. The location of each point mutation is provided when applicable.

AA Change	Type	Center	Number	Total Cases	Cancer Type	Location in Structure
E154*	Nonsense	Broad	3	170	Lung Adenocarcinoma	
E304*	Nonsense	Broad	3	170	Lung Adenocarcinoma	
V375fs	FS Deletion	WashU	5	240	Uterine	
L394*	Nonsense	MDAnderson	2	192	Endometrial	
K266N	Missense	WashU	5	240	Uterine	A domain
P117L	Missense	WashU	5	240	Uterine	Hinge between A and B domains, near active site
R455Q	Missense	WashU	5	240	Uterine	C domain, near FBP binding pocket
R516C	Missense	WashU	5	240	Uterine	C domain, on loop FBP binding pocket loop
R246S	Missense	Broad	3	170	Lung Adenocarcinoma	A domain
V417L	Missense	Broad	3	170	Lung Adenocarcinoma	C domain, near dimer-dimer interface
L144P	Missense	Broad	2	132	Stomach	B domain
R92H	Missense	Broad	2	132	Stomach	A domain
E282K	Missense	Broad	4	286	Head and Neck	A domain
R319L	Missense	Broad	4	286	Head and Neck	C domain, forms intersubunit salt bridge with E28
S222L	Missense	Broad	4	286	Head and Neck	A domain
T60M	Missense	Broad	4	286	Head and Neck	A domain
D354N	Missense	Broad	1	88	Bladder	A domain
L465M	Missense	Broad	1	88	Bladder	A domain
S287I	Missense	Broad	2	220	Colon	A domain
G415R	Missense	Baylor	1	418	Kidney	C domain, at dimer-dimer interface

METHODS

Generation of PKM2 Conditional Mice and Embryonic Fibroblasts (MEFs)

The relevant genomic DNA for the *PKM2* locus from 129S6/SvEvTac-derived TC1 embryonic stem (ES) cells was amplified using PCR and cloned into the pKOII targeting vector using standard molecular biology techniques (Bardeesy et al, 2002). The vector was introduced into TC1 ES cells by electroporation, selected with neomycin, and clones with homologous recombination at the *Pkm* locus were identified by Southern blot. The relevant genomic sequence encompassing *Pkm* exons 8 through 12 from the targeted ES cells was verified by DNA sequencing to confirm proper placement of the loxP sites and lack of any coding sequence mutations. Appropriately targeted ES cells were injected into blastocysts derived from C57/B6 mice and implanted into pseudo-pregnant females to generate chimeric animals. Germline transmission of the targeted allele was determined through breeding and confirmed with Southern blot. These mice were then crossed with FlpO-expressing transgenic mice to delete the neomycin resistance cassette and the FlpO transgene eliminated from the colony through breeding (Raymond & Soriano, 2007). MEFs were prepared from E13.5 *Pkm2* $^{+/+}$ *Cre-ER* or *Pkm2* $^{fl/fl}$ *Cre-ER* embryos using standard protocols. Where indicated, MEFs were treated with 500 nM 4-hydroxytamoxifen or mock treated and analyzed 4 days later.

Southern Blotting

Genomic DNA was prepared from embryonic stem cells or mouse tail tissue, digested with Asp718 (cuts at same site as KpnI, Roche), separated by agarose gel electrophoresis, neutral transferred to a membrane (Hybond XL, GE Healthcare), and UV cross-linked prior to radioactive probe hybridization using QuickHyb (Stratagene) according to the

manufacturers instructions. The DNA probes were prepared using a Rediprime II Kit (GE Healthcare), and probe binding was visualized by autoradiography.

PCR Genotyping

PCR genotyping was performed using forward (5′-TAGGGCAGGACCAAAGGATTCCCT-3′) and reverse (5′-CTGGCCCAGAGCCACTCACTCTTG-3′) primers to amplify the genomic locus including *Pkm* exon 10.

Quantitative RT-PCR and Analysis of PKM Splicing

Quantitative RT–PCR was performed on Trizol-extracted RNA using a High Capacity cDNA Reverse Transcription kit (Applied Biosystems). qPCR reactions were performed using Fast SYBR Green Master Mix (Applied Biosystems) and a Roche Light Cycler 480II thermocycler (Roche). *PKM2*, *PKM1*, and *PKLR* expression were reported relative to *GAPDH* expression. qPCR primers were: *PKM2* forward 5′- GTCTGGAGAAACAGCCAAGG-3′, *PKM2* reverse 5′-CGGAGTTCCTCGAATAGCTG-3′; *PKM1* forward 5′-GTCTGGAGAAACAGCCAAGG-3′, *PKM1* reverse 5′-TCTTCAAACAGCAGACGGTG-3′; *PKLR* forward 5′-AAGGGTCCCGAGATACGCA-3′, *PKLR* reverse 5′-CTGCAACGACCTGGGTGATA-3′; *GAPDH* forward 5′-AGCTTGTCATCAACGGGAAG-3′, *GAPDH* reverse 5′-TTTGATGTTAGTGGGGTCTCG-3′; *PDK1* forward 5′-GGACTTCGGGTCAGTGAATGC-3′, *PDK1* reverse 5′-TCCTGAGAAGATTGTCGGGGA-3′; *GLUT1* forward 5′-CAGTTCGGCTATAACACTGGTG-3′, *GLUT1* reverse 5′-GCCCCCGACAGAGAAGATG-3′; beta-actin forward 5′-GGCATAGAGGTCTTTACGGATGTC-3′, beta-actin reverse 5′-TATTGGCAACGAGCGGTTCC-3′. TaqMan probes were used for LDHa and Axin2. Quantification of mouse PKM splicing was performed as reported previously (Clower et al, 2010).

Western Blot Analysis and Immunohistochemistry

Western blots were performed using standard techniques with primary antibodies against PKM1 (Sigma, SAB4200094), PKM2 (Cell Signaling Technology, #4053), PKM (Cell Signaling Technology, #3190; abcam, ab6191), FLAG (Cell Signaling Technology, #2368), beta-actin (abcam, ab1801), or GAPDH (Cell Signaling Technology, #2118) and detected using HRP-conjugated secondary antibodies, and chemiluminescence. The anti-PKM antibody #3190 from Cell Signaling Technologies recognizes an epitope that includes G200. For immunohistochemistry, formalin-fixed, paraffin-embedded tissue sections were stained with the following primary antibodies following antigen retrieval: PKM1 (Cell Signaling Technology, #7067), PKM2 (Cell Signaling Technology, #4053 at 1:800 dilution), PCNA (Cell Signaling Technology, #2586 at 1:2000 dilution), Ki-67 (BD Pharmingen, 556003 at 1:100 dilution), Cleaved Caspase 3 (Cell Signaling Technology, #9661 at 1:400 dilution), and/or FLAG antigen (Cell Signaling Technology, #2368 at 1:250 dilution). Staining was performed on an automated stainer or using a DAB peroxidase substrate kit and/or a Vector Red alkaline phosphatase substrate kit (Vector Laboratories) according to the manufacturer's protocol. Stained sections were counterstained with haematoxylin. Quantification of PKM1/PCNA dual-stained tumor sections was performed using ImageJ image processing software (National Institutes of Health). All cells in each field were scored as PCNA-positive or -negative and PKM1-high or -low; four fields were scored for each of 3 allograft and 4 spontaneous tumors.

Histology

Haematoxylin and eosin staining was used for routine histology. Glycogen stores were visualized in formalin-fixed, paraffin-embedded tumor sections using periodic acid-Schiff

stain with or without pre-digestion with diastase. Neutral lipid stores were stained in fresh-frozen tumor sections with Oil Red O.

Tumor-Derived Cell Lines

Freshly dissected tumors were minced, disaggregated with warm trypsin and propagated in Dulbecco's Modified Eagle Medium supplemented with 10% fetal bovine serum, 2 mM glutamine, and penicillin/streptomycin. Once established, tumor cell lines were retrovirally infected with an MSCV-CreER^{T2}-puro vector and a pLHCX expression vector containing no insert, FLAG-PKM1 cDNA, or FLAG-PKM2 cDNA as described previously (Christofk et al, 2008a). Puromycin (2 μg/mL) and hygromycin (100 μg/mL) were used to select for cells with stable integration of the constructs, and 1 μM 4-hydroxytamoxifen was used to induce recombination of PKM2^{fl} alleles where indicated.

Allograft Tumor Experiments

PKM2$^{\Delta/\Delta}$ mouse tumor cell lines with stably integrated empty vector, pLHCX-FLAG-PKM1, or pLHCX-FLAG-PKM2 were suspended in sterile PBS, and 5×10^6 cells injected into the flanks of nu/nu mice. Tumor growth was monitored by caliper measurement in two dimensions, tumor volume was estimated by the equation $V = (\pi/6)(L*W^2)$, and tumors harvested for analysis at the time indicated.

Tissue Microarray Analysis

PKM2 and PKM1 expression in human breast cancers was determined using IHC as described above. We analyzed three tissue microarrays: US BioMax BR1504, a multi-tissue TMA containing tissue obtained from the archives of the Institute of Pathology at the University of Basel (Schraml et al, 1999; Baumhoer et al, 2008), and two breast cancer TMAs from Beth-Israel Deaconess Medical Center. Each TMA core was scored for PKM2

IHC intensity independently by both a pathologist (D.D.V.) and another member of the team (T.D.). Tumors that showed no positive staining for PKM2 were given a score of 0, those with weak staining were given a score of 1, and tumors with strong PKM2 staining were given a score of 2. PKM2 scores from one TMA (US BioMax BR1504) were quantified relative to tumor subtype as determined by IHC staining results provided by US BioMax. Statistical significance was determined by the Chi-square test.

Preparation of Recombinant Proteins

Human PKM2 cDNA or cDNA corresponding to the predicted mouse PKM-skip protein product was cloned in pET28a with an in-frame N-terminal 6x-HIS tag. Proteins were expressed in *E. coli* strain BL21(DE3) and purified using nickel–nitrilotriacetic acid (Ni-NTA) affinity chromatography as previously described (Anastasiou et al, 2012; Chapter 2).

Size Exclusion Chromatography

Recombinant PKM-skip protein was separated on a HiPrep 16/60 Sephacryl S-200 HR column (GE Healthcare) in 150 mM sodium chloride and 50 mM sodium phosphate, pH 7.2 as previously described (Anastasiou et al, 2012; Chapter 2). Fractions were analyzed by SDS-PAGE and proteins visualized by staining with Coomassie blue.

Pyruvate Kinase Assay

Pyruvate kinase activity of recombinant proteins was determined using a lactate dehydrogenase-linked assay as previously described (Anastasiou et al, 2012; Chapter 2). Assays were performed at 25°C in buffer containing 50 mM Tris pH 7.5, 100 mM KCl, 5 mM $MgCl_2$, and 100 U/ml lactate dehydrogenase with the following substrates: 500 μM PEP, 600 μM ADP, 180 μM NADH.

Protein Kinase Assay

Protein kinase activity was assayed as described previously (Gao et al, 2012). Briefly, purified recombinant His-tagged PKM-skip (10 μg/mL) was incubated with nuclear lysate (100 μg/mL) prepared from H1299 cells, ~1 μCi [γ-^{32}P]-ATP (Perkin Elmer) or ~0.1 μCi [^{32}P]-PEP (prepared as described in Vander Heiden et al (2010)), and kinase buffer (50 mM Tris-HCl [pH 7.5], 10 mM KCl, 50 mM $MgCl_2$, and 1 mM DTT) at 30°C for 1 hour. Nuclear lysate was prepared using a protocol modified from (Wang et al, 1994). Where indicated, 1 mM cold competitor ATP or PEP was added to the reaction. Reactions were stopped by addition of SDS-PAGE loading buffer and heated to 100°C. Reaction products were analyzed by SDS-PAGE and autoradiography.

Oxygen Consumption Assay

Oxygen consumption rates were measured at 37°C in standard growth medium using an Oxytherm electrode unit and Oxygraph software (Hansatech) in the presence or absence of 50 μM *R*-etomoxir.

Luciferase Reporter Assays

Cells were co-transfected with either a TOPFLASH, FOPFLASH, or HRE-luciferase reporter construct and a control *Renilla* luciferase construct (pRL-TK) at a 20:1 ratio using X-tremeGENE transfection reagent (Roche). Following treatment, cells were harvested and assayed using Dual-Luciferase Assay System reagents (Promega) and a Tecan Infinite M200 Pro plate reader. For experiments involving hypoxia, cells were incubated at 1% oxygen in a ProOx C21 C-chamber (BioSpherix).

Human Tumor DNA Sequence Analysis

Whole exome sequencing of 13 endometrioid endometrial tumors demonstrated a stop codon in exon 10 of PKM (Liang et al, 2012). Based on this observation, the PKM2 mutation was confirmed by Sequenom mass spectrometry of 234 human endometrial cancers. Additional mutations in PKM were identified through the cBIO portal (Cerami et al, 2012).

Mouse Glucose Infusion Studies

Venous catheters were implanted into the jugular vein of animals with allograft tumors 5-7 days before performing basal glucose turnover experiments as reported previously (Ayala et al, 2010; Jurczak et al, 2012). After surgical recovery, mice were fasted overnight before U-^{13}C-glucose was reconstituted in saline and infused into conscious mice for 120 min to achieve steady-state enrichments without perturbing endogenous glucose homeostasis. Next, mice were anesthetized with sodium pentobarbital injection and tissue was harvested within 5 minutes, snap frozen in liquid nitrogen using Biosqueezer (BioSpec Products), and stored at -80 C for subsequent analysis.

Mass Spectrometry Metabolite Measurement

Metabolites were extracted and resuspended for analysis with isotope labeled internal standards. The samples from Line 1 were analyzed as described previously (Jain et al, 2012). Briefly, metabolites were separated by isocratic elution (40% acetonitrile with 10 mM ammonium formate) from a C18 column (2.5 μm particle size, 2x50 mm, Shimadzu) at 300 ul/min using a Shimadzu Prominence UHPLC. For MS analysis an ABSCIEX 5500 QTRAP equipped with a SelexION was used with lactate isotopologues measured in negative ion mode. For GC/MS, dried metabolites from plasma were resuspended in 20 μl of 2% methoxyamine hydrochloride in pyridine (Thermo) and held at 37°C for 1.5 h. After dissolution and reaction, tert-butyldimethylsilyl derivatization was initiated by adding 25

µl *N*-methyl-*N*-(tert-butyldimethylsilyl)trifluoroacetamide + 1% tert-butyldimethylchlorosilane (Sigma) and incubating at 37°C for 1 h. GC/MS analysis was performed using an Agilent 7890A GC equipped with a 30m DB-35MS capillary column connected to an Agilent 5975C MS operating under electron impact ionization at 70 eV. One microliter of sample was injected in splitless mode at 270°C, using helium as the carrier gas at a flow rate of 1 ml min^{-1}. For measurement of pyruvate and lactate, the GC oven temperature was held at 100°C for 3 min and increased to 300°C at 3.5°C min^{-1}. The MS source and quadrupole were held at 230°C and 150°C, respectively, and the detector was run in scanning mode, recording ion abundance in the range of 100–605 m/z. MIDs were determined by integrating the appropriate ion fragments as described previously (Commisso et al, 2013). The samples from Line 2 were analyzed by hydrophilic interaction liquid chromatography (HILIC)/negative ion mode MS analyses using an Open Accela 1250 U-HPLC and a Q Exactive hybrid quadrupole orbitrap mass spectrometer (Thermo Fisher Scientific; Waltham, MA). Briefly, chromatography used a Luna NH2 column (Phenomenex; Torrance, CA) eluted at a flow rate of 400 µL/min with initial conditions of 10% mobile phase A (20 mM ammonium acetate and 20 mM ammonium hydroxide in water) and 90% mobile phase B (10 mM ammonium hydroxide in 75:25 v/v acetonitrile/methanol) followed by a 10 min linear gradient to 100% mobile phase A. Analyses were carried out using negative ion mode and raw LC-MS data were processed using TraceFinder (v 3.0, Thermo Scientific) software.

ACKNOWLEDGEMENTS

We thank Chu-Xia Deng for sharing the *BRCA1* mouse model, Luigi Terracciano and Luigi Tornillo for providing the multi-tissue TMA, and Cynthia Clower, Sarah-Maria Fendt,

Andrea J. Howell, Vivian M. Liu, Sophia Lunt, Katherine R. Mattaini, Benjamin A. Olenchock, and Kerry Pierce for technical assistance. Eric L. Bell provided advice and reagents. Denise G. Crowley, Michael Brown, Kathleen S. Cormier assisted with histology. This work was supported in part by NIH grants R01CA168653, 5P01CA117969, P30CA147882, 5P30CA14051, 5K08CA136983, DK059635, R01DK092606, R00CA131472, and ADA grant 7-12-BS-09. RAD and JH acknowledge support from the Belfer Foundation. MVH acknowledges additional support from the Smith Family Foundation, the Burroughs Wellcome Fund, the Damon Runyon Cancer Research Foundation, and the Stern family.

REFERENCES

Allali-Hassani A, Wasney GA, Chau I, Hong BS, Senisterra G, Loppnau P, Shi Z, Moult J, Edwards AM, Arrowsmith CH, Park HW, Schapira M, Vedadi M (2009) A survey of proteins encoded by non-synonymous single nucleotide polymorphisms reveals a significant fraction with altered stability and activity. *Biochem J* 424**:** 15-26

Anastasiou D, Poulogiannis G, Asara JM, Boxer MB, Jiang JK, Shen M, Bellinger G, Sasaki AT, Locasale JW, Auld DS, Thomas CJ, Vander Heiden MG, Cantley LC (2011) Inhibition of pyruvate kinase M2 by reactive oxygen species contributes to cellular antioxidant responses. *Science* 334**:** 1278-1283

Anastasiou D, Yu Y, Israelsen WJ, Jiang JK, Boxer MB, Hong BS, Tempel W, Dimov S, Shen M, Jha A, Yang H, Mattaini KR, Metallo CM, Fiske BP, Courtney KD, Malstrom S, Khan TM, Kung C, Skoumbourdis AP, Veith H, Southall N, Walsh MJ, Brimacombe KR, Leister W, Lunt SY, Johnson ZR, Yen KE, Kunii K, Davidson SM, Christofk HR, Austin CP, Inglese J, Harris MH, Asara JM, Stephanopoulos G, Salituro FG, Jin S, Dang L, Auld DS, Park HW, Cantley LC, Thomas CJ, Vander Heiden MG (2012) Pyruvate kinase M2 activators promote tetramer formation and suppress tumorigenesis. *Nat Chem Biol* 8**:** 839-847

Ayala JE, Samuel VT, Morton GJ, Obici S, Croniger CM, Shulman GI, Wasserman DH, McGuinness OP (2010) Standard operating procedures for describing and performing metabolic tests of glucose homeostasis in mice. *Dis Model Mech* 3**:** 525-534

Bardeesy N, Sinha M, Hezel AF, Signoretti S, Hathaway NA, Sharpless NE, Loda M, Carrasco DR, DePinho RA (2002) Loss of the Lkb1 tumour suppressor provokes intestinal polyposis but resistance to transformation. *Nature* 419**:** 162-167

Baumhoer D, Tornillo L, Stadlmann S, Roncalli M, Diamantis EK, Terracciano LM (2008) Glypican 3 expression in human nonneoplastic, preneoplastic, and neoplastic tissues: a tissue microarray analysis of 4,387 tissue samples. *Am J Clin Pathol* 129**:** 899-906

Cairns RA, Harris IS, Mak TW (2011) Regulation of cancer cell metabolism. *Nat Rev Cancer* 11**:** 85-95

Cerami E, Gao J, Dogrusoz U, Gross BE, Sumer SO, Aksoy BA, Jacobsen A, Byrne CJ, Heuer ML, Larsson E, Antipin Y, Reva B, Goldberg AP, Sander C, Schultz N (2012) The cBio cancer genomics portal: an open platform for exploring multidimensional cancer genomics data. *Cancer Discov* 2**:** 401-404

Chaneton B, Gottlieb E (2012) Rocking cell metabolism: revised functions of the key glycolytic regulator PKM2 in cancer. *Trends Biochem Sci* 37**:** 309-316

Chaneton B, Hillmann P, Zheng L, Martin AC, Maddocks OD, Chokkathukalam A, Coyle JE, Jankevics A, Holding FP, Vousden KH, Frezza C, O'Reilly M, Gottlieb E (2012) Serine is a natural ligand and allosteric activator of pyruvate kinase M2. *Nature* 491**:** 458-462

Chen M, David CJ, Manley JL (2012) Concentration-dependent control of pyruvate kinase M mutually exclusive splicing by hnRNP proteins. *Nat Struct Mol Biol* 19**:** 346-354

Christofk HR, Vander Heiden MG, Harris MH, Ramanathan A, Gerszten RE, Wei R, Fleming MD, Schreiber SL, Cantley LC (2008a) The M2 splice isoform of pyruvate kinase is important for cancer metabolism and tumour growth. *Nature* 452**:** 230-233

Christofk HR, Vander Heiden MG, Wu N, Asara JM, Cantley LC (2008b) Pyruvate kinase M2 is a phosphotyrosine-binding protein. *Nature* 452**:** 181-186

Clower CV, Chatterjee D, Wang Z, Cantley LC, Vander Heiden MG, Krainer AR (2010) The alternative splicing repressors hnRNP A1/A2 and PTB influence pyruvate kinase isoform expression and cell metabolism. *Proc Natl Acad Sci U S A* 107**:** 1894-1899

Commisso C, Davidson SM, Soydaner-Azeloglu RG, Parker SJ, Kamphorst JJ, Hackett S, Grabocka E, Nofal M, Drebin JA, Thompson CB, Rabinowitz JD, Metallo CM, Vander Heiden MG, Bar-Sagi D (2013) Macropinocytosis of protein is an amino acid supply route in Ras-transformed cells. *Nature* 497**:** 633-637

Cortes-Cros M, Hemmerlin C, Ferretti S, Zhang J, Gounarides JS, Yin H, Muller A, Haberkorn A, Chene P, Sellers WR, Hofmann F (2013) M2 isoform of pyruvate kinase is dispensable for tumor maintenance and growth. *Proc Natl Acad Sci U S A* 110**:** 489-494

David CJ, Chen M, Assanah M, Canoll P, Manley JL (2010) HnRNP proteins controlled by c-Myc deregulate pyruvate kinase mRNA splicing in cancer. *Nature* 463**:** 364-368

Dombrauckas JD, Santarsiero BD, Mesecar AD (2005) Structural basis for tumor pyruvate kinase M2 allosteric regulation and catalysis. *Biochemistry* 44**:** 9417-9429

Gao X, Wang H, Yang JJ, Liu X, Liu ZR (2012) Pyruvate kinase M2 regulates gene transcription by acting as a protein kinase. *Mol Cell* 45**:** 598-609

Goldberg MS, Sharp PA (2012) Pyruvate kinase M2-specific siRNA induces apoptosis and tumor regression. *J Exp Med* 209**:** 217-224

Hitosugi T, Kang S, Vander Heiden MG, Chung TW, Elf S, Lythgoe K, Dong S, Lonial S, Wang X, Chen GZ, Xie J, Gu TL, Polakiewicz RD, Roesel JL, Boggon TJ, Khuri FR, Gilliland DG, Cantley LC, Kaufman J, Chen J (2009) Tyrosine phosphorylation inhibits PKM2 to promote the Warburg effect and tumor growth. *Sci Signal* 2**:** ra73

Imamura K, Tanaka T (1972) Multimolecular forms of pyruvate kinase from rat and other mammalian tissues. I. Electrophoretic studies. *J Biochem* 71**:** 1043-1051

Jain M, Nilsson R, Sharma S, Madhusudhan N, Kitami T, Souza AL, Kafri R, Kirschner MW, Clish CB, Mootha VK (2012) Metabolite profiling identifies a key role for glycine in rapid cancer cell proliferation. *Science* 336**:** 1040-1044

Jurczak MJ, Lee AH, Jornayvaz FR, Lee HY, Birkenfeld AL, Guigni BA, Kahn M, Samuel VT, Glimcher LH, Shulman GI (2012) Dissociation of inositol-requiring enzyme (IRE1alpha)-mediated c-Jun N-terminal kinase activation from hepatic insulin resistance in conditional X-box-binding protein-1 (XBP1) knock-out mice. *J Biol Chem* 287**:** 2558-2567

Keller KE, Tan IS, Lee YS (2012) SAICAR stimulates pyruvate kinase isoform M2 and promotes cancer cell survival in glucose-limited conditions. *Science* 338**:** 1069-1072

Liang H, Cheung LW, Li J, Ju Z, Yu S, Stemke-Hale K, Dogruluk T, Lu Y, Liu X, Gu C, Guo W, Scherer SE, Carter H, Westin SN, Dyer MD, Verhaak RG, Zhang F, Karchin R, Liu CG, Lu KH, Broaddus RR, Scott KL, Hennessy BT, Mills GB (2012) Whole-exome sequencing combined with functional genomics reveals novel candidate driver cancer genes in endometrial cancer. *Genome Res* 22**:** 2120-2129

Luo W, Hu H, Chang R, Zhong J, Knabel M, O'Meally R, Cole RN, Pandey A, Semenza GL (2011) Pyruvate kinase M2 is a PHD3-stimulated coactivator for hypoxia-inducible factor 1. *Cell* 145**:** 732-744

Lv L, Li D, Zhao D, Lin R, Chu Y, Zhang H, Zha Z, Liu Y, Li Z, Xu Y, Wang G, Huang Y, Xiong Y, Guan KL, Lei QY (2011) Acetylation targets the M2 isoform of pyruvate kinase for degradation through chaperone-mediated autophagy and promotes tumor growth. *Mol Cell* 42**:** 719-730

Maquat LE (2004) Nonsense-mediated mRNA decay: splicing, translation and mRNP dynamics. *Nat Rev Mol Cell Biol* 5**:** 89-99

Mazurek S (2011) Pyruvate kinase type M2: a key regulator of the metabolic budget system in tumor cells. *Int J Biochem Cell Biol* 43**:** 969-980

Noguchi T, Inoue H, Tanaka T (1986) The M1- and M2-type isozymes of rat pyruvate kinase are produced from the same gene by alternative RNA splicing. *J Biol Chem* 261**:** 13807-13812

Parnell KM, Foulks JM, Nix RN, Clifford A, Bullough J, Luo B, Senina A, Vollmer D, Liu J, McCarthy V, Xu Y, Saunders M, Liu XH, Pearce S, Wright K, O'Reilly M, McCullar MV, Ho KK, Kanner SB (2013) Pharmacologic activation of PKM2 slows lung tumor xenograft growth. *Mol Cancer Ther* 12**:** 1453-1460

Raymond CS, Soriano P (2007) High-efficiency FLP and PhiC31 site-specific recombination in mammalian cells. *PLoS One* 2**:** e162

Salk JJ, Fox EJ, Loeb LA (2010) Mutational heterogeneity in human cancers: origin and consequences. *Annu Rev Pathol* 5**:** 51-75

Schraml P, Kononen J, Bubendorf L, Moch H, Bissig H, Nocito A, Mihatsch MJ, Kallioniemi OP, Sauter G (1999) Tissue microarrays for gene amplification surveys in many different tumor types. *Clin Cancer Res* 5**:** 1966-1975

Sonveaux P, Vegran F, Schroeder T, Wergin MC, Verrax J, Rabbani ZN, De Saedeleer CJ, Kennedy KM, Diepart C, Jordan BF, Kelley MJ, Gallez B, Wahl ML, Feron O, Dewhirst MW (2008) Targeting lactate-fueled respiration selectively kills hypoxic tumor cells in mice. *J Clin Invest* 118**:** 3930-3942

Vander Heiden MG, Plas DR, Rathmell JC, Fox CJ, Harris MH, Thompson CB (2001) Growth factors can influence cell growth and survival through effects on glucose metabolism. *Mol Cell Biol* 21**:** 5899-5912

Vander Heiden MG, Cantley LC, Thompson CB (2009) Understanding the Warburg effect: the metabolic requirements of cell proliferation. *Science* 324**:** 1029-1033

Vander Heiden MG, Locasale JW, Swanson KD, Sharfi H, Heffron GJ, Amador-Noguez D, Christofk HR, Wagner G, Rabinowitz JD, Asara JM, Cantley LC (2010) Evidence for an alternative glycolytic pathway in rapidly proliferating cells. *Science* 329**:** 1492-1499

Varghese B, Swaminathan G, Plotnikov A, Tzimas C, Yang N, Rui H, Fuchs SY (2010) Prolactin inhibits activity of pyruvate kinase M2 to stimulate cell proliferation. *Mol Endocrinol* 24**:** 2356-2365

Vaupel P, Kallinowski F, Okunieff P (1989) Blood flow, oxygen and nutrient supply, and metabolic microenvironment of human tumors: a review. *Cancer Res* 49**:** 6449-6465

Wang X, Sato R, Brown MS, Hua X, Goldstein JL (1994) SREBP-1, a membrane-bound transcription factor released by sterol-regulated proteolysis. *Cell* 77**:** 53-62

Wang Z, Chatterjee D, Jeon HY, Akerman M, Vander Heiden MG, Cantley LC, Krainer AR (2012) Exon-centric regulation of pyruvate kinase M alternative splicing via mutually exclusive exons. *J Mol Cell Biol* 4**:** 79-87

Xu X, Wagner KU, Larson D, Weaver Z, Li C, Ried T, Hennighausen L, Wynshaw-Boris A, Deng CX (1999) Conditional mutation of Brca1 in mammary epithelial cells results in blunted ductal morphogenesis and tumour formation. *Nat Genet* 22**:** 37-43

Yang W, Xia Y, Ji H, Zheng Y, Liang J, Huang W, Gao X, Aldape K, Lu Z (2011) Nuclear PKM2 regulates beta-catenin transactivation upon EGFR activation. *Nature* 480**:** 118-122

Yang W, Xia Y, Hawke D, Li X, Liang J, Xing D, Aldape K, Hunter T, Alfred Yung WK, Lu Z (2012a) PKM2 phosphorylates histone H3 and promotes gene transcription and tumorigenesis. *Cell* 150**:** 685-696

Yang W, Zheng Y, Xia Y, Ji H, Chen X, Guo F, Lyssiotis CA, Aldape K, Cantley LC, Lu Z (2012b) ERK1/2-dependent phosphorylation and nuclear translocation of PKM2 promotes the Warburg effect. *Nat Cell Biol* 14**:** 1295-1304

CHAPTER FOUR:
Cancer-Associated Amino Acid Substitutions in PKM2 Alter Enzyme Kinetics

William J. Israelsen, Vivian M. Liu, Andrea J. Howell, Matthew G. Vander Heiden

David H. Koch Institute for Integrative Cancer Research, Massachusetts Institute of Technology, Cambridge, Massachusetts, 02139, United States

This chapter is not published as of July 2014.

VML, AJH, and WJI generated mutant plasmids. WJI led the study, prepared all proteins with assistance from VML and AJH, and contributed Figure 1D. VML performed experiments presented in Figures 1, 2, 4, 5, and 6. AJH performed experiments presented in Figure 7.

ABSTRACT

Heterozygous mutations causing amino acid substitutions in conserved regions of pyruvate kinase M2 (PKM2) are found in some human cancers. Allosteric regulation of PKM2 pyruvate kinase activity impacts glucose metabolism and the proliferative capacity of cells. Understanding the functional effects of PKM2 mutations on pyruvate kinase activity will inform the selective pressure on the metabolism of cancer cells. Five novel PKM2 cancer mutants (P117L, R246S, G415R, R455Q, and R516C) were prepared and characterized with respect to substrate kinetics and activation by the allosteric activator fructose-1,6-bisphosphate (FBP). These PKM2 cancer mutants exhibited reduced maximal velocity, reduced substrate affinity, and/or altered response to activation by FBP. Kinetic parameters were determined for four additional PKM2 mutants (S37A, R399E, K433E, and H464A), which have been used to study aspects of enzyme function or regulation. These mutations also have global deleterious effects on enzyme function, highlighting the difficulty of engineering mutations that affect only one functional aspect of this highly conserved protein. The effects of single amino acid substitutions in PKM2 demonstrate that the protein is sensitive to small changes in primary structure; however, tumor cells appear to tolerate or select for reductions in pyruvate kinase activity, in line with the known down-regulation of PKM2 activity in proliferating cells.

INTRODUCTION

Mammalian pyruvate kinase isoforms function as homotetramers to catalyze the final step of glycolysis, which is the transfer of phosphate from phosphoenolpyruvate (PEP) to ADP to produce pyruvate and ATP. There are four mammalian pyruvate kinase isoforms, and the activity of each isoform is regulated in unique ways to suit its physiological role

(Mazurek, 2011; Gui et al, 2013). The muscle (PKM1) isoform is found in non-proliferating and highly catabolic tissues such as the heart, brain, and muscle (Imamura & Tanaka, 1972), where it functions as a highly active, constitutive tetramer with few regulatory inputs (Morgan et al, 2013). The liver (PKL), red blood cell (PKR) isoforms are subject to allosteric feed-forward activation by an upstream glycolytic intermediate, fructose-1,6-bisphosphate (FBP) (Taylor & Bailey, 1967; Koler & Vanbellinghen, 1968). Both PKL and PKR are inhibited by phosphorylation; the liver isoform in particular is under exquisite regulatory control to minimize futile cycles during gluconeogenesis (Kahn & Marie, 1982). The M2 isoform of pyruvate kinase (PKM2) is expressed in most tissue types not listed above, including the developing embryo and virtually all cancers studied to date (Imamura & Tanaka, 1972; Mazurek, 2011). In proliferating tissues, including cancer, its catalytic activity is tightly regulated to help balance the catabolic and anabolic needs of proliferating cells (Chaneton & Gottlieb, 2012).

PKM2 activity is modulated by a host of regulatory inputs. Like PKL and PKR, fructose-1,6-bisphosphate (FBP) is a major allosteric activator of PKM2 (Imamura et al, 1972), and its activity is also affected by other allosteric effectors, including phenylalanine, thyroid hormone T_3, and serine (Ashizawa et al, 1991a; Chaneton et al, 2012; Morgan et al, 2013). FBP binding increases affinity of PKM2 for one of its substrates, PEP, and stabilizes the PKM2 tetramer in its fully active conformation. The PKM2 tetramer assembles as a dimer of dimers, and the enzyme exists in a tetramer-dimer-monomer equilibrium; the less-active, FBP-free tetramer conformation is prone to dissociation to inactive monomer. Tetramer dissociation significantly reduces enzyme activity, while the binding of FBP favors tetramer assembly and results in an increase in V_{max} due to an apparent increase in

concentration of functional enzyme (Ashizawa et al, 1991a; Morgan et al, 2013). This association-dissociation phenomenon is also observed *in vivo* (Ashizawa et al, 1991b; Anastasiou et al, 2012; Merrins et al, 2013).

Release of FBP, and subsequent down-regulation of enzyme activity, is stimulated by interaction of the FBP-binding pocket of the enzyme with phosphotyrosine-containing proteins during growth signaling (Christofk et al, 2008). During proliferation, additional mechanisms serve to reduce pyruvate kinase activity, such as the lysine acetylation and degradation of the enzyme during nutrient-replete conditions (Lv et al, 2011). Reduction of PKM2 activity via intracellular signaling facilitates shunting of upstream glycolytic intermediates to biosynthetic pathways (Eigenbrodt et al, 1992), and pharmacologic activation of PKM2 in opposition to this signaling disrupts proliferative metabolism and is detrimental to cellular proliferation (Anastasiou et al, 2012). Genetic experiments using a mouse cancer model suggest that the PKM2 isoform itself is dispensable for proliferation if cells maintain pyruvate kinase activity at a sufficiently low level (Israelsen et al, 2013).

We recently reported 23 heterozygous missense mutations PKM2 that were found in human cancers (Israelsen et al, 2013). Pyruvate kinase is highly conserved, and PKM2 function appears to be sensitive to amino acid substitutions, even in solvent exposed residues (Allali-Hassani et al, 2009), suggesting that the PKM2 mutations occurring in human tumors will have some functional effect on the enzyme. Given that a reduction in intracellular pyruvate kinase activity supports proliferative metabolism, we hypothesized that these cancer mutations may reduce or abolish PKM2 function.

Several studies have also proposed non-glycolytic PKM2 activities in the context of cancer (Chaneton & Gottlieb, 2012), with amino acid substitutions in PKM2 used to

experimentally enhance or separate these non-glycolytic functions from the glycolytic function of the enzyme (Gao et al, 2012; Yang et al, 2012), or to alter the response of the enzyme to intracellular signaling or allosteric inputs (Christofk et al, 2008; Chaneton et al, 2012); however, the effects of these mutations on enzyme kinetics have not been well characterized. Given the importance of PKM2 function on the metabolism of proliferating cells, kinetic characterization is necessary to interpret experiments that use PKM2 mutations in the study of cancer cell proliferation and cell biology. We therefore determined the functional effects of these amino acid substitutions on PKM2 function.

RESULTS

Kinetic Behavior of Wild-type PKM2 and PKM1

Recombinant proteins are often produced as 6x-histidine-tagged versions that are purified using a one-step Ni-affinity protocol. As a poly-histidine tag does not alter the kinetic parameters of PKM2 (Dombrauckas et al, 2005), we sought to determine the viability of this method for preparing recombinant PKM2 proteins for kinetic analysis. 6x-His-PKM2 was prepared from bacterial lysate via binding to Ni-NTA beads, elution at high imidazole concentration, and dialysis. 6x-His-PKM2 (hereafter "PKM2") prepared using this one-step protocol was active and exhibited hyperbolic kinetics with respect to PEP substrate; however, the observed ability of the allosteric activator, FBP, to increase enzyme affinity for PEP or increase the maximal velocity of the enzyme was less than expected (Figure 1A). These results suggested that a large fraction of the enzyme was still bound by FBP from the bacterial lysate, as retention of bound FBP despite purification and dialysis of PKM2 has been previously reported (Christofk et al, 2008). In support of this hypothesis, independent preparations of PKM2 using the one-step purification produced enzyme with

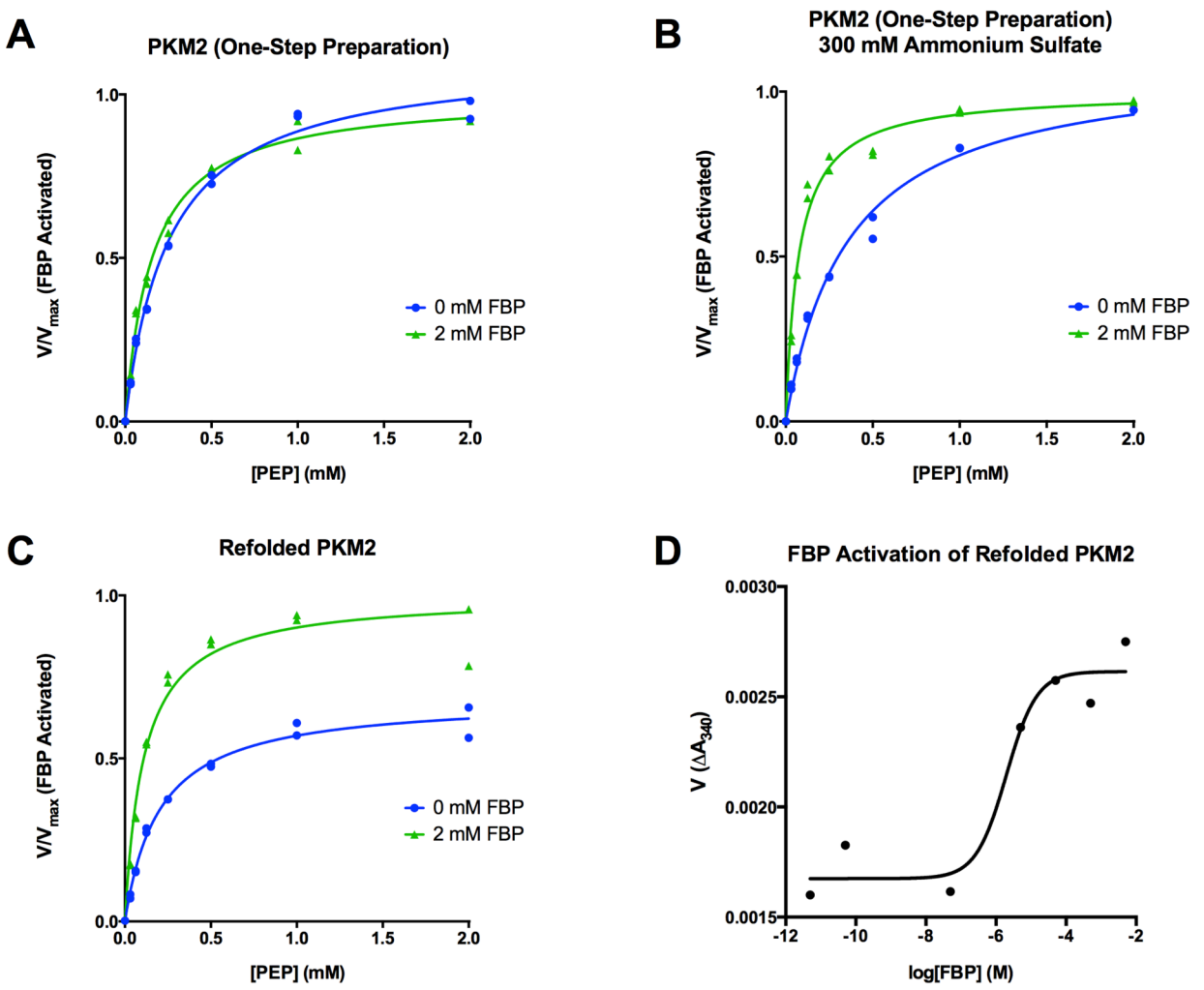

Figure 1. Steady-State Kinetics and FBP Activation of 6x-His-PKM2.
Individual data points are plotted, and assays were conducted using a saturating ADP concentration (5 mM). **(A)** PEP kinetics of PKM2 purified using the one-step protocol. **(B)** PEP kinetics of one-step purified PKM2 in the presence of 300 mM ammonium sulfate. **(C)** PEP kinetics of PKM2 refolded in the absence of FBP. **(D)** Activation of refolded PKM2 by FBP in the presence of subsaturating (0.125 mM) PEP and saturating (5 mM) ADP.

variable ability to be activated by FBP; however, this variability hindered detailed kinetic study of the enzyme. Ammonium sulfate precipitation has been used previously to remove allosteric effectors from liver pyruvate kinase preparations (El-Maghrabi et al, 1982; Blair & Walker, 1984); sulfate ions appear to interfere with the interaction between FBP and the liver enzyme (El-Maghrabi et al, 1982). The presence of 300 mM ammonium sulfate in the

kinetic assay of one-step purified PKM2 resulted in FBP increasing the affinity of the enzyme for PEP without affecting V_{max} (Figure 1B), suggesting that the PKM2 tetramer is incompletely saturated with bacterially-derived FBP under these conditions. To further improve the reproducibility of the assay and obtain PKM2 without pre-bound FBP, bacterially-produced PKM2 was isolated from inclusion bodies and refolded using an on-column refolding method. This refolded PKM2 exhibited robust activation by FBP, as evidenced by a decrease in apparent K_m for PEP and an increase in V_{max} (Figure 1C). The observed increase in V_{max} is consistent with an FBP-induced assembly of fully-active PKM2 tetramers; this behavior of the enzyme has been reported previously (Ashizawa et al, 1991a; Morgan et al, 2013). An activity-based determination of FBP activation of refolded PKM2 protein yielded an AC_{50} value of ~2 μM (Figure 1D), which is comparable to previously reported values for PKM2 activation (Morgan et al, 2013) and binding of FBP to non-phosphorylated PKL (El-Maghrabi et al, 1982).

A two-column preparation of native PKM2 allowed convenient isolation of FBP-responsive PKM2. Following affinity chromatography, PKM2 eluted as a dimer during preparative gel filtration (data not shown) and was activated by FBP (Figure 2A). FBP increased V_{max} and increased affinity for PEP, as evidenced by a reduction in K_m with respect to PEP. FBP had little effect on K_m with respect to ADP (Figure 2B). The qualitative similarity between refolded PKM2 and PKM2 that was prepared using the two-column purification suggests that the latter preparation is sufficient to separate PKM2 from the FBP originally found in the bacterial lysate. As expected, PKM1 protein prepared by the two-column method eluted largely as a tetramer (data not shown), exhibited hyperbolic kinetics with respect to PEP, and was not activated by FBP (Figure 2B). These behaviors of

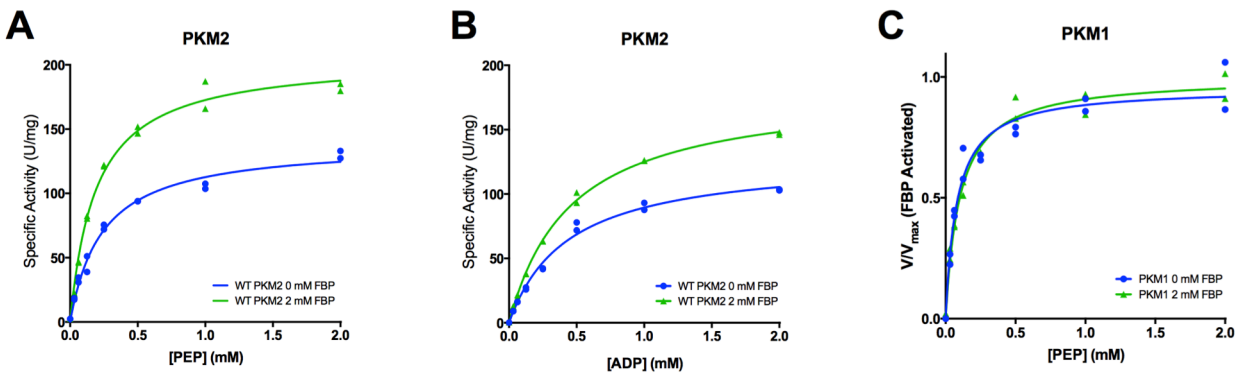

Figure 2. Steady-State Kinetics of 6x-His-PKM2 and 6x-His-PKM1 Prepared Using A Two-Column Purification.
All conditions were performed in duplicate and individual data points are shown. **(A)** PEP kinetics of PKM2 with saturating (5 mM) ADP. **(B)** ADP kinetics of PKM2 with saturating (5 mM) PEP. **(C)** PEP kinetics of PKM1 with saturating (5 mM) ADP.

PKM2 and PKM1 are similar to those reported previously (Dombrauckas et al, 2005; Morgan et al, 2013) and provide a baseline for understanding the effects of mutations on the kinetic parameters of PKM2.

Mutations in PKM2 from Human Cancers

We have previously reported missense mutations in PKM2 that were found in primary human cancers (Israelsen et al, 2013). These mutations are found throughout the primary structure of the enzyme, and we sought to determine if these mutations occurred in conserved residues. The protein sequences of different isoforms of pyruvate kinase from various species were aligned and the locations of all 23 mutations were determined (Figure 3). Nearly half (10/23) of the mutations were perfectly conserved across all species considered, suggesting that many of these residues may be important for enzyme function. Five mutations were chosen for in-depth analysis: P117L, R246S, G415R, R455Q, and R516C. These mutations are found at disparate locations in the tertiary structure of PKM2 and modify residues with varying degrees of conservation; 3 of these 5 mutations are perfectly conserved in the alignment shown in Figure 3.

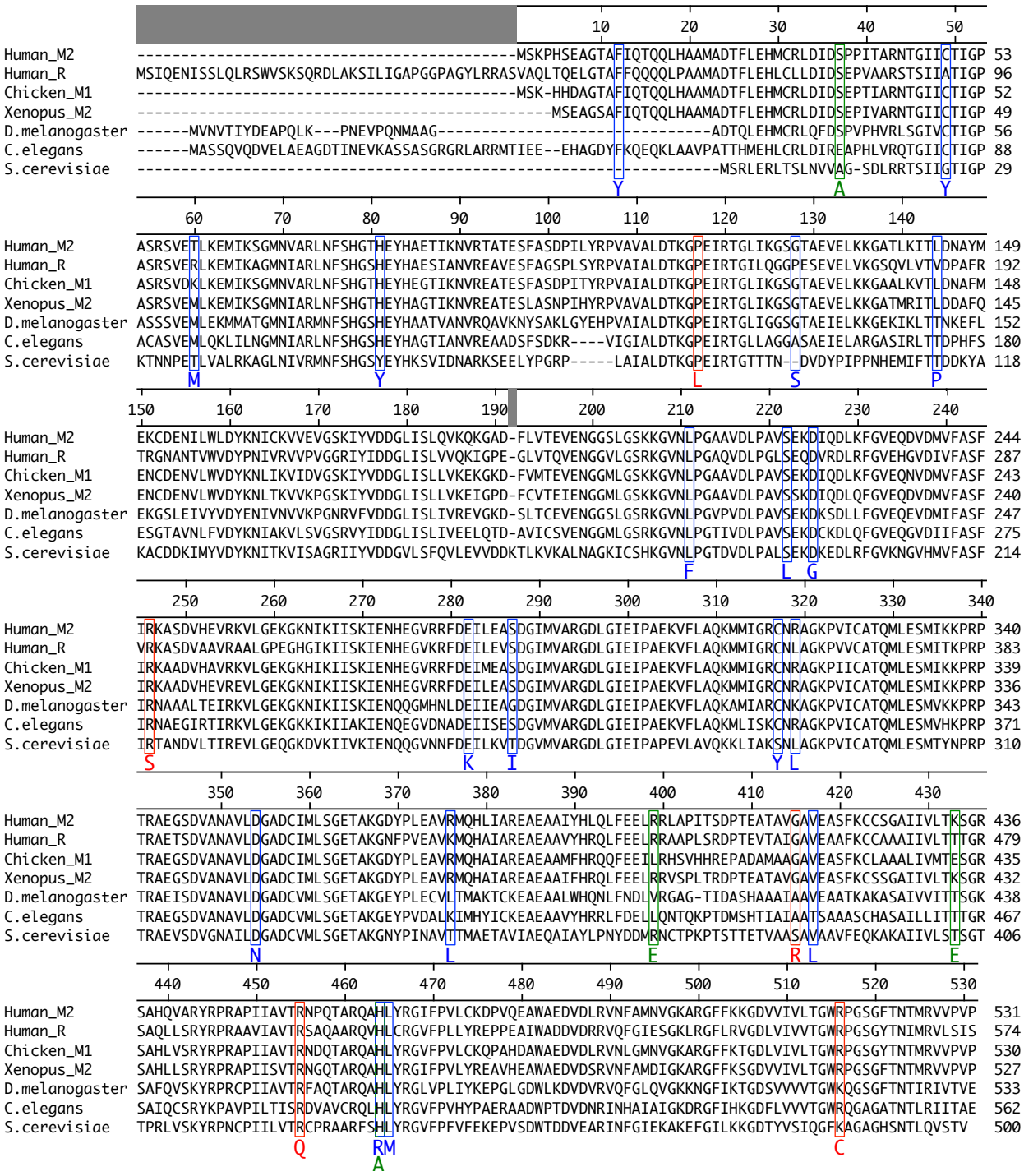

Figure 3. Multiple Sequence Alignment of Pyruvate Kinase Isoforms.
The locations of mutations from human cancers are marked with blue boxes. The cancer mutations characterized in this study are marked with red boxes. Green boxes mark residues from the literature that have been characterized here.

The P117L, R246S, G415R, R455Q, and R516C cancer mutants were prepared using the one-step purification method, and the kinetics of these enzymes were determined with respect to PEP and ADP (Figures 4 and 5). A functional FBP activation assay was also used to determine FBP AC_{50} values for WT, P117L, G415R, and R455Q as a proxy for FBP binding affinity (Figure 6). The location of these mutations and their effects on PKM2 function are described below.

P117 is found in the "hinge" region of the protein between the A and B domains that allows closure of the active site upon substrate binding; this proline residue is conserved from humans to *E. coli*. Despite a reduction in overall velocity, the P117L mutant retains near-wild-type affinity for PEP in the presence and absence of FBP, and the enzyme is capable of tetramerization in response to FBP binding as evidence by the FBP-induced increase in V_{max}. The main effect of the P117L substitution is to greatly reduce affinity of the enzyme for ADP. The K_m with respect to ADP is increased to 1.86 mM in the absence of FBP, and 2.44 mM in the presence of FBP. These data suggest that FBP acts on the PKM2 P117L mutant to stabilize a tetrameric form of the protein in a state of reduced ADP affinity. The discrepancy between the maximum velocities determined from the analyses of PEP- and ADP-dependent kinetic parameters is likely due to a failure of 5 mM ADP to saturate the enzyme; saturating ADP concentrations would likely yield V_{max} values for PEP that are comparable to those determined with respect to ADP. The P117L mutation has very little effect on FBP binding, as the AC_{50} for FBP is largely unchanged relative to refolded PKM2. Interestingly, a large, selective reduction of ADP binding affinity has been observed in the R119C mutant of PKM1 (Cheng et al, 1996). R119 also lies near the hinge

region and the active site cleft; however, the positive side chain of R119 is exposed in the active site and may play a more direct role in ADP binding than does P117.

R246 is partially solvent-exposed and is part of the TIM barrel of the A domain; it is located within 14 angstroms of the active site. In the wild-type protein, the positively-charged side chain of R246 forms interactions with the backbone oxygen of F244 and the negatively-charged side chain of D250. The R246S mutant displays a significant reduction in specific activity and is not activated by FBP. The disruption of enzyme activity is likely is due to changes in active site conformation caused by disruption of the tertiary structure through loss of structural interactions. The FBP binding status and quaternary structure of this mutant protein is unknown.

G415 is located at the dimer-dimer interface of the tetramer. This glycine is found on an α-helix at the interface and positioned such that the G415 of one subunit is in contact with the G415 of the subunit on the opposite side of the interface. The lack of a bulky side chain allows tight packing of the α-helices at the interface. The G415R substitution replaces the hydrogen side chain with a large, charged side chain, and this mutation appears to largely abolish FBP activation of the enzyme, presumably be interfering with the ability of the enzyme to assume a fully active conformation. PKM2 G415R exhibits cooperativity with respect to PEP binding in the absence (n_H = 1.6) of FBP, and this cooperativity is reduced in the presence of FBP (n_H = 1.2). The reduction of cooperativity and modest V_{max} increase caused by FBP suggest that FBP does indeed bind to the enzyme, but the G415R mutation abolishes any physiologically-meaningful FBP activation. The monomer-dimer-tetramer status of this mutant is unknown.

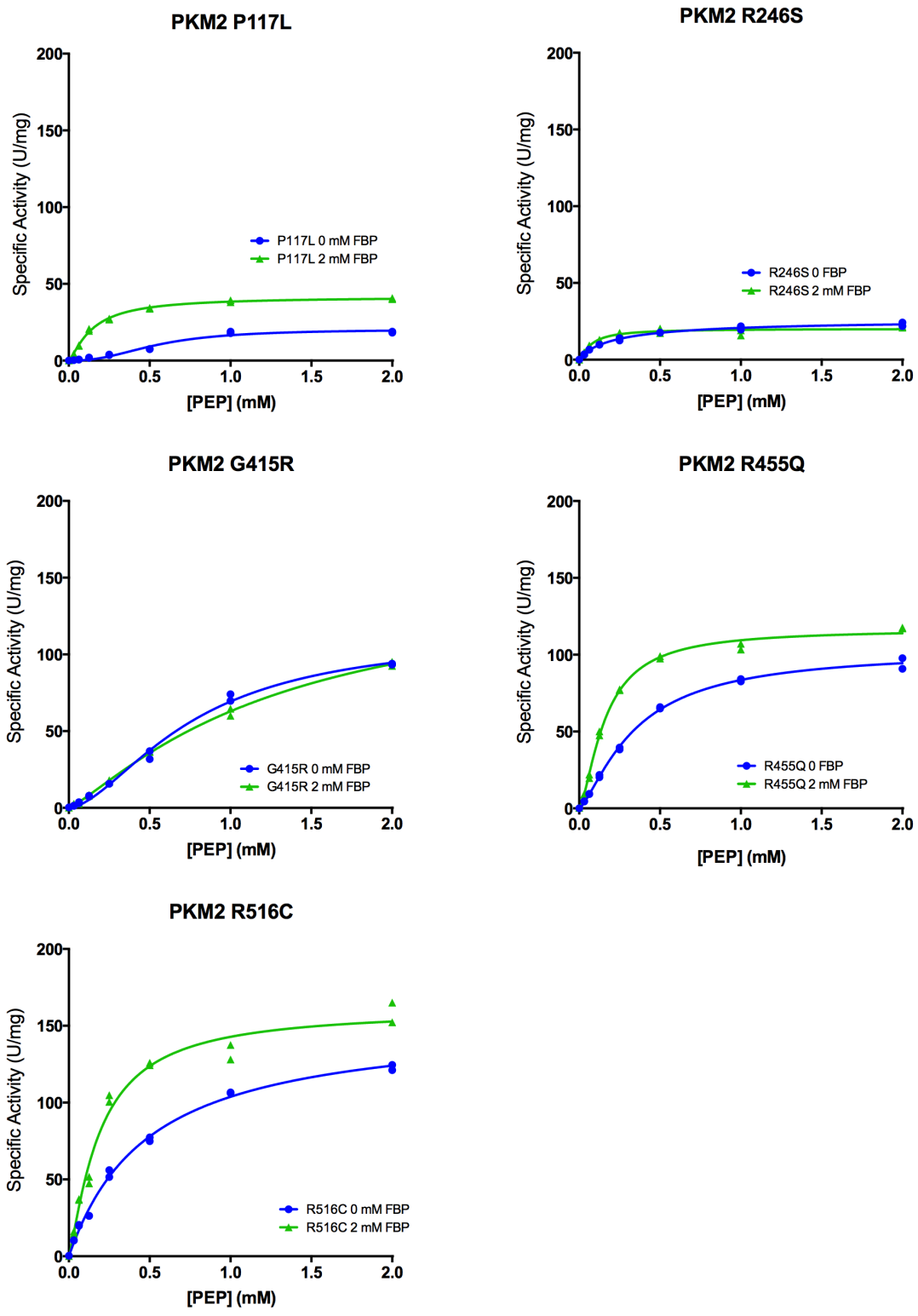

Figure 4. Steady-State Kinetics of PKM2 Cancer Mutants With Respect to PEP.
The ADP concentration was held constant at 5 mM. Assays were preformed in duplicate and all data points are shown.

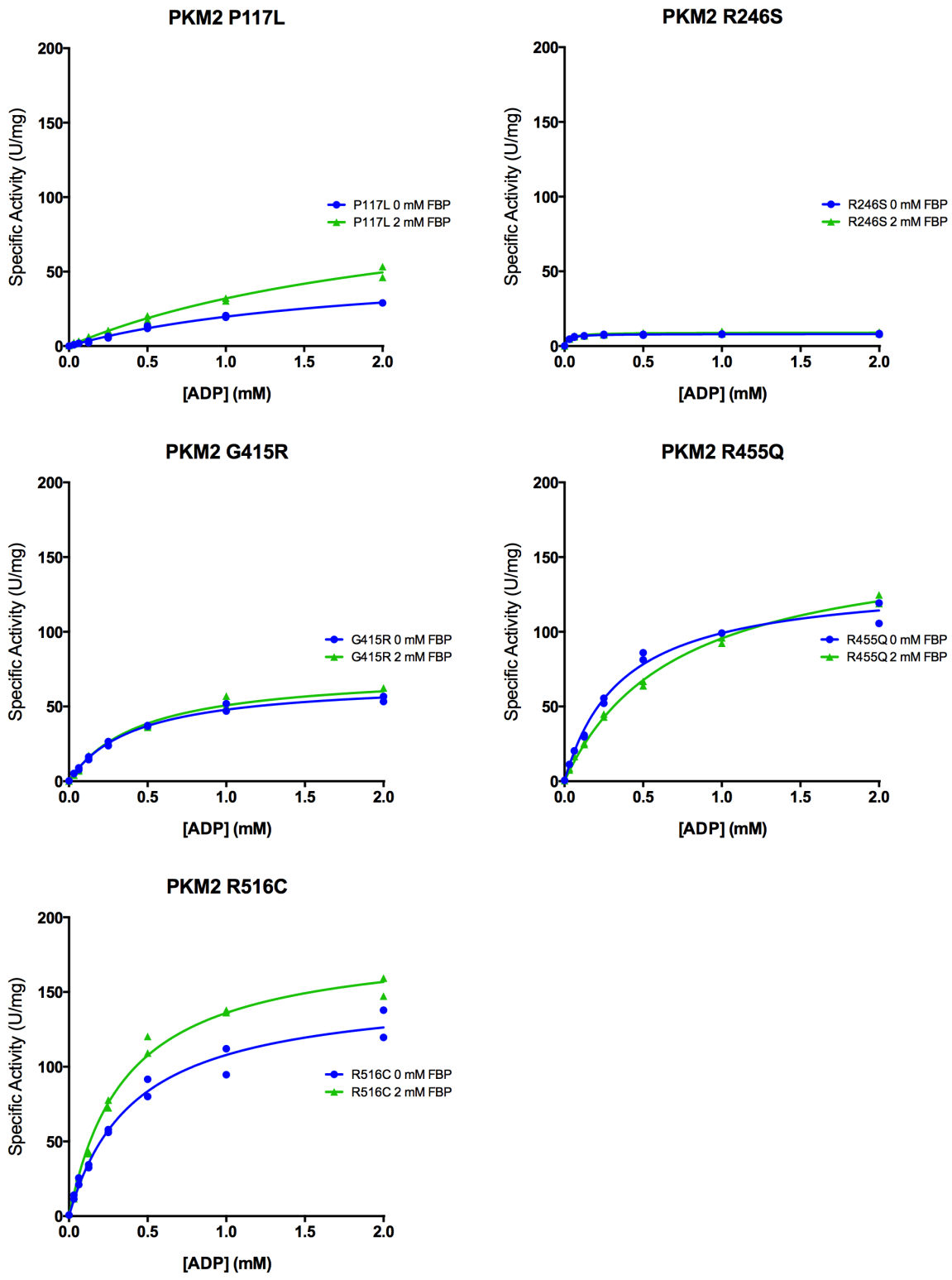

Figure 5. Steady-State Kinetics of PKM2 Cancer Mutants With Respect to ADP.
The PEP concentration was held constant at 5 mM. Assays were preformed in duplicate and all data points are shown.

R455 is located near the FBP binding pocket and interacts electrostatically with D476 and D485. Loss of charge due to the R455Q substitution might be expected to disrupt tertiary structure and affect FBP binding. This mutation appears to abolish the tight FBP binding exhibited by the wild-type enzyme, and increases the FBP AC_{50} to 84 μM, but the R455Q mutant retains near-wild-type enzymatic activity.

R516 is located on the FBP binding loop of the enzyme, but this residue is solvent-exposed and does not form contacts with other parts of the protein or bound FBP. The R516C mutant retains near-normal activity and kinetic parameters but also lacks the tight FBP binding exhibited by the wild-type enzyme.

A summary of kinetic parameters for PEP is given in Table 1; kinetic parameters for ADP are given in Table 2. Overall, the PKM2 mutants from human cancers had either lower maximal activity or reduced affinity for substrates and/or FBP when compared to wild-type PKM2. Despite the one-step preparation method, none of these mutant proteins remained fully activated by FBP following purification, suggesting that each of the mutations resulted either in a loss of the tight, wild-type FBP binding ability of the enzyme, or the mutation had even greater effects on enzyme function and kinetics.

Mutations in PKM2 Used to Study Enzyme Regulation and Function

Previous studies have introduced mutations in PKM2 to study enzyme regulation and separate protein functions (Christofk et al, 2008; Chaneton et al, 2012; Gao et al, 2012; Yang et al, 2012). These mutations have been reported to abolish various non-enzymatic aspects of protein function, or to alter the response of the enzyme to allosteric effectors; however their effects on the kinetic parameters of PKM2 have not been completely characterized. Given the alterations in enzyme function caused by the cancer-associated

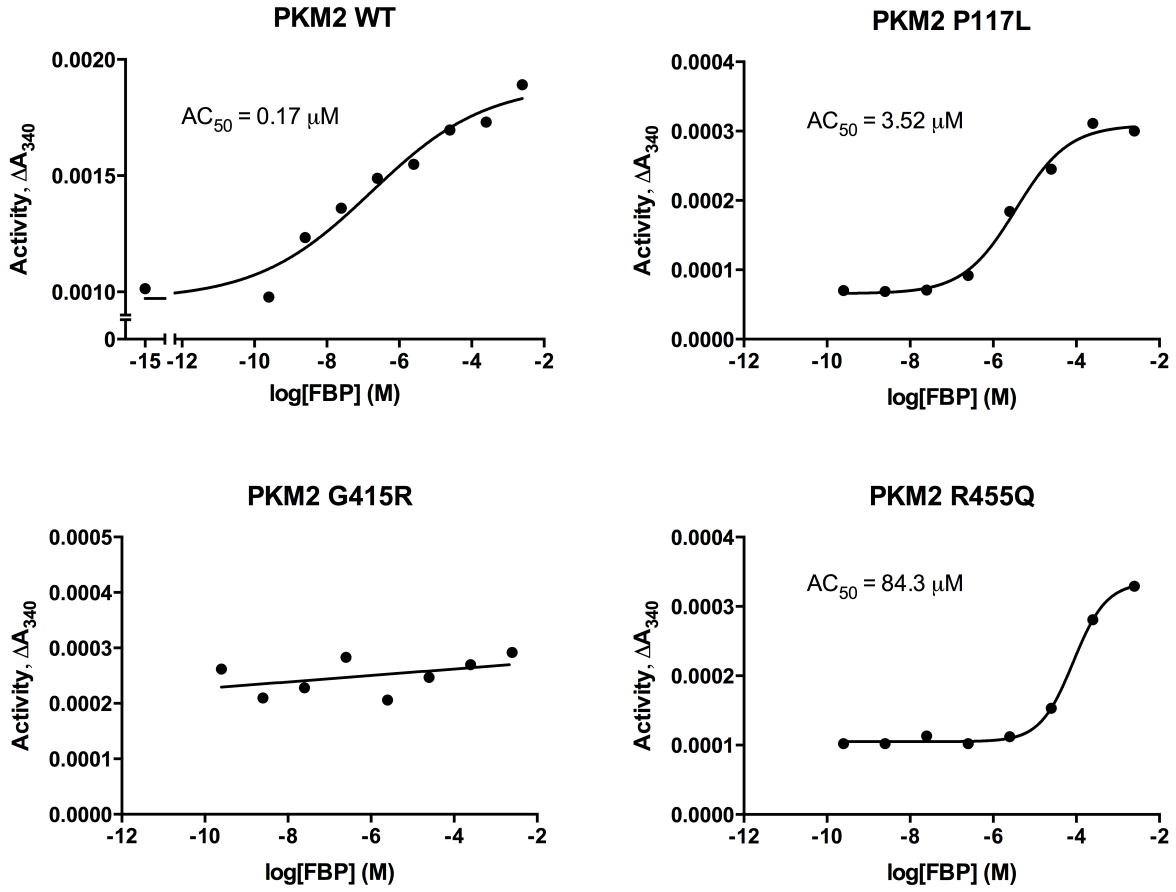

Figure 6. Activation of PKM2 and PKM2 Cancer Mutants by FBP.
Assays contained 5 mM ADP and PEP concentrations were chosen to minimize PEP-induced cooperativity: WT [PEP] = 0.125 mM, P117L [PEP] = 0.0625 mM, G415R [PEP] = 0.0625 mM, R455Q [PEP] = 0.5 mM). PKM2 WT data points are means of duplicate measurements. PKM2 mutant data points represent individual measurements. Data were fit to a sigmoid dose response curve with variable slope.

mutations, we sought to determine if these mutants from the literature also caused changes in kinetic parameters of PKM2. The substitutions considered include S37A, R399E, K433E, and H464A (Christofk et al, 2008; Chaneton et al, 2012; Gao et al, 2012; Yang et al, 2012). Except for R399E, these mutant enzymes were prepared using the two-column purification; all enzymes were assayed for kinetics with respect to PEP in the absence and presence of FBP (Figure 7).

Phosphorylation of PKM2 on S37 is purported to facilitate translocation of PKM2 to the nucleus, where it is involved in oncogenic signaling (Yang et al, 2012). The S37A mutation eliminates this phosphorylation event and drastically reduces orthotopic xenograft growth of glioblastoma in a mouse model. PKM2 S37A eluted as a dimer during preparative gel filtration (data not shown), yet was not responsive to FBP activation and exhibited a reduction in V_{max} with respect of PEP when compared to wild-type PKM2 (Figure 7, Table 1), indicating that the S37A mutation has a large effect on activity and regulation of the enzyme.

The R399E mutation results in loss of inter-subunit contacts across the dimer-dimer interface, and has been reported to be a constitutive dimer with enhanced protein kinase activity (Gao et al, 2012). PKM2 R399E exhibits increased cooperativity (n_H=1.2) in the absence of FBP when compared to wild-type PKM2 (n_H=1.0), and displays a reduced V_{max} both with and without FBP when compared to wild-type. FBP increases affinity of the R399E mutant enzyme for PEP, as evidenced by a large decrease in K_m. Of note is that despite the large effect of FBP on PEP binding affinity, no change is observed in V_{max} during FBP activation, suggesting a lack of tetramer assembly as is seen in the wild-type enzyme.

K433 is located on a loop that forms part of the FBP binding pocket. This positively-charged residue is reported to interact with phosphotyrosine residues on other proteins during intracellular signaling; these interactions facilitate the inactivation of PKM2 by causing release of the allosteric activator FBP (Christofk et al, 2008). The K433E substitution has been reported to interfere with phosphotyrosine-based FBP release, but not with FBP activation of the protein. PKM2 K433E eluted as a dimer from preparative gel filtration (data not shown) and was responsive to activation by FBP. FBP increased affinity

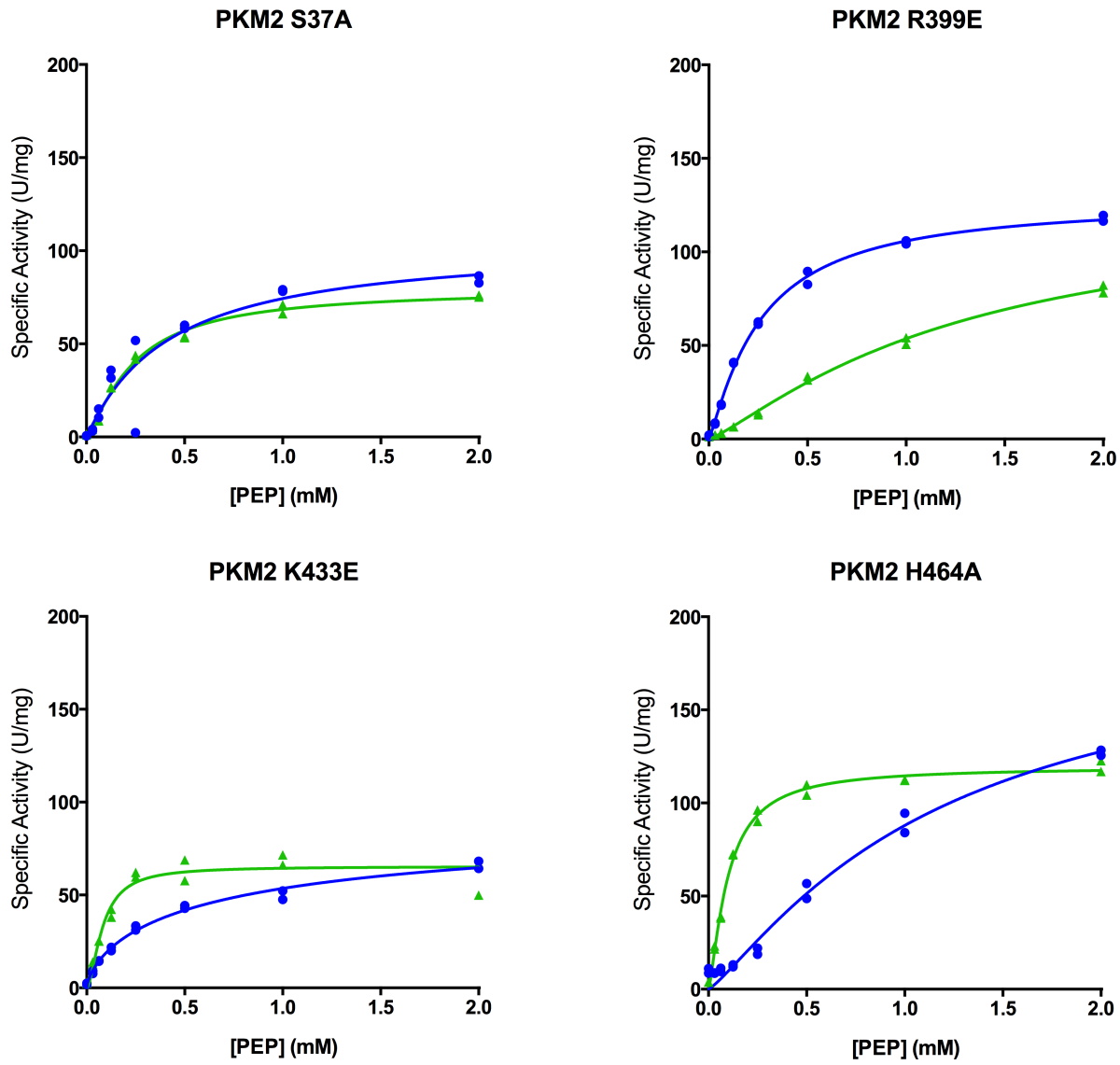

Figure 7. Steady-State Kinetics of PKM2 "Literature" Mutants With Respect to PEP.
The ADP concentration was held constant at 5 mM. Assays were preformed in duplicate and all data points are shown.

for PEP as evidenced by a decrease in K_m with respect to PEP; however, the mutant enzyme shows a greatly reduced V_{max} both with and without FBP as compared to the wild-type enzyme. Additionally, the inability of FBP to induce an increase in V_{max} suggests that the K433E mutant might be incapable of tetramerizing in response to FBP binding, and may function as a dimer.

Serine acts as an allosteric activator of PKM2 with a reported AC_{50} of 1.3 mM (Chaneton et al, 2012), and H464 is found in the serine/alanine/phenylalanine binding pocket (Williams et al, 2006; Chaneton et al, 2012; Morgan et al, 2013). Substitution of H464 with alanine was reported to abolish serine binding without affecting FBP activation (Chaneton et al, 2012). Our results confirm that PKM2 H464A is activated by FBP. When compared to wild-type enzyme, the H464A mutant reduces V_{max} in the FBP-bound state and increases the cooperativity of PEP binding in the absence of FBP.

DISCUSSION

Single amino acid substitutions affecting PKM2 have been found in human cancers. The mutations considered in this study tended to lower affinity of the enzyme for substrate, reduce its maximal activity, or alter its response to the allosteric activator, FBP. That these mutations would have functional effects is not surprising for two reasons. First, these mutations affect residues that are highly conserved, and many of the cancer mutations considered here are located near functional sites on the enzyme. Second, sensitivity of PKM2 to amino acid substitutions is consistent with prior studies regarding PKM2 mutations in other contexts. A previous study characterized mutations in PKM2 caused by SNPs in the human population and found that many of these missense mutations resulted in reduced enzyme activity, reduced thermal stability, or altered allosteric regulation (Allali-Hassani et al, 2009). Characterization of missense mutations of PKM2 in patients with Bloom Syndrome, the underlying cause of which is defective DNA damage repair, revealed that these mutations also negatively affected PKM2 function (Anitha et al, 2004; Akhtar et al, 2009; Gupta et al, 2010).

Wild-type PKM2 prepared using the one-step method was found to retain bound FBP, which rendered it already fully activated by FBP in the standard pyruvate kinase assay. Interestingly, the cancer mutants prepared using this method did not appear to retain FBP to the same extent, suggesting that single amino acid changes, at disparate locations in the enzyme, were each sufficient to abolish the tight FBP-binding characteristic of the wild-type enzyme. The high affinity of PKM2 for FBP is shared by other mammalian pyruvate kinase isoforms such as PKL, but not by the pyruvate kinase isoforms of unicellular organisms. The values reported here and elsewhere for half-maximal binding or half-maximal activation of mammalian pyruvate kinases are in the sub-micromolar to low micro-molar range (0.34-6.5 μM) (El-Maghrabi et al, 1982; Morgan et al, 2013). A reported value for the intracellular FBP concentration in mammalian cells is 80 μM (Srivastava & Bernhard, 1986), which is at least an order of magnitude greater than the concentration required for half-maximal activation of PKM2. In the absence of other allosteric inputs, mammalian pyruvate kinases are likely fully activated by FBP *in vivo*. In contrast, the $K_{0,5}$ values are around 45 μM for yeast pyruvate kinase (Murcott et al, 1992), and 70 μM for *E. coli* pyruvate kinase (Waygood et al, 1976). This might suggest that the yeast and *E. coli* pyruvate kinase isoforms are better suited to respond to changes in intracellular FBP concentration; however, the intracellular FBP concentrations of glucose-fed yeast and glucose-fed *E. coli* are 300 μM and 15 mM, respectively (Bennett et al, 2009; Xu et al, 2012). It therefore appears that the pyruvate kinase of mammals, yeast, and *E. coli* will be fully saturated with FBP – and thus fully activated – when the cells are in a fed state. Why the affinity of the enzyme for FBP does not fall within the dynamic range of intracellular FBP concentrations is a mystery, as sensitivity to fluctuations in FBP

concentration might be expected to allow fine-tuning of glycolytic flux through pyruvate kinase via feed-forward activation. It is possible that FBP activation of pyruvate kinase in unicellular organisms instead acts more as an on-off switch upon glucose withdrawal or change of carbon source. The mammalian isoforms may have traded some allosteric control for regulation by intracellular signaling to allow appropriate metabolic behavior in the multicellular context of specialized tissues. Inactivation of PKL by phosphorylation during gluconeogenesis in the liver is one example (Ishibashi & Cottam, 1978), and inactivation of PKM2 due to FBP release caused by growth signaling in proliferating cells is another (Christofk et al, 2008).

The presence of PKM2 mutations in human cancers demonstrates that tumor cells tolerate, and perhaps select for, reduction in PKM2 activity. These mutations may be advantageous for the proliferation of cancer cells because they lower pyruvate kinase activity, as the ability of the cell to down-regulate pyruvate kinase activity is important for the proliferative metabolic program (Anastasiou et al, 2012; Israelsen et al, 2013). The retention of one wild-type copy of PKM2 could provide metabolic flexibility by allowing up-regulation of PKM2 activity when the cancer cell must survive suboptimal nutrient or growth conditions.

The mutations that have been used to study non-canonical PKM2 functions were all sufficient to alter some aspect of the normal enzymatic function of PKM2. As all of these mutations seemed to have an effect that is similar to, or greater than, the magnitude of the effect observed in cancer associated mutations, changes in glycolytic enzyme activity could be responsible for at least some of the phenotypes found in cells expressing these mutants. These findings also argue that isolating mutations in PKM2 that abolish or alter only one

function of the protein without affecting enzyme kinetics is difficult. The use of PKM2 mutants to study aspects of cell biology that are linked to cell proliferation will require careful consideration of both the metabolic consequences of those mutants and their effects on other enzyme functions.

It is important to note that the determination of kinetic parameters has been done using homotetramers. While sole experimental expression of the non-cancer mutations has been the norm, the cancer mutations have all been found to be heterozygous. As a consequence of this, the mutated form of the enzyme is co-expressed with wild-type enzyme in the affected cancer cell. A similar situation has been found in individuals with Bloom syndrome who harbor heterozygous missense mutations in PKM2 as a consequence of DNA damage (Anitha et al, 2004). Like the mutations studied here, the single amino acid substitutions found in Bloom Syndrome patients alter enzyme kinetics (Akhtar et al, 2009), and the mutant subunits are capable of forming heterotetramers with wild-type PKM2 (Gupta et al, 2010). PKM2 has also been observed to form heterotetramers with PKM1 and PKL (Cardenas & Dyson, 1978; Anastasiou et al, 2012), and heterotetramerization is likely to occur between wild-type PKM2 and PKM2 mutants, as even chicken PKM1 and bovine PKL can combine into functional tetramers (Cardenas et al, 1975). The kinetic parameters of heterotetramers containing wild-type and cancer mutation subunits remain to be determined, but prior works suggests that they are likely to be intermediate between the kinetics of homotetramers of the mutant and wild-type enzymes (Cardenas & Dyson, 1973; Hubbard & Cardenas, 1975).

TABLES

Table 1. **Kinetic Parameters for PEP in the Presence and Absence of 2 mM FBP for Wild-Type and Mutant PKM2.**
Substrate-velocity data were fit using Michaelis-Menten (M) or Hill (H) models.

Enzyme	FBP	K_m (mM)	V_{max} (U/mg)	n_H	FBP AC_{50} (μM)	Fit/R^2
PKM2	-	0.255	111%*	(1.0)		M/0.9934
(One-Step	+	0.156	100%*	(1.0)	-	M/0.9908
Preparation)						
PKM2	-	0.360	110%*	(1.0)		M/0.9904
(One-Step/300mM	+	0.074	100%*	(1.0)	-	M/0.9862
Ammonium Sulfate)						
PKM2	-	0.203	68.5%*	(1.0)		M/0.9898
(Refolded)	+	0.110	100%*	(1.0)	1.98	M/0.9739
PKM1	-	0.080	95.5%*	(1.0)		M/0.9654
	+	0.101	100%*	(1.0)	-	M/0.9840
PKM2	-	0.238	139.4	(1.0)		M/0.9880
(Two-Column Prep.)	+	0.192	205.7	(1.0)	0.17	M/0.9925
PKM2 P117L	-	0.546	20.4	2.4		H/0.9746
	+	0.147	41.6	1.3	3.52	H/0.9974
PKM2 R246S	-	0.234	26.4	0.9		H/0.9926
	+	0.075	20.2	1.3	-	H/0.9693
PKM2 G415R	-	0.765	113.6	1.7		H/0.9958
	+	1.305	149.7	1.2	-	H/0.9987
PKM2 R455Q	-	0.345	103.0	1.4		H/0.9981
	+	0.162	116.6	1.5	84.3	H/0.9972
PKM2 R516C	-	0.483	153.3	1.0		H/0.9961
	+	0.191	161.1	1.2	-	H/0.9833
PKM2 S37A	-	0.416	104.3	1.0		H/0.8897
	+	0.241	79.4	1.3	-	H/0.9923
PKM2 R399E	-	1.291	126.8	1.2		H/0.9966
	+	0.263	128.0	1.2	-	H/0.9975
PKM2 K433E	-	0.705	96.7	0.7		H/0.9885
	+	1.677	65.4	1.7	-	H/0.9501
PKM2 H464A	-	1.187	195.9	1.2		H/0.9825
	+	0.098	119.3	1.4	-	H/0.9946

* Maximum velocities relative to the FBP condition.

Table 2. Michaelis-Menten Kinetic Parameters for ADP in the Presence and Absence of 2 mM FBP for Wild-Type and Mutant PKM2.

Enzyme	FBP	K_m (mM)	V_{max} (U/mg)	R^2
PKM2	-	0.435	128.3	0.9916
(Two-Column Prep.)	+	0.458	182.2	0.9985
PKM2 P117L	-	1.864	56.5	0.9945
	+	2.442	110.0	0.9915
PKM2 R246S	-	0.022	8.1	0.9907
	+	0.029	9.0	0.9769
PKM2 G415R	-	0.413	67.6	0.9946
	+	0.457	73.9	0.9880
PKM2 R455Q	-	0.363	135.0	0.9894
	+	0.706	163.0	0.9970
PKM2 R516C	-	0.412	152.3	0.9835
	+	0.360	185.0	0.9927

METHODS

PCR Mutagenesis

Human PKM2 cDNA was previously cloned into pET-28a with an in-frame N-terminal 6x-His tag (Christofk et al, 2008). PCR mutagenesis was used to generate mutations in the PKM2 coding sequence. The thermal conditions for mutagenesis PCR were 90 s at 98°C, followed by 16 cycles of 10 s at 98°C, 30 s at 55°C, and 10 min at 72°C, with an additional 10 min final elongation step at 72°C. The forward primers used were as follows (5'-3', underlined bases indicate mutations):

S37A: CGCCTGGACATTGATTACCCACCCATCACAGCC;

P117L: CTAGACACTAAAGGACTTGAGATCCGAACTGGG;

R246S: TTTGCGTCATTCATCAGCAAGGCATCTGATGTC;

R399E: TTATTTGAGGAACTCGAACGCCTGGCGCCCATT;

G415R: GAAGCCACCGCCGTGCGTGCCGTGGAGGCCTCC;

K433E: ATAATCGTCCTCACCGAGTCTGGCAGGTCTGCT;

R455Q: ATCATTGCTGTGACCCAGAATCCCCAGACAGCT;

H464A: ACAGCTCGTCAGGCCGCCCTGTACCGTGGCATC;

R516C: GTGCTGACCGGATGGTGCCCTGGCTCCGGCTTC. The reverse primer sequences are the reverse complement of the forward primers. Successful mutagenesis was verified by sequencing the coding region of the plasmid using T7 promoter and terminator primers.

Native Protein Expression and Purification

Wild-type and mutant PKM2 proteins were expressed in *E. coli* BL21(DE3) (Invitrogen) and the soluble protein was purified from the cell lysates. A 50 mL starter culture was inoculated with a colony of freshly transformed *E. coli* and grown at 37°C overnight in LB

broth containing 50 μg/mL of kanamycin (LB-kan). The starter culture was diluted 1/40 into 1 L LB-kan containing 2 mM $MgCl_2$. The expression culture was grown at 37°C to OD_{600} of 0.7 and induced for 6 hours at 25°C with 0.5 mM isopropyl β-D-1-thiogalactopyranoside (IPTG). Following centrifugation, the cell pellet was snap frozen using liquid nitrogen or stored at -80°C prior to use. All subsequent steps were performed on ice or at 4°C. The cell pellet from 1 L of culture was resuspended in a total of 60 mL Buffer A (50 mM Tris, pH 7.5, 10 mM $MgCl_2$, 300 mM KCl, 10% glycerol, 5 mM imidazole) containing two protease inhibitor tablets (Roche, 11836170001). Resuspended cells were lysed by sonication and the lysate was clarified by centrifugation at 20,000 *g* for 45 minutes. The supernatant was filtered using a 0.22 μm filter and applied to a Ni^{2+}-charged IMAC column (GE Healthcare HisTrap 1mL) using an Äkta FPLC system. The column was washed with 15 column volumes of Wash Buffer (50 mM Tris, pH 7.5, 10 mM $MgCl_2$, 300 mM KCl, 20 mM imidazole), then with 20 column volumes of Wash Buffer containing 20% Elution Buffer (50 mM Tris, pH 7.5, 10 mM $MgCl_2$, 250 mM KCl, 250 mM imidazole), and the protein was eluted with a 6 column volume linear gradient from 20% to 100% Elution Buffer. Fractions containing the protein of interest were pooled and concentrated using Amicon Ultra centrifugal filters (Millipore, UFC903024) and run on a gel filtration column (GE Healthcare HiPrep 16/60, Sephacryl S-200) in Buffer B (25 mM Bis-Tris Propane, pH 7.5, 10 mM $MgCl_2$, 25 mM KCl). Fractions of interest were again pooled and spin-concentrated. Glycerol was added to the concentrated protein to 20% v/v and the proteins were aliquotted, frozen in liquid nitrogen, and stored at -80°C. The concentration of purified PKM2 was determined by absorbance at 280 nm using an extinction coefficient of 29,910 $M^{-1}cm^{-1}$.

One-Step hPKM2 Purification

E. coli BL21 (DE3) cells were transformed, induced, pelleted, and frozen as above. The cell pellet was resuspended in Buffer C (50 mM Tris, pH 8.5; 10 mM $MgCl_2$; 300 mM NaCl; 10% glycerol; 5mM imidazole), lysed by sonication and clarified as above, and the supernatant was collected and β-mercaptoethanol (BME) was added to 0.1% (v/v) final concentration. Recombinant protein was bound to Ni-NTA (nickel-nitrilotriacetic acid) agarose beads (Qiagen 30210, 4 mL bead volume per 1 L of culture) by shaking for 1 hour on ice. Beads were batch-washed 4 times with 30 mL Buffer D (50 mM Tris, pH 8.5, 10 mM $MgCl_2$, 300 mM NaCl, 10% glycerol, 30 mM imidazole) and packed into a gravity flow column at 4°C. Bound protein was eluted with Buffer E (50 mM Tris pH 8.5, 10 mM $MgCl_2$, 250 mM NaCl, 10% glycerol, 250 mM imidazole) and collected in 1 mL fractions. The three fractions containing the peak of eluted protein were identified using the Bradford assay, pooled, and dialyzed against 1 L Buffer F (50 mM Tris pH 7.5, 10 mM $MgCl_2$, 25 mM NaCl, 20% glycerol, 21 mM β-mercaptoethanol) for a total 24 hours at 4°C, with one change of buffer after 12 hours.

Inclusion Body Production and On-Column Refolding

E. coli strain BL21 (DE3) transformed with pET28a-6x-His-PKM2 was grown in 1 L of LB-kan containing 5% (w/v) sucrose at 37°C. The culture was induced at OD_{600} of 0.4 with 1 mM IPTG and shaking continued for 3 hours at 37°C. Following centrifugation, the cell pellet was resuspended in Buffer G (50 mM Tris pH 7.5, 100 mM KCl, 20% glycerol; 60 mL per 1 L culture) and lysed by sonication. Inclusion bodies were isolated by centrifugation at 15,000 *g* for 15 minutes, washed twice with Inclusion Body Wash Buffer 1 (50 mM Tris pH 7.5, 10 mM EDTA, 2% Triton X-100, 500 mM NaCl, 5 mM DTT), once with Inclusion

Body Wash Buffer 2 (50 mM Tris pH 7.5), and collected in a pre-weighed tube. The inclusion body pellet was resolubilized overnight at 4°C in 1 mL of Resuspension Buffer (50 mM Tris pH 8.0, 6 M guanidinium, 40 mM imidazole, 5 mM DTT) per 30 mg wet pellet weight. A gravity flow column was packed with Ni-NTA beads (2 mL) at 22°C and washed with 4 column volumes (CV) of Resuspension Buffer. Resolubilized protein was applied to the column and the column was washed with 15 CV of Column Wash Buffer (50 mM Tris pH 8.0, 4 M urea, 40 mM imidazole, 1 mM DTT). To initiate refolding, the column was washed with 4 CV of Refolding Buffer (50 mM Bis-Tris Propane pH 8.0, 100 mM KCl, 20% glycerol, 2 mM $MgCl_2$). The column outlet was stopped and refolding continued at 22°C for 1 h. Protein was eluted using Buffer H (50 mM Bis-Tris Propane pH 8.0, 100 mM KCl, 20% glycerol, 2 mM $MgCl_2$, 250 mM imidazole, 1 mM DTT). Fractions (1 mL) containing protein were pooled and DTT was added to a final concentration of 25 mM.

Protein Visualization

Purified proteins were subjected to SDS-PAGE separation using 8% polyacrylamide gels and visualized by Coomassie blue staining. Images of stained gels were obtained using a LI-COR Biosciences Odyssey imager.

Kinetic Assays

A lactate-dehydrogenase-linked spectrophotometric assay was used to determine pyruvate kinase activity by measuring the oxidation of NADH via absorbance at 340 nm. The reaction buffer consisted of 50 mM Bis-Tris Propane pH 7.5, 200 mM KCl, 15 mM $MgCl_2$, 100 units/mL lactate dehydrogenase (LDH), 2 mM ADP (or PEP), 180 μM NADH and PEP (or ADP) at variable (from 0 to 2 mM) or saturating (5 mM) concentrations as indicated. Enzymes were pre-incubated with or without 50 mM FBP prior to the start of the assay,

and the reaction was initiated by adding reaction buffer to enzyme to a final volume of 100 µL in a well of a 96-well plate. Final FBP concentration was 5 mM when present in the assay. Final pyruvate kinase concentrations were chosen to allow convenient measurement of initial rate measurements; for example, wild-type enzymes were assayed at concentrations near 1 µg/mL. The reaction was monitored using a Tecan Infinite M200 Pro plate reader. K_m and V_{max} values were calculated by fitting the initial rate data using GraphPad Prism software. One unit is defined as the amount of pyruvate kinase activity causing oxidation of one µmole of NADH per minute at 25°C in the LDH-linked assay.

FBP Activation Assay

Enzymes were pre-incubated in concentrations of FBP as indicated and the reaction was started by addition of reaction buffer containing the same FBP concentration. PEP concentrations were chosen to be insufficient to induce cooperativity. Apparent half maximal activating concentration (AC_{50}) values for FBP binding were determined by fitting to data to a sigmoid dose response curve with variable slope using GraphPad Prism software.

REFERENCES

Akhtar K, Gupta V, Koul A, Alam N, Bhat R, Bamezai RN (2009) Differential behavior of missense mutations in the intersubunit contact domain of the human pyruvate kinase M2 isozyme. *J Biol Chem* 284**:** 11971-11981

Allali-Hassani A, Wasney GA, Chau I, Hong BS, Senisterra G, Loppnau P, Shi Z, Moult J, Edwards AM, Arrowsmith CH, Park HW, Schapira M, Vedadi M (2009) A survey of proteins encoded by non-synonymous single nucleotide polymorphisms reveals a significant fraction with altered stability and activity. *Biochem J* 424**:** 15-26

Anastasiou D, Yu Y, Israelsen WJ, Jiang JK, Boxer MB, Hong BS, Tempel W, Dimov S, Shen M, Jha A, Yang H, Mattaini KR, Metallo CM, Fiske BP, Courtney KD, Malstrom S, Khan TM, Kung C, Skoumbourdis AP, Veith H, Southall N, Walsh MJ, Brimacombe KR, Leister W, Lunt SY, Johnson ZR, Yen KE, Kunii K, Davidson SM, Christofk HR, Austin CP, Inglese J, Harris MH, Asara JM, Stephanopoulos G, Salituro FG, Jin S, Dang L, Auld DS, Park HW, Cantley LC, Thomas CJ, Vander Heiden MG (2012) Pyruvate kinase M2 activators promote tetramer formation and suppress tumorigenesis. *Nat Chem Biol* 8**:** 839-847

Anitha M, Kaur G, Baquer NZ, Bamezai R (2004) Dominant negative effect of novel mutations in pyruvate kinase-M2. *DNA Cell Biol* 23**:** 442-449

Ashizawa K, McPhie P, Lin KH, Cheng SY (1991a) An in vitro novel mechanism of regulating the activity of pyruvate kinase M2 by thyroid hormone and fructose 1, 6-bisphosphate. *Biochemistry* 30**:** 7105-7111

Ashizawa K, Willingham MC, Liang CM, Cheng SY (1991b) In vivo regulation of monomer-tetramer conversion of pyruvate kinase subtype M2 by glucose is mediated via fructose 1,6-bisphosphate. *J Biol Chem* 266**:** 16842-16846

Bennett BD, Kimball EH, Gao M, Osterhout R, Van Dien SJ, Rabinowitz JD (2009) Absolute metabolite concentrations and implied enzyme active site occupancy in Escherichia coli. *Nat Chem Biol* 5**:** 593-599

Blair JB, Walker RG (1984) Rat liver pyruvate kinase: influence of ligands on activity and fructose 1,6-bisphosphate binding. *Arch Biochem Biophys* 232**:** 202-213

Cardenas JM, Dyson RD (1973) Bovine pyruvate kinases. II. Purification of the liver isozyme and its hybridization with skeletal muscle pyruvate kinase. *J Biol Chem* 248**:** 6938-6944

Cardenas JM, Blachly EG, Ceccotti PL, Dyson RD (1975) Properties of chicken skeletal muscle pyruvate kinase and a proposal for its evolutionary relationship to the other avian and mammalian isozymes. *Biochemistry* 14**:** 2247-2252

Cardenas JM, Dyson RD (1978) Mammalian pyruvate kinase hybrid isozymes: tissue distribution and physiological significance. *J Exp Zool* 204**:** 361-367

Chaneton B, Gottlieb E (2012) Rocking cell metabolism: revised functions of the key glycolytic regulator PKM2 in cancer. *Trends Biochem Sci* 37**:** 309-316

Chaneton B, Hillmann P, Zheng L, Martin AC, Maddocks OD, Chokkathukalam A, Coyle JE, Jankevics A, Holding FP, Vousden KH, Frezza C, O'Reilly M, Gottlieb E (2012) Serine is a natural ligand and allosteric activator of pyruvate kinase M2. *Nature* 491**:** 458-462

Cheng X, Friesen RH, Lee JC (1996) Effects of conserved residues on the regulation of rabbit muscle pyruvate kinase. *J Biol Chem* 271**:** 6313-6321

Christofk HR, Vander Heiden MG, Wu N, Asara JM, Cantley LC (2008) Pyruvate kinase M2 is a phosphotyrosine-binding protein. *Nature* 452**:** 181-186

Dombrauckas JD, Santarsiero BD, Mesecar AD (2005) Structural basis for tumor pyruvate kinase M2 allosteric regulation and catalysis. *Biochemistry* 44**:** 9417-9429

Eigenbrodt E, Reinacher M, Scheefers-Borchel U, Scheefers H, Friis R (1992) Double role for pyruvate kinase type M2 in the expansion of phosphometabolite pools found in tumor cells. *Crit Rev Oncog* 3**:** 91-115

El-Maghrabi MR, Claus TH, McGrane MM, Pilkis SJ (1982) Influence of phosphorylation on the interaction of effectors with rat liver pyruvate kinase. *J Biol Chem* 257**:** 233-240

Gao X, Wang H, Yang JJ, Liu X, Liu ZR (2012) Pyruvate kinase M2 regulates gene transcription by acting as a protein kinase. *Mol Cell* 45**:** 598-609

Gui DY, Lewis CA, Vander Heiden MG (2013) Allosteric regulation of PKM2 allows cellular adaptation to different physiological states. *Sci Signal* 6**:** pe7

Gupta V, Kalaiarasan P, Faheem M, Singh N, Iqbal MA, Bamezai RN (2010) Dominant negative mutations affect oligomerization of human pyruvate kinase M2 isozyme and promote cellular growth and polyploidy. *J Biol Chem* 285**:** 16864-16873

Hubbard DR, Cardenas JM (1975) Kinetic properties of pyruvate kinase hybrids formed with native type L and inactivated type M subunits. *J Biol Chem* 250**:** 4931-4936

Imamura K, Tanaka T (1972) Multimolecular forms of pyruvate kinase from rat and other mammalian tissues. I. Electrophoretic studies. *J Biochem* 71**:** 1043-1051

Imamura K, Taniuchi K, Tanaka T (1972) Multimolecular forms of pyruvate kinase. II. Purification of M2-type pyruvate kinase from Yoshida ascites hepatoma 130 cells and comparative studies on the enzymological and immunological properties of the three types of pyruvate kinases, L, M1, and M2. *J Biochem* 72**:** 1001-1015

Ishibashi H, Cottam GL (1978) Glucagon-stimulated phosphorylation of pyruvate kinase in hepatocytes. *J Biol Chem* 253**:** 8767-8771

Israelsen WJ, Dayton TL, Davidson SM, Fiske BP, Hosios AM, Bellinger G, Li J, Yu Y, Sasaki M, Horner JW, Burga LN, Xie J, Jurczak MJ, DePinho RA, Clish CB, Jacks T, Kibbey RG, Wulf GM, Di Vizio D, Mills GB, Cantley LC, Vander Heiden MG (2013) PKM2 isoform-specific deletion reveals a differential requirement for pyruvate kinase in tumor cells. *Cell* 155**:** 397-409

Kahn A, Marie J (1982) Pyruvate kinases from human erythrocytes and liver. *Methods Enzymol* 90 Pt E**:** 131-140

Koler RD, Vanbellinghen P (1968) The mechanism of precursor modulation of human pyruvate kinase I by fructose diphosphate. *Adv Enzyme Regul* 6**:** 127-142

Lv L, Li D, Zhao D, Lin R, Chu Y, Zhang H, Zha Z, Liu Y, Li Z, Xu Y, Wang G, Huang Y, Xiong Y, Guan KL, Lei QY (2011) Acetylation targets the M2 isoform of pyruvate kinase for degradation through chaperone-mediated autophagy and promotes tumor growth. *Mol Cell* 42**:** 719-730

Mazurek S (2011) Pyruvate kinase type M2: a key regulator of the metabolic budget system in tumor cells. *Int J Biochem Cell Biol* 43**:** 969-980

Merrins MJ, Van Dyke AR, Mapp AK, Rizzo MA, Satin LS (2013) Direct measurements of oscillatory glycolysis in pancreatic islet beta-cells using novel fluorescence resonance energy transfer (FRET) biosensors for pyruvate kinase M2 activity. *J Biol Chem* 288**:** 33312-33322

Morgan HP, O'Reilly FJ, Wear MA, O'Neill JR, Fothergill-Gilmore LA, Hupp T, Walkinshaw MD (2013) M2 pyruvate kinase provides a mechanism for nutrient sensing and regulation of cell proliferation. *Proc Natl Acad Sci U S A* 110**:** 5881-5886

Murcott TH, Gutfreund H, Muirhead H (1992) The cooperative binding of fructose-1,6-bisphosphate to yeast pyruvate kinase. *EMBO J* 11**:** 3811-3814

Srivastava DK, Bernhard SA (1986) Metabolite transfer via enzyme-enzyme complexes. *Science* 234**:** 1081-1086

Taylor CB, Bailey E (1967) Activation of liver pyruvate kinase by fructose 1,6-diphosphate. *Biochem J* 102**:** 32C-33C

Waygood EB, Mort JS, Sanwal BD (1976) The control of pyruvate kinase of Escherichia coli. Binding of substrate and allosteric effectors to the enzyme activated by fructose 1,6-bisphosphate. *Biochemistry* 15**:** 277-282

Williams R, Holyoak T, McDonald G, Gui C, Fenton AW (2006) Differentiating a ligand's chemical requirements for allosteric interactions from those for protein binding. Phenylalanine inhibition of pyruvate kinase. *Biochemistry* 45**:** 5421-5429

Xu YF, Zhao X, Glass DS, Absalan F, Perlman DH, Broach JR, Rabinowitz JD (2012) Regulation of yeast pyruvate kinase by ultrasensitive allostery independent of phosphorylation. *Mol Cell* 48**:** 52-62

Yang W, Zheng Y, Xia Y, Ji H, Chen X, Guo F, Lyssiotis CA, Aldape K, Cantley LC, Lu Z (2012) ERK1/2-dependent phosphorylation and nuclear translocation of PKM2 promotes the Warburg effect. *Nat Cell Biol* 14**:** 1295-1304

CHAPTER FIVE:
Discussion and Future Directions

SUMMARY

Proliferating cells must regulate intracellular metabolism to fuel biosynthesis, and the M2 isoform of pyruvate kinase has been investigated for its role in cancer metabolism for almost 40 years. The work presented in this thesis shows that expression of the PKM2 isoform allows metabolic flexibility in the cell and permits anabolic metabolism.

PKM2 expression appears to be important for anabolic metabolism due to the response of the enzyme to intracellular signals that down-regulate its activity in response to growth signaling (Christofk et al, 2008b). If PKM2 is important because its activity can be decreased, we reasoned that artificially increasing pyruvate kinase activity in the cell would oppose the ability of the cell to engage a proliferative metabolic program. Opposing the down-regulation of PKM2 by artificially increasing intracellular pyruvate kinase activity does indeed inhibit tumor proliferation (Anastasiou et al, 2012; Chapter 2). Exogenous expression of constitutively active PKM1 and activation of endogenous PKM2 using novel small molecule activators both cause defects in xenograft growth and disruption of anabolic metabolism. These latter results have since been repeated by others using PKM2 activators with different chemical structures but similar mechanisms of action (Kung et al, 2012; Parnell et al, 2013). High, unregulated pyruvate kinase activity thus appears to be dominant in its effect on proliferation and proliferative metabolism. The PKM2 protein remained the only isoform expressed in activator-treated cells, which suggested that enzyme activity may be more important than the presence of a particular PK isoform.

We next sought to determine if the PKM2 isoform is required for tumor formation and growth. Deletion of the M2-specific exon in a mouse model of BRCA1-deficient breast

cancer accelerated tumor formation despite effective loss of PKM2 expression (Israelsen et al, 2013; Chapter 3), and similar results were obtained in a model of colon cancer driven by loss of the *APC* tumor suppressor gene (Appendix A). These results demonstrated that the PKM2 isoform is not required for tumor formation. Interestingly, regulation of PKM splicing in PKM2-null tumors allowed variable expression of PKM1. High PKM1 expression was found in non-proliferative cells, while proliferative cells had little PKM1 expression, suggesting that variable, compensatory PKM1 expression was recapitulating the PK activity levels that would be normally present in the proliferating and non-proliferating cells due to regulation of PKM2 activity. Exogenous PKM1 expression was sufficient to hinder growth in PKM2-null cells, again demonstrating the growth-suppressive function of high pyruvate kinase activity. Thus, the PKM2 protein itself is not required for proliferation, and the importance of PKM2 appears to be due to its responsiveness to down-regulation by growth signaling in proliferating cells.

Evaluation of human tumors for mutations revealed heterozygous mutations in PKM2 (Israelsen et al, 2013; Chapter 3). The mutations included recurrent nonsense mutations in *PKM* exon 10, which is specific for the PKM2 isoform. The truncations caused by these nonsense mutations are predicted to result in unstable, non-functional PKM proteins. In addition to three nonsense mutations, 23 missense mutations in the PKM gene were identified. Characterization of the kinetic parameters of five of these mutant enzymes showed that the amino acid substitutions result in reduced activity or disrupted response to allosteric activation by fructose-1,6-bisphosphate (Chapter 4). These results demonstrate that some human tumors tolerate, and possibly select for, reduced pyruvate kinase activity. That these mutations are heterozygous suggests that there is selective

pressure to maintain some pyruvate kinase activity, as an ability to up-regulate pyruvate kinase activity may be beneficial to allow catabolic metabolism during times of nutrient stress that may occur during tumor initiation or growth of tumor cells in an inappropriate microenvironment.

We conclude that PKM2 expression facilitates down-regulation of intracellular pyruvate kinase activity, which is beneficial for anabolic metabolism during proliferation. Pharmacological activation of PKM2, replacement of PKM2 with PKM1, or expression of PKM1 in addition to endogenous PKM2 all result in high, unregulatable pyruvate kinase activity which is detrimental to a cell's ability to proliferate. The PKM2 isoform is not required in a mouse model of breast cancer, nor is it required for growth of cells in culture. Although the PKM2 isoform is not required for cell proliferation, regulation of PKM2 activity allows metabolic flexibility and supports proliferative metabolism.

DISCUSSION

Limitations of *In Vitro* Assays of PKM2 Kinetics

Most routine characterization of enzyme kinetic parameters is performed using purified enzyme in assay conditions that meet the assumptions of the Michaelis-Menten model. These assumptions include the stipulations that the enzyme concentration is much lower than the substrate concentration, that there is no reverse reaction, and that the substrate concentration does not change over the course of the measurement. The kinetic assay thus normally contains a very small amount of purified enzyme in a buffered solution with relatively high substrate concentrations. In the case of PKM2, there are two main limitations to relating the behavior of the enzyme *in vitro* to conditions *in vivo*: the huge

dilution required to assay PKM2 *in vitro*, and the high concentrations of reaction products (ATP and pyruvate) in the cytosol that are absent from the *in vitro* kinetic assay.

PKM2 has high specific activity, and due to physical limitations of conducting assays of pyruvate kinase activity without using stopped flow techniques, pyruvate kinase must be assayed at a very dilute concentration so that it is possible to record measurable initial rates. In a plate reader format, recombinant PKM2 is conveniently assayed using a final concentration of approximately 1 μg/mL (subunit concentration = ~17 nM) (Chapter 4; Morgan et al, 2013). The reported association constant for PKM2, assuming a simple tetramer-monomer equilibrium, is 0.04 nM^{-3} (Ashizawa et al, 1991a); if the assumptions of this model are accurate, ~18% of the PKM2 subunits will exist as dissociated monomers at equilibrium under standard assay conditions. In contrast, the intracellular pyruvate kinase concentration has been estimated to be around 10 mg/ml in rabbit muscle, and estimates of the total intracellular protein concentration in a variety of cell types fall near the 200-300 mg/ml range (Srivastava & Bernhard, 1986b). PKM2 may thus be approximately 10,000-fold more concentrated in the cell than in the activity assay, and the apparent *in vivo* concentration of the enzyme is further increased by molecular crowding due to the extremely high concentration of proteins in the cytosol. The combination of high cytosolic PKM2 concentration and molecular crowding greatly favors tetramer association *in vivo*. The *in vitro* assay is thus not a perfect representation of *in vivo* kinetics and is potentially complicated by spontaneous dissociation of PKM2 tetramers. Assay conditions more or less favorable to tetramer dissociation may explain the differences in PKM2 kinetics with respect to PEP and FBP that have been reported by various groups (Appendix B). We and others have reported hyperbolic substrate kinetics for purified PKM2, with an FBP-induced

increase in maximal velocity of the enzyme (Chapter 4; Morgan et al, 2013). This behavior of the enzyme is consistent with the enzyme existing in a tetramer-monomer or tetramer-dimer equilibrium and with FBP stabilizing the active tetramer form of PKM2. Other workers have reported sigmoidal kinetics for PKM2 with respect to PEP (Imamura et al, 1972; Dombrauckas et al, 2005). In this case, the simplest explanation for cooperativity of PEP binding is the allosteric activation of additional subunits in an intact tetramer; it may be that the assay conditions used by those workers (e.g., solutions containing 25% glycerol) favored tetramer stabilization. We have, however, been unable to replicate these findings despite considerable effort. A more complete understanding of PKM2 activity *in vivo* will require additional work and may be hampered by the technical difficulty of replicating a cytosol-like environment.

The high concentrations of products of the pyruvate kinase reaction further complicate the direct application of *in vitro* assay findings to the function of the enzyme *in vivo*. The change in free energy between the reactants and the products of the forward pyruvate kinase reaction is thought to greatly favor the transfer of phosphate from PEP to ATP; PEP is the highest energy phosphorylated metabolite (Mazurek et al, 2002). In contrast to the *in vitro* assay conditions, where ATP and pyruvate concentrations are negligible, cells maintain a high ATP/ADP ratio and the pyruvate concentration in the cell is non-negligible. The high ATP/ADP ratio in the cell likely reduces the driving force favoring the forward reaction, and some workers have suggested that the mass action of the products and the reactants of the pyruvate kinase reaction may place the reaction near equilibrium and even allow reversal in some instances (Dyson et al, 1975; Dobson et al, 2002). Finally, a third assumption is challenged by the observation that the pyruvate

kinase concentration in the cell is very high relative to the intracellular metabolite concentrations (Srivastava & Bernhard, 1986a). The conditions faced by PKM2 in the cytosol therefore do not meet the assumptions of Michaelis-Menten kinetics, which highlights potential limitations in applying *in vitro* kinetic parameters to intracellular reactions.

Biochemical assays, such as size exclusion chromatography, result in significant dilution of proteins isolated from lysates. We have used size exclusion to determine the effects of small molecule activators on PKM2 stability (Anastasiou et al, 2012; Chapter 2). In this case, PKM2 from cancer cell lines or xenograft tumors exhibited significant tetramer dissociation, but one is left to wonder if dissociation is an artifact of dilution. It may be that phosphotyrosine-induced FBP release *in vivo* simply allows entry of the PKM2 tetramer into a less active conformation, similar to the state of PKL or PKR tetramers that are inactivated by phosphorylation. There is, however, some evidence that the PKM2 tetramer does in fact dissociate *in vivo.* Ashizawa et al (1991b) generated monoclonal antibodies specific for the monomeric form of PKM2 and used immunofluorescence of fixed cells to show that PKM2 apparently dissociated into a monomeric form when intracellular FBP concentrations were reduced upon glucose starvation. More recently, work using a genetically-encoded PKM2 FRET sensor system has demonstrated a similar phenotype (Merrins et al, 2013). In this case, expression of PKM2 fused to fluorescent proteins allowed live imaging of insulin-secreting cells which showed apparent oscillations of PKM2 association and dissociation in phase with addition metabolic fluctuations.

Additional work is needed to fully understand the tetramer-dimer-monomer dynamics of PKM2 *in vivo.* The metabolic consequences of changes in PKM2 activity and/or

multimer status have yet to be fully explored. Dissociated PKM2 subunits might interact with other proteins, and controversial roles for PKM2 dimers or monomers have been proposed, but a clear function for non-tetramers in cells has not been defined.

PKM2 Regulation and Lactate Production: A Case for Channeling?

Changes in pyruvate kinase activity alter cellular metabolism. Cancer cells expressing PKM1 exhibited greater oxygen consumption and reduced lactate production, suggesting that the normal down-regulation of PKM2 activity apparently favors lactate production at the expense of pyruvate oxidation in the mitochondria (Christofk et al, 2008a). Similar results were obtained in PKM2-expressing cancer cells that were treated with PKM2 activators: lactate production falls when PKM2 enzymatic activity is artificially increased (Anastasiou et al, 2012; Chapter 2). Conversely, lactate production is increased when PKM2 activity is reduced as a result of intracellular signaling. Prolactin stimulation of cells expressing the prolactin receptor results in Janus kinase 2 (JAK2)-mediated tyrosine phosphorylation; this signaling cascade causes a reduction of intracellular PKM2 activity and an increase in lactate production (Varghese et al, 2010). The mechanism by which pyruvate kinase activity affects the fate of pyruvate, a product of its reaction, is unknown.

The pyruvate produced by pyruvate kinase is, in general, either reduced to lactate in an NADH-dependent reaction catalyzed by lactate dehydrogenase (LDH) or transported into the mitochondria where it is converted to acetyl-CoA and CO_2 by pyruvate dehydrogenase (PDH). Although it is unclear how pyruvate kinase activity affects the fate of pyruvate, this effect appears to depend on pyruvate kinase activity alone. There are

several possible explanations for the effect of pyruvate kinase activity on the fate of the product of its reaction.

The first of these hypotheses invokes substrate channeling. The pro-proliferative signaling cascade in the cell may change the localization of PKM2 with respect to LDH or the mitochondria to increase the probability that pyruvate is acted upon by LDH. In this hypothetical scenario, destabilization of the PKM2 tetramer may allow PKM2 monomers or dimers to associate with LDH in the cytosol, and the proximity of the two enzymes would favor conversion of pyruvate to lactate. Cytosolic complexes of various glycolytic enzymes have been found. These complexes have included LDH, enolase, and phosphoglycerate kinase (Simon et al, 1989), or glyceraldehyde-3-phosphate dehydrogenase, enolase, phosphoglycerate kinase, and pyruvate kinase (Mazurek et al, 1996). Despite observations such as these, evidence for channeling of pyruvate to LDH is lacking, and cytosolic substrate channeling remains a controversial field with little definitive data (Mendes et al, 1995).

A second hypothesis is that PKM2 activity regulates lactate production by causing indirect global changes to the metabolic network. This idea is plausible, as changes in pyruvate kinase activity have been shown to affect other metabolic pathways, and changes in the cytosolic NAD^+/NADH ratio can have a major impact on pyruvate to lactate conversion. Inhibition of PKM2 due to reactive oxygen species increases pentose phosphate pathway flux (Anastasiou et al, 2011). Downregulation of PKM2 appears to be important for flux through the serine biosynthesis pathway; pharmacological activation of PKM2 disrupts serine production and causes serine auxotrophy in certain cancer cell lines (Kung et al, 2012). Work presented here found activator-induced changes in the sizes of pools of metabolites that are important for anabolic processes (Anastasiou et al, 2012;

Chapter 2). Analysis of glycolytic fluxes using stable isotope tracers will further our understanding of the role of PKM2 activity on intracellular metabolic fluxes, and careful characterization of the NAD^+/NADH ratio in cells with active and inactive pyruvate kinase may help explain changes in the balance between lactate production and mitochondrial pyruvate oxidation.

Is a Product of the *PKM* Gene Required?

Genetic elimination of PKM2 in a tumor context demonstrated that PKM2 is dispensable for tumor growth (Israelsen et al, 2013; Chapter 3); however, PKM2 is expressed in the developing embryo and many adult tissues. This raises the question of whether PKM2 is required for normal organismal development and function. Null alleles of both PKM1 and PKM2 have been generated in the Vander Heiden laboratory, and maintenance of these animals by the author and others has demonstrated that both PKM1-null and PKM2-null animals are viable and compensate for lack of PKM1 or PKM2 in specific tissues, respectively, via expression of the other PKM isoform (Talya Dayton, personal communication). Because some product of the *Pkm* gene is always expressed in the tissues of these animals, it may be that normal tissues require some pyruvate kinase activity, although whether pyruvate kinase activity is required in all cell types within tissues remains an open question.

The spontaneous *Pkm* loss-of-function mutation (*PK-3^r*) isolated in laboratory mice (Johnson et al, 1981) provided information that speaks both to the requirement for pyruvate kinase activity and to endogenous regulation of pyruvate kinase expression. Given that the *PK-3^r* allele results in complete loss of function, it is interesting to note that animals with only one functional *Pkm* gene had about 50-60% of normal pyruvate kinase

activity in the PKM2-expressing kidney and PKM1-expressing heart (Johnson et al, 1981; Peters & Andrews, 1984). This lack of compensation in pyruvate kinase expression in heterozygous animals indicates a lack of intracellular feedback on expression from the *Pkm* gene. The implications of this are two-fold: first, the cell is apparently unable to detect intracellular pyruvate kinase activity and adjust expression accordingly (indeed, there is no plausible mechanism for this type of sensing), and second, PKM1 and/or PKM2 protein levels are apparently not involved in regulation of their own expression in the context of these tissues.

The *PK-3*^{r} allele is lethal when homozygous, and this lethality occurs early in development, around the time of implantation of the embryo (Lewis & Johnson, 1983). Unfortunately the *PK-3*^{r} allele is uncharacterized at the molecular level and the mice are no longer in existence, so the possibility remains that the developmental lethality of the *PK-3*^{r} allele is due to a defect in a closely-linked gene or genes. If the lethality of this allele is, in fact, due to loss of pyruvate kinase expression, this would suggest that the developing mouse embryo requires expression of at least one product of the *Pkm* gene.

While pyruvate kinase acts as the ATP payoff step of glycolysis, there is some evidence for an alternative glycolytic pathway that involves the conversion of PEP to pyruvate via the transfer of phosphate to histidine 11 of phosphoglycerate mutase (PGAM) (Vander Heiden et al, 2010). This PEP phosphatase activity does not generate ATP, but would be sufficient to allow continued glycolysis given sufficient flux through this pathway. The protein or proteins catalyzing this reaction are unknown. If the lethality of the *PK-3*^{r} allele is due solely to loss of pyruvate kinase, the alternative pyruvate kinase activity does not appear capable of replacing PKM2 during embryogenesis.

Molecular Function And Alternative Activities Of PKM2

PKM2 is unique in that intracellular signaling reduces enzyme activity by precipitating release of the allosteric activator FBP (Christofk et al, 2008b). This signaling-induced FBP release has been reported to rely on interaction of the phosphotyrosine with a lysine residue (K433) that is found at the FBP binding site. Analysis of crystal structures of PKM2 with bound FBP shows that K433 forms an electrostatic interaction with the phosphate group attached to the C1 carbon of FBP. FBP and phosphotyrosine-peptides appear to compete for a binding site on PKM2 (Christofk et al, 2008b; Allali-Hassani et al, 2009). The K433E mutant is unable to bind phosphotyrosine peptides, but retains some affinity for FBP, which might be explained by binding of phosphotyrosine peptides to the FBP binding site in a manner that involves K433 but produces fewer favorable contacts than does FBP binding. Kinetic analysis of the K433E mutant shows that FBP binding increases affinity for PEP but does not increase V_{max}. These results suggest that PKM2 K433E is either a constitutive tetramer with reduced V_{max}, or that it is incapable of forming tetramers in response to FBP binding (Chapter 4). Additional work is needed to determine the FBP binding affinity and tetramer status of this mutant.

Given that the apparent AC_{50} of FBP for PKM2 is approximately an order of magnitude lower than the reported FBP concentration in mammalian cells (Srivastava & Bernhard, 1986a; Srivastava & Bernhard, 1986b; Morgan et al, 2013; Chapter 4), sustained phosphotyrosine signaling would be needed to inactivate PKM2 by continually competing for FBP binding. PKM2 would be expected to bind FBP and enter an active conformation once the growth signal has been withdrawn and phosphotyrosine levels fall. This type of

input on PKM2 activity ensures that PKM2 activity is reduced only when growth signaling in active in the cell.

A tyrosine phosphatase inhibitor, pervanadate, has been used to artificially increase phosphotyrosine levels in the cell, and treatment of cells with pervanadate results in PKM2 tetramer destabilization and a corresponding reduction in enzyme activity (Christofk et al, 2008b; Anastasiou et al, 2012; Chapter 2). Pervanadate, which is a peroxide form of the vanadate anion, is an irreversible inhibitor that works by modifying the catalytic cysteine of the phosphatase (Huyer et al, 1997). Pervanadate is quickly converted to vanadate in the presence of reducing agents; the vanadate ion acts as a competitive phosphatase inhibitor by binding to the active site of the phosphatase in place of phosphate.

The sulfate ion interferes with FBP binding to PKL (El-Maghrabi et al, 1982), and sulfate ions have been shown to bind to the effector sites of *Leishmania* pyruvate kinase and stabilize the crystal form in an active state (Tulloch et al, 2008). High concentrations of sulfate appear to remove some bound FBP from one-step purified PKM2 to allow FBP activation in a kinetic assay (Chapter 4). Because the sulfate ion is capable of interfering with FBP binding, presumably via direct competition for the FBP binding site, one may wonder if the vanadate ion has a similar effect on the enzyme. The vanadate ion does not directly affect the catalytic activity of PKM1, but has been reported to inhibit other glycolytic enzymes such as phosphoglycerate mutase (Climent et al, 1981). Additionally, PKM2 activity is reduced and the tetramer is destabilized by oxidation of cysteine 358 (Anastasiou et al, 2011). This raises the possibility that pervanadate might act directly on PKM2 by modifying this cysteine residue.

SAICAR, an intermediate in purine nucleotide synthesis, has been reported to activate both the pyruvate kinase and putative protein kinase activities of PKM2 (Keller et al, 2012; Keller et al, 2014). Pyruvate kinase is most active as a glycolytic enzyme when it is a tetramer, but work by others has argued that non-tetrameric PKM2 is responsible for protein kinase activity (Gao et al, 2012; Gao et al, 2013; Lv et al, 2013). Regardless of tetramer state, some structural change in PKM2 would be necessary to allow binding of different substrates. This raises questions about how SIACAR binding can enhance two activities that require different enzyme conformations. The site of SAICAR binding is unknown, but work using two mutants – K433E and Q393K, which is SAICAR-insensitive – suggested that SAICAR activation is separable from FBP activation of the enzyme (Keller et al, 2012). The Q393K substitution changes a residue at the novel binding pocket that is bound by multiple classes of small molecule activators (Anastasiou et al, 2012; Chapter 2; Kung et al, 2012; Parnell et al, 2013), suggesting that SAICAR may bind at this site and not at the FBP binding site. A crystal structure of PKM2 bound to SAICAR would provide a definitive answer to this question and help to shed light on the molecular mechanism of SAICAR activation.

PKM2 has been reported to act as a PEP-dependent protein kinase (Gao et al, 2012; Yang et al, 2012; Keller et al, 2014). The proposed mechanism of this protein kinase activity requires binding of the protein substrate to the ADP binding site, and the presence of ADP has been reported to interfere with protein kinase activity, which supports that argument. The ability of SAICAR to activate both the pyruvate kinase and putative protein kinase activities of the enzyme would suggest that activation of both activities is dependent on increased affinity of the enzyme for PEP, the phosphate donor, and the low μM K_m for

PEP for the protein kinase activity of SAICAR-activated PKM2 has led others to suggest that the active protein kinase state is the active R-state of PKM2 (Keller et al, 2014). Barring SAICAR-induced refolding of the enzyme, the active form of the PKM2 protein kinase is thus predicted to be a stabilized tetramer. This brings up two difficulties in understanding the published data regarding the protein kinase activity of PKM2. First, all reports to date have shown clearly that PKM2 has protein kinase activity but PKM1 does not. The active sites of these enzymes are identical in amino acid sequence and virtually identical in structure (Morgan et al, 2013); the PKM1 isoform and the active tetramer form of PKM2 are essentially the same enzyme and exhibit nearly identical kinetic parameters (Ibsen et al, 1981). It is therefore not clear why PKM2 would be a protein kinase when PKM1 is not, as there is no clear molecular distinction between the active sites. Second, it is also unclear how the active site allows binding and phosphorylation of more than 140 protein substrates (Keller et al, 2014) while still maintaining specificity of nucleotide substrate binding. It is thus extremely difficult to rationalize the molecular mechanism by which PKM2, but not PKM1, acts as a triple-specificity kinase which is capable of transferring phosphate from PEP to nucleotide substrates, to threonine residues on protein substrates, and to tyrosine residues on protein substrates.

The ability to unambiguously detect PKM2-dependent protein kinase activity is complicated by the ATP-producing activity of the enzyme. Incubation of cell lysates with ^{32}P-labeled PEP results in transfer of radiolabeled phosphate to multiple proteins, as visualized by autoradiography following SDS-PAGE (Israelsen et al, 2013; Chapter 3), but the pattern of phosphorylated proteins appears to be the same as that obtained with γ-^{32}P-ATP, a substrate for ATP-dependent protein kinases found in the cell. The presence of

excess cold competitor ATP inhibits phosphorylation of protein by radiolabeled ATP, and interestingly, cold competitor ATP successfully competes away most PEP-dependent phosphorylation. These results suggest that PEP-dependent phosphorylation requires the ATP-generating activity of pyruvate kinase; if this is the case, the PEP-dependent phosphorylation events occur when the radiolabeled ATP produced by PKM2 is available as a substrate for protein kinases in the lysate. These results thus imply that ADP present in the cell lysate is acts as a substrate to allow generation of radiolabeled ATP from radiolabeled PEP by PKM2, and that this labeled ATP is responsible for most, if not all, of the phosphorylation events observed.

An alternative explanation for the ability of ATP to compete away PEP-dependent phosphorylation is that the protein kinase activity of PKM2 is inhibited by the 1 mM ATP used as competitor. This alternative explanation is unlikely, because the reported intracellular ATP concentration of mammalian cells is 8 mM (Srivastava & Bernhard, 1986a). In a doubly-hypothetical situation, this proposed ATP inhibition of PKM2 protein kinase activity might be overcome by SAICAR activation of PKM2 protein kinase; however, these ideas have not been tested experimentally, and careful biochemical characterization of the putative protein kinase activity of PKM2 is lacking. Finally, lack of requirement for PKM2 by tumors, and the existence of PKM2-null mice, which have no overt phenotype, raises questions about whether any PKM2 protein kinase activity is physiologically relevant.

FINAL PERSPECTIVE

The work presented in this thesis addresses the importance of PKM2 in cancer. Expression of PKM2 facilitates cancer metabolism by allowing the cell to titrate pyruvate kinase activity, and down-regulation of PKM2 activity in response to growth signaling is important for proliferation. Pyruvate kinase activity can be artificially increased by exogenous expression of PKM1 or through the use of novel small molecule PKM2 activators. High, unregulatable pyruvate kinase activity due to these treatments disrupts proliferative metabolism and hinders xenograft tumor growth. Despite expression of PKM2 in most, if not all, cancers, the M2 isoform of pyruvate kinase is not required for tumor development or growth, as was demonstrated by PKM2 deletion in a mouse model of breast cancer. Following excision of *Pkm* exon 10 in this model, the unique splicing of the *Pkm* gene allows variable PKM1 expression, and low PKM1 expression in a subset of cancer cells is conducive to their proliferation. Pyruvate kinase is thus an important point of metabolic regulation, and the amount of pyruvate kinase activity in the cell appears to be more important than the particular pyruvate kinase isoform.

REFERENCES

Allali-Hassani A, Wasney GA, Chau I, Hong BS, Senisterra G, Loppnau P, Shi Z, Moult J, Edwards AM, Arrowsmith CH, Park HW, Schapira M, Vedadi M (2009) A survey of proteins encoded by non-synonymous single nucleotide polymorphisms reveals a significant fraction with altered stability and activity. *Biochem J* 424**:** 15-26

Anastasiou D, Poulogiannis G, Asara JM, Boxer MB, Jiang JK, Shen M, Bellinger G, Sasaki AT, Locasale JW, Auld DS, Thomas CJ, Vander Heiden MG, Cantley LC (2011) Inhibition of pyruvate kinase M2 by reactive oxygen species contributes to cellular antioxidant responses. *Science* 334**:** 1278-1283

Anastasiou D, Yu Y, Israelsen WJ, Jiang JK, Boxer MB, Hong BS, Tempel W, Dimov S, Shen M, Jha A, Yang H, Mattaini KR, Metallo CM, Fiske BP, Courtney KD, Malstrom S, Khan TM, Kung C, Skoumbourdis AP, Veith H, Southall N, Walsh MJ, Brimacombe KR, Leister W, Lunt SY, Johnson ZR, Yen KE, Kunii K, Davidson SM, Christofk HR, Austin CP, Inglese J, Harris MH, Asara JM, Stephanopoulos G, Salituro FG, Jin S, Dang L, Auld DS, Park HW, Cantley LC, Thomas CJ, Vander Heiden MG (2012) Pyruvate kinase M2 activators promote tetramer formation and suppress tumorigenesis. *Nat Chem Biol* 8**:** 839-847

Ashizawa K, McPhie P, Lin KH, Cheng SY (1991a) An in vitro novel mechanism of regulating the activity of pyruvate kinase M2 by thyroid hormone and fructose 1, 6-bisphosphate. *Biochemistry* 30**:** 7105-7111

Ashizawa K, Willingham MC, Liang CM, Cheng SY (1991b) In vivo regulation of monomer-tetramer conversion of pyruvate kinase subtype M2 by glucose is mediated via fructose 1,6-bisphosphate. *J Biol Chem* 266**:** 16842-16846

Christofk HR, Vander Heiden MG, Harris MH, Ramanathan A, Gerszten RE, Wei R, Fleming MD, Schreiber SL, Cantley LC (2008a) The M2 splice isoform of pyruvate kinase is important for cancer metabolism and tumour growth. *Nature* 452**:** 230-233

Christofk HR, Vander Heiden MG, Wu N, Asara JM, Cantley LC (2008b) Pyruvate kinase M2 is a phosphotyrosine-binding protein. *Nature* 452**:** 181-186

Climent F, Bartrons R, Pons G, Carreras J (1981) Effect of vanadate on phosphoryl transfer enzymes involved in glucose metabolism. *Biochem Biophys Res Commun* 101**:** 570-576

Dobson GP, Hitchins S, Teague WE, Jr. (2002) Thermodynamics of the pyruvate kinase reaction and the reversal of glycolysis in heart and skeletal muscle. *J Biol Chem* 277**:** 27176-27182

Dombrauckas JD, Santarsiero BD, Mesecar AD (2005) Structural basis for tumor pyruvate kinase M2 allosteric regulation and catalysis. *Biochemistry* 44**:** 9417-9429

Dyson RD, Cardenas JM, Barsotti RJ (1975) The reversibility of skeletal muscle pyruvate kinase and an assessment of its capacity to support glyconeogenesis. *J Biol Chem* 250**:** 3316-3321

El-Maghrabi MR, Claus TH, McGrane MM, Pilkis SJ (1982) Influence of phosphorylation on the interaction of effectors with rat liver pyruvate kinase. *J Biol Chem* 257**:** 233-240

Gao X, Wang H, Yang JJ, Liu X, Liu ZR (2012) Pyruvate kinase M2 regulates gene transcription by acting as a protein kinase. *Mol Cell* 45**:** 598-609

Gao X, Wang H, Yang JJ, Chen J, Jie J, Li L, Zhang Y, Liu ZR (2013) Reciprocal regulation of protein kinase and pyruvate kinase activities of pyruvate kinase M2 by growth signals. *J Biol Chem* 288**:** 15971-15979

Huyer G, Liu S, Kelly J, Moffat J, Payette P, Kennedy B, Tsaprailis G, Gresser MJ, Ramachandran C (1997) Mechanism of inhibition of protein-tyrosine phosphatases by vanadate and pervanadate. *J Biol Chem* 272**:** 843-851

Ibsen KH, Chiu RH, Park HR, Sanders DA, Roy S, Garratt KN, Mueller MK (1981) Purification and properties of mouse pyruvate kinases K and M and of a modified K subunit. *Biochemistry* 20**:** 1497-1506

Imamura K, Taniuchi K, Tanaka T (1972) Multimolecular forms of pyruvate kinase. II. Purification of M2-type pyruvate kinase from Yoshida ascites hepatoma 130 cells and comparative studies on the enzymological and immunological properties of the three types of pyruvate kinases, L, M1, and M2. *J Biochem* 72**:** 1001-1015

Israelsen WJ, Dayton TL, Davidson SM, Fiske BP, Hosios AM, Bellinger G, Li J, Yu Y, Sasaki M, Horner JW, Burga LN, Xie J, Jurczak MJ, DePinho RA, Clish CB, Jacks T, Kibbey RG, Wulf GM, Di Vizio D, Mills GB, Cantley LC, Vander Heiden MG (2013) PKM2 isoform-specific deletion reveals a differential requirement for pyruvate kinase in tumor cells. *Cell* 155**:** 397-409

Johnson FM, Chasalow F, Anderson G, Macdougal P, Hendren RW, Lewis SE (1981) A variation in mouse kidney pyruvate kinase activity determined by a mutant gene on chromosome 9. *Genet Res* 37**:** 123-131

Keller KE, Tan IS, Lee YS (2012) SAICAR stimulates pyruvate kinase isoform M2 and promotes cancer cell survival in glucose-limited conditions. *Science* 338**:** 1069-1072

Keller KE, Doctor ZM, Dwyer ZW, Lee YS (2014) SAICAR induces protein kinase activity of PKM2 that is necessary for sustained proliferative signaling of cancer cells. *Mol Cell* 53**:** 700-709

Kung C, Hixon J, Choe S, Marks K, Gross S, Murphy E, DeLaBarre B, Cianchetta G, Sethumadhavan S, Wang X, Yan S, Gao Y, Fang C, Wei W, Jiang F, Wang S, Qian K, Saunders J, Driggers E, Woo HK, Kunii K, Murray S, Yang H, Yen K, Liu W, Cantley LC, Vander Heiden MG, Su SM, Jin S, Salituro FG, Dang L (2012) Small molecule activation of PKM2 in cancer cells induces serine auxotrophy. *Chem Biol* 19**:** 1187-1198

Lewis SE, Johnson FM (1983) Dominant and recessive effects of electrophoretically detected specific locus mutations. In *Utilization of Mammalian Specific Locus Studies in Hazard Evaluation and Estimation of Genetic Risk*, de Serres FJ, Sheridan W (eds), pp 267-278. New York: Plenum Press

Lv L, Xu YP, Zhao D, Li FL, Wang W, Sasaki N, Jiang Y, Zhou X, Li TT, Guan KL, Lei QY, Xiong Y (2013) Mitogenic and oncogenic stimulation of K433 acetylation promotes PKM2 protein kinase activity and nuclear localization. *Mol Cell* 52**:** 340-352

Mazurek S, Hugo F, Failing K, Eigenbrodt E (1996) Studies on associations of glycolytic and glutaminolytic enzymes in MCF-7 cells: role of P36. *J Cell Physiol* 167**:** 238-250

Mazurek S, Grimm H, Boschek CB, Vaupel P, Eigenbrodt E (2002) Pyruvate kinase type M2: a crossroad in the tumor metabolome. *Br J Nutr* 87 Suppl 1**:** S23-29

Mendes P, Kell DB, Welch GR (1995) Metabolic channeling in organized enzyme systems: experiments and models. *Advances in Molecular and Cell Biology* 11**:** 1-19

Merrins MJ, Van Dyke AR, Mapp AK, Rizzo MA, Satin LS (2013) Direct measurements of oscillatory glycolysis in pancreatic islet beta-cells using novel fluorescence resonance energy transfer (FRET) biosensors for pyruvate kinase M2 activity. *J Biol Chem* 288**:** 33312-33322

Morgan HP, O'Reilly FJ, Wear MA, O'Neill JR, Fothergill-Gilmore LA, Hupp T, Walkinshaw MD (2013) M2 pyruvate kinase provides a mechanism for nutrient sensing and regulation of cell proliferation. *Proc Natl Acad Sci U S A* 110**:** 5881-5886

Parnell KM, Foulks JM, Nix RN, Clifford A, Bullough J, Luo B, Senina A, Vollmer D, Liu J, McCarthy V, Xu Y, Saunders M, Liu XH, Pearce S, Wright K, O'Reilly M, McCullar MV, Ho KK, Kanner SB (2013) Pharmacologic activation of PKM2 slows lung tumor xenograft growth. *Mol Cancer Ther* 12**:** 1453-1460

Peters J, Andrews SJ (1984) The Pk-3 gene determines both the heart, M1, and the kidney, M2, pyruvate kinase isozymes in the mouse; and a simple electrophoretic method for separating phosphoglucomutase-3. *Biochem Genet* 22**:** 1047-1063

Simon M, Spahr PF, Dainous F (1989) The proteins associated with the soluble form of p36, the main target of the src oncogene product in chicken fibroblasts, are glycolytic enzymes. *Biochem Cell Biol* 67**:** 740-748

Srivastava DK, Bernhard SA (1986a) Metabolite transfer via enzyme-enzyme complexes. *Science* 234**:** 1081-1086

Srivastava DK, Bernhard SA (1986b) Enzyme-enzyme interactions and the regulation of metabolic reaction pathways. *Curr Top Cell Regul* 28**:** 1-68

Tulloch LB, Morgan HP, Hannaert V, Michels PA, Fothergill-Gilmore LA, Walkinshaw MD (2008) Sulphate removal induces a major conformational change in Leishmania mexicana pyruvate kinase in the crystalline state. *J Mol Biol* 383**:** 615-626

Vander Heiden MG, Locasale JW, Swanson KD, Sharfi H, Heffron GJ, Amador-Noguez D, Christofk HR, Wagner G, Rabinowitz JD, Asara JM, Cantley LC (2010) Evidence for an alternative glycolytic pathway in rapidly proliferating cells. *Science* 329**:** 1492-1499

Varghese B, Swaminathan G, Plotnikov A, Tzimas C, Yang N, Rui H, Fuchs SY (2010) Prolactin inhibits activity of pyruvate kinase M2 to stimulate cell proliferation. *Mol Endocrinol* 24**:** 2356-2365

Yang W, Zheng Y, Xia Y, Ji H, Chen X, Guo F, Lyssiotis CA, Aldape K, Cantley LC, Lu Z (2012) ERK1/2-dependent phosphorylation and nuclear translocation of PKM2 promotes the Warburg effect. *Nat Cell Biol* 14**:** 1295-1304

APPENDIX A:
PKM2 Deletion in Colon Cancer Driven by *APC* Loss

INTRODUCTION

In collaboration with Kenneth E. Hung and Mark J. Sinnamon, we sought to determine if PKM2 is required for development of colon tumors. Mice harboring a conditional *Pkm2* allele (Israelsen et al, 2013) were crossed to mice with a conditional allele of the *APC* tumor gene and the effect of PKM2 deletion on tumor formation was determined. In this model of colon cancer, a section of distal colon is ligated and adenovirus expressing Cre recombinase is introduced into the lumen of the colon, which results in APC loss in infected cells and tumor initiation (Hung et al, 2010). Disease progression is followed over time by endoscopy.

RESULTS

There was no significant difference in survival between *Pkm2*$^{flox/flox}$ and *Pkm2*$^{+/+}$ mice (Figure 1), nor were there significant differences between cohorts in tumor penetrance at three weeks post-induction, at 6 weeks post-induction, or in overall tumor penetrance (Figure 2). Tumor penetrance is defined as the fraction of mice developing one or more tumors.

Interestingly, some *Pkm2*$^{flox/flox}$ mice developed more than one tumor, while no control mice ever developed more than one tumor. The multiplicity of the colon tumors (defined as number of tumors per tumor-bearing mouse) was therefore greater in the *Pkm2*$^{flox/flox}$ mice (Figure 3), with the mean number of tumors per tumor-bearing mouse being statistically significantly greater in the *Pkm2*$^{flox/flox}$ mice at the 6 week and "Final" time points ($p=0.003$ and $p=0.013$, respectively; unpaired two-tailed t-test). The reduction of multiplicity in the *Pkm2*$^{flox/flox}$ mice between 6 weeks and the "Final" time point is

explained by an increase in penetrance (i.e., additional *Pkm2*$^{flox/flox}$ mice each developed only one tumor).

The overall effect of increased tumor multiplicity in the *Pkm2*$^{flox/flox}$ mice is a greater number of tumors in that cohort compared to the control cohort (Figure 4).

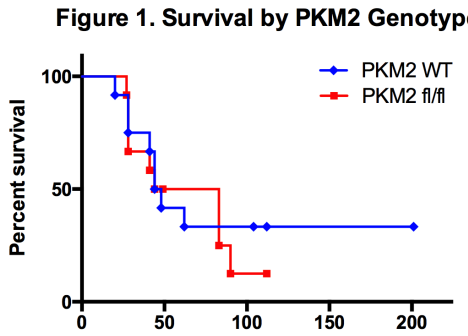

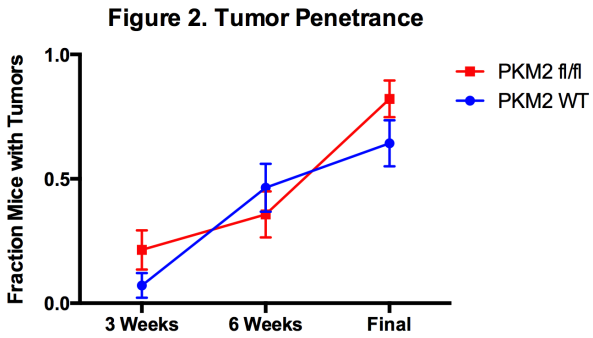

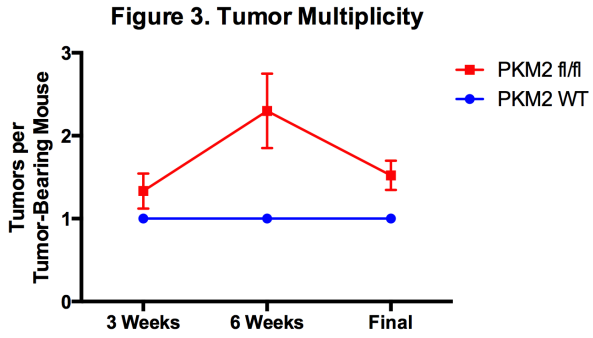

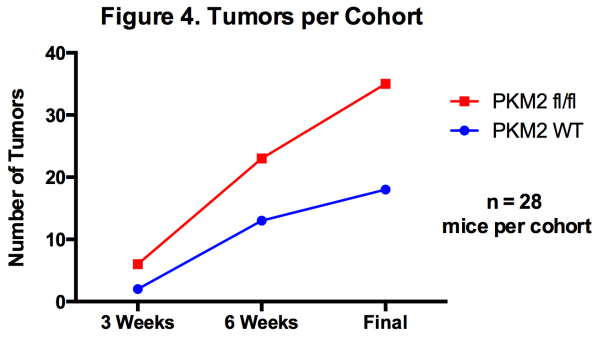

DISCUSSION

Deletion of PKM2 upon tumor initiation due to APC loss has no effect on survival or the fraction of mice developing tumors; however, PKM2 conditional mice that did develop tumors developed, on average, more than one tumor. PKM2 thus does not appear to be required for tumor growth in this model of colon cancer, and PKM2 loss may enhance tumor initiation or growth. An accelerating effect of PKM2 loss has been observed previously (Israelsen et al, 2013). Final conclusions from these experiments await

characterization of the tumors and verification of effective PKM2 deletion in the tumor cells.

REFERENCES

Hung KE, Maricevich MA, Richard LG, Chen WY, Richardson MP, Kunin A, Bronson RT, Mahmood U, Kucherlapati R (2010) Development of a mouse model for sporadic and metastatic colon tumors and its use in assessing drug treatment. *Proc Natl Acad Sci U S A* 107**:** 1565-1570

Israelsen WJ, Dayton TL, Davidson SM, Fiske BP, Hosios AM, Bellinger G, Li J, Yu Y, Sasaki M, Horner JW, Burga LN, Xie J, Jurczak MJ, DePinho RA, Clish CB, Jacks T, Kibbey RG, Wulf GM, Di Vizio D, Mills GB, Cantley LC, Vander Heiden MG (2013) PKM2 isoform-specific deletion reveals a differential requirement for pyruvate kinase in tumor cells. *Cell* 155**:** 397-409

APPENDIX B:
Table of Published Pyruvate Kinase Kinetic Parameters

A Comparison of Published Pyruvate Kinase Kinetic Parameters

PKM2	**PEP**				**ADP**				
Species (origin)	**K_m** (-FBP)	**K_m** (+FBP)	**n_H** (-FBP)	**n_H** (+FBP)	**K_m** (-FBP)	**K_m** (+FBP)	**Temp** (°C)	**pH**	**Reference**
Rat (PKM2 from liver)	500 µM						25	7.5	(Imamura & Tanaka, 1972)
Rat (hepatoma cells)	400 µM		1.4-1.5	1.0			24	7.4	(Imamura et al, 1972)
Chicken (liver)	330 µM	40 µM	2.1	1.0				7.5	(Strandholm et al, 1975)
Pig (kidney)	250 µM	70 µM			300 µM		30	7.5	(Berglund & Humble, 1979)
Mouse (kidney)	190 µM	26 µM			270 µM	300 µM	37	7.5	(Ibsen et al, 1981)
Mouse (kidney)	90 µM	35 µM			320 µM	380 µM	37	7.0	(Ibsen et al, 1981)
Rat M2 (insect cells)	180 µM	52 µM	2.3	1.2	320 µM		37	7.5	(Ikeda et al, 1997)
Human (*E. coli*-refold)	2100 µM	170 µM	1.6	1.0	340 µM	240 µM	32	8.0	(Dombrauckas et al, 2005)
Human (*E. coli*-native)	460 µM	47 µM	2.1	1.0	190 µM	180 µM	25	7.5	(Akhtar et al, 2009)
Human (*E. coli*-native)	860 µM	100 µM	1.2	1.0			37	7.4	(Morgan et al, 2013)

PKM1	**PEP**				**ADP**				
Species (origin)	**K_m** (-FBP)	**K_m** (+FBP)	**n_H** (-FBP)	**n_H** (+FBP)	**K_m** (-FBP)	**K_m** (+FBP)	**Temp** (°C)	**pH**	**Reference**
Rabbit (muscle)	0.86 µM						25	7.5	(Bücher & Pfleiderer, 1955)
Rat (muscle)	75 µM						25	7.5	(Tanaka et al, 1967)
Rat (muscle)	75 µM		1.0	1.0			24	7.4	(Imamura et al, 1972)
Cow (muscle)	40 µM		0.93	0.94			25	7.0	(Cardenas & Dyson, 1973)
Cow (muscle)	39 µM						25	7.0	(Cardenas et al, 1973)
Chicken (pectoralis)	40 µM		1.0					7.5	(Strandholm et al, 1975)
Chicken (pectoralis)	50 µM				300 µM		25		(Cardenas et al, 1975)
Pig (muscle)	20 µM				300 µM		30	7.5	(Berglund & Humble, 1979)
Mouse (muscle)	35 µM	28 µM			280 µM	300 µM	37	7.5	(Ibsen et al, 1981)
Mouse (muscle)	35 µM	33 µM			290 µM	380 µM	37	7.0	(Ibsen et al, 1981)

PKL	**PEP**				**ADP**				
Species (origin)	**K_m** (-FBP)	**K_m** (+FBP)	**n_H** (-FBP)	**n_H** (+FBP)	**K_m** (-FBP)	**K_m** (+FBP)	**Temp** (°C)	**pH**	**Reference**
Rat (liver)	830 µM						25	7.5	(Tanaka et al, 1967)
Rat (liver)	830 µM		2.0	1.0			24	7.5	(Imamura et al, 1972)
Cow (liver)	500 µM	80 µM	2.1	1.2			25	7.0	(Cardenas & Dyson, 1973)
Rat (liver)	600 µM	60 µM					25	7.5	(Taylor & Bailey, 1967)
Cow (liver)	660 µM	69 µM	2.5	1.1			25	7.5	(Hubbard & Cardenas, 1975)
Pig (liver)	300 µM						30	7.5	(Berglund & Humble, 1979)

This table is not exhaustive. References are given in full starting on the next page.

See also:

Kahn A, Marie J (1982) Pyruvate kinases from human erythrocytes and liver. *Methods Enzymol* 90 Pt E**:** 131-140
Cardenas JM (1982) Pyruvate kinase from bovine muscle and liver. *Methods Enzymol* 90 Pt E**:** 140-149
Imamura K, Tanaka T (1982) Pyruvate kinase isozymes from rat. *Methods Enzymol* 90 Pt E**:** 150-165

REFERENCES

Akhtar K, Gupta V, Koul A, Alam N, Bhat R, Bamezai RN (2009) Differential behavior of missense mutations in the intersubunit contact domain of the human pyruvate kinase M2 isozyme. *J Biol Chem* 284**:** 11971-11981

Berglund L, Humble E (1979) Kinetic properties of pig pyruvate kinases type A from kidney and type M from muscle. *Arch Biochem Biophys* 195**:** 347-361

Bücher T, Pfleiderer G (1955) Pyruvate kinase from muscle: Pyruvate phosphokinase, pyruvic phosphoferase, phosphopyruvate transphosphorylase, phosphate—transferring enzyme II, etc. Phosphoenolpyruvate+ ADP⇌ Pyruvate+ ATP. *Methods Enzymol* 1**:** 435–440

Cardenas JM, Dyson RD (1973) Bovine pyruvate kinases. II. Purification of the liver isozyme and its hybridization with skeletal muscle pyruvate kinase. *J Biol Chem* 248**:** 6938-6944

Cardenas JM, Dyson RD, Strandholm JJ (1973) Bovine pyruvate kinases. I. Purification and characterization of the skeletal muscle isozyme. *J Biol Chem* 248**:** 6931-6937

Cardenas JM, Blachly EG, Ceccotti PL, Dyson RD (1975) Properties of chicken skeletal muscle pyruvate kinase and a proposal for its evolutionary relationship to the other avian and mammalian isozymes. *Biochemistry* 14**:** 2247-2252

Dombrauckas JD, Santarsiero BD, Mesecar AD (2005) Structural basis for tumor pyruvate kinase M2 allosteric regulation and catalysis. *Biochemistry* 44**:** 9417-9429

Hubbard DR, Cardenas JM (1975) Kinetic properties of pyruvate kinase hybrids formed with native type L and inactivated type M subunits. *J Biol Chem* 250**:** 4931-4936

Ibsen KH, Chiu RH, Park HR, Sanders DA, Roy S, Garratt KN, Mueller MK (1981) Purification and properties of mouse pyruvate kinases K and M and of a modified K subunit. *Biochemistry* 20**:** 1497-1506

Ikeda Y, Tanaka T, Noguchi T (1997) Conversion of Non-allosteric Pyruvate Kinase Isozyme into an Allosteric Enzyme by a Single Amino Acid Substitution. *J Biol Chem* 272**:** 20495-20501

Imamura K, Tanaka T (1972) Multimolecular forms of pyruvate kinase from rat and other mammalian tissues. I. Electrophoretic studies. *J Biochem* 71**:** 1043-1051

Imamura K, Taniuchi K, Tanaka T (1972) Multimolecular forms of pyruvate kinase. II. Purification of M2-type pyruvate kinase from Yoshida ascites hepatoma 130 cells and comparative studies on the enzymological and immunological properties of the three types of pyruvate kinases, L, M1, and M2. *J Biochem* 72**:** 1001-1015

Morgan HP, O'Reilly FJ, Wear MA, O'Neill JR, Fothergill-Gilmore LA, Hupp T, Walkinshaw MD (2013) M2 pyruvate kinase provides a mechanism for nutrient sensing and regulation of cell proliferation. *Proc Natl Acad Sci U S A* 110**:** 5881-5886

Strandholm JJ, Cardenas JM, Dyson RD (1975) Pyruvate kinase isozymes in adult and fetal tissues of chicken. *Biochemistry* 14**:** 2242-2246

Tanaka T, Harano Y, Sue F, Morimura H (1967) Crystallization, characterization and metabolic regulation of two types of pyruvate kinase isolated from rat tissues. *J Biochem* 62**:** 71-91

Taylor CB, Bailey E (1967) Activation of liver pyruvate kinase by fructose 1,6-diphosphate. *Biochem J* 102**:** 32C-33C

The End.